2014

Sediment and Organic Carbon Burial in Englebright Lake, CA over the Last Century

Christina Rose Pondell
College of William and Mary - Virginia Institute of Marine Science

Sediment and Organic Carbon Burial in Englebright Lake, CA over the Last Century

---

A Dissertation

Presented to

The Faculty of the School of Marine Science

The College of William and Mary in Virginia

In Partial Fulfillment

of the requirements for the Degree of

Doctor of Philosophy

---

by

Christina Rose Pondell

2014

APPROVAL SHEET

This dissertation is submitted in partial fulfillment of

the requirements for the degree of

Doctor of Philosophy

Christina R. Pondell

Christina R. Pondell

Approved, by the Committee, July 2014

Elizabeth A. Canuel, Ph.D.
Advisor

Aaron J. Beck, Ph.D.

Mark J. Brush, Ph.D.

John D. Milliman, Ph.D.

Steve A. Kuehl, Ph.D.

Scott A. Wright, Ph.D.
USGS California Water Science Center
Sacramento, California

TABLE OF CONTENTS

ACKNOWLEDGEMENTS

I am greatly appreciative for the support and advice from so many people who have helped me to complete this dissertation. First, thank you, Dr. Elizabeth Canuel, for your patience, your guidance, and for all of your support. Your passion for science inspires me to dig deeper and ask the tough questions, remembering that there is always more to be learned.

Thank you Drs. Aaron Beck, Steve Kuehl, John Milliman, Scott Wright and Mark Brush, my committee members, for your recommendations and advice, and for your many provocative questions. You encouraged me to take a step back, get a new perspective, and try and focus on the bigger picture, and you definitely kept me on my toes for these last few years.

To the administration and staff at VIMS who ensure everything runs smoothly, especially Dr. Iris Anderson, Dr. Linda Schaffner, Cynthia Harris and Cindy Hornsby. Thank you for helping me stay organized and focused, and for helping me develop professional network and make connections with the local community and with the broader scientific community.

I would be remiss if I didn't acknowledge the teachers, students, fellows, and the management team of the GK-12 PERFECT program. For two years they worked with me outside of the lab, and I learned the coolest science from some of the most interesting people I know.

Without the support of my lab mates, I would not be the same person today. Thank you Erin, Steph, Sarah, Emily, Hadley, Amanda, Arash, Yuehan, George, Matt, and Paul for all the long days in the lab, and for the longer—and hotter—days in the field. Above of all, thank you for all the laughs.

Finally, to my friends, my family, and to Robert: thank you. Thank you for your support, for the motivation, and for your understanding, even when you couldn't understand all of the dam carbon mumbo-jumbo. I am forever grateful to you.

LIST OF TABLES

LIST OF FIGURES

Page

ABSTRACT

The proliferation of dams has impacted over 67% of the world's largest rivers, degrading ecosystems, severing river-watershed connectivity, and reducing water, sediment, and carbon supply from rivers to the coastal ocean by 20 to 100%. Many studies have focused on the downstream impacts of dams, but few have quantified the amounts and quality of organic matter stored within impoundments. This study examined organic carbon (OC) sources and accumulation in a reservoir in northern California to characterize the organic matter retained in terrestrial systems by these man-made structures and relate the amounts and quality of OC to mining, damming and flood events in the watershed. Englebright Lake was chosen for the study site because high sedimentation rates, resulting from 19th century hydraulic gold mining, offered high-resolution records of historic (1940-2002) change, detailed records of land-use and flood events provided a history of the watershed, and the construction of an upstream dam in 1970 offered the opportunity to analyze its hydrologic impacts. Sediments from Englebright Lake as well as soil, vegetation and aquatic samples from the lake and its watershed were analyzed as part of this study. Measured plutonium radioisotope profiles were used to calculate sediment and OC accumulation rates, and organic matter was characterized using total organic carbon (TOC) and nitrogen (TN) content, stable carbon and nitrogen isotopes ($\delta^{13}C$ and $\delta^{15}N$), and fatty acid, sterol, and lignin biomarkers. OC signatures from end-member samples were used to describe aquatic (plankton and algae) and terrigenous (soil and plant) sources and interpret sediment OC profiles in Englebright Lake. Mass accumulation rates of OC ranged from 0.8 to 216 $kg_{OC}\ m^{-2}\ yr^{-1}$, with the highest mass accumulation rates corresponding to flood events. During the 60-year record measured in this study, 0.36 Tg OC were buried in Englebright Lake, 64% of which was from terrigenous sources (based on data from a two end-member $\delta^{13}C$ mixing model). Flood events in 1964 and 1997 had a significant impact on OC accumulation, and terrigenous biomarkers, including long chain fatty acids (LCFA), lignin phenols (Σ8), and plant sterols (stigmasterol, campesterol, sitosterol), increased 2 to 5 times in delta front cores during these events. Aquatic biomarkers in bottomset deposits responded to the upstream dam construction, and concentrations of aquatic sterols (27-nor-24-cholesta-5,22-dien-3β-ol and cholesta-5,22-dien-3β-ol) increased after 1970, while diacid concentrations (a terrigenous biomarker) decreased following the construction of the dam. Records of hydraulic mining impacts were observed as a thick layer of OC-poor (TOC < 0.1%) sediments accumulating between 1950 and 1980 in topset deposits. Overall, the OC sequestered in Englebright Lake suggests that the magnitude of the carbon sink provided by dams and impoundments is substantial, and should be considered in global carbon cycle budgets as well as in plans for future dam construction or removal projects.

Sediment and Organic Carbon Burial in Englebright Lake, CA over the Last Century

CHAPTER 1: INTRODUCTION

The Global Impact of Dams and Reservoirs

The construction of dams and reservoirs is perhaps one of the most significant ways in which humans have altered terrestrial and aquatic ecosystems and has important consequences for the transfer of carbon between land-ocean systems (Walling 2006). In 2001 the number of artificial lakes and reservoirs exceeded 800,000 and covered an area of 500,000km^3, about 3% of the surface of the earth (Friedl and Wuest 2002). These impoundments have been built to provide drinking water, hydropower, irrigation, and flood control to surrounding communities, but they also prevent sediment, nutrients, and organic matter from travelling further downstream. Together, these impoundments hold more than 30% of all river sediments on a global scale (Meybeck and Vörösmarty 2005), and on an annual basis, the amount of organic carbon (OC) stored in lakes and reservoirs is comparable to the amount of OC delivered by rivers to the ocean (Downing et al. 2008).

Artificial lakes and reservoirs created by dams influence the way sediment and organic carbon travel through and between ecosystems, and moderate the delivery of sediment and associated materials to downstream environments. A majority of major rivers worldwide have been dammed multiple times, greatly reducing the amount of sediment being deposited in coastal systems. In many cases the reduction in sediment load can be greater than 75%, as seen in the Sao Francisco River in Brazil, the Chao Phraya River in Thailand, and the Yellow River in China (Walling 2006). In some river systems, as in the Nile River and the Columbia River, the sediment load at the delta of the river has been reduced to zero as a result of damming practices (Walling 2006). With reduced sediment supply to coastal systems, the effects of sea level transgression are more severe and coastlines quickly succumb to encroaching water levels (Milliman et al. 1989, Syvitski and Milliman 2007, Blum and Roberts 2009).

Dams not only change the transport of sediment through rivers, but also change the flux of materials associated with sediments, including particulate organic matter, to downstream ecosystems. Dams trap coarse sediments and particulate organic matter in their reservoirs while allowing finer sediments and dissolved organic matter to continue to flow downstream (Vörösmarty et al. 2003, Walling 2006, Dai et al. 2008). They also trap sediment-associated nutrients and contaminants such as mercury (Alpers et al. 2006), and dams have the potential to influence climate change because they release greenhouse gases such as CO_2 and CH_4 during microbial decomposition of organic matter sequestered in reservoirs (St Louis et al. 2000). Additionally, dams increase the retention time of rivers, leading to more primary production in the water column as microalgae take advantage of the increased nutrient concentrations and light availability in the reservoir (Friedl and Wuest 2002, Meybeck 2003, Das et al. 2008). Previous studies have focused primarily on the accumulation of sediment and total organic matter in reservoirs (e.g., Downing et al. 2008).

On a per area basis, the sequestration of OC in reservoirs is considerable and can be up to three times higher than marine environments, such as vegetated habitats, that are thought to be significant carbon sinks (Dean and Gorham 1998). These systems are an important sink for OC, and likely represent a significant change in the global carbon cycle as a direct response to human activities. To date, only a few studies have investigated the composition and abundance of OC sequestered in reservoir sediments and ecosystem implications (Houel et al. 2006, Weissenberger et al. 2010, Oelbermann and Schiff 2010). This study builds on this body of work by investigating changes in the rates of carbon accumulation and sources of organic carbon using organic biomarker analysis of sediment cores collected from a reservoir in California as a model system.

Background

The Sacramento-San Joaquin River Delta located in the Central Valley of California (Delta, hereafter) exemplifies a system highly vulnerable to environmental change (e.g., Knowles 2002, Cloern et al. 2011, Cloern and Jassby 2012). High rates of land

subsidence (most of the Delta is below sea level), extensive land use change, an unstable system of protective levees, and extensive tectonic activity in the Delta watershed make this system particularly vulnerable to the influences of rising sea level on the region. Over the last 50 years the population in the Delta watershed, which includes the watersheds of both the Sacramento River and the San Joaquin River, has increased from about 750,000 to almost 2 million people. During this same time period, much of the land was converted from wetlands to agriculture and grazing land and subsequently has become increasingly urbanized (Sickman et al. 2007, Canuel et al. 2009).

Further compounding the stresses on the Delta ecosystem from anthropogenic demands are the expected effects of climate change, including warming, reduced snowpack and altered precipitation patterns (Duffy et al. 2007, Bonfils et al. 2008, Cayan et al. 2008b, Cloern et al. 2011). Altered precipitation patterns are expected to transform river runoff patterns resulting in earlier peak flows (Stewart et al. 2004, Hayhoe et al. 2004). Greater variability in rainfall is also predicted, which will lead to increases in the frequency and violence of the winter floods as well as increased occurrence of droughts (Dettinger 2011, Pierce et al. 2012). Shifts in the runoff regime are expected to exacerbate existing problems with flood control infrastructure, including the 110,000 km of levees and dams that line the waterways in the delta's drainage basin (Cloern et al. 2011). Along with the levees, hundreds of dams and water diversions built to control water flow are already under significant stress, and failures like those of the Lower Jones Tract levee in 1980 and the Sherman and Mandeville levee in 1972 have created major floods and millions of dollars in damage to the Central Valley area (Lund et al. 2007).

Altered precipitation patterns are one of many of the dramatic responses to climate change expected in the near future; higher temperatures are also predicted by 2060 (Cloern et al. 2011, Pierce et al. 2012). Higher temperatures will result in elevated sea level and increases in the frequency of droughts that will impact coastal and agricultural communities, including regions like the Delta (Rahmstorf 2010, Cloern et al. 2011). In the Delta, sea level is expected to rise 13-86cm by 2100 (Cayan et al. 2008a), which will

put more strain on infrastructure and reduce the amount of freshwater in the area. Increased duration and frequency of droughts will amplify the demand for freshwater in the drainage basin and in other areas of the state that depend on the Central Valley and the Delta for freshwater (Cloern et al. 2011). The combined effects of precipitation increases, sea level rise, and more demands for freshwater will put more stress on an already weak infrastructure network along the waterways of the Delta watershed.

Recent studies of sediment and total organic carbon (TOC) in sediment cores collected from the Delta document decreasing rates of accumulation since the 1970's. These changes were considered in light of changes in land use and precipitation and it was found that anthropogenic influences dominated over climate change during this time period (Canuel et al. 2009). In a separate study, (Wright and Schoellhamer 2004) documented reductions in total suspended loads in the Sacramento River for this time period. They suggested that water diversion programs, specifically accumulation behind dams, might account for the reduction in suspended sediment concentrations in the Delta.

California has been damming rivers for over 150 years. Initially, these dams were built to trap mining debris and, more recently, have been used to divert water for drinking, irrigation, and flood control. In northern California, most rivers travel from the high Sierra Nevada Mountains, across the Central Valley, and deposit water, sediments, and organic matter in their deltas and in the Pacific Ocean. Since these rivers have their origins in the high, easily erodible mountains, their sediment loads are generally high (Milliman and Syvitski 1992) so the potential for dams to have major impacts on the transfer of sediments, as well as organic matter and other associated materials transported by rivers, is significant.

Study Site

Englebright Lake on the Yuba River in California was chosen as a representative site for this study because its watershed is one of the most heavily mined in the state (James 2005), leading to high erosion, and therefore, high accumulation rates in the reservoir.

The Yuba River is located in northern California, northeast of Sacramento, with its headwaters in the Sierra Nevada Mountain Range. Conifer forests at higher elevations, and oak and chaparral communities at lower elevations, dominate the Yuba River watershed, while agriculture and urban regions cover less than two percent of the watershed area. The North, Middle and South Yuba River tributaries make up the upper Yuba River, and they flow from the mountains where they join to create the Yuba River just north (upriver) of the Englebright Dam. The California Debris Commission completed the Englebright Dam in December 1940 for the purpose of controlling floodwaters to the Central Valley region around Marysville by trapping mining debris from future hydraulic-mine sites (Snyder et al. 2004a). Currently, the dam is used for a minor supply of hydroelectric power and its 14 km long reservoir is used for recreation.

Both the Middle and the South Yuba Rivers were extensively dammed to control mine tailings resulting from some of the heaviest hydraulic gold mining activity in the Yuba River watershed during the Gold Rush era in California (Gilbert 1917). However, a majority of these dams were small in size, constructed solely to retain mining sediments, and many have since failed (James 2005). Small dams on the North Yuba River were also built to control mining debris, but the transport of materials in this tributary was significantly altered in 1970 by the addition of the New Bullards Bar dam (NBB). This large dam created a reservoir with a surface area of 19km^2, which traps much of the sediment and organic matter moving through the North Yuba River, and altered the hydrologic regime in Englebright Lake.

Previous Studies

The Yuba River above Englebright Dam is the location of the California Bay-Delta Authoritiy's (CBDA) Upper Yuba River Studies Program (UYRSP). This program was initiated in 2001 in an effort to reintroduce Chinook salmon and steelhead trout species to the upper Yuba River (Snyder et al. 2004a). Because the Englebright Dam prevents upriver migration of anadromous fish, several options were considered: (1) the addition of a salmon ladder for the fish to circumnavigate the dam, (2) lowering the dam, or (3)

complete removal of the dam. To determine the feasibility of this project and the consequences of releasing the sediment from behind the dam to downstream ecosystems, the United States Geological Society (USGS) surveyed the geology of Englebright Lake.

The USGS measured bathymetry of the Englebright Lake in 2001 (Childs et al. 2003), and by comparing this bathymetric survey to the Army Corps of Engineers survey taken in 1939, before the dam was constructed, they determined the volume of sediment trapped by the dam to be 21,890,000 m^3. This accumulation of sediment represents a reduction in the original storage capacity by 25.5% (Snyder et al. 2004a). In 2002, the USGS returned to conduct an extensive coring campaign of the reservoir sediments. Sediments were collected from twenty-nine piston cores at 6 locations along the thalweg of Englebright Lake, and measurements of grain size, organic content, mercury content, and radioactivity (^{137}Cs) allowed the team of researchers to characterize the sedimentation regime in the lake (Childs et al. 2003, Snyder et al. 2004b, 2004c, 2004a, Alpers et al. 2006, Snyder et al. 2006).

While the USGS created a comprehensive geological description of Englebright Lake, no research was undertaken to characterize the organic carbon buried in the lake. Studies of organic carbon stored in reservoir sediments are relatively limited but have the potential to provide insights about the role of dams in carbon sequestration as well as the potential effects of carbon removal on downstream ecosystem. This study builds on the USGS effort by characterizing the amount and composition of organic carbon sequestered in the Englebright Lake study system. The objectives of this study are threefold: (1) determine the sources of organic carbon to Englebright Lake, (2) examine how carbon accumulates on temporal and spatial scales in this reservoir and (3) relate changes in upstream tributaries to biomarkers in lake sediments.

Approach

Sources of organic matter delivered to Englebright Lake over its 60-year history were traced using sediment core records of lignin and lipid biomarker compounds and stable

isotopes of carbon and nitrogen ($d^{13}C$ and $d^{15}N$). Stable carbon isotopes are useful biomarkers of organic matter source due to differences in the ratio of ^{13}C to ^{12}C resulting from different sources of inorganic carbon and different pathways of carbon fixation (Libes 2009). Generally, vascular plants (-27‰) have lower $\delta^{13}C$ values than marine algae (-21 to -19‰), providing a useful tool for differentiating between terrigenous and marine organic matter in estuarine and coastal environments (Cloern et al. 2002). $d^{15}N$ values are used to observe changes in primary production, variations in nitrogen inputs and diagenetic alteration (Gu 2009, Lu et al. 2010, Vreča and Muri 2010). Interpretation of $d^{15}N$ can be difficult because many of the signal variations overlap, such as values for soils (0‰-12‰), sewage effluents (10‰-20‰) and fertilizer inputs (5‰-7‰). Thus, $\delta^{13}C$ and $d^{15}N$ are best used in combination with other tracers such as organic biomarkers.

Lipid biomarkers, including fatty acids and sterols, can be uniquely linked to algal, bacterial, and vascular plant sources (Bianchi and Canuel 2011). Fatty acids and sterols are useful biomarkers because they provide the ability to use differences in their molecular structure to distinguish among phytoplankton, zooplankton, bacteria and terrestrial plants (Waterson and Canuel 2008). For example, fatty acids can be used to differentiate between organic matter sources by comparing the carbon chain length, levels of unsaturation (double bonds), and the number and location of alkyl (methyl) branches. Marine and freshwater phytoplankton are uniquely comprised of polyunsaturated fatty acids (e.g., 20:5w3), while terrestrial plants are characterized by long chain (C_{20}-C_{28}) saturated fatty acids and branched fatty acids are unique to bacterial sources (Waterson and Canuel 2008).

Lignin phenols make up the macromolecules used as structural components in vascular plants (Hedges and Mann 1979). These biomarkers are unique to vascular plants. This, in addition to its refractory nature, makes lignin an excellent biomarker for tracing terrigenous organic matter in aquatic environments. A suite of phenols, products from the oxidation of the lignin macromolecule, is used to distinguish between woody material and soft tissue, like leaves or needles, and between gymnosperm (cone-bearing plants)

and angiosperm (flower-bearing plants) tissues (Hedges and Mann 1979). Ratios of lignin phenols also offer insight into the degree of degradation in vascular plant materials (Ertel and Hedges 1984). Moreover, changes in the concentration and distribution of lignin can be used to determine responses to land use and vegetation modification in the watershed.

The time chronology of the sediment cores used for this study was established using radiochronometric methods (e.g., ^{137}Cs, $^{239+240}Pu$). Studies have shown the application of $^{239+240}Pu$ to date coarse sediments (Kuehl et al. 2012) in a manner similar to ^{137}Cs, whose affinity for fine grain sizes restricts the application of this radiochronometric method to systems dominated by clays and silts (Cundy and Croudace 1995). $^{239+240}Pu$ offer greater sensitivity to measure low concentration of radioisotopes associated with coarse grain size. In Englebright Lake, where sediments are characterized by a combination of fine and coarse sediments, plutonium isotopes offer an opportunity to determine sediment chronology for all six sediment cores, regardless of their dominant grain size.

These organic biomarkers and proxies allowed for the classification of organic matter sources in Englebright Lake, which were then related to climate and anthropogenic impacts in the watershed. The following chapters discuss the biomarker results and address the three objectives that guided this study.

Objective 1: Identify OM sources in Englebright Lake. This objective is addressed in Chapters 3 and 5 of the dissertation. Chapter 3 presents results from a study that characterized the sources of organic carbon to Englebright Lake by measuring the biomarker and stable isotope composition of soil and vegetation samples collected from the upper Yuba River watershed and from aquatic samples collected from the lake. Concentrations of fatty acid (FA), sterol, and lignin biomarkers, as well as $d^{13}C$ and $d^{15}N$, were used to address this objective. Later, in Chapter 5, the biomarkers identified through this study were applied to interpretation of the sediment cores collected from Englebright Lake.

Objective 2: Determine spatial and temporal controls of OC accumulation in Englebright Lake. The second objective is addressed in the work presented in Chapters 2, 4, and 5 of this dissertation. In Chapter 2, sediment accumulation rates are calculated using depth profiles of $^{239+240}$Pu activities. These sedimentation rates are then applied to TOC presented in Chapter 4 to discuss the mass accumulation rates and burial of OC in Englebright Lake. Sources of this OC are identified with $d^{13}C$ and $d^{15}N$ in Chapter 4 and using the organic biomarker composition in Chapter 5. Multiple proxies including sediment and OC accumulation rates, TOC, $d^{13}C$ and $d^{15}N$, and organic matter biomarkers were used to provide insight into spatial and temporal patters of OC accumulation in Englebright Lake.

Objective 3: Evaluate the response of OC signatures in Englebright Lake to changes in the watershed. This objective was addressed in Chapters 3, 4, and 5 using trends in biomarker, TOC and stable isotope accumulation over the 60-year history of the sediments deposited within Englebright Lake. Changes in aquatic and terrigenous OM sources in the sediment record, identified from end-member samples (Chapter 3) in the watershed, were related to flood events and changes in the hydrologic regime (Chapters 4 and 5).

The goal of this study was to characterize the organic carbon accumulating behind dams using Englebright Lake as a representative system. This dissertation describes the magnitude of carbon burial in this system and the significance of the response of organic carbon accumulation to climate- and human-driven events in the watershed.

Literature Cited

Alpers, C. N., M. P. Hunerlach, M. C. Marvin-DiPasquale, R. C. Antweiler, B. K. Lasorsa, J. F. DeWild, and N. P. Snyder. 2006. Geochemical Data for Mercury, Methylmercury, and Other Constituents in Sediments from Englebright Lake, California, 2002. Page 95. U.S. Geological Survey Data Series 151.

Bianchi, T. S., and E. A. Canuel. 2011. Chemical Biomarkers in Aquatic Ecosystems. Princeton University Press, Princeton.

Blum, M., and H. Roberts. 2009. Drowning of the Mississippi Delta due to insufficient sediment supply and global sea-level rise. Nature Geoscience 2:488–491.

Bonfils, C., P. B. Duffy, B. D. Santer, T. Wigley, and D. B. Lobell. 2008. Identification of external influences on temperatures in California. Climatic Change 87 (Suppl 1):S43–S55.

Canuel, E., E. Lerberg, R. Dickhut, S. Kuehl, T. Bianchi, and S. Wakeham. 2009. Changes in sediment and organic carbon accumulation in a highly-disturbed ecosystem: The Sacramento-San Joaquin River Delta (California, USA). Mar Pollut Bull 59:154–163.

Cayan, D. R., P. D. Bromirski, K. Hayhoe, and M. Tyree. 2008a. Climate change projections of sea level extremes along the California coast. Climatic Change 87 (Suppl 1):S57-S73.

Cayan, D., E. Maurer, M. Dettinger, M. Tyree, and K. Hayhoe. 2008b. Climate change scenarios for the California region. Climatic Change 87 (Suppl 1):S21-S42.

Childs, J., N. Snyder, and M. Hampton. 2003. Bathymetric and geophysical surveys of Englebright Lake, Yuba-Nevada Counties, California. Page 20. U.S. Geological Survey Open-File Report 03-383.

Cloern, J. E., and A. D. Jassby. 2012. Drivers of change in estuarine-coastal ecosystems: Discoveries from four decades of study in San Francisco Bay. Reviews of Geophysics 50:RG4001.

Cloern, J. E., E. A. Canuel, and D. Harris. 2002. Stable carbon and nitrogen isotope composition of aquatic and terrestrial plants of the San Francisco Bay estuarine system. Limnology and Oceanography 47:713–729.

Cloern, J. E., N. Knowles, L. R. Brown, D. Cayan, M. D. Dettinger, T. L. Morgan, D. H.

Schoellhamer, M. T. Stacey, M. van der Wegen, R. W. Wagner, and A. D. Jassby. 2011. Projected evolution of California's San Francisco Bay-Delta-River system in a century of climate change. PLoS ONE 6:e24465.

Cundy, A. B., and I. W. Croudace. 1995. Physical and chemical associations of radionuclides and trace metals in estuarine sediments: an example from Poole Harbour, Southern England. Journal of Environmental Radioactivity 29:191–211.

Dai, S., S. Yang, and A. Cai. 2008. Impacts of dams on the sediment flux of the Pearl River, southern China. CATENA 76:36–43.

Das, B., R. Nordin, and A. Mazumder. 2008. An alternative approach to reconstructing organic matter accumulation with contrasting watershed disturbance histories from lake sediments. Environmental Pollution 155:117–124.

Dean, W., and E. Gorham. 1998. Magnitude and significance of carbon burial in lakes, reservoirs, and peatlands. Geology 26:535–538.

Dettinger, M. 2011. Climate Change, Atmospheric Rivers, and Floods in California – A Multimodel Analysis of Storm Frequency and Magnitude Changes. Journal of the American Water Resources Association 47:514–523.

Downing, J., J. Cole, J. Middelburg, R. Striegl, C. Duarte, P. Kortelainen, Y. Prairie, and K. Laube. 2008. Sediment organic carbon burial in agriculturally eutrophic impoundments over the last century. Global Biogeochemical Cycles 22:GB1018.

Duffy, P. B., C. Bonfils, and D. Lobell. 2007. Interpreting recent temperature trends in California. Eos, Transactions American Geophysical Union 88:409–410.

Ertel, J. R., and J. I. Hedges. 1984. The lignin component of humic substances: Distribution among soil and sedimentary humic, fulvic, and base-insoluble fractions. Geochimica et Cosmochimica Acta.

Friedl, G., and A. Wuest. 2002. Disrupting biogeochemical cycles - Consequences of damming. Aquatic Sciences 64:55–65.

Gilbert, G. K. 1917. Hydraulic-mining Débris in the Sierra Nevada. U.S. Geological Survey Professional Paper.

Gu, B. 2009. Variations and controls of nitrogen stable isotopes in particulate organic matter of lakes - Springer. Oecologia.

Hayhoe, K., D. Cayan, C. B. Field, P. C. Frumhoff, E. P. Maurer, N. L. Miller, S. C. Moser, S. H. Schneider, K. N. Cahill, E. E. Cleland, L. Dale, R. Drapek, R. M.

Hanemann, L. S. Kalkstein, J. Lenihan, C. K. Lunch, R. P. Neilson, S. C. Sheridan, and J. H. Verville. 2004. Emissions pathways, climate change, and impacts on California. Proceedings of the National Academy of Sciences 101:12422–12427.

Hedges, J., and D. Mann. 1979. The characterization of plant tissues by their lignin oxidation products. Geochimica et Cosmochimica Acta 43:1803–1807.

Houel, S., P. Louchouarn, M. Lucotte, R. Canuel, and B. Ghaleb. 2006. Translocation of soil organic matter following reservoir impoundment in boreal systems: Implications for in situ productivity. Limnology and Oceanography 51:1497–1513.

James, L. A. 2005. Sediment from hydraulic mining detained by Englebright and small dams in the Yuba basin. Geomorphology 71:202–226.

Knowles, N. 2002. Potential effects of global warming on the Sacramento/San Joaquin watershed and the San Francisco estuary. Geophysical Research Letters 29:1891.

Kuehl, S. A., M. E. Ketterer, and J. L. Miselis. 2012. Extension of 239+ 240 Pu sediment geochronology to coarse-grained marine sediments. Continental Shelf Research 36:83–88.

Libes, S. 2009. Introduction to Marine Biogeochemistry, 2nd edition. Elsevier, Oxford.

Lu, Y., P. A. Meyers, T. H. Johengen, B. J. Eadie, and J. A. Robbins. 2010. δ15N values in Lake Erie sediments as indicators of nitrogen biogeochemical dynamics during cultural eutrophication. Chemical Geology 273:1-7.

Lund, J. R., E. Hanak, W. Fleenor, R. Howitt, J. Mount, and P. Moyle. 2007. Envisioning futures for the Sacramento-San Joaquin Delta. Public Policy Institute of California.

Meybeck, M. 2003. Global analysis of river systems: from Earth system controls to Anthropocene syndromes. Philosophical Transactions of the Royal Society B-Biological Sciences 358:1935–1955.

Meybeck, M., and C. Vörösmarty. 2005. Fluvial filtering of land-to-ocean fluxes: from natural Holocene variations to Anthropocene. Comptes Rendus Geoscience 337:107–123.

Milliman, J., and J. Syvitski. 1992. Geomorphic/Tectonic Control of Sediment Discharge to the Ocean: The Importance of Small Mountainous Rivers. The Journal of Geology 100:525–544.

Milliman, J., J. Broadus, and F. Gable. 1989. Environmental and Economic Implications of Rising Sea Level and Subsiding Deltas: The Nile and Bengal Examples. Ambio

18:340–345.

Oelbermann, M., and S. L. Schiff. 2010. The Redistribution of Soil Organic Carbon and Nitrogen and Greenhouse Gas Production Rates During Reservoir Drawdown and Reflooding. Soil Science 175:72–80.

Pierce, D. W., T. Das, D. R. Cayan, E. P. Maurer, N. L. Miller, Y. Bao, M. Kanamitsu, K. Yoshimura, M. A. Snyder, L. C. Sloan, G. Franco, and M. Tyree. 2012. Probabilistic estimates of future changes in California temperature and precipitation using statistical and dynamical downscaling. Climate Dynamics 40:839–856.

Rahmstorf, S. 2010. A new view on sea level rise : article : Nature Reports Climate Change. Nature reports climate change.

Sickman, J. O., M. J. Zanoli, and H. L. Mann. 2007. Effects of Urbanization on Organic Carbon Loads in the Sacramento River, California. Water Resources Research 43:W11422.

Snyder, N. P., D. M. Rubin, C. N. Alpers, J. R. Childs, J. A. Curtis, L. E. Flint, and S. A. Wright. 2004a. Estimating accumulation rates and physical properties of sediment behind a dam: Englebright Lake, Yuba River, northern California. Water Resources Research 40:W11301.

Snyder, N., C. Alpers, L. Flint, J. Curtis, M. Hampton, B. Haskell, and D. Nielson. 2004b. Report on the May-June 2002 Englebright Lake deep coring campaign. Page 32.

Snyder, N., J. Allen, C. Dare, M. Hampton, G. Schneider, R. Wooley, C. ALPERS, AND M. MARVIN-DIPASQUALE. 2004c. Sediment grain-size and loss-on-ignition analyses from 2002 Englebright Lake coring and sampling campaigns. Page 46.

Snyder, N., S. Wright, C. Alpers, L. Flint, C. Holmes, and D. Rubin. 2006. Reconstructing depositional processes and history from reservoir stratigraphy: Englebright Lake, Yuba River, northern California. Journal of Geophysical Research 111:F04003.

St Louis, V., C. Kelly, E. Duchemin, J. Rudd, and D. Rosenberg. 2000. Reservoir surfaces as sources of greenhouse gases to the atmosphere: A global estimate. BioScience 50:766–775.

Stewart, I. T., D. R. Cayan, and M. D. Dettinger. 2004. Changes in Snowmelt Runoff Timing in Western North America under a `Business as Usual' Climate Change Scenario. Climatic Change 62:217–232.

Syvitski, J. P. M., and J. D. Milliman. 2007. Geology, Geography, and Humans Battle for Dominance over the Delivery of Fluvial Sediment to the Coastal Ocean 115:1-19. dxdoiorgproxywmedu.

Vörösmarty, C., M. Meybeck, B. Fekete, K. Sharma, P. Green, and J. Syvitski. 2003. Anthropogenic sediment retention: major global impact from registered river impoundments. Global and Planetary Change 39:169–190.

Vreča, P., and G. Muri. 2010. Sediment organic matter in mountain lakes of north-western Slovenia and its stable isotopic signatures: records of natural and anthropogenic impacts. Hydrobiologia 648:35–49.

Walling, D. 2006. Human impact on land-ocean sediment transfer by the world's rivers. Geomorphology 79:192–216.

Waterson, E., and E. Canuel. 2008. Sources of sedimentary organic matter in the Mississippi River and adjacent Gulf of Mexico as revealed by lipid biomarker and [delta] 13CTOC analyses. Organic Geochemistry 39:422–439.

Weissenberger, S., M. Lucotte, S. Houel, and N. Soumis. 2010. Modeling the carbon dynamics of the La Grande hydroelectric complex in northern Quebec. Ecological Modelling 221:610-620.

Wright, S., and D. Schoellhamer. 2004. Trends in the Sediment Yield of the Sacramento River, California, 1957-2001. San Francisco Estuary and Watershed Science 2:Article 2.

CHAPTER 2: APPLICATION OF PLUTONIUM ISOTOPES TO THE SEDIMENT GEOCHRONOLOGY OF COARSE-GRAINED SEDIMENTS FROM ENGLEBRIGHT LAKE, CALIFORNIA (USA)

Pondell, C.R.

Canuel, E.A.

Beck, A J.

Kuehl, S.A

Abstract

This study uses an impoundment in northern California as a model system to examine the application of plutonium isotopes in lacustrine environments where the combination of coarse and fine sediments complicates the determination of sediment accumulation rates using traditional methods. Inductively coupled plasma mass spectrometry (ICP-MS) was used to quantify plutonium isotopes, and low limits of detection associated with this method allowed for the detection of plutonium in sand fractions as well as clay and silt fractions. Although measurable levels of plutonium were found in the sand fractions, over 75% of the total plutonium activity was measured in the fine grain-size fractions (< 63μm). Strong correlations between cesium activity and plutonium activity in fine-grain sediments ($r = 0.81\text{-}0.98$, $p < 0.005$) suggest that plutonium isotopes may be a useful substitute for cesium isotopes in coarse-grain sediments where cesium is typically below detection. Sediment accumulation rates calculated from grain-size normalized plutonium activity profiles ranged from 6 to 145 cm yr^{-1} in Englebright Lake, and reflected changes in sediment supply from the watershed in response to flood events and human impacts including hydraulic mining and dam construction. This study extends the application of plutonium isotopes for sediment geochronology of aquatic environments dominated by coarse sediments and provides new information that contributes to a better understanding of the processes influencing sediment deposition in Englebright Lake.

Introduction

The determination of sediment accumulation rates in lakes has become important in many areas of research, including anthropogenic pollution (Fernández et al. 2000, Li et al. 2012), paleoclimate (Karabanov et al. 2000, Moore et al. 2001, Quillmann et al. 2010), and biogeochemical cycling (Hollander and Smith 2001, Andrade et al. 2010). Since the 1970s, radioisotopes such as ^{210}Pb and ^{137}Cs have been employed to understand recent (< 100 years) sediment accumulation in lacustrine (Krishnaswamy et al. 1971) and marine systems (Koide et al. 1972). Recent advances in radioisotope detection methods, such as mass spectrometry for measuring long-lived isotopes and improvements in detection limits (Ketterer et al. 2002, Wendt and Trautmann 2005), have refined sediment-dating techniques by applying numerous anthropogenic (e.g., ^{90}Sr, ^{137}Cs, ^{239}Pu, ^{240}Pu) and natural radioisotopes (e.g., ^{210}Pb, ^{234}Th, ^{7}Be) to study various environmental systems over multiple time scales with high accuracy and resolution (Hall and McCave 2000, Leithold et al. 2005, Zhu and Olsen 2009, Kretschmer et al. 2010, Matisoff and Whiting 2011).

^{137}Cs isotope profiles have been used in many marine and freshwater systems over the past several decades to provide chronostratigraphic control. The usefulness of this anthropogenic radioisotope has been proven repeatedly and in various environments throughout the world (Ritchie and McHenry 1990, Hermanson 1990, Sanchez-Cabeza et al. 1999, McHenry et al. 2010). ^{137}Cs has a well known environmental fallout record due to its production during nuclear fission in nuclear weapons and nuclear reactors (Ritchie and McHenry 1990). Using nuclear fallout records and environmental samples, studies identified 1954 as the date of first detection of ^{137}Cs (Longmore 1982) and 1963 at the date of maximum ^{137}Cs deposition (Carter and Moghissi 1977) in sediments and soils. However, the usefulness of cesium from nuclear weapons fallout is decreasing with time due to its relatively short half-life (30.2 years). More than 50 years have passed since the peak in nuclear weapons testing and almost 75% of the initial ^{137}Cs has decayed away; analysis of ^{137}Cs activity and its usefulness as a radiochronometric tracer will thus become more limited with time.

Plutonium isotopes offer a possible alternative to cesium for sediment geochronology, especially in recent years as analytical measurements of these isotopes have advanced and become more precise (Ketterer et al. 2002, Kenna 2002). Plutonium isotopes have a similar global environmental input function to ^{137}Cs, resulting from fallout from nuclear weapons testing in the mid 20th century, and can be used in the same way to identify the 1954 (initial input) and 1963 (peak input) horizons in sediment cores. Plutonium isotopes, however, are much longer-lived than ^{137}Cs with half-lives on the order of 10^3 to 10^4 years, and thus will remain at detectable levels in sediments longer than ^{137}Cs. Recent advances with inductively coupled plasma mass spectrometry (ICP-MS) have reduced the limit of detection for plutonium isotopes (Ketterer et al. 2002), and allow for its application to systems dominated by coarse sediments with inherently low concentrations of particle-reactive elements (Watters et al. 1983). Additionally, plutonium isotopes show little remobilization in sediments, except under oxidizing conditions when the dominant Pu(IV) species is oxidized to the more mobile Pu(V) and Pu(VI) oxidation states (Kaplan et al. 2004, 2007). These properties suggest that plutonium isotopes can indeed be a useful replacement for ^{137}Cs as a tool for sediment geochronology.

Several recent studies have explored the application of plutonium isotopes as a dating tool in fine-grained sediments from marine (Smith et al. 1986, Kershaw et al. 1999, Gulin et al. 2002, Kuehl et al. 2012) and lacustrine sediments (Jaakkola et al. 1983, Ketterer et al. 2004, Zheng et al. 2008, Wu et al. 2010), and have shown that these isotopes provide accurate sediment chronologies in many systems where ^{137}Cs could not be applied. Previous studies have also focused on the novel application of $^{239}Pu/^{240}Pu$ to determine the source of plutonium in the environment, whether it is from global fallout or a more local plutonium source (Ketterer et al. 2004, Zheng et al. 2008). Few studies have used the sum of ^{239}Pu and ^{240}Pu isotopes to explore their application in systems dominated by coarse sediments (Kuehl et al., 2012), where traditional isotopes like ^{137}Cs and ^{210}Pb have high uncertainties associated with measuring low radioisotope concentrations in sandy sediments, such as estuarine and shelf environments, where the combination of fine

sediments from the marine system mix with coarse river sediment inputs. The current study extends the use of plutonium isotopes as a dating tool to a mountainous lake system in northern California, where anthropogenic disturbance, combined with a highly erodible watershed, results in high accumulation of sediments with a range of grain sizes. The results presented here support the application of $^{239+240}$Pu for dating sediments in systems dominated by a mixture of sediment inputs.

Study Site

Sediments for this study were collected from Englebright Lake in northern California (Figure 2-1), an impoundment created in 1940. Its watershed an area of the Sierra Nevada Mountains most heavily mined during the Gold Rush of the late 1800s (James 2005). Hydraulic mining within the Englebright Lake watershed resulted in extensive erosion and therefore, high sedimentation rates in the reservoir. The material that accumulates in Englebright Lake is a combination of fine and coarse sediments with organic carbon contents ranging from 0.03% to as high as 30.24% (C. Pondell, unpublished data).

The U.S. Geological Survey (USGS) collected six piston cores from Englebright Lake in 2002 (Figure 2-1) that captured the accumulation history of the lake since construction of Englebright Dam in 1940. The USGS collected ~60 samples (representing approximately 1 year of accumulation for each sample) from three of the downstream, fine-grained cores for ^{137}Cs radioisotopic analysis, and the cesium profiles showed a clear peak in two of the three cores (Snyder et al. 2006). The peak in ^{137}Cs corresponded to the 1963 maximum fallout horizon and allowed for the calculation of accumulation rates for these two sites. The association between these anthropogenic-derived isotopes and fine-grained sediments allowed for interpretation of these two cores, but the third core, containing a combination of coarse and fine- grain sediments and high organic matter (12-30%), exhibited a complicated cesium profile that was difficult to correlate to the 1963 event horizon (Snyder et al. 2006). Other information about sediment accumulation, such as seismic stratigraphy, is not available for Englebright Lake due to the high concentration

of biogenic gas in the sediments and the narrow shape of the reservoir that prevented sub-bottom profilers from penetrating the reservoir floor (Childs et al. 2003).

This study revisits the radioisotope work in Englebright Lake and applies plutonium isotopes to provide chronostratigraphic control in a system dominated by coarse sediments. The six cores collected by the USGS in 2002 were further sub-sampled in 2009 for organic carbon measurements (presented in a later paper) and plutonium isotope analyses. Sediment intervals of 10 to 20 cm were collected from each core, with a greater sample frequency in cores 1, 4 and 7 to capture a high-resolution record of sediment accumulation in Englebright Lake. Cores 8 and 9 had coarse grain sediments, so larger sediment volumes, and lower temporal resolution, were necessary for analyses; fewer samples were collected from core 6 due to a more disturbed sediment record resulting from coring practices at this site.

Methods

Grain Size Separation

Selected sediment samples from each core collected from Englebright Lake were analyzed to determine whether plutonium was preferentially associated with a particular grain size. Ten to fifty grams of sediment were separated into sand (>63 μm), silt (4 μm - 63 μm), and clay (< 4 μm) size fractions using the procedure described by Salemi et al. (2010). Briefly, samples were separated into sand and mud fractions using a 63 μm sieve. The mud was then washed into a graduated cylinder and brought up to 1000 mL volume with deionized water. To separate the mud fraction into silt (4 μm - 63 μm) and clay (< 4 μm) size fractions, graduated cylinders were thoroughly mixed, and then at a specific time (dependent on temperature and calculated using Stokes Law) the suspended material was siphoned into a large beaker (Salemi et al., 2010). This was repeated two more times to ensure complete separation between the clay particles remaining in suspension and the silt particles that settled on the bottom of the cylinder. The sand, silt, and clay fractions

were then dried at 60°C for approximately one week and weighed. The percent sand, silt, and clay (Table 2-1) were within 15% of the reported values from previous grain size analysis (Snyder et al., 2004a). Each fraction was then analyzed for plutonium as described below.

Sample Preparation

Fine-grained sediment samples were analyzed for concentrations of ^{239}Pu and ^{240}Pu isotopes following the method outlined in Ketterer et al. (2002). Five grams of sediment were first combusted at 600°C for 24 hours to remove organic material, and then approximately 35 mBq of ^{242}Pu standard (NIST 4334) were added to the combusted samples as a yield tracer. Samples were leached with 20 mL of concentrated nitric acid for 24 hours at 75°C. The leachate was then diluted to 50 mL with deionized water and filtered through 0.7 μm glass fiber filters. One gram of $NaNO_2$ and 0.1 g of iron were added to the diluted leachate to transform all plutonium species to the tetravalent state, which is necessary for extraction using tetravalent actinide (TEVA) resin (Horwitz et al. 1995). Samples were allowed to equilibrate with 0.1g of TEVA resin (EIChrom, Darien IL, TE-B25-A, 100-150 μm) for 90-120 minutes.

Coarse sediments were expected to yield much lower plutonium activities. As a result, any samples from cores 8 and 9 that had a mean grain size > 100 μm required larger samples. For these cores, 50 g of sediment were prepared for plutonium analysis using larger amounts of reagents to accommodate the increased sample size. These samples were combusted at 600°C for 24 hours and spiked with approximately 35 mBq of ^{242}Pu. They were then acid leached at 75°C using 50 mL of concentrated nitric acid for 24 hours. The leachate was diluted to 100 mL with deionized water and filtered through 0.7 μm glass fiber filters. Iron (0.1 g) and $NaNO_2$ (1 g) were added to the leachate and the samples equilibrated with 0.15 g of TEVA resin for 90-120 minutes.

The remaining TEVA resin chromatography was performed the same way for both the 5 g and 50 g samples. The TEVA resin was loaded with actinide ions (including uranium, thorium and plutonium) during equilibration and then was passed into a column with a 35-μm frit to retain the TEVA resin material. Five rinses of 2M nitric acid and two rinses of 8M hydrochloric acid were poured through the column to remove uranium and thorium isotopes from the TEVA resin. Plutonium isotopes were eluted and collected from the column using a rinse of deionized water (1 mL), followed by 0.05M ammonium oxalate (1 mL) and a final rinse with deionized water (1 mL).

Samples (3 mL) were then analyzed by direct injection using a ThermoFisher Element2 ICP-MS operated in low-resolution mode for ^{239}Pu, ^{240}Pu, and ^{242}Pu. Measured ^{238}U was used to correct for the $^{238}U^{1}H$ interference on ^{239}Pu. The $^{238}U^{1}H/^{238}U$ ratio was generally less than 10^{-4}, consistent with previous work (e.g., Ketterer et al. 2004), and corrections represented ~10% of the ^{239}Pu signal. The activity of the ^{239}Pu and ^{240}Pu isotopes was calculated using ratios of ^{239}Pu and ^{240}Pu to the added ^{242}Pu standard, and the mass and specific activity of ^{239}Pu, ^{240}Pu, and ^{242}Pu isotopes. The sum of the $^{239+240}$Pu isotopic activity is reported here.

Data Analysis

Statistical analyses were performed using R-studio version 0.97.332. Pearson correlation coefficients and student's t-test were run on plutonium and cesium activities and accumulation rates measured in this study and from Snyder et al. (2006). The sampling intervals were not the same for the cesium and plutonium analyses. Snyder et al. (2006) collected samples based on stratigraphic layering, which resulted in intervals that ranged from 5 to 100 cm, whereas sample intervals for plutonium analysis were constant (10 or 20 cm) for each core. Therefore, the correlation analysis compared plutonium and cesium activities from samples at similar depths in each core.

Uncertainty in the $^{239+240}$Pu grain-size normalized activity was determined using the error propagation equation (Lindberg 2000). The standard deviations used for this calculation

included the standard deviation for the grain size data (Snyder et al. 2004a) and the standard deviation from duplicate samples analyzed for plutonium activity.

Sediment accumulation rates were calculated for select time periods using information about the known input of plutonium to the environment. For instance, the date of first appearance for plutonium in environmental samples is 1954 and the date of maximum plutonium concentration is 1963. This information and the assumption that all six sediment cores collected from Englebright Lake represented sediment accumulation from construction of the dam in 1940 to collection of the cores in 2002 were used to calculate vertical sediment accumulation rates from the plutonium activity profiles. The bottom of each core was identified as the 1940 horizon based on contact during coring with an impenetrable layer of gravel assumed to be the pre-dam river bottom, as well as the calculation of sediment thickness from pre-dam bathymetric records (Childs et al. 2003). Accumulation rates were determined using the depth of first appearance of plutonium (identified as the deepest sample with activities above the detection limit) and the depth of maximum grain-size normalized plutonium activity, when available. Uncertainty associated with these rates was calculated by using the standard deviation associated with the range of accumulation rates calculated from horizons above and below the depths of first appearance and maximum activity.

Quality Control

In order to optimize the amount of information we could obtain from the limited amount of sediment available, samples were analyzed for plutonium concentration after the sediments had been extracted for lipid biomarkers using a 2:1 (v:v) mixture of dichloromethane: methanol. In a separate experiment (see Supplemental Information), it was determined that this extraction did not affect the plutonium activity in the sediment (two-sample t-test, $p > 0.1$). The detection limits ($3\sigma_{Blank}$) for 3 mL of plutonium solution were 0.01 Bq kg^{-1} for 5 g samples and 0.001 Bq kg^{-1} for 50 g samples. Additionally, a standard reference material (SRM) (NIST 4350b) was extracted with every ten sediment samples to evaluate the method accuracy. Measured values of

$^{239+240}$Pu from these SRM samples were 0.506 ± 0.004 Bq kg^{-1}, which compares favorably to the reported value of 0.508 Bq kg^{-1}.

Results

Grain Size Analysis

Plutonium activities were most strongly associated with fine grain sizes, particularly grain sizes smaller than 63 μm (Table 2-1). Less than 25% of the total plutonium activity was in the sand fraction, with only trace amounts (< 1%) of plutonium detected in the coarsest samples. Greater than 75% of the plutonium activity in all core samples was associated with the mud fraction (silt and clay, < 63 μm). Therefore, all plutonium activities reported here are normalized to the percent mud using grain size data from Snyder et al. (2004).

Vertical Core Profiles

Measurable $^{239+240}$Pu activities were detected in all cores collected from Englebright Lake, including those cores dominated by coarse sediments (Figure 2-2). Plutonium activities in the lake sediments ranged from 0.002 Bq kg^{-1} to 1.5 Bq kg^{-1}, and grain-size normalized plutonium activities were between 0.012 Bq kg_{mud}^{-1} and 7.9 Bq kg_{mud}^{-1}. Grain-size normalized plutonium activities were similar in the two cores collected from the deepest section of the lake (cores 1 and 6) and the two cores collected from the shallowest region of the lake (cores 8 and 9), with maximum grain-size normalized plutonium activities between 1 to 1.9 Bq kg_{mud}^{-1}. In contrast, maximum grain-size normalized plutonium activities measured in the two cores from the delta front region of Englebright Lake (cores 4 and 7) were 3 to 8 times higher than maximum activities observed in the rest of the lake (Figure 2-2).

Grain-size normalized plutonium activity profiles were similar in five of the six sediment cores from Englebright Lake, with low or non-detectable activities in the bottom of each

core increasing to a peak in activity, and then decreasing again at shallower depths in the core (Figure 2-2). The depths of maximum grain-size normalized plutonium activity were shallowest in cores from the deep-water region of the lake (cores 1 and 6), deepest near the delta front (cores 4 and 7), and at an intermediate depth in the cores collected from the shallow water region of Englebright Lake (Figure 2-2, Table 2-2). In core 8, the shallow water core closest to where the Yuba River enters the lake, the $^{239+240}$Pu profile did not show a peak in plutonium activities. Instead, the profile for this core continued to increase as the depths become shallower, suggesting that the depth of peak activity was not captured in our sample collections. As a result, accumulation rates calculated from the depth of maximum activity for core 8 could not be determined based on $^{239+240}$Pu profiles, but accumulation between 1940 and 1954 was determined using the depth of first appearance (Table 2-2).

Sediment Accumulation Rates

Depths of first appearance and maximum activity of plutonium were determined from these grain-size normalized plutonium activity profiles in order to calculate sediment accumulation rates in Englebright Lake over three periods of time: 1940-1954, 1954-1963, and 1963-2002 (Table 2-2). The accumulation rates ranged from 6 to 145 cm yr^{-1} throughout the lake, and the highest rates of accumulation were found in cores 7, 8 and 9, in the region of the lake closest to the river input (i.e., furthest from the dam). Sediment accumulation was highest during the early history of the lake, prior to 1963 (Figure 2-3).

Discussion

Plutonium isotopes have been investigated as an alternative to cesium isotopes for dating sediment horizons due to the similar input functions and longer radioactive half-lives (Carpenter and Beasley 1981, Kaplan et al. 2004, 2007). These data provide further support for the application of plutonium isotopes in a sediment system with mixed grain sizes, which was difficult to date using ^{137}Cs. Results from this study demonstrate the value of using $^{239+240}$Pu to date coarse grain sediments and as a replacement for ^{137}Cs since

decay makes the anthropogenic ^{137}Cs increasingly unreliable as a radiochronometric dating tool.

Affinity of plutonium isotopes for fine and coarse sediments

Englebright Lake is a system defined by a combination of fine and coarse sediments, and with mean grain sizes ranging from clay to gravel, the distribution of sediment grain size can change drastically over just a few centimeters depth range (Snyder et al. 2004a). Therefore, plutonium activities associated with sand, silt and clay fractions were analyzed for six samples representing a range in mean grain sizes and grain size class distribution encompassing sediment characteristics at the study site. Previous studies have documented increased adsorption of heavy metals (i.e., Fe, Mn, and Zn) and radionuclides including ^{230}Th, ^{210}Pb, and ^{137}Cs to the fine-grain fraction of freshwater and marine sediments due to increased surface area and clay mineral content (Cundy and Croudace 1995, Singh et al. 1999, Kretschmer et al. 2010). The observations from Englebright Lake sediments are consistent with these previous findings. These data show that most of the plutonium activity is associated with the mud fraction (< 63 μm) where the higher surface area can provide more sites for plutonium to bind.

The benefits of plutonium analysis in sediments from this system derive from the improved lower limit of detection associated with ICP-MS measurements that allows for the detection of plutonium activity in coarse sediments. Measurable plutonium activities were observed in the sand fraction, but at lower levels than in the fine-grained sediments likely due to their lower surface area. Results from cores dominated by coarse grain sizes (>98% sand in samples from cores 8 and 9) suggest that less than one percent of the total plutonium activity was present in the sand fraction (Table 2-1). The higher relative contributions of plutonium activity found in the sand fraction for the other cores (12 to 22% from cores 1, 6, 4 and 7) may reflect incomplete separation of fine grains while sieving or plutonium bound to organic materials larger then 63μm (Loyland Asbury et al. 2001) rather than indicating the plutonium bound specifically to coarse sediment grains.

For the analysis of plutonium isotopes in sandy sediments larger sample sizes are needed, and plutonium activities in all samples should be normalized to fine grain sizes (< 63 μm) to account for the preferential association of plutonium isotopes to fine sediments.

Correlation of Plutonium and Cesium Isotopes

Accumulation rates in the combination of fine and coarse sediments in Englebright Lake have proven to be difficult to study using the more traditional dating methods of ^{137}Cs and ^{210}Pb (Snyder et al. 2006), but the addition of plutonium isotopes offers more insight into the deposition and accumulation processes occurring in this system. Previous studies of Englebright Lake sediments focused on ^{137}Cs, which was useful for dating fine-grain cores 1 and 4 in the deep region of the lake (Snyder et al. 2006). These cores had ^{137}Cs profiles with well-defined 1954 and 1963 horizons, which indicated accumulation rates on the order of 8 to 55 cm yr^{-1}. However, when ^{137}Cs was applied to core 7 collected from the top of the delta front, the combination of sandy, silty, and organic rich laminations resulted in multiple peaks due to the affinity of ^{137}Cs for clay minerals and coarse organic matter (Cundy and Croudace 1995), which complicated the isotope profile and prevented a reliable dating profile using ^{137}Cs alone. We compared the cesium profiles from Snyder et al. (2006) with the $^{239+240}Pu$ profiles from this study (Figure 2-4) and found a strong positive correlation between the plutonium and cesium isotope activities (Pearson Coefficient = 0.81-0.98; $p < 0.005$). The strong correlation between cesium and plutonium activities verifies the application of plutonium in cores 1 and 4, and identifies the depth of the 1963 maximum fallout horizon with overlapping cesium and plutonium peaks in core 7 (Figure 2-4). These findings are similar to other studies of plutonium in lake systems (Jaakkola et al. 1983, Ketterer et al. 2004, Zheng et al. 2008, Wu et al. 2010), showing that plutonium and cesium have similar behavior in freshwater environments. Additionally, the strong correlation between ^{137}Cs and $^{239+240}Pu$ suggests that if there is remobilization of these isotopes in the lake system, both isotopes are affected similarly. However, based on previous studies, mobilization of plutonium isotopes is not expected (Carpenter and Beasley 1981) unless there are major changes in pH or oxidation state in the system (Kaplan et al. 2004, 2007), and the correlation of

plutonium with cesium, which is strongly sorbed to illite clay and effectively non-mobile in freshwater systems (Cundy and Croudace 1995), does not support this type of remobilization in Englebright Lake sediments.

The correlation between plutonium and cesium isotope activities in the three sediment cores from Englebright Lake provides confidence for determining accumulation rates from the plutonium profiles for two additional cores from the lake. Core 6, dominated by fine sediments, and core 9, consisting of mostly coarse sediments, were not analyzed previously for cesium, but the plutonium activity profiles in these cores are similar to the plutonium profiles for cores 1, 4 and 7. As a result, plutonium activity profiles can be extended to cores 6 and 9 to provide sediment accumulation rate data that augment previous estimates based on stratigraphic position and grain size distribution (Snyder et al. 2006).

One core in the lake (core 8) showed a different plutonium trend than the other five cores, in that there was no observed sub-surface peak in grain-size normalized plutonium activities. Plutonium activities in core 8 show only an increasing trend as depth in the core shallows (e.g., from 12 to 6 m). This could result from high sediment accumulation rates in the early history of the lake accumulation and a sampling strategy that was inappropriate for the accumulation patterns at this location in Englebright Lake. Core 8 is the site closest to the convergence of the three tributaries at the upstream end of the lake, which is a relatively high-energy location in Englebright Lake. Snyder et al. (2006) divided the depositional regime in this core into foreset deposition and topset deposition based on studies of deltaic deposition by Gilbert (1890). According to Snyder et al. (2006), this site experienced foreset deposition, which was defined by high rates of accumulation of coarse sediment (Gilbert 1890) until the mid 1950's, followed by topset deposition, or lower rates of accumulation of coarse materials. High sediment accumulation rates during the initial phase (before mid-1950's) would lead to a shallower horizon of maximum plutonium activity at this site relative to the other locations, especially if the accumulation rates associated with the topset deposition were

particularly low. This could explain why the horizon of maximum plutonium activity was not observed below 5m in core 8, and implies that peak plutonium activity likely occurred in shallower horizons that were not captured by our sampling. Unfortunately, due to logistical and financial reasons, we were unable to resample core 8 and perform additional plutonium analyses.

Throughout the depositional history of this basin, most plutonium activity measurements ranged from 0.03 to 1.2 Bq kg_{mud}^{-1}, but peak grain-size normalized activities in the two delta front cores (cores 4 and 7) were 6 to 7 times greater than peak grain-size normalized plutonium activity in the four remaining cores. One explanation for these relatively high plutonium activities may be that the peak plutonium accumulation was captured in cores 4 and 7 where the sampling interval was greatest, and in cores 1, 6, 8 and 9, the sampling strategy did not allow us to capture the sediment horizon with highest plutonium activity. This uncertainty is reflected in the standard deviation associated with the depth of maximum activity (Table 2-2) and in the highlighted area describing the peak plutonium activity shown in Figure 2-2. Furthermore, the strong correlation between plutonium activity and organic matter in sediments (correlation between $^{239+240}Pu$ and organic carbon content from all samples: Pearson Coefficient = 0.67, $p < 0.001$) may also explain why peak plutonium activities in cores 4 and 7 were greater than peak plutonium activities observed throughout the rest of the study site (Livens and Singleton 1991, Agapkina et al. 1995, Loyland Asbury et al. 2001). In cores 4 and 7 from Englebright Lake a layer of material characterized by relatively fine sediment and high organic carbon content (12 to 32% organic carbon) was deposited during a large flood in 1964 (Table 2-3). Accumulation from this event was focused at the delta front (cores 4 and 7), and the combination of high organic content and relatively fine sediments may explain why plutonium activities from these horizons differ from activities measured in other sediments from Englebright Lake.

Sediment Accumulation in Englebright Lake

Sediment accumulation rates calculated from the plutonium activities compare well to accumulation rates calculated by Snyder et al. (2006), especially when differences between the methods of accumulation rate estimation are considered (Figure 2-3). Snyder et al. (2006) calculated vertical sediment accumulation rates using grain size data, hydrological reports, straigraphic position, and ^{137}Cs profiles, when appropriate. Sediment accumulation rates determined using plutonium isotopes were calculated using the depth of first detection of the isotopes, the depth of maximum activity, and using the assumption that the sediment record collected covers the time period from 1940-2002, meaning that the bottom of each core was deposited in 1940 (as evidenced by the pre-dam gravel beds identified at the bottom of each core; Childs et al. 2003) and the top of each core is the 2002 horizon. Sediment accumulation rates from the three cores within six kilometers of Englebright Dam (cores 1 and 4) are similar when calculated using plutonium and cesium or other geologic proxy data. Accumulation rates calculated from plutonium profiles in core 6 offer higher resolution, and three rates of accumulation could be determined, while accumulation rates from Snyder et al (2006) were only able to provide an average accumulation rate for this core.

When compared to accumulation rates calculated from plutonium activity profiles in cores 7, 8 and 9 from the shallow region of the lake, the accumulation rates estimated from stratigraphic position, grain size distributions, and hydrological history underestimate the rate at which material accumulates during the early history of Englebright Lake (1940-1954) and overestimate accumulation during the period of frequent flood events (1954-1963) (Figure 2-3). However, this apparent discrepancy may be due to different time intervals over which these accumulation rates were estimated. While this study attempted to compare accumulation rates over similar time periods, this could not always be done due to analytical differences between methods. In cores 7 and 9, for example, accumulation calculated from $^{239+240}Pu$ between 1940-1954 and 1954-1963 are compared to accumulation rates from Snyder et al. (2006) calculated between 1940-1960 and 1960-1964. Regardless, trends in sediment accumulation rates calculated using plutonium track trends observed in accumulation rates calculated with cesium and

geologic proxies (Snyder et al., 2006), and in general, these accumulation rates were not significantly different.

The additional sediment core chronologies determined from plutonium activity profiles provide insights about the complex processes, including floods and mining activities in the watershed, that influence accumulation in Englebright Lake over time (Table 2-3). The sedimentation pattern in Englebright Lake has been described as a typical example of a Gilbert-type delta with different regions of the lake dominated by bottomset, foreset, and topset deposition (Snyder et al. 2006). The accumulation rates calculated from plutonium activity profiles allow us to examine the evolution of these depositional regimes throughout the history of Englebright Lake and develop a conceptual model to explain the accumulation patterns in the lake (Figure 2-5). Cores 1, 6 and 4 from the deep-water region of the lake are dominated, for example, by bottomset deposition throughout the entire history of Englebright Lake. Bottomset deposition occurs as the suspended sediment load settles from the water column (Gilbert 1890), and in the deep water region of Englebright Lake the suspended load settles and accumulates as fine clay and silt, with a few fine sand horizons (Snyder et al. 2004a). The relatively low accumulation rates for these two cores reflect this bottomset depositional environment, especially in core 1 where sediment accumulation rates only range between 6 cm yr^{-1} and 12 cm yr^{-1}. Core 6 also has low accumulation rates when compared to the other cores throughout the lake, but there is an increase in accumulation rates between 1940-1954 and 1954-1963 that mirrors accumulation trends in core 4 (Figure 2-3, Table 2-2). In cores 4 and 6, sediment accumulation between 1954-1963 was greater than accumulation before and after this period ($p \leq 0.001$), and accumulation rates of1940-1954 and 1963-2002 are the same. Between 1954 and 1963, four of the largest flood in this system in this system occurred (Table 2-3), and trends in accumulation rates from cores 4 and 6 suggest that these cores are influenced by turbidity currents or hyperpycnal flows associated with these flood events. However, this increase in accumulation in cores 4 and 6 is not observed in core 1, suggesting that sediment deposition in the region of the lake nearest the Englebright Dam is dominated by water column settling, and not by high density

sediment flows. This implies that the suspended sediment load may not respond to flood events in the watershed. Additionally, accumulation rates in core 1 doubled after 1963 relative to rates before 1963 (Figure 2-3, Table 2-2). This may signify that more of the material that is being delivered to Englebright Lake is being transported in the suspended load rather than the bed load, and is dominated by fine grain material (Curtis et al. 2006). Changes in sediment accumulation during the later part of Englebright Lake's history were examined further as part of the discussion on the impact of the New Bullards Bar dam on sediment accumulation in the lake after 1970 (see below).

The delta front cores (4 and 7) reflect periods of bottomset and foreset deposition since completion of Englebright Dam in 1940 (Snyder et al. 2006). Bottomset deposition dominated cores 4 and 7 in the early history of the lake between 1940 and 1954 (Figure 2-5). During this time accumulation rates were relatively low for these two cores, reflecting the deposition of suspended material in this region when the delta front was further upstream. Between 1954 and 1963, accumulation rates at the delta front increased 2- to 3-fold. This increase in accumulation reflects inputs from four flood events in the system (e.g., 1955, 1960, 1962, and 1963) during this time period when the mean daily discharge from Englebright Lake was greater than 1500 $m^3 s^{-1}$ (U.S. Geological Survey gauging station 11418000). During the floods, the increased inputs of material to Englebright Lake resulted in the progradation of the delta front from the shallow reaches of the lake upstream of core 8 to the current location of the delta front at core 7 (Snyder et al. 2006). The calculated sediment accumulation rate of 154 cm yr^{-1} at core 7 between 1954 and 1963 is the highest accumulation in Englebright Lake, and likely reflects the transition from bottomset to foreset accumulation. Foreset accumulation in core 7 is defined by high accumulation of sandy material on a sloping surface, which is first seen at this core's location during the 1964 flood. During this flood event, the delta front moved to its current location at core 7, and the deposition at core 4 becomes defined as distal foreset/bottomset (Snyder et al. 2006). This region is dominated by sediment remobilization at the delta front via turbidity currents during flood and lake level draw-down events (Blais and Kalff 1995), observed in the sediment record as sandy

laminations punctuating the normal bottomset accumulation of fine silt and clay (Snyder et al., 2006).

Accumulation rates calculated between 1963 and 2002 reflect a period in the lake's history of lower sediment accumulation driven by a combination of (1) decreases in the frequency of floods in the watershed, (2) construction of the New Bullards Bar (NBB) dam across the North Yuba River in 1970, (3) changes in the hydrology of Englebright Lake associated with the construction of the NBB (i.e., fewer draw-down events), and (4) decreasing inputs from mine tailings as these sediments are washed from the Yuba River tributaries and into Englebright Lake (Snyder et al., 2006). Between 1963 and 2002 there was only one large flood event in 1997 and one smaller flood in 1986 (Snyder et al. 2006). The New Bullards Bar dam, even though it inundated an area already dammed by a smaller dam, likely altered sediment supply from the North Yuba River by decreasing the amount of sediment and by trapping coarse sediments while still allowing some of the finer material to pass (Vörösmarty et al. 2003). This could change the characteristics of the sediment accumulating in Englebright Lake by increasing the amount of fine grain material transported as the suspended load, as seen in the increase in accumulation at core 1 after 1970. Additionally, after the construction of the NBB, annual lake level draw-downs in Englebright Lake ceased, modifying sediment deposition throughout the lake. Before 1970, topset deposits were exposed during lake draw-downs, and fine sediments were winnowed away and redeposited in the bottomset deposits or bypassed the dam as part of the suspended sediment load. With the discontinuation of these draw-downs, sediment accumulation patterns throughout the lake would change, and may be part of the reason that accumulation rates are lower in more recent sediments (1963-2002) than in the older sediment deposits (1940-1954) in most sediment cores (Figure 2-3).

Sediments in the shallow water region of the lake are dominated by coarse sand and gravel accumulation due to their close proximity to river input. During the earliest history of the lake (1940-1954) the location of the delta front was in this shallow region of the lake, which is reflected in the high accumulation of silty sands in cores 8 and 9.

Between 1954 and 1963 there is a distinct layer of coarse (> 70 μm), organic matter poor (< 0.1 %), pale grey sediments, which differs from the light brown color that dominates the remaining sediments in the lake (Snyder et al. 2004b). This layer could represent mine tailings that were washed from the watershed during the floods of 1955 and 1964 and transported to Englebright Lake. Due to the heavy mining activity in the Yuba River watershed during the late 19th century Gold Rush, there would be large volumes of mobile mine tailings in the watershed (Gilbert 1917, James 2005). The larger grain sizes associated with these tailings would limit their transport to flood events when the energy in the river was great enough to transport this material downstream as part of the bed load. Coarse material from mining activity in the Englebright Lake watershed would likely accumulate in the upstream reaches of Englebright Lake where the energy of the river decreases as it enters the lake. Inorganic geochemical data provides further evidence that material in cores 8 and 9 may result from hardrock gold mining. Tailings from hardrock gold mining in the Sierra Nevada Mountain Range contain elevated concentrations of naturally occurring arsenic, antimony, and lead, in addition to the mercury added to facilitate gold extraction (Ashley 2002, Alpers et al. 2006). Profiles of arsenic, antimony and lead for cores 8 and 9 show a horizon between 5 and 15 m with higher concentrations of these metals (Alpers et al., 2006), which corresponds to sediments deposited between 1954 and 1963. Sediment accumulation rates after 1963 decrease drastically, reflecting a change in depositional regime from foreset accumulation to topset accumulation (Snyder et al. 2006). Lower accumulation rates after 1963 and sediment properties may also indicate the absence of mine tailings (Wright and Schoellhamer 2004), showing that the mine tailings were washed from the Yuba River watershed and into Englebright Lake prior to and during the major flood in 1964.

Conclusions

In the Englebright Lake system, a combination of coarse and fine sediments and high concentrations of biogenic gas make it difficult to constrain accumulation rates using traditional approaches. Plutonium isotopes provide an alternative method for examining

accumulation patterns in this impoundment following the construction of the dam that created the lake. Strong correlations between $^{239+240}Pu$ and ^{137}Cs isotopes in some cores indicate that the behavior of these isotopes is similar in freshwater environments. Additionally, $^{239+240}Pu$ was detected in clay, silt, and sand fractions, but did show a stronger affinity for fine grain sizes (< 63 μm). This work indicates that $^{239+240}Pu$ can be applied as a sediment geochronometer in freshwater systems dominated by coarse and fine-grained sediment accumulation. Accumulation rates calculated from grain-size normalized plutonium activity profiles were used to explore different depositional settings in the lake over three time periods and compare them to flood and land-use impacts in the lake's watershed.

References

Agapkina, G. I., F. A. Tikhomirov, A. I. Shcheglov, W. Kracke, and K. Bunzl. 1995. Association of Chernobyl-derived 239 + 240Pu, 241Am, 90Sr and 137Cs with organic matter in the soil solution. Journal of Environmental Radioactivity 29:257–269.

Alpers, C. N., M. P. Hunerlach, M. C. Marvin-DiPasquale, R. C. Antweiler, B. K. Lasorsa, J. F. DeWild, and N. P. Snyder. 2006. Geochemical Data for Mercury, Methylmercury, and Other Constituents in Sediments from Englebright Lake, California, 2002. Page 95. U.S. Geological Survey Data Series 151.

Andrade, C. F., H. E. Jamieson, T. K. Kyser, T. Praharaj, and D. Fortin. 2010. Biogeochemical redox cycling of arsenic in mine-impacted lake sediments and co-existing pore waters near Giant Mine, Yellowknife Bay, Canada. Applied Geochemistry 25:199–211.

Ashley, R. P. 2002. Geoenvironmental model for low-sulfide gold-quartz vein deposits. Progress on geoenvironmental models for selected mineral deposits types 2:176.

Blais, J. M., and J. Kalff. 1995. The influence of lake morphometry on sediment focusing. Limnology and Oceanography 40:582–588.

Carpenter, R., and T. M. Beasley. 1981. Plutonium and americium in anoxic marine sediments: Evidence against remobitization. Geochimica et Cosmochimica Acta 45:1917–1930.

Carter, M. W., and A. A. Moghissi. 1977. Three decades on nuclear testing. Health Physics 33:55–71.

Childs, J., N. Snyder, and M. Hampton. 2003. Bathymetric and geophysical surveys of Englebright Lake, Yuba-Nevada Counties, California. Page 20. U.S. Geological Survey Open-File Report 03-383.

Cundy, A. B., and I. W. Croudace. 1995. Physical and chemical associations of radionuclides and trace metals in estuarine sediments: an example from Poole Harbour, Southern England. Journal of Environmental Radioactivity 29:191–211.

Curtis, J., L. Flint, C. Alpers, S. Wright, and N. Snyder. 2006. Sediment Transport in the Upper Yuba River Watershed, California, 2001-2003. U.S. Geological Survey Scientific Report 2005-5246:74.

Fernández, P., R. M. Vilanova, C. Martínez, P. Appleby, and J. O. Grimalt. 2000. The Historical Record of Atmospheric Pyrolytic Pollution over Europe Registered in the

Sedimentary PAH from Remote Mountain Lakes. Environmental Science & Technology 34:1906–1913.

Gilbert, G. K. 1890. Lake Bonneville. US Geological Survey.

Gilbert, G. K. 1917. hydraulic-mining debris in the Sierra Nevada. US Geological Survey Professional Paper:105-154.

Gulin, S. B., G. G. Polikarpov, V. N. Egorov, J. M. Martin, and E. al. 2002. Radioactive contamination of the north-western Black Sea sediments. Estuarine, Coastal and Shelf Science 54:541–549.

Hall, I. R., and I. N. McCave. 2000. Palaeocurrent reconstruction, sediment and thorium focussing on the Iberian margin over the last 140 ka. Earth and Planetary Science Letters 178:151–164.

Hermanson, M. H. 1990. 210Pb and 137Cs chronology of sediments from small, shallow Arctic lakes. Geochimica et Cosmochimica Acta 54:1443–1451.

Higgo, J. J. W., and L. V. C. Rees. 1986. Adsorption of actinides by marine sediments: effect of the sediment/seawater ratio on the measured distribution ratio. Environ. Sci. Technol 20:483–490.

Hollander, D. J., and M. A. Smith. 2001. Microbially mediated carbon cycling as a control on the δ13C of sedimentary carbon in eutrophic Lake Mendota (USA): new models for interpreting isotopic excursions in the sedimentary record. Geochimica et Cosmochimica Acta 65:4321–4337.

Horwitz, E. P., M. L. Dietz, R. Chiarizia, H. Diamond, S. L. Maxwell III, and M. R. Nelson. 1995. Separation and preconcentration of actinides by extraction chromatography using a supported liquid anion exchanger: application to the characterization of high-level nuclear waste solutions. Analytica Chimica Acta 310:63–78.

Jaakkola, T., K. Tolonen, P. Huttunen, and S. Leskinen. 1983. The use of fallout 137Cs and 239,240Pu for dating of lake sediments. Hydrobiologia 103:15–19.

James, L. A. 2005. Sediment from hydraulic mining detained by Englebright and small dams in the Yuba basin. Geomorphology 71:202–226.

Kaplan, D. I., B. A. Powell, D. I. Demirkanli, R. A. Fjeld, F. J. Molz, S. M. Serkiz, and J. T. Coates. 2004. Influence of Oxidation States on Plutonium Mobility during Long-Term Transport through an Unsaturated Subsurface Environment. Environ. Sci. Technol 38:5053–5058.

Kaplan, D. I., B. A. Powell, M. C. Duff, D. I. Demirkanli, M. Denham, R. A. Fjeld, and F. J. Molz. 2007. Influence of Sources on Plutonium Mobility and Oxidation State Transformations in Vadose Zone Sediments. Environ. Sci. Technol 41:7417–7423.

Karabanov, E. B., A. A. Prokopenko, D. F. Williams, and G. K. Khursevich. 2000. A new record of Holocene climate change from the bottom sediments of Lake Baikal. Palaeogeography, Palaeoclimatology, Palaeoecology 156:211–224.

Kenna, T. C. 2002. Determination of plutonium isotopes and neptunium-237 in environmental samples by inductively coupled plasma mass spectrometry with total sample dissolution. Journal of Analytical Atomic Spectrometry 17:1471–1479.

Kershaw, P. J., D. C. Denoon, and D. S. Woodhead. 1999. Observations on the redistribution of plutonium and americium in the Irish Sea sediments, 1978 to 1996: concentrations and inventories. Journal of Environmental Radioactivty 44:191–221.

Ketterer, M. E., B. R. Watson, G. Matisoff, and E. al. 2002. Rapid dating of recent aquatic sediments using Pu activities and 240Pu/239Pu as determined by quadrupole inductively coupled plasma mass spectrometry. Environmental Science & Technology 36:1307–1311.

Ketterer, M. E., K. M. Hafer, V. J. Jones, and E. al. 2004. Rapid dating of recent sediments in Loch Ness: inductively coupled plasma mass spectrometric measurements of global fallout plutonium. Science of The Total Environment 322:221–229.

Koide, M., A. Soutar, and E. D. Goldberg. 1972. Marine geochronology with210Pb. Earth and Planetary Science Letters 14:442–446.

Kretschmer, S., W. Geibert, M. M. Rutgers van der Loeff, and G. Mollenhauer. 2010. Grain size effects on 230Thxs inventories in opal-rich and carbonate-rich marine sediments. Earth and Planetary Science Letters 294:131–142.

Krishnaswamy, S., D. Lal, J. M. Martin, and M. Meybeck. 1971. Geochronology of lake sediments. Earth and Planetary Science Letters 11:407–414.

Kuehl, S. A., M. E. Ketterer, and J. L. Miselis. 2012. Extension of 239+ 240 Pu sediment geochronology to coarse-grained marine sediments. Continental Shelf Research 36:83–88.

Leithold, E., D. Perkey, N. Blair, and T. Creamer. 2005. Sedimentation and carbon burial on the northern California continental shelf: the signatures of land-use change. Continental Shelf Research 25:349–371.

Li, H. B., S. Yu, G. L. Li, and H. Deng. 2012. Lead contamination and source in Shanghai in the past century using dated sediment cores from urban park lakes. Chemosphere 88:1161–1169.

Lingberg, V. 2002. Uncertainties and error propagation-Part I of a manual on uncertainty, graphing, and the Vernier Caliper. Rochester Institute of Technology.

Livens, F. R., and D. L. Singleton. 1991. Plutonium and americium in soil organic matter. Journal of Environmental Radioactivity 13:323–339.

Longmore, M. E. 1982. The caesium-137 dating technique and associated applications in Australia-a review. Archaeometry: An Australasion Perspective:310–321.

Loyland Asbury, S. M., S. P. Lamont, and S. B. Clark. 2001. Plutonium Partitioning to Colloidal and Particulate Matter in an Acidic, Sandy Sediment: Implications for Remediation Alternatives and Plutonium Migration. Environ. Sci. Technol 35:2295–2300.

Matisoff, G., and P. J. Whiting. 2011. Measuring Soil Erosion Rates Using Natural (7Be, 210Pb) and Anthropogenic (137Cs, 239,240Pu) Radionuclides. Pages 487–519 *in* Handbook of Environmental Isotope Geochemistry. Springer Berlin Heidelberg, Berlin, Heidelberg.

McHenry, J. R., J. C. Ritchie, and A. C. Gill. 2010. Accumulation of fallout cesium 137 in soils and sediments in selected watersheds. Water Resources Research 9:676–686.

Moore, J. J., K. A. Hughen, G. H. Miller, and J. T. Overpeck. 2001. Little Ice Age recorded in summer temperature reconstruction from vared sediments of Donard Lake, Baffin Island, Canada. Journal of Paleolimnology 25:503–517.

Quillmann, U., A. Jennings, and J. Andrews. 2010. Reconstructing Holocene palaeoclimate and palaeoceanography in Ìsafjarðardjúp, northwest Iceland, from two fjord records overprinted by relative sea-level and local hydrographic changes. Journal of Quaternary Science 25:1144–1159.

Ritchie, J. C., and J. R. McHenry. 1990. Application of radioactive fallout cesium-137 for measuring soil erosion and sediment accumulation rates and patterns: a review. Journal of environmental quality 19:215-233.

Salemi, E., U. Tessari, and N. C. M. Mastrocicco. 2010. Improved gravitational grain size separation method. Applied Clay Science 48:612–614.

Sanchez-Cabeza, J. A., P. Masqué, I. Ani-Ragolta, and E. al. 1999. Sediment

accumulation rates in the southern Barcelona continental margin (NW Mediterranean Sea) derived from 210 Pb and 137 Cs chronology. Progress in Oeanography 44:313-332.

Singh, A. K., S. I. Hasnain, and D. K. Banerjee. 1999. Grain size and geochemical partitioning of heavy metals in sediments of the Damodar River - a tributary of the lower Ganga, India. Environmental Geology 39:90–98.

Smith, D. G., and H. M. Jol. 1997. Radar structure of a Gilbert-type delta, Peyto Lake, Banff National Park, Canada. Sedimentary Geology 113:195–209.

Smith, J. N., B. P. Boudreau, and V. Noshkin. 1986. Plutonium and 210 Pb distributions in northeast Atlantic sediments: subsurface anomalies caused by non-local mixing. Earth and Planetary Science Letters 81:15-28..

Snyder, N. P., D. M. Rubin, C. N. Alpers, J. R. Childs, J. A. Curtis, L. E. Flint, and S. A. Wright. 2004a. Estimating accumulation rates and physical properties of sediment behind a dam: Englebright Lake, Yuba River, northern California. Water Resources Research 40:W11301.

Snyder, N., C. Alpers, L. Flint, J. Curtis, M. Hampton, B. Haskell, and D. Nielson. 2004b. Report on the May-June 2002 Englebright Lake deep coring campaign. Page 32.

Snyder, N., J. Allen, C. Dare, M. Hampton, G. Schneider, R. Wooley, C. Alpers, and M. Marvin-DiPasquale. 2004c. Sediment grain-size and loss-on-ignition analyses from 2002 Englebright Lake coring and sampling campaigns. Page 46.

Snyder, N., S. Wright, C. Alpers, L. Flint, C. Holmes, and D. Rubin. 2006. Reconstructing depositional processes and history from reservoir stratigraphy: Englebright Lake, Yuba River, northern California. Journal of Geophysical Research 111:F04003.

Vörösmarty, C., M. Meybeck, B. Fekete, K. Sharma, P. Green, and J. Syvitski. 2003. Anthropogenic sediment retention: major global impact from registered river impoundments. Global and Planetary Change 39:169–190.

Watters, R. L., T. E. Hakonson, and L. J. Lane. 1983. The Behavior of Actinides in the Environments. Radiochimica Acta 32:89-103.

Wendt, K., and N. Trautmann. 2005. Recent developments in isotope ratio measurements by resonance ionization mass spectrometry. International Journal of Mass Spectrometry 242:161-168.

Wright, S., and D. Schoellhamer. 2004. Trends in the Sediment Yield of the Sacramento River, California, 1957-2001. San Francisco Estuary and Watershed Science 2:Article 2.

Wu, F., J. Zheng, H. Liao, and M. Yamada. 2010. Vertical distributions of plutonium and 137Cs in lacustrine sediments in northwestern China: quantifying sediment accumulation rates and source identifications. Environmental Science and Technology 44:2911-2917.

Zheng, J., F. Wu, M. Yamada, H. Liao, C. Liu, and G. Wan. 2008. Global fallout Pu recorded in lacustrine sediments in Lake Hongfeng, SW China. Environmental Pollution 152:314-321.

Zhu, J., and C. R. Olsen. 2009. Beryllium-7 atmospheric deposition and sediment inventories in the Neponset River estuary, Massachusetts, USA. Journal of Environmental Radioactivity 100:192–197.

Figure 2-1. Map of cores collected from Englebright Lake.
Englebright Lake is located in northern California, and a map of its watershed is shown in the insert. The six sediment cores examined in this study are identified with labeled points in the lake.

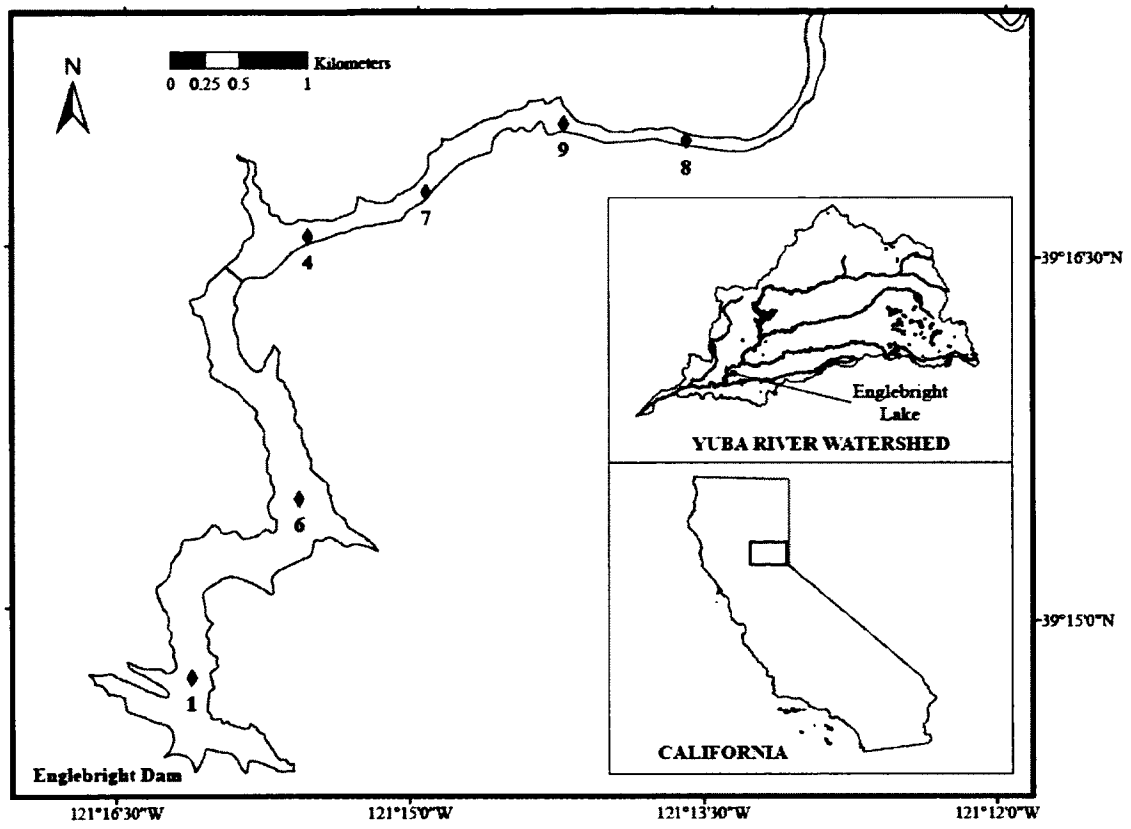

Figure 2-2. Depth profiles of plutonium activity.
Depth profiles (shown in meters below sediment surface) of plutonium activity (open symbols) and grain size normalized plutonium activity (filled symbols) show peaks in plutonium activity for five of the six sediment cores (all except Core 8) collected from Englebright Lake. Profiles are arranged by location in the lake, with the cores closest to the dam on the left and the cores closest to the mouth of the tributaries flowing into Englebright Lake on the right. The two cores from each region are plotted on the same axis: the left panels (cores 1 and 6) show plutonium activities for cores collected from the deepest part of the lake, the middle panels (cores 4 and 7) represent cores collected from near the delta front, and the right panels (cores 9 and 8) show plutonium activities for cores collected from the shallowest region in the lake. Error bars represent the combined standard deviation incorporating uncertainty associated with both the grain size and plutonium activity measurements. Grey shaded areas indicate the 1963 horizon.

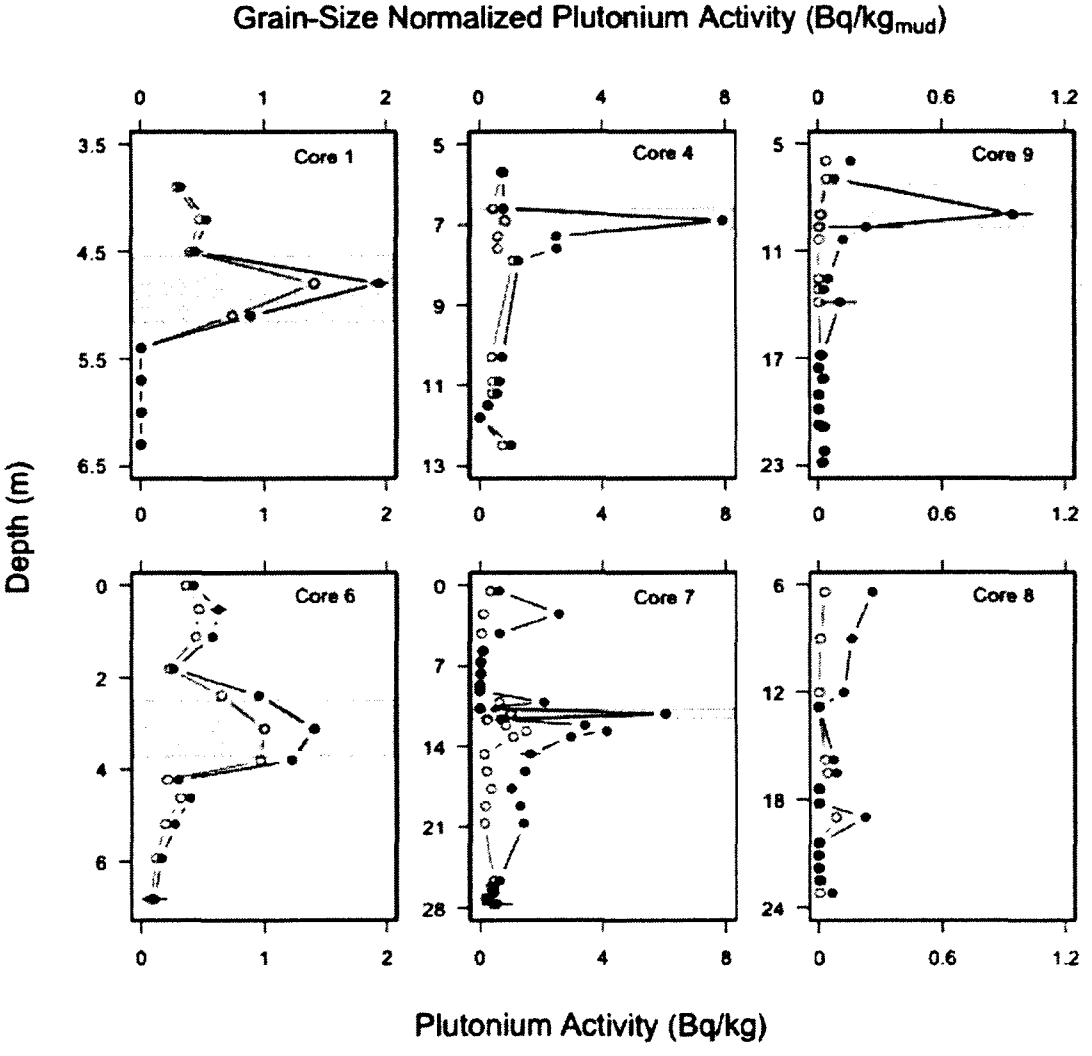

Figure 2-3. Spatial variability of accumulation rates in Englebright Lake. Sediment accumulation rates calculated from grain size normalized plutonium activities were highly variable on temporal and spatial scales in Englebright Lake. Average accumulation rates from 1940-1954, 1954-1963, and 1963-2002 for each core are shown with grey bars. Accumulation rates for 1954-1963 and 1963-2002 from core 8 (last core on the right) were not available because our sampling did not capture the peak in plutonium activity. The error bars represent one standard deviation from the average accumulation rate calculated from the three sediment horizons at, below, and above the depth of first detection and maximum grain size normalized plutonium activity. Accumulation rates from 1954-1963 are significantly higher than accumulation before and after this time period for all cores, expect core 1 and between 1940-1954 and 1954-1963 in core 9 (ANOVA and post-hoc tests, $p = 0.04$ for 1940-1954 and 1954-1963 accumulation rates in core 6 and $p \leq 0.001$ for all other comparisons) The open diamond symbols show the accumulation rates for similar time periods determined from other geological proxies by Snyder et al. (2006).

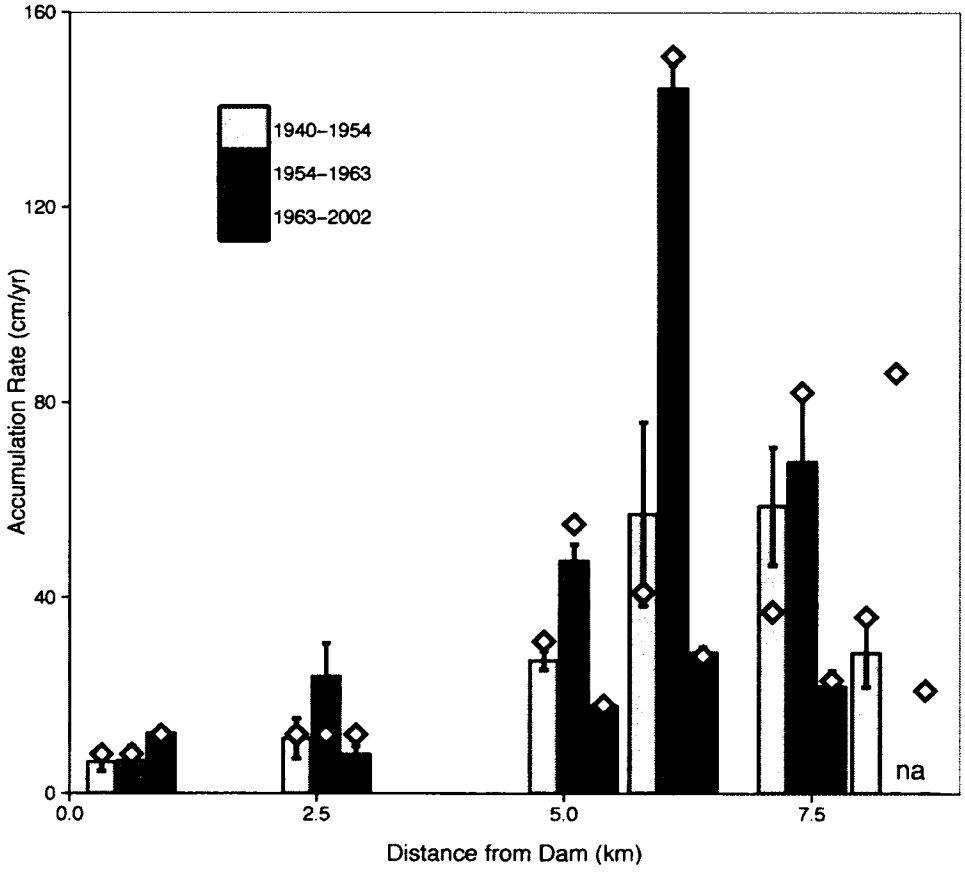

Figure 2-4. Comparison of cesium and plutonium activity profiles.
Depth profiles (in meters below sediment surface) of grain size normalized plutonium (solid line) and cesium (dashed line) activities show how well the radioisotopes compare to each other. Cesium data are from Snyder et al. (2006).

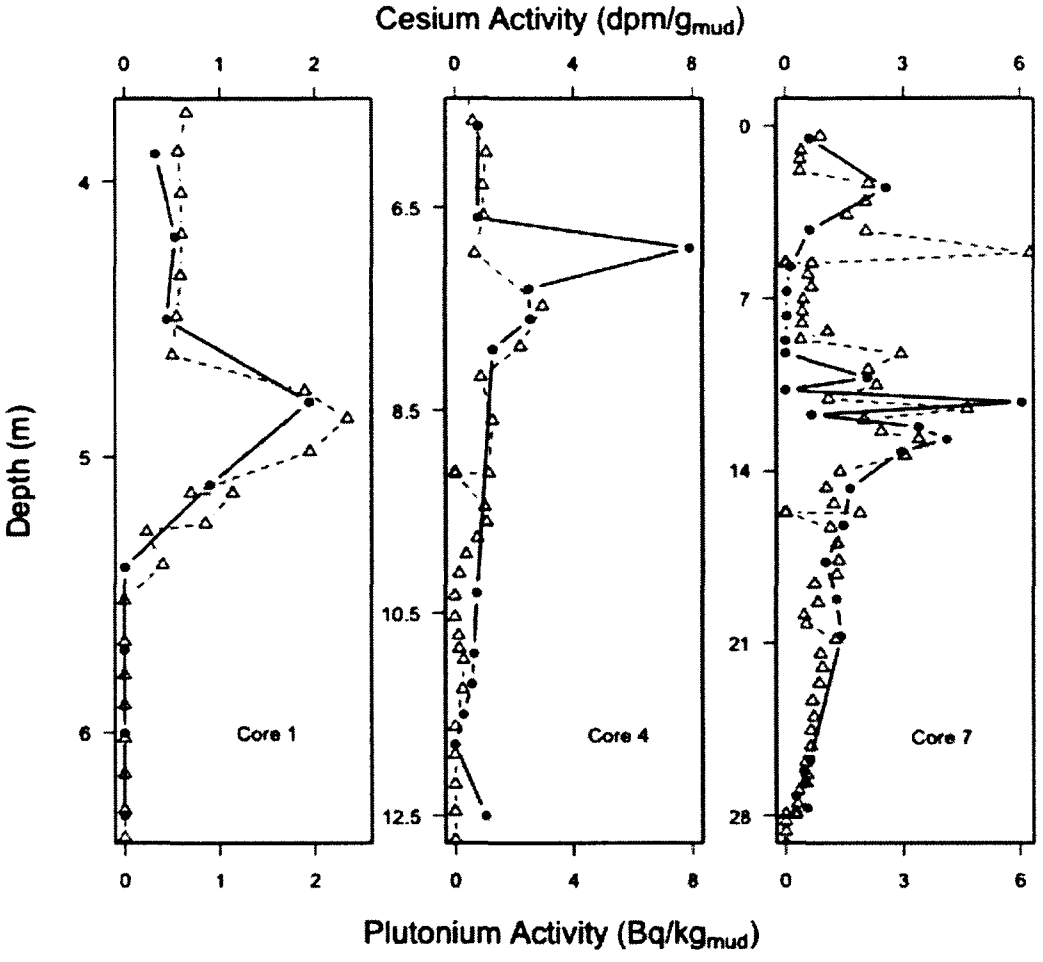

Figure 2-5. Conceptual diagram of Englebright Lake sediment accumulation.
Conceptual figure showing regional sediment accumulation patterns in Englebright Lake and their relation to sediment input from the Yuba River. The sediment accumulation between 1939 and 2001 along the river thalweg is depicted, and regions of bottomset, foreset, and topset deposition are highlighted by different patterns in the figure. The six cores discussed in this study are identified by triangles labeled with the core number. This figure is based on data presented by Snyder et al. (2006).

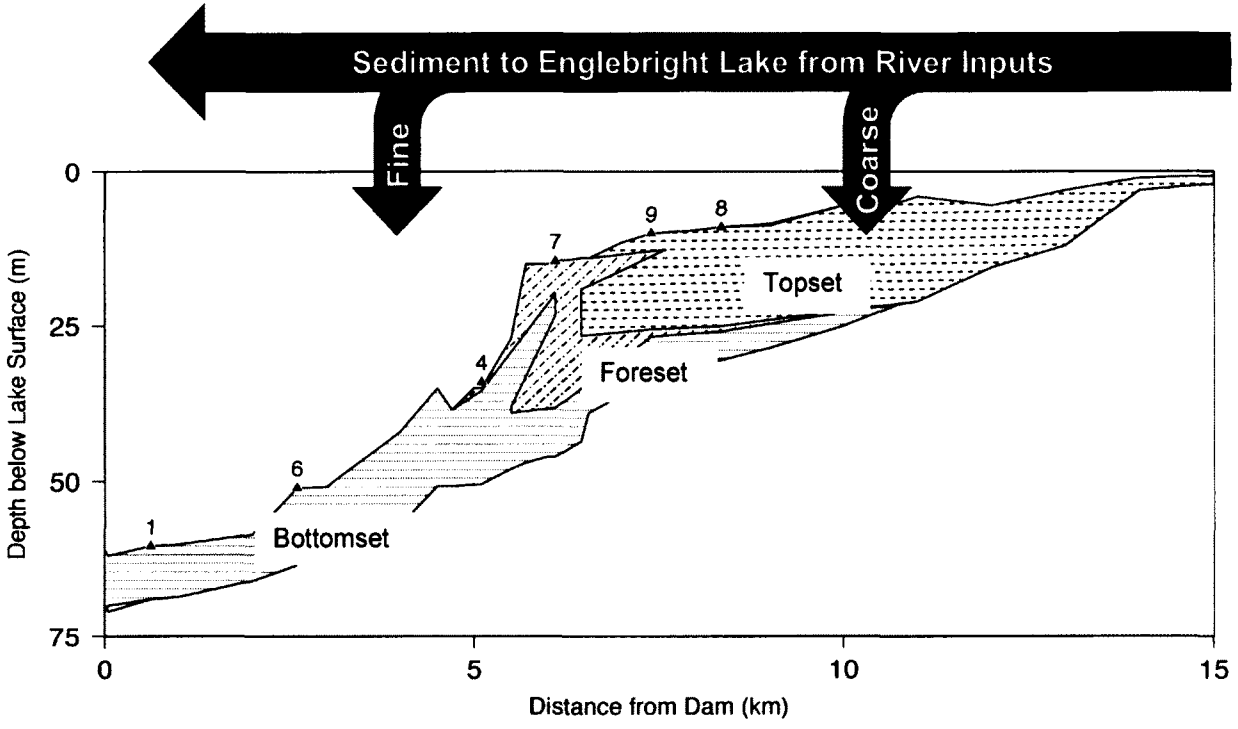

Table 2-1. Plutonium activities in sand, silt, and clay grain size fractions.
Results from an experiment to determine whether plutonium isotopes were associated with particular sediment grain size fractions. One sample from each core was analyzed and the mean grain size of these samples, determined with a Beckman-Coulter LS 100Q particle-size analyzer by the U.S. Geological Survey, is shown here (Snyder et al. 2004). Samples were then separated into three size fractions: sand (>63μm), silt (4 to 63μm) and clay (<4μm), and the percent sand, silt, and clay are reported here. The highest proportion of the plutonium activity was associated with the clay size in all of the sediment cores except Core 8 where activity was higher in the silt fraction. Because >75% of the measured plutonium was associated with the mud fraction, or those particles less than 63μm in diameter, plutonium activities were normalized to the mud fraction (% silt + % clay) for each sample using grain size data from Snyder et al. (2004).

Core Number	Mean Grain Size (μm)	Sand (%)	Silt (%)	Clay (%)	Pu in Sand Fraction (%)	Pu in Silt Fraction (%)	Pu in Clay Fraction (%)	Pu in Mud Fraction (Silt + Clay; %)
1	17.1	24.0	72.2	3.8	20.54	24.15	**55.31**	**79.46**
6	23.0	14.7	76.0	9.3	12.77	23.02	**64.21**	**87.23**
4	35.4	71.8	26.3	1.9	13.77	29.20	**57.03**	**86.23**
7	74.8	63.3	34.4	2.3	21.96	28.82	**49.22**	**78.04**
9	2848.0	98.0	1.6	0.2	0.74	9.31	**89.95**	**99.26**
8	2000.0	98.1	1.6	0.3	0.67	**58.19**	41.14	**99.33**

Table 2-2. Accumulation rates calculated from plutonium activity profiles.
The depths of first appearance and maximum activity of $^{239+240}Pu$ were used to calculate average accumulation rates during three periods of sedimentation in Englebright Lake: 1940-1954, 1954-1963, and 1963-2002. The depths of first appearance and maximum activity calculated from ^{137}Cs profiles (Snyder et al., 2006) are shown in parentheses for cores 1, 4, and 7. na=not available.

	Distance from Dam (km)	Depth of First Appearance (m)	Depth of Maximum Activity (m)	Average Accumulation Rate (cm/yr)		
				1940-1954	1954-1963	1963-2002
1	0.625	5.4 ± 0.26 (5.27)	4.8 ± 0.26 (4.86)	6.4 ± 1.9	6.7 ± 2.9	12.3 ±0.7
6	2.6	5.25 ± 0.57	3.11 ± 0.62	11.2 ± 4.1	23.8 ± 6.8	8.0 ± 1.6
4	5.1	11.2 ± 0.26 (11.25)	6.9 ± 0.31 (7.47)	27.1 ± 1.9	47.4 ± 3.4	17.8 ± 0.8
7	6.1	24.2 ± 2.63 (27.93)	11.2 ± 0.44 (na)	57.1 ± 18.8	144.4 ± 4.8	28.7 ± 1.1
9	7.4	14.6 ± 1.70	8.50 ± 1.22	58.7 ± 12.1	67.8 ± 13.5	21.8 ± 3.1
8	8.35	19.2 ± 0.97	na	28.6 ± 6.9	na	na

Table 2-3. List of events in Yuba River watershed.
Key events in California's history, including floods and land-use, influence the sediment accumulation record in Englebright Lake.

Date	Event influencing sediment record in Englebright Lake
2002	USGS coring campaign of Englebright Lake
1997	Flood affects Sierra Nevada region of California
1986	Flood affects northern one third of California
1970	New Bullards Bar dam constructed across North Yuba River
1964	Flood affects northern one third of California
1963	Flood in the Yuba River watershed
1962	Flood in the Yuba River watershed
1960	Flood in the Yuba River watershed
1955	Flood affects Sierra Nevada region of California
1950	Statewide flood
1941	Englebright Dam completed on the Yuba River
1848	Gold mining era in California begins

Table 2-4. Results from lipid-extraction experiment.
Results from an experiment to test the effect of lipid extraction on the plutonium activity of Englebright Lake sediments show that there is no significant difference between plutonium activities measured from lipid-extracted sediments and from unaltered sediments. Sediment cores collected from Englebright Lake by the USGS were subsampled to be analyzed for organic carbon, including lipid biomarkers, and plutonium activities. The sample size, especially in the coarse-grained sediments, was not always large enough for all analyses, so an experiment was designed to test if the lipid extraction method would impact the plutonium activity. The lipid extraction method involves using an accelerated solvent extractor (ASE) with a 2:1 (v/v) dichloromethane to methanol mixture of solvents at high temperature and pressure to extract lipids from the sediments. Three samples were selected based on their different sediment characteristics (i.e., mean grain size and grain size distribution) and on the amount of sample available for analysis. Three replicates of lipid extracted samples and unaltered samples were analyzed for plutonium with ICP-MS, and the average and standard deviation of plutonium activity are reported here. Differences between plutonium activities in lipid extracted sediments and unaltered sediments were determined with a two-tailed student's t-test, and p-values ≥ 0.1 indicate that lipid extraction prior to plutonium analysis does not change the plutonium activity in a sample.

Sample ID	Preparation	Replicates	$^{239+240}$Pu (Bq kg^{-1})	p-value from Student's t-test
7C-4H-2 66-76	Lipid Extraction	3	0.037 ± 0.004	
7C-4H-2 66-76	Unaltered Sediment	3	0.046 ± 0.007	0.16
6F-2H-2 80-100	Lipid Extraction	3	0.962 ± 0.025	
6F-2H-2 80-100	Unaltered Sediment	3	0.990 ± 0.007	0.14
8C-3H-2 78-98	Lipid Extraction	3	0.007 ± 0.004	
8C-3H-2 78-98	Unaltered Sediment	3	0.015 ± 0.006	0.10

CHAPTER 3: MULTI-BIOMARKER ANALYSIS OF ORGANIC MATTER IN A SIERRA NEVADA LAKE AND ITS WATERSHED

Pondell, C.R.

Canuel, E.A

Abstract

Organic matter in sediments includes a mixture of sources, often making it difficult to resolve their biological origins. In this study, we surveyed organic matter sources from the Upper Yuba River watershed in northern California to identify specific biomarkers to differentiate between aquatic and terrigenous sources of organic matter. Multiple classes of organic proxies, including sterols, fatty acids, lignin phenols and stable isotopes were measured in soils, vegetation, charcoal and freshwater plankton collected from the study system to characterize the organic signatures in the representative end member sources. Sterols, including 27-nor-24-cholesta-5,22-dien-3β-ol, cholesta-5,22-dien-3β-ol, brassicasterol and cholesterol, and positive $\delta^{15}N$ values were associated with aquatic organic matter sources (freshwater plankton and suspended particulate organic matter), whereas lignin phenols, long chain fatty acids and diacids characterized terrigenous organic matter (soils, charcoal and vegetation). Variability within terrigenous samples was explained by relative contributions from higher plants (diacids and C18:1ω9t) and fungi and bacteria (branched fatty acids and C18:1ω7). Trends in organic carbon and biomarker signatures in soil samples emphasize the influence of human land-use through an inverse relationship between OM content and the degree of human disturbance. These data expand upon previous biomarker research defining organic signatures in source material and provide useful proxies for identifying organic matter in freshwater systems in the study region.

Introduction

Understanding how human activities, land use and climate change have altered continental landscapes over time presents many challenges for geochemists, archaeologists and paleoecologists trying to decipher lake sediment records. Deforestation, agriculture and urbanization, for example, strongly modify continental landscapes by changing the amounts and kinds of vegetation, altering nutrient loadings, and increasing soil erosion and exposure to weathering processes (Regnier et al. 2013, Bauer et al. 2013). While many studies focus on coastal landscapes such as estuaries and the land-ocean margin, where human activities have contributed to profound ecosystem changes (e.g., Zimmerman and Canuel 2002, Lotze et al. 2006), considerably less is known about continental systems such as lakes and reservoirs, particularly those in mountainous regions. Reliable proxies for soils and vegetation are needed to better understand how human activities and climate have altered terrestrial ecosystems and to interpret lake and river sediment records.

Biomarkers, chemical compounds whose origin can be linked to a specific organic source, have been used in many environments to trace organic matter (OM) inputs and transformation processes (Bianchi and Canuel 2011). Unique biomarkers have been identified for different OM sources, including, for example, short chain fatty acids and sterols like dinosterol which are indicative of microalgae (Volkman 1986, Zimmerman and Canuel 2002), and branched fatty acids and specific amino acids which are indicative of bacterial sources (Canuel and Martens 1993, Veuger et al. 2007). Biomarkers have proven to be effective tools for quantifying terrestrial inputs to marine environments using lignin phenols (e.g., Hedges and Mann 1979, Goni et al. 1998, Houel et al. 2006), tracing wastewater effluent and human contamination with sterols such as corprostanol (Jeng and Han 1996, Eganhouse and Sherblom 2001), or determining the contribution of terrestrial and marine OM sources in an estuary using lipid biomarker compounds (Canuel 2001, Waterson and Canuel 2008). However, geochemical approaches to understanding OM sources in lakes, rivers, and terrestrial systems generally characterize

bulk sediment and soil signatures with proxies such as total organic carbon (TOC), total nitrogen (TN), and stable carbon and nitrogen isotopes ($\delta^{13}C$ and $\delta^{15}N$) (Vreča and Muri 2006, Masiello and Druffel 2012). A variety of limnology studies have employed biomarkers for understanding how OM sources change in response to impacts in the watershed (eg. Meyers 1997).

Of the studies that have used biomarkers to investigate OM in terrestrial and aquatic systems, the most common strategy is to focus on one class of biomarker to understand the origin and/or response of a particular source of OM to an outside influence, such as human land-use or long-term climate change. For example, Ouellet et al. (2009) used lignin to demonstrate the importance of terrigenous OM as a vector for mercury from watersheds to lakes and Van Metre et al. (1997) used organochlorine compounds to trace historic declines in water quality from reservoirs adjacent to human population centers. While biomarkers have proven useful for understanding ecosystems with a few different OM sources, in systems with many sources of OM, using a single class of biomarkers limits the amount of information that can be obtained. In complex systems, such as estuaries and coastal environments, multiple biomarkers and proxies, including stable isotopes, provide a more complete description of OM sources within the system (e.g., Goni et al. 1998, Yunker et al. 2005). For example, using organic carbon and stable isotope data, Das et al. (2008) attributed human land-use changes, specifically an increase in agricultural practices, to increased OM accumulation due to cultural eutrophication in nearby lake sediments, whereas Muri et al. (2004) used multiple classes of lipid biomarkers to delineate biogeochemical cycles, including sources, accumulation, and preservation, in an remote mountain lake. Multi-proxy studies have advanced the understanding of the ecosystem response to various stressors by allowing for the identification of multiple OM sources and interactions between these sources.

One limitation of using biomarkers in aquatic systems is that they are influenced by plant species and the physical environment (Meyers 1994) and general assumptions about biomarkers for aquatic or terrigenous OM may not hold across all study systems. This

study examined biomarker signatures of the dominant OM sources in the Yuba River and Englebright Lake, and their watersheds, in northern California in order to optimize the application of biomarkers to small, mountainous rivers and similar aquatic systems. The sterol, fatty acid, lignin, and stable carbon and nitrogen isotope composition of soil, vegetation, charcoal and freshwater plankton were examined. The biomarker composition of these materials were then used to distinguish between aquatic and terrigenous OM sources, contributing to an improved understanding of anthropogenic and climate change effects within the watershed of this study system.

Study Site

The Yuba River drains a 3470 km^2 watershed located in the Sierra Nevada mountain range in northern California, and includes three tributaries: the North Yuba River, Middle Yuba River and South Yuba River. These three tributaries converge at Englebright Lake, the downstream extent of the upper Yuba River watershed (Figure 3-1). The Yuba River watershed experiences a Mediterranean climate, with hot, dry summers, and precipitation occurring primarily between October and April. River discharge is controlled by winter storms and spring snowmelt. The upper Yuba River watershed has a population of approximately 16,000 people and only 1.6% of the watershed is considered urban (Federal 2000). The headwaters of the Yuba River and its tributaries lie at elevations greater than 2780 m where the soils exhibit minimal horizon development or are of volcanic origin (Staff 2013). At these elevations, the dominant vegetation is mixed conifer forest, dominated by Ponderosa pine and Douglas fir, while at lower elevations in the watershed, soils become more developed and fertile, and the vegetation cover changes to oak woodlands and chaparral communities. Forest and woodland land cover dominate the upper Yuba River watershed, and recent human land-use in the watershed is limited to logging operations (Curtis et al. 2006), water diversions (James 2005), and agriculture, including rangeland, cropland, and vineyards (Federal 2000). In contrast, during the mid 19^{th} century the upper Yuba River watershed was heavily impacted by hydraulic gold mining (Wright and Schoellhamer 2004, James 2005), which contributed to high sediment yields in the upper Yuba River (Gilbert 1917).

Methods

Sample Collection

A total of 37 samples were collected throughout the upper Yuba River watershed in July 2011 and July 2012 to characterize the signatures of multiple sources of OM (Figure 3-1). Samples included fresh vegetation, leaf litter and bark, charcoal samples from recent forest fire sites, soils, plankton, algae, and suspended particulate matter from lake water (Table 3-1).

Soil and Charcoal. Soil and charcoal samples were collected from agricultural, mining, forest and urban sites in the upper Yuba River watershed. The top 1 cm of soil was collected with a 16 cm^2 diameter push core. At all sites, three cores were collected from a 1-m^2 area and combined into a single soil sample (~15 g). Two additional samples were collected from subsurface soil horizons exposed at outcrops near roads. Charred vegetation from two recent forest fires were collected as charcoal samples. Soil sample colors were recorded using the Munsell Soil Color Index (Table 3-1) and then stored at -80°C before they were freeze-dried for organic analyses. Freeze-dried samples were sieved through 1.19 mm mesh to remove coarse gravel and plant material, and homogenized with mortar and rubber pestle to a fine powder before analysis.

Vegetation. Vegetation samples represented the dominant plant species in the watershed, and included pine, fir and oak trees, grasses, moss, and ferns (Table 3-1). The tissues included hard bark, leaves and needles, flowers, and litter samples. Samples were collected from two forested sites, one agricultural site, and from the shoreline of Englebright Lake, corresponding to locations where soil or aquatic samples were collected. All vegetation samples were stored at -80°C, freeze-dried, and homogenized with a mortar and pestle prior to analysis.

Aquatic (Freshwater Plankton). Aquatic samples were collected from Englebright Lake to define autochthonous OM sources. Plankton samples were collected with a 0.5 m diameter, 63 μm mesh plankton net at three locations in Englebright Lake. At sites 1 and 2, the plankton net was deployed to a depth of 8 m and a vertical tow was collected through the water column. At Site 3, near the confluence of Englebright Lake and the South Yuba River, a strong current prevented sample collection using a vertical plankton tow. Instead, the plankton net was deployed at the water surface for 30 seconds in a 1.9 $m^3 s^{-1}$ current (USGS station 11417500). Following collection, the plankton samples were transferred to pre-combusted glass jars for storage. At each site, three plankton tows were collected to characterize the > 63 μm plankton assemblage in the lake. The plankton samples were then filtered through 0.7 μm pre-combusted glass fiber filters, stored at -80°C, and freeze-dried before elemental analysis.

Suspended particulate organic matter (POM) samples were collected concurrently at each of the sites where plankton samples were obtained. For biomarker samples, 20 L of lake water were collected with a peristaltic pump and filtered through 0.7 μm pre-combusted glass fiber filters. These filters were frozen at -80°C and stored until they could be analyzed for lipid biomarkers. POM samples for total organic carbon (TOC), total nitrogen (TN) and stable isotopes, were obtained from three replicate water samples (500 mL each) and filtered through 0.7 μm pre-combusted glass fiber filters. These samples represented the > 0.7 μm plankton assemblage.

Algal biofilm samples from Englebright Lake were collected by scraping algae from the floating dock and buoy on the shoreline with an acetone rinsed spatula. The biofilm was filtered through pre-weighed 0.7 μm pre-combusted glass fiber filters, frozen at -80°C, and freeze-dried. Before being analyzed for lipid biomarkers, the filters were weighed to determine the dry weight of the sample. Together, these three types of samples describe the general freshwater plankton signal in Englebright Lake.

Organic Proxy Analysis

TOC, TN, and Stable Isotope Analyses. Small aliquots (5 to 50 mg) of soils, vegetation, and plankton were acidified with dilute HCl to remove inorganic carbon (Hedges and Stern 1984) and dried overnight at 60°C before being analyzed with a Carlo Erba Elemental Analyzer to measure total organic carbon (TOC) and total nitrogen (TN) content. Filters with particulate samples from lake water were placed in a desiccator with 6N HCl and fumed overnight to remove inorganic carbon. Filters were then dried for a minimum of four days before being packaged and analyzed for TOC and TN content with the Carlo Erba Elemental Analyzer. Replicate analyses (n = 2 to 4) were run for all samples and the variation between samples was generally less than 5%, but was higher in samples with lower OM concentrations.

Samples for stable carbon and nitrogen isotope ($\delta^{13}C$ and $\delta^{15}N$) analyses were prepared similarly. Stable carbon and nitrogen isotope ratios were measured with a Costech ECS 4010 CHNSO Analyzer (Costech Analytical Technologies, Inc.) connected to a Delta V Advantage Isotope Ratio Mass Spectrometer with the Conflo IV interface (Thermo Electron North America, LLC). All stable carbon and nitrogen isotope values are reported relative to standard reference materials ($\delta^{13}C$: PeeDee Belemnite limestone; $\delta^{15}N$: atmospheric nitrogen).

Lipid Biomarker Analysis. Samples were analyzed for lipid biomarkers following the procedure outlined by (Waterson and Canuel 2008). Briefly, aliquots of soils (10 to 50 g), vegetation (1 to 5 g) and whole water filters were extracted with a mixture of dichloromethane (DCM) and methanol (2:1, v/v) at 80°C and 1200 psi using an accelerated solvent extractor. Extracts were partitioned according to (Bligh and Dyer 1959) using a 1:1:0.9 solution of DCM, methanol, and NaCl (20% aqueous solution) to separate organic extracts from the aqueous phase. The organic fraction was saponified and neutral and acidified fractions were extracted (Canuel and Martens 1993). Neutral lipids were separated into lipid compound classes using silica gel columns and fractions

containing sterols and alcohols were collected. The acidified lipids were methylated and fatty acid methyl ethers (FAMEs) were purified using silica gel columns. Sterol and alcohol fractions were derivatized with N,O-Bis(trimethylsilyl)trifluoroacetamide (BSTFA) prior to analysis with an Agilent 7890A GC (DB-5MS 30m x 0.32mm column with 0.25μm film) connected to an Agilent 5975C mass spectrometer. FAME fractions were analyzed with an HP5890 series II GC (DB-23 60m x 0.32mm, 0.25μm film). Compounds were quantified relative to internal standards (C_{21} FAME for FAME analysis and 5α-cholestane for sterol analysis) and were blank corrected prior to data analysis. The average recovery of nonadecanol and 5α-androstanol (surrogate compounds added at the beginning of the analysis) from this analysis was greater than 65%, and variation between blank-corrected replicate samples was less than 20%.

Lignin Biomarker Analysis. Lignin phenols were measured following the method described by(Louchouarn et al. 2000). Soil, charcoal,and vegetation samples were weighed so approximately 4 mg of organic carbon were analyzed for each sample. Lignin analyses were not conducted on the aquatic samples because the samples were not large enough and because these samples were not expected to contain lignin (Hedges and Mann 1979). Samples were loaded into stainless steel vessels with 330 mg of CuO, 150 mg $Fe(NH_4)Mg$, and 2 to 3 mL of 2N NaOH. The CuO oxidation reaction occurred as samples were stirred and heated for 3 hours at 154°C in a modified GC oven. A standard surrogate solution containing ethyl-vanillin and *trans*-cinnamic acid was then mixed into the vessels, the solution was decanted, and vessels were rinsed twice with 1N NaOH. Lignin oxidation products were separated from this solution with three rinses of ethyl acetate. Samples sat over Na_2SO_4 overnight to remove water and were dried with a Zymark TurbVap II solvent concentrator before being redissolved in pyridine and derivatized with BSTFA. Lignin oxidation products were measured with an Agilent 7890A GC (DB-5MS 30m x 0.32mm column with 0.25μm film) connected to an Agilent 5975C mass spectrometer using 1,3,5-triisopropylbenzene as an internal standard to compute the concentrations of 13 lignin phenol compounds. Peak areas were blank-

corrected prior to analysis, and the average variation between replicate samples was approximately 20%.

Total lignin concentrations normalized to dry mass of sediment (Σ8) were calculated as the sum of vanillyl, syringyl, and cinnamyl lignin phenols (Hedges and Ertel 1982) and were normalized to TOC to calculated total lignin yields (Λ8). Ratios of syringyl to vanillyl phenols (S/V) and cinnamyl to vanillyl phenols (C/V) were used to differentiate between vascular plant tissues (Hedges and Mann 1979). Acid to aldehyde ratios of vanillyl phenols [(Ad/Al)v] and 3,5-dihydroxybenzoic acid to vanillyl phenol ratios (3,5-Bd:V) provided information regarding the degradation state of organic matter derived from vascular plants (Hedges and Mann 1979, Hedges and Ertel 1982) .

Data Analysis

Peak areas were integrated using the Chem Station software package (Agilent) and converted to concentrations. These values were analyzed for statistical differences using R-Studio version 0.98.507. In order to identify differences in OM sources in the upper Yuba River watershed, principal components analysis (PCA) was performed on fatty acid, sterol, alcohol and lignin biomarker data. PCA is a data-exploration method that simplifies complex data sets into a small number of principal components (PC) to describe factors controlling variation within the data. Prior to this analysis, biomarker values were blank-corrected and any undetected values were replaced with the biomarker detection limit, or one-half the minimum detected concentration of each variable (Yunker et al. 2005). Biomarker concentrations were then normalized to the total fatty acid, sterol, or alcohol concentration to reduce artifacts related to large concentration differences (Yunker et al. 2005). Each biomarker value was divided by the geometric mean of that variable across all samples and log transformed. Biomarker variables were auto-scaled by subtracting the mean and then dividing by standard deviation from each value within a variable class. These normalization steps created a dataset that was

unaffected by negative bias or closure (Yunker et al. 2005). PCA was performed with 37 observations (samples) and 31 variables (lipid and lignin biomarkers).

Lipid, lignin, TOC and TN data that did not meet the assumption of normality required for the statistical analyses, were log-transformed prior to regression, correlation, and t-test analysis. Stable carbon and nitrogen values were not transformed for statistical analyses because they met the required assumptions. Data reported here are either presented on a mass-normalized ($\mu g\ g^{-1}$) or percent basis.

Results

TOC, TN, and Stable Isotopes

TOC ranged from 0.27 to 46.96% dry weight in soil, vegetation and plankton samples and was approximately 80 $\mu g\ L^{-1}$ for the POM samples (Table 3-2). As expected, %TOC was higher in the vegetation ($p < 0.001$) and freshwater plankton ($p < 0.001$) samples than in the soil samples (Figure 3-2a). Within the soil samples %TOC content was higher in forest soils than agricultural soils ($p = 0.003$) or urban soils ($p < 0.005$); mining and subsurface soils had significantly lower %TOC ($p < 0.001$) (Figure 3-3a). TN varied between 0.01 and 6.25%, and was highest for the plankton samples collected from sites 1 and 2 in Englebright Lake (Figure 3-2b). Mining and subsurface soils had the lowest %TN ($p < 0.001$ for student's t-test between mining and agriculture, forest, and urban soils and between subsurface and forest soils; $p = 0.005$ between subsurface soils and agriculture and urban soils) and agricultural and forest soils had the highest %TN (Table 3-2, Figure 3-3d).

Carbon to nitrogen ratios ($C:N_a$) ranged from 5.6 to 81.5, and were lowest in freshwater plankton samples (8.5 ± 3.4, $p < 0.02$) and highest in plant samples (55.7 ± 21.2, $p < 0.005$) (Table 3-2, Figure 3-4a). The variability in $C:N_a$ ratios from soil samples was high (10.8 – 35.8); agricultural soils had significantly lower $C:N_a$ ratios than forest soils

($p = 0.004$). Unlike TOC, $C:N_a$ ratios did not exhibit any relationship with levels of human impact (Figure 3-4b).

$\delta^{13}C$ ranged from -33 to -23‰. Freshwater plankton samples had significantly lower $\delta^{13}C$ values (-31.72 ± 2.39‰) than the terrigenous (vegetation and soil) samples (-28.1 ± 2.1‰, $p = 0.012$) (Table 3-2; Figure 3-2c). $\delta^{15}N$ ranged from -11 to 3‰, with the lowest values associated with the vegetation samples (-7.62 ± 1.02‰), especially from the gymnosperm and tree bark samples. The freshwater plankton samples had significantly higher $\delta^{15}N$ values (1.48 ± 2.73‰, $p < 0.001$) (Table 3-2; Figure 3-5a).

Lipid Biomarkers

Total sterol concentrations ranged from below detection (BD) to 5416.4 μg g^{-1}, and carbon normalized total sterol concentration ranged from BD to 14.4 μg mg_{TOC}^{-1}. Carbon normalized sterols were higher ($p < 0.05$) in aquatic (1.8 ± 1.6 μg mg_{TOC}^{-1}) and plant (2.4 ± 3.0 μg mg_{TOC}^{-1}) samples than in soil (1.3 ± 3.5 μg mg_{TOC}^{-1}) and char (0.3 ± 0.1 μg mg_{TOC}^{-1}) samples. The dominant sterols included 27-nor-methylchoesta-5,22-dien-3β-ol, cholesta-5,22-dien-3β-ol, cholest-5-en-3β-ol (cholesterol), 24-methylcholesta-5,22-dien-3β-ol (brassicasterol), 24-methylcholest-5-en-3β-ol (campesterol), 24-ethylcholesta-5,22-dien-3β-ol (stigmasterol), 24-ethylcholest-5-en-3β-ol (sitosterol) (Table 3-3). Sterols such as 27-nor-methylchoesta-5,22-dien-3β-ol, and cholesta-5,22-dien-3β-ol, typically assigned to aquatic sources, were detected in all aquatic samples, as well as V9 and AS2. The proportion of brassicasterol and cholesterol to the total sterol concentration was higher in aquatic samples ($p = 0.02$-0.04 and $p < 0.01$, respectively), while the proportion of plant sterols (stigmasterol, campesterol and sitosterol) was higher in vegetation samples than in aquatic ($p = 0.01$) and soil samples ($p = 0.002$).

Total fatty acid (FA) concentrations ranged from 6.8 to 8422.9 μg g^{-1}, or 1.2 to 25.2 μg mg_{TOC}^{-1} on a carbon-normalized basis. TOC-normalized total FA concentrations were higher in the aquatic samples (23.8 ± 1.4 μg mg_{TOC}^{-1}) than in soil (3.9 ± 2.1 μg mg_{TOC}^{-1}),

char (3.2 ± 0.3 μg mg_{TOC}^{-1}), and plant (5.1 ± 2.1 μg mg_{TOC}^{-1}) samples ($p < 0.003$). Saturated FA comprised the largest fraction (mean = 60 ± 14% of total FA), and short chain FA (SCFA = C_{12}+ C_{14}+ C_{16}+ C_{18}; mean = 34.0 ± 16.0% of total FA) concentrations were higher than long chain FA (LCFA = C_{24}+ C_{25}+ C_{26}+ C_{27}+ C_{28}+ C_{29}+ C_{30}+ C_{31}+ C_{32}; mean = 13.7 ± 10.5% of Total FA) in all samples, except the mixed bark sample (V9). LCFA varied across sample types with significantly higher contributions in soils (17.7 ± 9.6%), charcoal (19.3 ± 15.3%) and vegetation (12.5 ± 10.0%) than in the aquatic samples (1.2 ± 1.5%, $p < 0.01$ for all three one-sided t-tests). Significant differences in the concentration of polyunsaturated FA (PUFA) between the samples were only evident for the C_{18} PUFAs, and not for C_{16} PUFAs or C_{20}+C_{22} PUFAs. C_{18} PUFAs were more abundant in the vegetation samples than in aquatic ($p = 0.015$) or soil ($p < 0.001$) samples. On average, monounsaturated fatty acids made up 19.6 ± 8.4% of the total fatty acid composition among samples, branched fatty acids (BrFA) and diacids were less than 20% of the total fatty acids in all samples, and diacids were not detected in any aquatic samples.

Lignin Biomarkers

Total lignin concentration (Σ8) ranged from 0.01 to 43.96 mg g^{-1}, and carbon normalized lignin concentration (Λ8) ranged from 0.18 to 11.39 mg/100 mg_{TOC}. Σ8 was highest in vegetation and charcoal samples ($p < 0.01$), and soil samples from the mine sites and from the subsurface horizons had the lowest lignin concentrations (Table 3-3). Ratios of syringyl to vanillyl phenols (S/V) and cinnamyl to vanillyl phenols (C/V) phenols showed a wide rage of values (S/V = 0.002 – 5.61 and C/V = 0.02 – 5.76), with the greatest range observed in the vegetation samples. There was no significant difference in C/V or S/V detected between plant, charcoal, and soil samples. (Ad/Al)v and 3,5-Bd:V were higher in soil and charcoal samples than in the vegetation samples ($p < 0.001$ and $p = 0.02$, respectively); (Ad/Al)v ranged from 0.13 – 1.04 and 3,5-Bd:V ranged from 0.0 to 0.7 across all soil, vegetation and charcoal samples (Table 3-5).

Principal Components Analysis (PCA)

PCA was used to determine sources of variability in the lipid and lignin biomarker data. An initial PCA was run on all samples using only the lipid biomarkers (Figure 3-6a), and PC-1 and PC-2 described 23.9% and 16.9% of the variability of the fatty acid and sterol data, respectively. Freshwater plankton samples grouped together with negative scores on PC-1, vegetation samples generally had positive scores on PC-1, and soil samples had negative scores on PC-1 and PC-2. Cholesterol and C18:1ω7 had the most negative loadings on PC-1, and C16:0 (0.356) and diacids (-0.304) had the most extreme values on PC-2 (Figure 3-6b).

A second PCA was run using all biomarker data, including fatty acids, sterols, and lignin, but only using the vegetation, soil, and charcoal samples (Figure 3-6c). PC-1 and PC-2 from this second PCA explained 25.3% and 14.5% of the variability in the biomarker data, respectively. Vegetation samples grouped together with positive PC-1 scores, and soils grouped together with negative PC-1 scores. Overall, sample groupings were driven by Σ8 (0.343), odd-numbered monounsaturated FA (Odd MUFA) (-0.354), and BrFA (-0.308) on PC-1 and by C18:1ω7 (0.379), C18:1ω9c (0.393), C18:1ω9c (-0.246), and diacids (-0.251) on PC-2 (Figure 3-6d).

Discussion

Bulk Signatures from the Upper Yuba River Watershed

TOC, TN, and C:N_a. The TOC and TN content of samples collected from the upper Yuba River watershed varied widely across the OM sources analyzed in this study. As expected, TOC and TN were highest in the living plant and plankton samples, and lower in soil and charcoal samples (Figure 3-2). The lower TOC and TN content associated with soil samples is consistent with increased OM processing through plant litter decomposition and microbial and fungal degradation associated with soil OM formation (Wedin et al. 1995), and the lower TOC content of charcoal is likely caused by exposure

to extreme heat in fires (Turney et al. 2006). The soil samples suggest that both TOC and TN contents decrease as a result of human land-use. The average TOC content was highest in forest samples and decreased in agricultural, urban, mining samples (Figure 3-3). TN content behaved similarly to TOC content across different soil types, but was elevated in agricultural samples, likely reflecting the addition of nitrogen to soils to increase agricultural efficiency (Compton and Boone 2000). Charcoal signatures are intermediate of soil and vegetation signatures (Figure 3-5b), reflecting the oxidation of vegetation and litter as a result of forest fires and as part of the formation of soil OM (Quideau et al. 2001, González-Pérez et al. 2004).

$C:N_a$ ratios also can differentiate aquatic from terrigenous OM sources. The low $C:N_a$ ratios in freshwater plankton samples ($C:N_a < 10$, except for PL3) collected from Englebright Lake are consistent with aquatic OM sources (Meyers 1994, Kaushal and Binford 1999) (Figure 3-4a). $C:N_a$ ratios are higher in terrigenous samples, with typical values ranging between 20 and 85.5, consistent with $C:N_a$ ratios in higher plants (Hedges and Oades 1997, Cloern et al. 2002). Soil and charcoal samples have intermediate $C:N_a$ values associated with the decomposition or combustion of plant matter. However, average $C:N_a$ ratios in soils was high (21.49 ± 9.10) compared to reported soil $C:N_a$ ratios (10-12) (Hedges and Oades 1997, Onstad et al. 2000), and in agricultural soils (12.6 ± 1.3) is comparable to these reported values. High $C:N_a$ ratios in most of the soils collected from the upper Yuba River watershed may reflect the average grain size. For example, $C:N_a$ in sands are usually higher (15-45) than $C:N_a$ in silt (13-25) or clay-sized particles (7-13) (Hedges and Oades 1997).

Stable Isotopes. Using stable isotopes to differentiate among OM sources in aquatic systems has had mixed results. McConnachie and Petticrew (2006), for example, used $\delta^{13}C$ and $\delta^{15}N$ to successfully model inputs from soil, salmon, and algal sources. In contrast, Cloern et al. (2002) examined seasonal variability in $\delta^{13}C$ and $\delta^{15}N$ values for marsh and estuarine plants and soil samples throughout the San Francisco Bay estuary,

and concluded that variation among and across sources was too great, and that the use of stable isotopes alone could not differentiate between OM sources in the San Francisco Estuary. In the upper Yuba River system, $\delta^{15}N$ values for freshwater plankton samples were higher than $\delta^{15}N$ values for plant, soil, and charcoal samples ($p < 0.01$). This is consistent with greater processing of nitrogen in aquatic samples from Englebright Lake (Cifuentes et al. 1988) than in terrigenous OM from the watershed. Results from this study suggest that $\delta^{15}N$ can be used to trace OM sources given the highly negative values found in higher plants (-11 to -4‰), slightly negative values measured in soils (-3 to -1‰), and positive values observed in aquatic samples (0 to 3‰) (Figure 3-2d).

$\delta^{13}C$ values also distinguish between terrigenous and aquatic samples because $\delta^{13}C$ in freshwater plankton samples are lower than $\delta^{13}C$ signatures in vegetation, char and soil (Figure 3-2c). In general, $\delta^{13}C$ values less than -31‰ indicate aquatic OM sources whereas $\delta^{13}C$ values greater than -31‰ suggest terrigenous OM sources. Of the 37 samples collected for this study, $\delta^{13}C$ values from three samples did not follow this trend: plankton collected from site 3 in Englebright Lake (PL3), one subsurface soil sample (SS1) and one charcoal sample (CC2) (Table 3-2). The $\delta^{13}C$ value for PL3 suggests mixing between aquatic and terrigenous OM sources in Englebright Lake, and will be discussed in more detail in a later section. The unexpectedly low $\delta^{13}C$ values in the charcoal and subsurface soil samples reflect degradation processes (i.e., burning or decomposition) influencing these samples.

Stable carbon isotope values within the terrigenous samples were variable and may reflect similarities in the source of OM in soil and vegetation samples, specifically the decay continuum from plant litter inputs to the formation of soil OM (Melillo et al. 1989). Plant litter decay and soil formation processes may lead to a small amount of isotope fractionation (2-4‰; Connin et al. 1997), which explains some of the variability observed among the $\delta^{13}C$ values of the terrestrial samples. However, an isotope bi-plot of $\delta^{15}N$ vs $\delta^{13}C$ values shows resolution between vegetation, soil, and aquatic samples,

whereas the regions of overlap indicate similarities between the OM sources (Figure 3-5a). In the upper Yuba River system, bulk elemental and stable isotopic values can differentiate between OM sources (Figure 3-5) and these parameters can be used in conjunction with biomarker data to enhance our ability to identify aquatic and terrigenous OM sources.

Biomarker Signatures in Aquatic Samples

Results from the PCA suggest that concentrations of aquatic sterols and cholesterol drive differences between aquatic and terrigenous sources (Figure 3-6a,b). Aquatic sterols (cholesta-5,22-dien-3β-ol and 27-nor-24-methylcholesta-5,22-dien-3β-ol) are found almost exclusively in aquatic samples collected from Englebright Lake. Cholesta-5,22-dien-3β-ol, a biomarker for diatoms (Volkman 1986, Barrett et al. 1995), was measured in freshwater plankton at concentrations similar to measured values from estuarine and river sediments (Mudge and Norris 1997, Volkman et al. 2008). 27-nor-24-methylcholesta-5,22-dien-3β-ol has been associated with marine dinoflagellate species (Goad and Withers 1982, Mansour et al. 1999); however, the absence of dinosterol (a sterol specific to dinoflagellates) in samples collected from Englebright Lake suggests against the presence of dinoflagellates in Englebright Lake. Instead, 27-nor-24-methylcholesta-5,22-dien-3β-ol detected in the aquatic samples may reflect contributions from other microalgae or from the bacterial biodegradation of diatoms (Holba et al. 1998). The presence of Odd MUFA and BrFA in aquatic samples support contributions from bacterial OM sources to these Englebright Lake samples (Volkman et al. 1980, Canuel and Martens 1993). Further evidence of the dominance of diatoms in the aquatic community of Englebright Lake comes from the presence of brassicasterol in aquatic samples. Brassicasterol has been identified in many aquatic systems as a biomarker for diatoms and other microalgae (Cranwell 1976, Kumari et al. 2013). In the upper Yuba river watershed, contributions from brassicasterol, while not exclusive to aquatic samples, were highest in aquatic samples from Englebright Lake. Brassicasterol was higher in the small size fraction (> 0.7 μm) of freshwater plankton in Englebright Lake

(8% - 20%) than in the larger fraction (> 63 μm) of freshwater plankton (1% -3%), suggesting that these two size fractions may represent different plankton communities.

Cholesterol also contributed to differences between aquatic and terrigenous OM sources (Figure 3-6a,b), and provides information about the aquatic community described by large plankton (> 63 μm) samples from Englebright Lake. Cholesterol dominates the sterol composition in many microalgae species (Volkman 2003), as well as in crustaceans, insects, and zooplankton carcasses (Volkman 1986,Volkman et al. 1987, Kanazawa 2001). In Englebright Lake, cholesterol was the dominant sterol (75% - 85%) in plankton (> 63 μm) collected from sites 1 and 2. The high percentage of cholesterol, and the small contributions from algal biomarkers in these samples, suggests that the plankton community (> 63μm) in Englebright Lake was likely comprised of crustaceans, such as amphipods, or other zooplankton.

Variation within the aquatic samples was also evident in the composition of FA, specifically SCFA (Figure 3-6a,b). SCFA, especially C_{16} and C_{18}, are non-specific fatty acids and have been detected in samples from diverse species (Ruess and Chamberlain 2010). However, SCFA are routinely found to be the dominant FA in aquatic samples, including seagrasses, marsh grasses and macro and microalgae (Volkman et al. 1980, Canuel and Martens 1993). In samples collected from the upper Yuba River watershed, SCFA are ubiquitous, but generally dominate the FA composition of aquatic samples (> 50% of total FA, except POM2 and ALG) (Table 3-3). Interestingly, trends in the variation within the aquatic samples highlight changes in OM composition throughout Englebright Lake. For example, as the distance from the dam increased (i.e., from site 1 at the dam to site 2 to site 3 near the river confluence), biomarker signatures from aquatic samples became more similar to soils (i.e., PC-2 scores decreased). This trend was evident for all freshwater plankton samples (Figure 3-6a), and indicates mixing between terrigenous and aquatic OM sources at the river confluence that decreases with distance from the river.

Biomarker Signatures in Vegetation

Plant sterols and multiple FA groups characterized terrigenous OM sources in the upper Yuba River watershed. Campesterol, stigmasterol and sitosterol have been ascribed to higher plants in previous studies (Huang and Meinschein 1979, Volkman et al. 1987, González-Pérez et al. 2011), and were investigated as a potential terrigenous biomarker for this study system. Concentrations of campesterol and stigmasterol varied across all samples, with no significant differences in the distribution of these sterols. However, contributions of sitosterol comprised over 85% of the total sterol concentration in all vegetation samples, higher than concentrations measured in any of the aquatic samples ($p < 0.01$).

FA and lignin biomarkers supplement sterol biomarker data, and in samples collected from the upper Yuba River watershed several FA groups provide supporting data that allow us to distinguish between aquatic and terrigenous OM sources. Concentrations of LCFA, C_{18} PUFA, and $C_{22:0}$, diacids, and total lignin phenols ($\Sigma 8$) were higher in terrigenous samples than in aquatic samples ($p < 0.01$ for aquatic vs. terrigenous values from these biomarkers), and were highest in plant samples collected from the watershed ($p < 0.01$). These biomarkers have been used as to trace terrestrial OM sources in many soil, estuarine and marine sediment studies (Almendros et al. 1996, Mudge and Norris 1997, Zimmerman and Canuel 2002, Waterson and Canuel 2008, González-Pérez et al. 2011). Further, diacids, a biomarker for plant leaves and roots (Volkman et al. 1980, Zelles 1999, Mueller et al. 2012), were only detected in terrigneous samples from the upper Yuba River watershed, and not freshwater plankton samples from Englebright Lake. Together, these biomarkers identify higher plant inputs from the upper Yuba River watershed.

Biomarkers in Soils and Charcoal

The presence of diacids and high concentrations of LCFA, $C_{22:0}$, C_{18} PUFA and Σ8 prove to be excellent biomarkers for terrigneous OM in Englebright Lake, but concentrations of these biomarkers differ between soil and plant samples. Σ8 and C_{18} PUFA were highest in plant samples ($p < 0.01$), as expected because higher plants synthesize C_{18} PUFAs and lignin (Σ8) as structural components. The presence of these biomarkers, in additiona to concentrations of diacids and brassicasterol, reflects the incorporation of vascular plant matter into soil OM. Concentrations of diacids are highest in soil samples, likely reflecting high inputs from the suberin component of roots (Mueller et al. 2012). Concentrations of brassicasterol in soils are unexpected because brassicasterol is commonly used as a biomarker for microalgae diatoms. However, brassicasterol is produced by organisms from the *Brassicaceae* plant family (Schaeffer et al. 2001, Piironen et al. 2003, González-Pérez et al. 2011), a medium-sized family of mostly agricultural plants (e.g., broccoli, cabbage and mustard). Several species from this family are invasive weeds in North America that are well adapted to thrive in cleared areas such as mine pits or along roadsides (Pyšek and Pyšek 1998, Meekins et al. 2001), and the presence of brassicasterol in soil samples suggests a relatively high abundance of *Brassicaceae* in the upper Yuba River watershed.

In addition to the biomarkers indicating inputs from higher plants in soil OM signatures, biomarkers for bacterial and fungi also comprise OM signatures in soils. Concentrations of Odd MUFA and BrFA indicate bacterial inputs (Volkman et al. 1980, Canuel and Martens 1993), and concentrations of C18:1w5 likely reflect fungal biomass contributed during biodegradation of plant OM during the formation of soils (Weete et al. 1985, Zelles 1999). Bacteria and fungi are responsible for the degradation of soil OM, and this is reflected in high (Ad/Al)v from lignin phenols. (Ad/Al)v range from 0.31 to 1.05 in soils from the upper Yuba River, showing that the amount of degradation of soils varies from fresh to highly degraded (Goñi et al. 1993). Biomarkers indicative of bacterial and fungal sources allow for the distinction between higher plants and soils that comprise the general terrigenous OM signature in Englebright Lake.

Variability in Soil and Plant Signatures.

Loadings from the PCA analysis of terrigenous samples suggests that differences between plant samples or between soil samples arise from concentrations of diacids and C18:1 biomarkers (Figure 3-6b). Samples V4, V5, and V8 (representing needles or leaves from fir, pine, and oak trees) are described by concentrations of C18:1ω9t and diacids. High concentrations of these biomarkers likely reflect inputs from conifer plants (C18:1ω9t, Mueller et al. 2012) and from the cutin found in leaves and bark from these samples (diacids, Volkman et al. 1980). The PCA results for the terrigenous samples (Figure 3-6b) suggest that scores for vegetation samples representing agricultural and lakeshore grasses and ferns (V1, V2, V7, V11, and V12) are driven by high concentrations of 18:1ω9c and C18:1ω7, indicating increased inputs from bacterial or fungal sources (Stahl and Klug 1996, Zelles 1999). However, it is more likely that values for these vegetation samples reflect low concentrations of 18:1ω9t and diacids, indicating that, as expected, the cutin coating for leaves and bark is not a major component in grasses and ferns.

Instead, loadings from 18:1ω9c and C18:1ω7 explain PCA scores for soil samples, where bacterial and fungal decomposition are expected to affect OM sources. Almost all soil samples have positive loadings on PC-2, indicating they have undergone oxidative degradation associated with bacterial and fungal activity. The urban soils (US2, US3, and US4) were expected to be more similar to the other degraded soils but instead fall in their own region of the score plot (Figure 3-6c). These samples were collected at elevations above 380 m where there is a transition from andisol to entisol soils (Staff 2013). Entisol soils (US2, US3, and US4) are undeveloped, and therefore, have undergone less degradation associated with soil formation. All other soil samples are andisols, which are more developed, and as expected, are more degraded (i.e., higher (Ad/Al)v ratios). The only other soil sample with negative PC-2 scores was collected from an organic farm

(AS2) where soil may be enriched in OM in an effort to increase agricultural efficiency through fertilizer use, and therefore, appears to be less degraded.

The soil samples generally group together by soil type, with mining and subsurface soils grouping closely together, and agricultural and forest samples creating additional groups (Figure 3-6c). Several biomarkers analyzed in samples from the study site show an interesting trend that tracks the decreasing %TOC (Fig 3a) in soils and may explain the grouping observed in the PCA (e.g., TOC is correlated to total FA [$r = 0.60$, $p < 0.001$], LCFA [$r = 0.83$, $p < 0.001$], plant sterols [$r = 0.064$, $p < 0.001$], and $\Sigma 8$ [$r = 0.77$, $p < 0.001$]). An examination of the relationship of the percent of several biomarkers reveals some deviations from the inverse relationship between the degree of soil modification from human land-use and contribution from select biomarkers. For example, diacids in the urban soils significantly higher that diacids concentrations from other soil samples ($p < 0.01$) (Figure 3-3e), which may indicate a source of diacids (e.g., higher density of roots resulting from landscaping; Mueller et al. 2012) in areas near roadways and urban centers.

Brassicasterol was unexpectedly high in subsurface and mining soils (Figure 3-3b), and may reflect the abundance of the invasive weeds from the *Brassicaceae* family that would take advantage of the vegetation-free mine pits. Additionally, brassicasterol has been traced to fungal sources in soils (Weete et al. 1985), and the high concentrations of brassicasterol in subsurface soil samples may reflect fungal degradation in these samples. Further, high (Ad/Al)v in subsurface and mining soils (Figure 3-3f) and high 3,5-Bd:V ratios are consistent with the highly processed nature of the mining and subsurface soils ($p < 0.05$ for higher values of both (Ad/Al)v and 3,5-Bd:V in mining/subsurface soils than in agricultural/urban/forest soils). High 3,5-Bd:V indicate increased inputs from soil organic matter (Prahl et al. 1994, Houel et al. 2006), and high (Ad/Al)v indicate an increasing degree of degradation (Hedges et al. 1988, Goñi et al. 1993, Opsahl and Benner 1995). The combination of high (Ad/Al)v and 3,5-Bd:V in mining and

subsurface soils emphasizes that hydraulic mining impacts soil OM to the same extent as biodegradation processes during soil formation (subsurface soils).

Deviations from data trends. While most of the samples from this study follow the trends described above, there are deviations that reveal insights into some of the processes governing the organic carbon signatures in the upper Yuba River watershed. For instance, evidence from multiple proxies and biomarkers, including $C:N_a$, $\delta^{13}C$, $\delta^{15}N$, and sterols from freshwater plankton samples collected at site 3 in Englebright Lake indicate inputs from terrigenous and aquatic OM sources (Figure 3-5 and 6a, b). The location of site 3 in Englebright Lake, within 200 m of the confluence of the South Yuba River and Englebright Lake, explains why OM signatures from this site had a stronger terrigenous signature than other freshwater plankton signatures collected from the lake. Data from this site highlight the mixing that is occurring between suspended sediment load and aquatic primary production as the rivers enter the lake system.

Biomarker values from the mining and subsurface soils were usually more similar to each other than the other soil signatures. The mining and subsurface soils provide examples of sites in the upper Yuba River watershed that are more degraded than other samples collected for this study, and therefore would have OM signatures that reflect recalcitrant soil OM sources rather than the more labile vegetation and litter sources. For example, the mining soils were pressure washed from mountain-sides and mixed in a slurry of mercury to remove gold before being rinsed again and discarded (James 2005). The two mining samples were highly processed, which was clear upon visual inspection as these soils were bleached of color. Organic carbon content and biomarker signatures reflect this hydraulic mine processing. Subsurface samples were collected to determine if the major source of organic material to the Yuba River was from subsurface horizons as stated by (O'Geen et al. 2010). These samples have undergone degradation from bacteria and fungi, as well as oxidation and leaching as a result of soil horizon formation (Quideau et al. 2001). These processes may be responsible for the observed similarities between subsurface and mine tailing samples.

Sterol signatures in soils from the organic farm were significantly different from other agricultural soils, and from soils collected throughout the watershed. This sample was the only soil sample that had measurable concentrations of 27-nor-24-methylcholesta-5,22-dien-3β-ol in addition to corprostanol (5b-cholestan-3β-ol), 24-ethylcholestan-7-en-3β-ol, and several stanol compounds. The detection of these sterols may reflect the fertilizer addition. These sterols suggest that organic fertilizer contained manure (corprostanol and cholesterol; Peng et al. 2005), and the increased contribution of stanols as compared to other soils samples indicated a degree of sterol degradation (Nishimura 1978), which may be the result of composting.

Conclusions

A combination of sterols, fatty acids, lignin phenols, and stable carbon and nitrogen isotopes distinguished signatures of terrestrial OM from aquatic OM signatures in a small watershed in northern California. Biomarker and stable isotope data from soil, vegetation, charcoal, and freshwater plankton samples provide unique identifiers to distinguish between aquatic and terrigenous OM sources.

1. Aquatic OM sources were dominated by sterols such as 27-nor-24-methylcholesta-5,22-dien-3β-ol and cholesta-5,22-dien-3β-ol, and by $\delta^{15}N$ values > 1.2‰.
2. Higher plant OM sources were dominated by high concentrations of plant sterols (stigmasterol, campesterol, and sitosterol), long chain fatty acids, lignin phenols, and by the presence of diacids.
3. Fatty acid and lignin biomarkers show a range in soils, from "fresher" soils with inputs from vegetation or litter to highly processed soils with lower TOC content and microbial (bacterial and fungi) signatures. Additionally, trends in OM signatures in soils emphasize the impact of human disturbance in the watershed

with an increasing degree of human modification resulting in lower OM signatures.

A multi-proxy approach to identify OM sources from samples collected in the upper Yuba River watershed in the Sierra Nevada Mountain Range describe processes impacting OM signatures throughout the watershed. This research identifies several lipid biomarkers in plankton and soil that provide specific information about the organisms contributing to aquatic and terrigenous OM signatures in this system, but many biomarker signatures that have been described as purely marine or terrestrial in estuarine and coastal research are detected across aquatic and terrigenous samples measured here. While this study emphasizes gaps in our knowledge of biomarker composition of terrestrial OM resulting from marine- and soil-centric research, it also highlights an opportunity to combine knowledge and research strategies from marine and soil geochemistry to explore biomarkers from an ecosystem-wide perspective.

References

Almendros, G., J. Sanz, and F. Velasco. 1996. Signatures of lipid assemblages in soils under continental Mediterranean forests. European Journal of Soil Science 47:183–196.

Barrett, S. M., J. K. Volkman, G. A. Dunstan, and J.-M. LeRoi. 1995. Sterols of 14 species of marine diatoms (*Bacillariophyta*). Journal of Phycology 31:360–369.

Bauer, J. E., W.-J. Cai, P. A. Raymond, T. S. Bianchi, C. S. Hopkinson, and P. A. G. Regnier. 2013. The changing carbon cycle of the coastal ocean. Nature 504:61–70.

Bianchi, T. S., and E. A. Canuel. 2011. Chemical Biomarkers in Aquatic Ecosystems. Princeton University Press, Princeton.

Bligh, E. C., and W. J. Dyer. 1959. A rapid method of total lipid extraction and purification. Can J Biochem Physiol.

Canuel, E. A. 2001. Relations between river flow, primary production and fatty acid composition of particulate organic matter in San Francisco and Chesapeake Bays: a multivariate approach. Organic Geochemistry 32:563–583.

Canuel, E., and C. Martens. 1993. Seasonal variations in the sources and alteration of organic matter associated with recently-deposited sediments. Organic Geochemistry 20:563–577.

Cifuentes, L. A., J. H. Sharp, and M. L. Fogel. 1988. Stable carbon and nitrogen isotope biogeochemistry in the Delaware estuary. Limnol Oceanogr.

Cloern, J. E., E. A. Canuel, and D. Harris. 2002. Stable carbon and nitrogen isotope composition of aquatic and terrestrial plants of the San Francisco Bay estuarine system. Limnology and Oceanography 47:713–729.

Compton, J. E., and R. D. Boone. 2000. Long-term impacts of agriculture on soil carbon and nitrogen in New England forests. Ecology 81:2314–2330.

Connin, S. L., R. A. Virginia, and C. P. Chamberlain. 1997. Carbon isotopes reveal soil organic matter dynamics following arid land shrub expansion. Oecologia 110:374–386.

Cranwell, P. A. 1976. Decomposition of aquatic biota and sediment formation: lipid components of two blue-green algal species and of detritus resulting from microbial

attack. Freshwater Biology 6:481–488.

Curtis, J., L. Flint, C. Alpers, S. Wright, and N. Snyder. 2006. Sediment Transport in the Upper Yuba River Watershed, California, 2001-2003. U.S. Geological Survey Scientific Report 2005-5246:74.

Das, B., R. Nordin, and A. Mazumder. 2008. An alternative approach to reconstructing organic matter accumulation with contrasting watershed disturbance histories from lake sediments. Environmental Pollution 155:117–124.

Eganhouse, R. P., and P. M. Sherblom. 2001. Anthropogenic organic contaminants in the effluent of a combined sewer overflow: impact on Boston Harbor. Marine Environmental Research.

Federal, M. (ED.). 2000. Landsat GeoCover EMT+2000 Edition Mosaics, 1st edition. USGS. http://www.landcover.org.

Gilbert, G. K. 1917. hydraulic-mining debris in the Sierra Nevada. US Geological Survey Professional Paper:105-154.

Goad, L. J., and N. Withers. 1982. Identification of 27-nor-(24R)-24-methylcholesta-5,22-dien-3β-ol and brassicasterol as the major sterols of the marine dinoflagellateGymnodinium simplex. Lipids 17:853–858.

Goni, M., K. Ruttenberg, and T. Eglinton. 1998. A reassessment of the sources and importance of land-derived organic matter in surface sediments from the Gulf of Mexico. Geochimica et Cosmochimica Acta 62:3055–3075.

González-Pérez, J. A., F. J. González-Vila, and M. E. Arias. 2011. Geochemical and ecological significance of soil lipids under Rhododendron ponticum stands. Environmental Chemistry Letters 9:453–464.

González-Pérez, J. A., F. J. González-Vila, G. Almendros, and H. Knicker. 2004. The effect of fire on soil organic matter—a review. Environment International 30:855–870.

Goñi, M. A., B. Nelson, and R. A. Blanchette. 1993. Fungal degradation of wood lignins: Geochemical perspectives from CuO-derived phenolic dimers and monomers. Geochimica et Cosmochimica Acta 57:3985–4002.

Hedges, J. I., and J. H. Stern. 1984. Carbon and nitrogen determinations of carbonate-containing solids [In sediments, sediment trap materials and plankton]. Limnology and Oceanography.

Hedges, J. I., and J. M. Oades. 1997. Comparative organic geochemistries of soils and marine sediments. Organic Geochemistry 27:319–361.

Hedges, J. I., R. A. Blanchette, K. Weliky, and A. H. Devol. 1988. Effects of fungal degradation on the CuO oxidation products of lignin: A controlled laboratory study. Geochimica et Cosmochimica Acta 52:2717–2726.

Hedges, J., and D. Mann. 1979. The characterization of plant tissues by their lignin oxidation products. Geochimica et Cosmochimica Acta 43:1803–1807.

Hedges, J., and J. Ertel. 1982. Characterization of lignin by gas capillary chromatography of cupric oxide oxidation products. Anal. Chem. 54:174–178.

Holba, A. G., L. I. P. Dzou, W. D. Masterson, W. B. Hughes, B. J. Huizinga, M. S. Singletary, J. M. Moldowan, M. R. Mello, and E. Tegelaar. 1998. Application of 24-norcholestanes for constraining source age of petroleum. Organic Geochemistry 29:1269–1283.

Houel, S., P. Louchouarn, M. Lucotte, R. Canuel, and B. Ghaleb. 2006. Translocation of soil organic matter following reservoir impoundment in boreal systems: Implications for in situ productivity. Limnology and Oceanography 51:1497–1513.

Huang, W.-Y., and W. G. Meinschein. 1979. Sterols as ecological indicators. Geochimica et Cosmochimica Acta 43:739–745.

James, L. A. 2005. Sediment from hydraulic mining detained by Englebright and small dams in the Yuba basin. Geomorphology 71:202–226.

Jeng, W.-L., and B.-C. Han. 1996. Coprostanol in a Sediment Core from the Anoxic Tan-Shui Estuary, Taiwan. Estuarine, Coastal and Shelf Science 42:727–735.

Kanazawa, A. 2001. Sterols in marine invertebrates. Fisheries Science 67:997-1007.

Kaushal, S., and M. W. Binford. 1999. Relationship between C:N ratios of lake sediments, organic matter sources, and historical deforestation in Lake Pleasant, Massachusetts, USA - Springer. Journal of Paleolimnology.

Kumari, P., M. Kumar, C. Reddy, B. Jha, and H. Dominguez. 2013. Algal lipids, fatty acids and sterols. Functional ingredients from algae for foods and nutraceuticals:87–134.

Lotze, H. K., H. S. Lenihan, B. J. Bourque, and R. H. Bradbury. 2006. Depletion, degradation, and recovery potential of estuaries and coastal seas. Science 312.

Louchouarn, P., S. Opsahl, and R. Benner. 2000. Isolation and quantification of dissolved lignin from natural waters using solid-phase extraction and GC/MS. Analytical Chemistry 72:2780–2787.

Mansour, M. P., J. K. Volkman, and A. E. Jackson. 1999. The fatty acid and sterol composition of five marine dinoflagellates. Journal of Phycology 35:710–720.

Masiello, C. A., and E. R. M. Druffel. 2012. Carbon isotope geochemistry of the Santa Clara River. Global Biogeochemical Cycles 15:407–416.

McConnachie, J. L., and E. L. Petticrew. 2006. Tracing organic matter sources in riverine suspended sediment: implications for fine sediment transfers. Geomorphology 79:13–26.

Meekins, J. F., H. E. Ballard Jr, and B. C. McCarthy. 2001. Genetic Variation and Molecular Biogeography of a North American Invasive Plant Species (Alliaria petiolata, Brassicaceae). International Journal of Plant Sciences 162:161–169.

Melillo, J. M., J. D. Aber, A. E. Linkins, A. Ricca, B. Fry, and K. J. Nadelhoffer. 1989. Carbon and nitrogen dynamics along the decay continuum: Plant litter to soil organic matter. Pages 53–62 *in* Ecology of Arable Land .... Ecology of Arable Lands-Perspectives and Challenges, Dordrecht.

Meyers, P. A. 1994. Preservation of elemental and isotopic source identification of sedimentary organic matter. Chemical Geology.

Meyers, P. A. 1997. Organic geochemical proxies of paleoceanographic, paleolimnologic, and paleoclimatic processes. Organic Geochemistry 27:213–250.

Mudge, S. M., and C. E. Norris. 1997. Lipid biomarkers in the Conwy Estuary (North Wales, U.K.): a comparison between fatty alcohols and sterols. Marine Chemistry 57:61–84.

Mueller, K. E., P. J. Polissar, J. Oleksyn, and K. H. Freeman. 2012. Differentiating temperate tree species and their organs using lipid biomarkers in leaves, roots and soil. Organic Geochemistry 52:130–141.

Muri, G., S. G. Wakeham, T. K. Pease, and J. Faganeli. 2004. Evaluation of lipid biomarkers as indicators of changes in organic matter delivery to sediments from Lake Planina, a remote mountain lake in NW Slovenia. Organic Geochemistry 35:1083–1093.

Nishimura, M. 1978. Geochemical characteristics of the high reduction zone of stenols in Suwa sediments and the environmental factors controlling the conversion of stenols

into stanols. Geochimica et Cosmochimica Acta.

O'Geen, A. T., R. A. Dahlgren, A. Swarowsky, K. W. Tate, D. J. Lewis, and M. J. Singer. 2010. Research connects soil hydrology and stream water chemistry in California oak woodlands. California Agriculture, University of California 64:78–84.

Onstad, G. D., D. E. Canfield, and P. D. Quay. 2000. Sources of particulate organic matter in rivers from the continental usa: lignin phenol and stable carbon isotope compositions. Geochimica et Cosmochimica Acta 20:3530-3546.

Opsahl, S., and R. Benner. 1995. Early diagenesis of vascular plant tissues: Lignin and cutin decomposition and biogeochemical implications. Geochimica et Cosmochimica Acta 59:4889–4904.

Ouellet, J.-F., M. Lucotte, R. Teisserenc, S. Paquet, and R. Canuel. 2009. Lignin biomarkers as tracers of mercury sources in lakes water column. Biogeochemistry 94:123–140.

Peng, X., G. Zhang, B. Mai, J. Hu, K. Li, and Z. Wang. 2005. Tracing anthropogenic contamination in the Pearl River estuarine and marine environment of South China Sea using sterols and other organic molecular markers. Marine Pollution Bulletin 50:856–865.

Piironen, V., J. Toivo, R. Puupponen-Pimi, and A.-M. Lampi. 2003. Plant sterols in vegetables, fruits and berries. Journal of the Science of Food and Agriculture 83:330–337.

Prahl, F. G., J. R. Ertel, M. A. Goñi, and M. A. Sparrow. 1994. Terrestrial organic carbon contributions to sediments on the Washington margin. Geochimica et Cosmochimica Acta 14:3035-3048.

Pyšek, P., and P. Pyšek. 1998. Is There a Taxonomic Pattern to Plant Invasions? Oikos 82:282.

Quideau, S. A., O. A. Chadwick, A. Benesi, R. C. Graham, and M. A. Anderson. 2001. A direct link between forest vegetation type and soil organic matter composition. Geoderma 104:41–60.

Regnier, P., P. Friedlingstein, P. Ciais, F. T. Mackenzie, N. Gruber, I. A. Janssens, G. G. Laruelle, R. Lauerwald, S. Luyssaert, A. J. Andersson, S. Arndt, C. Arnosti, A. V. Borges, A. W. Dale, A. Gallego-Sala, Y. Goddéris, N. Goossens, J. Hartmann, C. Heinze, T. Ilyina, F. Joos, D. E. LaRowe, J. Leifeld, F. J. R. Meysman, G. Munhoven, P. A. Raymond, R. Spahni, P. Suntharalingam, and M. Thullner. 2013. Anthropogenic perturbation of the carbon fluxes from land to ocean. Nature Geoscience 6:597–607.

Ruess, L., and P. M. Chamberlain. 2010. The fat that matters: Soil food web analysis using fatty acids and their carbon stable isotope signature. Soil Biology and Biochemistry 42:1898–1910.

Schaeffer, A., R. Bronner, and P. Benveniste. 2001. The ratio of campesterol to sitosterol that modulates growth in Arabidopsis is controlled by STEROL METHYLTRANSFERASE 2;1. The Plant Journal 25:605–615.

Staff, S. S. (ED.). 2013. Web Soil Survey. National Resources Conservation Service, United States Department of Agriculture. http://websoilsurvey.sc.egov.usda.gov/App/WebSoilSurvey.aspx.

Stahl, P. D., and M. J. Klug. 1996. Characterization and differentiation of filamentous fungi based on Fatty Acid composition. Applied and Environmental Microbiology.

Turney, C. S. M., D. Wheeler, and A. R. Chivas. 2006. Carbon isotope fractionation in wood during carbonization. Geochimica et Cosmochimica Acta 70:960–964.

Van Metre, P., E. Callender, and C. Fuller. 1997. Historical trends in organochlorine compounds in river basins identified using sediment cores from reservoirs. Environ. Sci. Technol.

Veuger, B., B. D. Eyre, D. Maher, and J. J. Middelburg. 2007. Nitrogen incorporation and retention by bacteria, algae, and fauna in a subtropical, intertidal sediment: An in situ 15N-labeling study. Limnology and Oceanography 52:1930–1942.

Volkman, J. 2003. Sterols in microorganisms. Applied microbiology and Biotechnology 60:495–506.

Volkman, J. K. 1986. A review of sterol markers for marine and terrigenous organic matter. Organic Geochemistry 9:83–99.

Volkman, J. K., J. W. Farrington, and R. B. Gagosian. 1987. Marine and terrigenous lipids in coastal sediments from the Peru upwelling region at 15°S: Sterols and triterpene alcohols. Organic Geochemistry 11:463–477.

Volkman, J. K., R. B. Johns, F. T. Gillan, G. J. Perry, and H. J. Bavor Jr. 1980. Microbial lipids of an intertidal sediment—I. Fatty acids and hydrocarbons. Geochimica et Cosmochimica Acta 44:1133–1143.

Volkman, J., A. Revill, D. Holdsworth, and D. Fredericks. 2008. Organic matter sources in an enclosed coastal inlet assessed using lipid biomarkers and stable isotopes. Organic Geochemistry 39:689–710.

Vreča, P., and G. Muri. 2006. Changes in accumulation of organic matter and stable carbon and nitrogen isotopes in sediments of two Slovenian mountain lakes(Lake Ledvica and Lake Planina), induced by eutrophication changes. Limnology and Oceanography 51:781–790.

Waterson, E., and E. Canuel. 2008. Sources of sedimentary organic matter in the Mississippi River and adjacent Gulf of Mexico as revealed by lipid biomarker and [delta] 13CTOC analyses. Organic Geochemistry 39:422–439.

Wedin, D. A., L. L. Tieszen, B. Dewey, and J. Pastor. 1995. Carbon isotope dynamics during grass decomposition and soil organic matter formation. Ecology.

Weete, J. D., M. Kulifaj, C. Montant, W. R. Nes, and M. Sancholle. 1985. Distribution of sterols in fungi. II. Brassicasterol in Tuberand Terfeziaspecies. Canadian Journal of Microbiology 31:1127–1130.

Wright, S., and D. Schoellhamer. 2004. Trends in the Sediment Yield of the Sacramento River, California, 1957-2001. San Francisco Estuary and Watershed Science 2:Article 2.

Yunker, M. B., L. L. Belicka, H. R. Harvey, and R. W. Macdonald. 2005. Tracing the inputs and fate of marine and terrigenous organic matter in Arctic Ocean sediments: A multivariate analysis of lipid biomarkers. Deep Sea Research Part II: Topical Studies in Oceanography 52:3478–3508.

Zelles, L. 1999. Fatty acid patterns of phospholipids and lipopolysaccharides in the characterisation of microbial communities in soil: a review. Biology and Fertility of Soils 29:111–129.

Zimmerman, A. R., and E. A. Canuel. 2002. Sediment geochemical records of eutrophication in the mesohaline Chesapeake Bay. Limnology and Oceanography 47:1084–1093.

Figure 3-1. Map of sample locations in the upper Yuba River watershed. This map shows the land cover (GLC 2000 from the Joint Research Centre of the European Commission) and sample locations in the upper Yuba River watershed in northern California, and includes the North, Middle, and South Yuba rivers and Englebright Lake. Colored triangles identify the location of 37 end-member samples collected throughout the watershed to characterize the organic matter signatures in this system. Triangles plotted on top of each other indicate a sampling location where multiple samples were collected. The inset shows all of the samples collected on and near Englebright Lake.

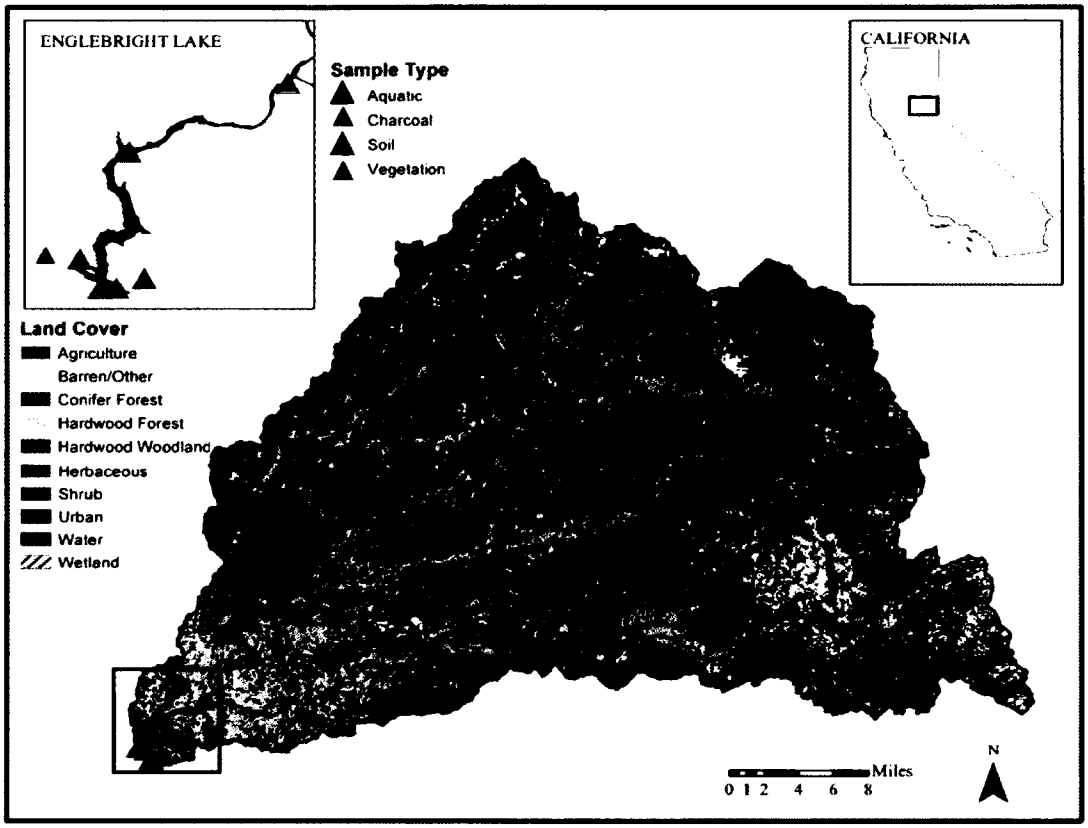

Figure 3-2. Organic carbon proxy values for each end member sample type. Boxplots showing total organic carbon (a), total nitrogen (b), stable carbon isotope values (c), and stable nitrogen isotope values (d). These data highlight some of the differences between aquatic, soil, charcoal, and plant OM sources.

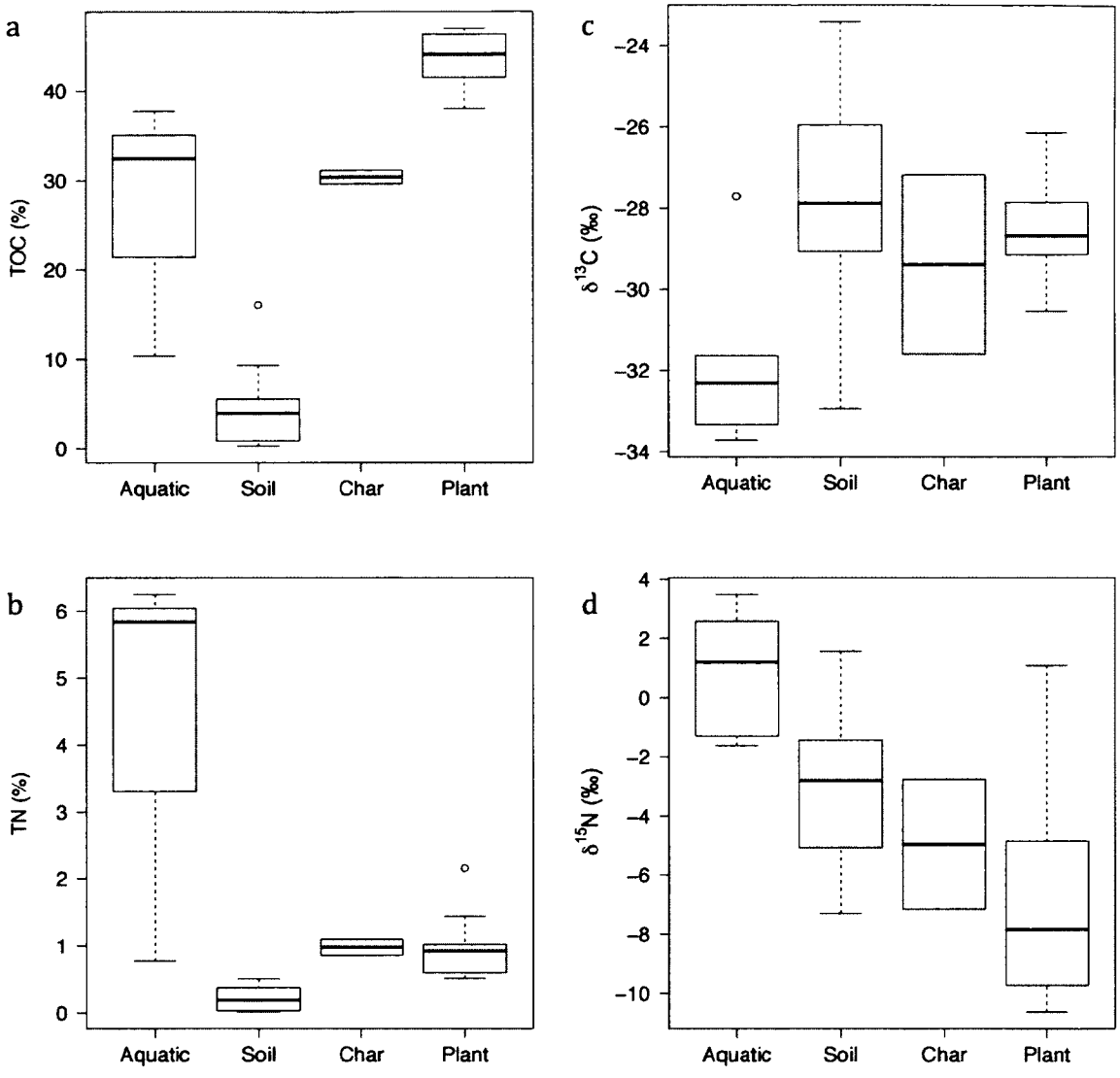

Figure 3-3. TOC, TN, and biomarkers for soil end member samples.
Boxplots showing OC proxies and biomarker signatures for soils collected from the upper Yuba River watershed. Several of the variables show a trend with level of anthropogenic impact going from most impacted (mining) to least impacted (forest). %TOC (a), %TN (b), brassicasterol (c), diacids (d), Λ8 (e), and (Ad/Al)v (f) are shows to highlight some of the variations between these soil OM signatures.

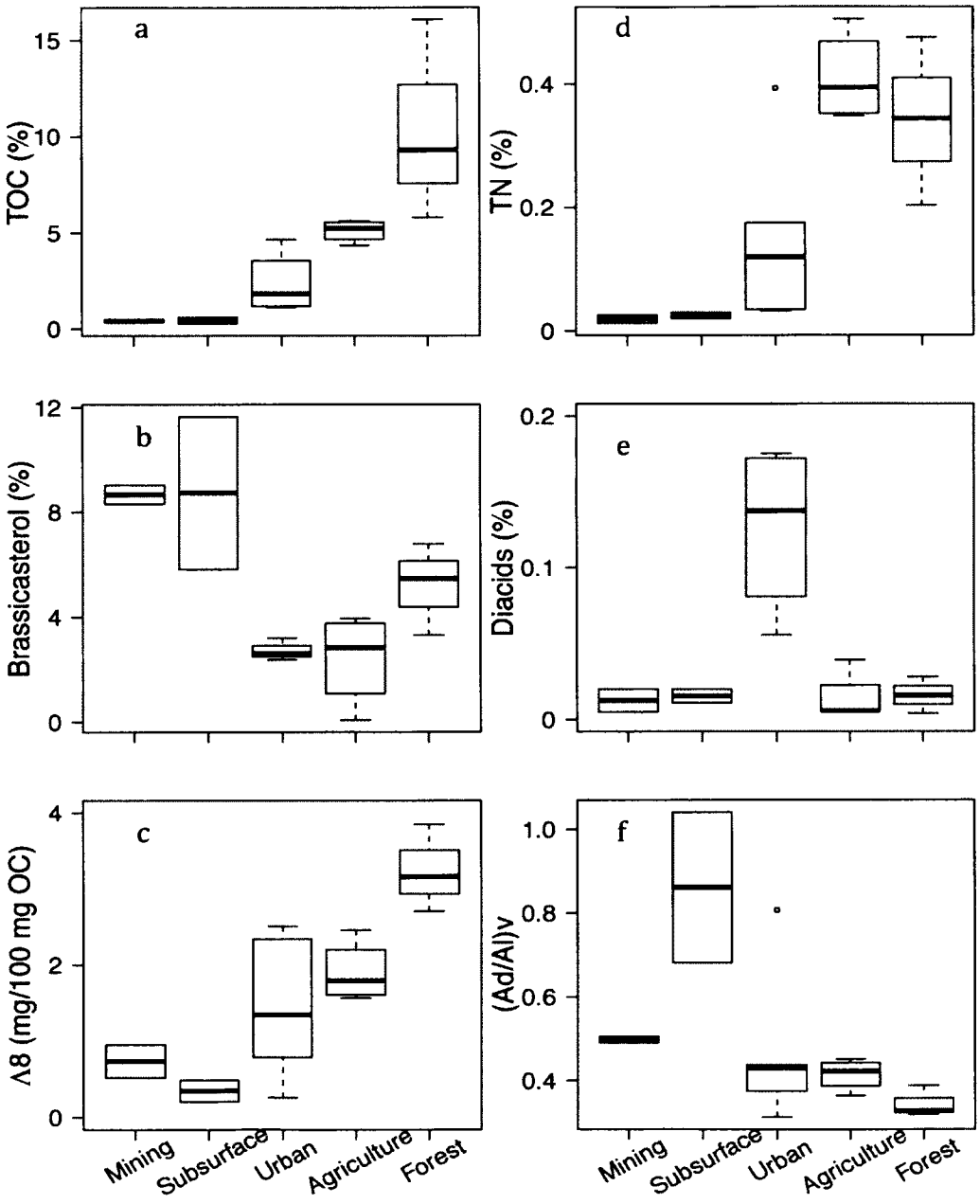

Figure 3-4. $C:N_a$ for groups of end member samples and types of soil samples. Boxplots showing differences in $C:N_a$ between OM sources (a) and between soil types (b).

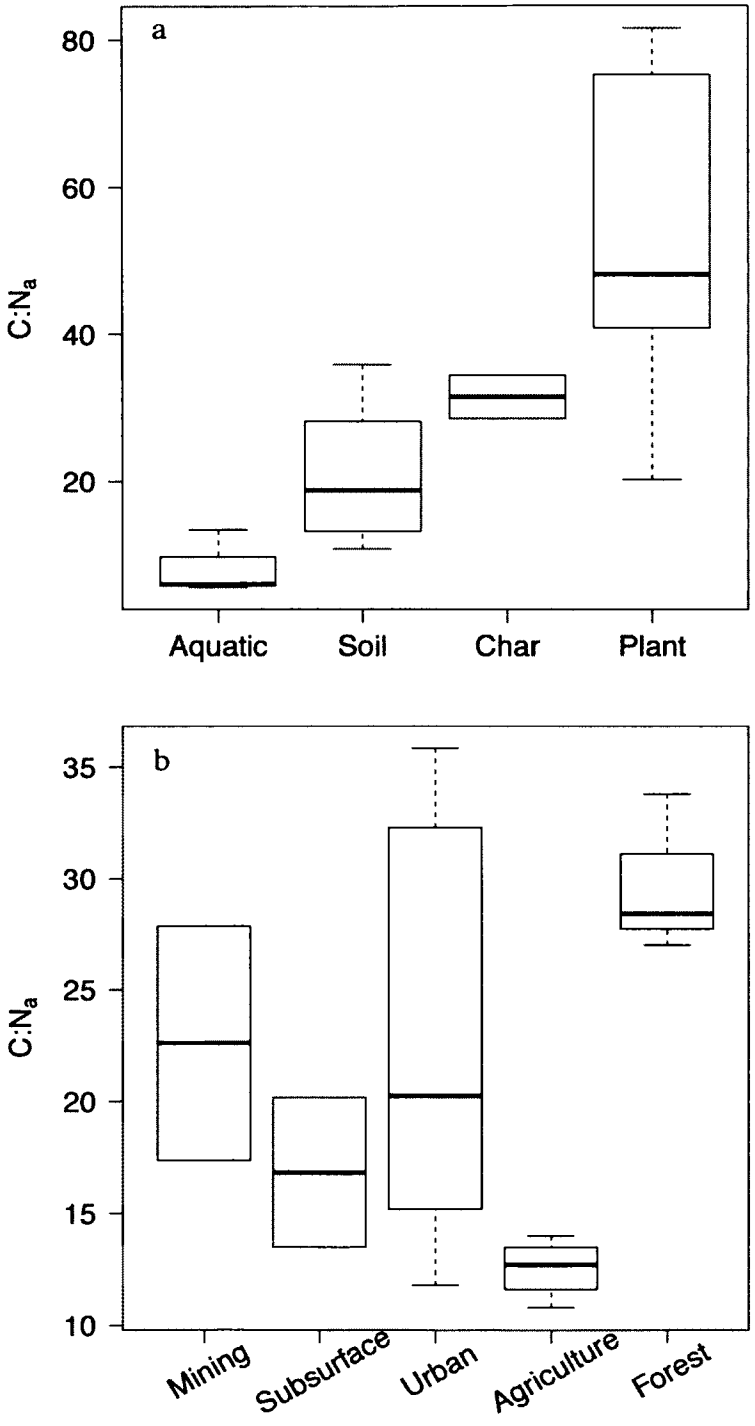

Figure 3-5. Bi-plots of stable carbon and nitrogen isotopes and TOC and TN. Biplots of stable carbon and nitrogen isotopes (a) and of TOC and TN (b) provide a visualization of the different signatures of soil, plant, and aquatic organic matter sources. The three boxes represent the mean ± standard deviation for aquatic, soil, and plant OM. There is evidence of overlap between the isotope values for these sources, emphasizing the amount of variation within these groupings and suggesting the need for additional proxy data to clearly define the aquatic, soil, and plant samples.

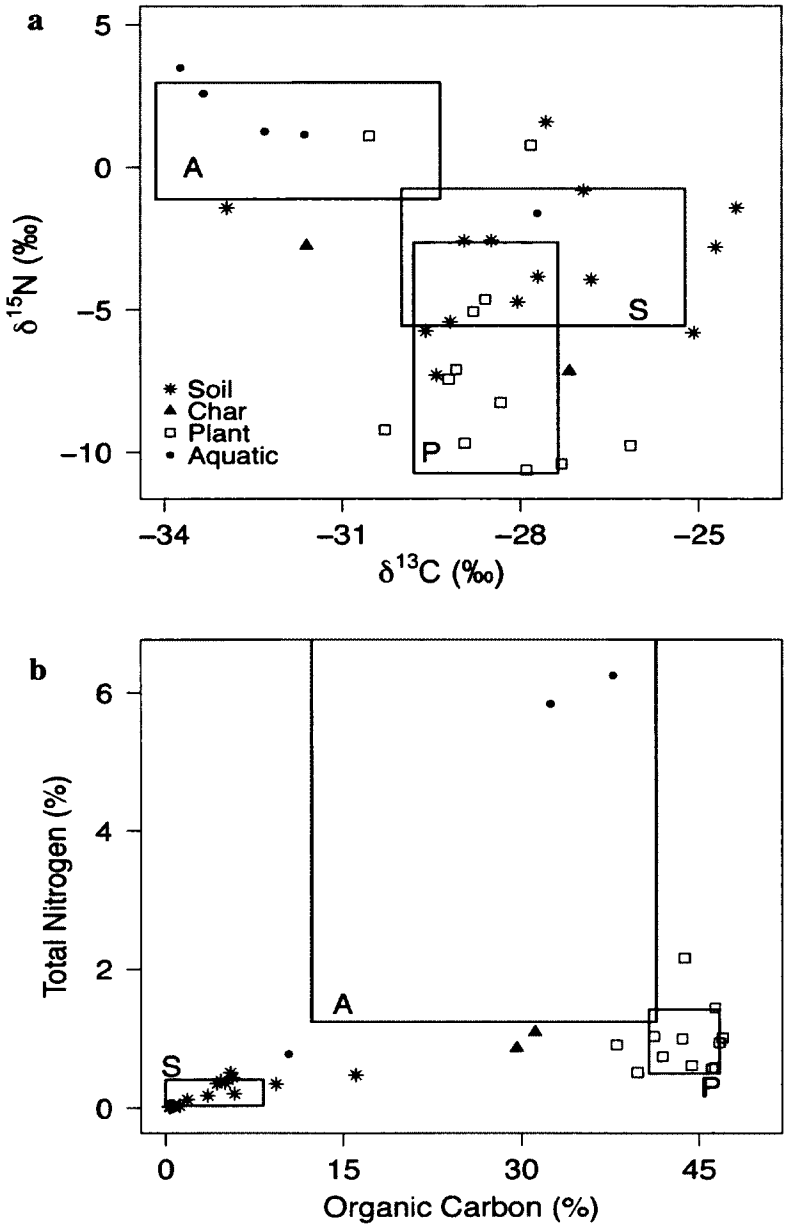

Figure 3-6. End member results from Principle Components Analysis.
These plots show the scores (panels a and c) and loadings (panels b and d) for two Principal Components Analyses that were run to evaluate the source of variability in OM samples collected from the upper Yuba River watershed. Plots of the scores highlight differences between aquatic (blue), plant (green), soil (purple) and charcoal (black) OM sources. PCA 1 (panels a and b) analyzed differences between aquatic and terrigenous OM sources using fatty acid, sterol, and alcohol biomarkers. PCA 2 focused exclusively on terrigenous OM sources and included both lipid and lignin biomarkers.

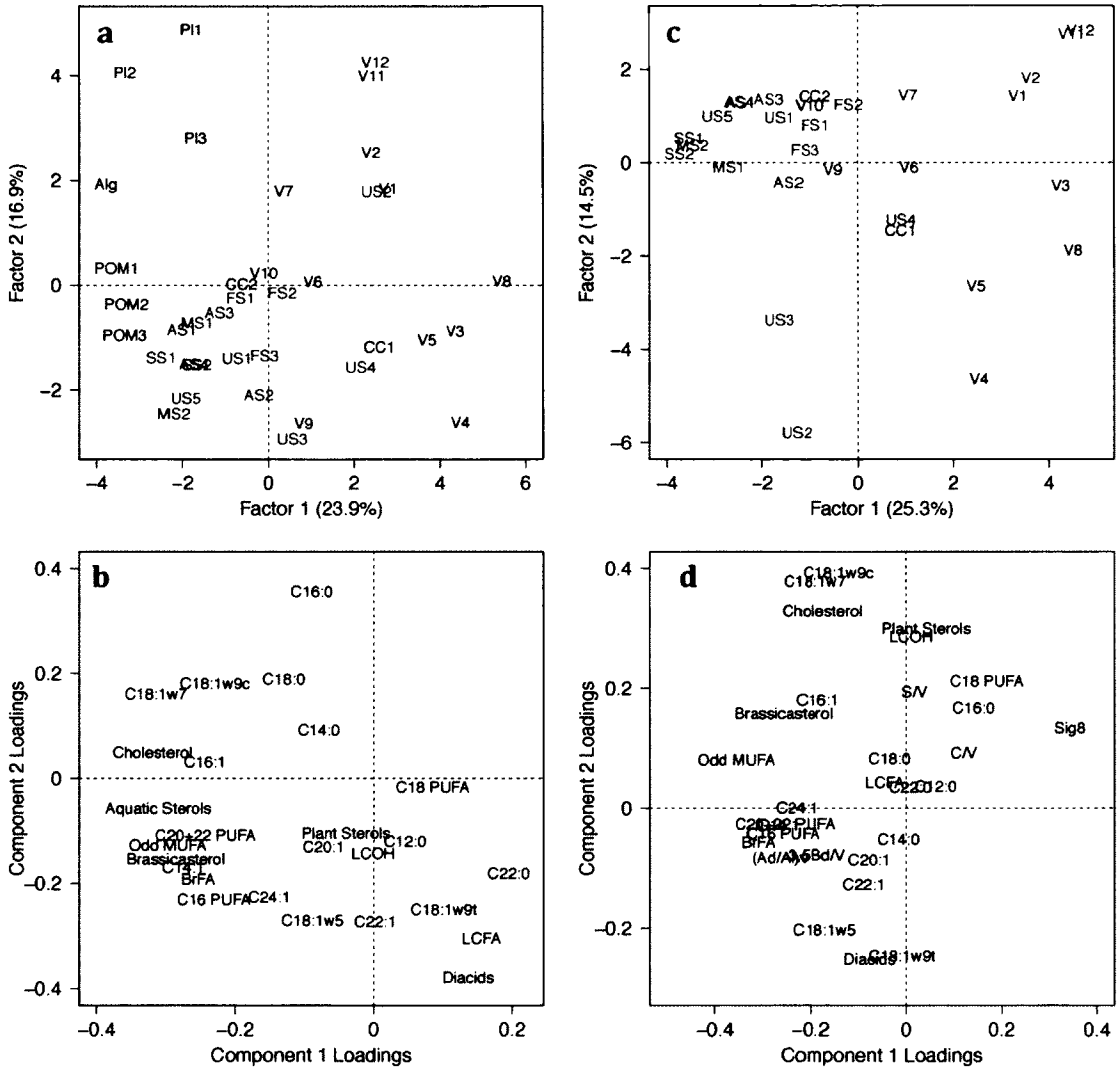

Table 3-1. Description of end member samples.
Description of samples collected from upper Yuba River watershed. The IDs are assigned based on the type of OM source represented by each sample collected from the North Yuba River (NYR), Middle Yuba River (MYR), South Yuba River (SYR), and Englebright Lake. In these samples MS = mining soils, US = urban soils, FS = forest soils, SS = subsurface soils, AS = agricultural soils, CC = charcoal, V = vegetation, PL = plankton, POM = particulate matter collected from lake water, and ALG = algal biofilm. The Munsell Soil Color is reported in parentheses in the description for all soil samples

ID	Type	Latitude	Longitude	Description
MS1	Soil	39° 22' 13"N	120° 59' 50"W	Mining soil, North Columbia Mine (10YR 7/2)
MS2	Soil	39° 22' 00"N	120° 55' 32"W	Mining soil, Malakoff Diggins SHP[a] (2.5Y 7/2)
US1	Soil	39° 22' 11"N	121° 06' 17"W	Urban soil, North San Juan (2.5Y 4/4)
US2	Soil	39° 19' 13"N	120° 33' 54"W	Urban soil, HWY 80 construction Site (2.5Y 3/3)
US3	Soil	39° 20' 03"N	120° 24' 12"W	Urban soil, Donner Summit PUD[b] (2.5Y 3/3)
US4	Soil	39° 33' 57"N	120° 38' 09"W	Urban soil, Sierra City (2.5Y 5/3)
US5	Soil	39° 33' 36"N	120° 49' 43"W	Urban soil, Downieville (2.5Y 6/3)
FS1	Soil	39° 24' 28"N	120° 58' 11"W	Forest soil, MYR watershed (7.5Y 3/3)
FS2	Soil	39° 22' 24"N	120° 46' 18"W	Forest soil, SYR watershed (2.5Y 6/2)
FS3	Soil	39° 23' 55"N	121° 07' 57"W	Forest soil, NYR watershed (7.5YR 5/6)
SS1	Soil	39° 14' 36"N	121° 15' 19"W	Subsurface soil, roadside outcrop (10YR 5/6)
SS2	Soil	39° 23' 50"N	121° 08' 00"W	Subsurface soil, lakeside outcrop (10YR 5/6)
AS1	Soil	39° 14' 53"N	121° 16' 32"W	Agricultural soil, rangeland (7.5YR 4/4)
AS2	Soil	39° 22' 17"N	121° 04' 22"W	Agricultural soil, organic farm (7.5YR 4/3)
AS3	Soil	39° 20' 21"N	121° 03' 25"W	Agricultural soil, vineyard (10YR 4/4)
AS4	Soil	39° 20' 20"N	121° 03' 19"W	Agricultural soil, vineyard (10YR 4/3)
CC1	Charcoal	39° 23' 55"N	121° 07' 57"W	Litter, natural forest fire site
CC2	Charcoal	39° 14' 56"N	121° 17' 11"W	Litter, natural controlled fire site
V1	Vegetation	39° 14' 53"N	121° 16' 32"W	*Trifolium hirtum* (Rose Clover)
V2	Vegetation	39° 14' 53"N	121° 16' 32"W	*Linum bienne* (Narrow Leaf Flax)

V3	Vegetation	39° 14' 53"N	121° 16' 32"W	*Bromus secalinus* (Chess Brome)
V4	Vegetation	39° 22' 24"N	120° 46' 18"W	*Pseudotsuga menziesii* (Douglas Fir)
V5	Vegetation	39° 22' 24"N	120° 46' 18"W	*Pinus lambertiana* (Sugar Pine), fresh needles
V6	Vegetation	39° 22' 24"N	120° 46' 18"W	*Pinus lambertiana* (Sugar Pine), needle litter
V7	Vegetation	39° 23' 55"N	121° 07' 57"W	*Pteridium aquilinum* (Western Bracken Fern)
V8	Vegetation	39° 23' 55"N	121° 07' 57"W	*Quercus chrysolepis* (Canyon Oak)
V9	Vegetation	39° 23' 55"N	121° 07' 57"W	Mixed bark samples
V10	Vegetation	39° 14' 28"N	121° 15' 51"W	*Leskeella nervosa* (Leskeella moss)
V11	Vegetation	39° 14' 28"N	121° 15' 51"W	*Scutellaria galerculuta* (Marsh Skullcap)
V12	Vegetation	39° 14' 28"N	121° 15' 51"W	*Juncus effusus* (Common Rush)
PL1	Aquatic	39° 14' 28"N	121° 15' 52"W	Plankton, 26 ft vertical tow in Englebright Lake
PL2	Aquatic	39° 16' 33"N	121° 13' 20"W	Plankton, 26 ft vertical tow in Englebright Lake
PL3	Aquatic	39° 17' 39"N	121° 12' 40"W	Plankton, 30 s tow in 1.9 m^3 s^{-1} current
POM1	Aquatic	39° 14' 28"N	121° 15' 52"W	POM filtered through 0.7 μm filter
POM2	Aquatic	39° 16' 33"N	121° 15' 40"W	POM filtered through 0.7 μm filter
POM3	Aquatic	39° 17' 39"N	121° 12' 40"W	POM filtered through 0.7 μm filter
ALG	Aquatic	39° 14' 26"N	121° 16' 02"W	Algae biofilm scraped from dock

a: State Historic Park, b: Public Utility District

Table 3-2. List of proxy data for end member samples.
TOC, TN, $C:N_a$ and stable isotope values for soil, vegetation and aquatic samples collected from the upper Yuba River watershed. Samples for which values were below detection are noted as not detected (n.d.). The mean and standard deviation are reported for soil, char, vegetation, and aquatic sample groups.

ID	TOC (%)	TN (%)	$C:N_a$	$\delta^{13}C_{TOC}$	$\delta^{15}N_{TN}$
MS1	0.36	0.01	27.87	-26.81	-3.94
MS2	0.45	0.03	17.38	-27.71	-3.84
US1	4.63	0.39	11.79	-27.57	1.57
US2	1.12	0.03	32.29	-28.54	n.d.
US3	1.17	0.03	35.85	-24.36	-1.44
US4	3.55	0.18	20.25	-23.42	-0.57
US5	1.82	0.12	15.20	-24.71	-2.80
FS1	5.78	0.20	28.42	-25.09	-5.80
FS2	16.05	0.48	33.78	-29.59	-5.75
FS3	9.29	0.34	27.01	-28.05	-4.73
SS1	0.27	0.02	13.50	-32.94	-1.44
SS2	0.61	0.03	20.17	-28.49	-2.57
AS1	4.33	0.35	12.42	-29.41	-7.30
AS2	5.45	0.50	10.80	-26.94	-0.82
AS3	5.61	0.43	12.99	-29.18	-5.43
AS4	5.00	0.36	14.01	-28.94	-2.59
Soil	4.09 ± 4.12	0.22 ± 0.18	21.49 ± 9.10	-27.61 ± 2.39	-3.16 ± 2.40
CC1	31.15	1.09	28.56	-27.18	-7.16
CC2	29.61	0.86	34.43	-31.60	-2.76
Charcoal	30.38 ± 1.09	0.98 ± 0.16	30.54 ± 3.59	-29.39 ± 3.12	-4.96 ± 3.11
V1	41.89	0.74	56.58	-29.21	-7.44
V2	44.37	0.61	72.53	-29.08	-7.10

V3	39.80	0.51	77.86	-30.29	-9.22
V4	46.69	0.94	49.77	-28.94	-9.69
V5	46.31	0.58	79.68	-26.15	-9.77
V6	46.96	1.01	46.51	-27.90	-10.62
V7	43.75	2.16	20.28	-28.79	-5.06
V8	46.33	1.44	32.19	-28.33	-8.25
V9	46.07	0.57	81.51	-27.31	-10.41
V10	41.15	1.03	39.95	-28.59	-4.64
V11	38.02	0.91	41.78	-30.54	1.09
V12	43.57	1.00	43.78	-27.82	0.77
Vegetation	43.74 ± 2.96	0.96 ± 0.46	55.73 ± 21.19	-28.58 ± 1.21	-6.69 ± 4.05
PL1	37.73	6.25	6.04	-33.72	3.48
PL2	32.46	5.84	5.56	-33.33	2.58
PL3	10.37	0.78	13.38	-27.71	-1.62
POM1	n.d.	n.d.	n.d.	n.d.	n.d.
POM2	0.18a	0.02a	9.88	-31.63	1.13
POM3	0.16a	0.02a	7.96	-32.31	1.26
ALG	n.d.	n.d.	n.d.	n.d.	-1.29
Aquatic	26.85 ± 14.52	4.29 ± 3.05	8.50 ± 3.40	-31.74 ± 2.39	0.92 ± 2.04

a: TOC and TN for POM samples are reported in mg L^{-1}, and are not included in the calculation of mean aquatic TOC and TN

Table 3-3. Fatty acids biomarker concentrations for end member samples.
Fatty Acid (FA) data for samples collected from the upper Yuba River watershed. Long chain FA (LCFA), short chain FA (SCFA), polyunsaturated C16, C18, and C20+C22 FA, branched FA (BrFA) and diacids are reported as percent (%) of the total FA. Total FA are reported in $\mu g\ g^{-1}$.

ID	LCFA	SCFA	Polyunsaturated FA			BrFA	Diacids	Total FA ($\mu g\ g^{-1}$)
			C16	C18	C20+C22			
Soil								
MS1	11.6	47.3	0.0	5.5	0.0	0.6	2.0	25.8
MS2	17.4	25.6	0.0	14.2	2.0	3.8	0.5	19.2
US1	27.7	19.4	0.0	2.5	0.0	3.9	17.5	100.8
US2	2.8	31.5	0.0	0.0	0.0	0.0	5.6	57.0
US3	7.7	11.5	0.0	1.9	15.3	0.0	16.9	59.2
US4	11.2	16.5	0.0	26.4	0.0	0.0	10.6	134.0
US5	26.6	12.3	0.0	8.9	0.7	2.8	0.0	47.3
FS1	15.3	46.7	0.0	4.3	0.0	2.0	0.4	205.9
FS2	27.3	30.3	0.0	5.4	0.0	1.1	1.6	319.4
FS3	29.5	25.7	0.0	3.1	0.0	2.7	2.8	189.6
SS1	9.3	31.7	0.0	7.8	0.5	1.5	2.0	15.8
SS2	6.5	19.6	0.0	20.5	2.4	1.2	1.1	54.2
AS1	12.3	23.9	0.0	6.9	1.3	2.4	0.6	162.7
AS2	22.5	20.4	0.0	9.7	0.0	4.1	3.9	64.2
AS3	35.4	16.8	0.0	4.4	0.3	1.8	0.5	125.2
AS4	18.8	21.7	0.0	10.5	1.5	3.2	0.5	130.8
Charcoal								
CC1	30.2	19.5	0.0	4.9	0.0	1.9	7.2	929.7
CC2	8.5	33.9	0.0	21.7	0.2	1.3	0.3	1011.5
Vegetation								
V1	15.5	38.1	0.0	20.4	0.0	0.0	1.1	1244.2
V2	11.3	40.2	0.0	12.1	0.8	0.0	0.8	2604.8

V3	15.3	28.1	0.0	19.5	0.0	0.0	1.9	1550.4
V4	10.5	19.0	0.0	29.3	1.7	6.1	8.4	2951.3
V5	10.7	31.8	0.0	13.8	0.0	1.1	6.3	1861.7
V6	4.6	37.2	0.0	29.7	0.3	1.3	0.2	4504.6
V7	8.1	41.4	0.0	21.6	2.3	0.4	0.0	3060.9
V8	20.1	29.0	0.0	24.7	0.0	0.0	4.9	1923.1
V9	39.8	9.0	0.0	7.4	0.6	2.1	8.1	808.7
V10	4.4	17.0	0.0	45.0	13.3	0.9	2.6	1820.8
V11	6.7	35.9	0.0	37.7	0.0	0.0	0.0	1745.1
V12	3.2	29.8	0.0	44.2	0.0	0.0	0.0	3125.1
Aquatic								
PL1	15.5	57.2	0.0	2.1	0.3	2.9	0.0	8422.9
PL2	11.3	59.0	0.0	3.4	0.5	2.8	0.0	8185.4
PL3	15.3	68.1	0.0	1.2	0.2	1.4	0.0	2470.7
POM1	10.5	50.9	0.0	18.4	2.2	1.0	0.0	12.4[a]
POM2	10.7	34.9	0.0	31.4	0.0	1.8	0.0	10.5[a]
POM3	4.6	58.5	0.0	3.5	0.0	1.5	0.0	6.8[a]
ALG	8.1	43.8	1.9	16.0	3.0	1.8	0.0	1477.5

a: TOC and TN for POM samples are reported in $\mu g\ L^{-1}$

Table 3-4. Sterol biomarker concentrations for end member samples.
Sterol data for samples collected from the upper Yuba River watershed are presented as a percent (%) of the total sterol concentration. Aquatic sterols include 27-nor-methylcholesta-5,22-dien-3β-ol and cholesta-5,22-dien-3β-ol, and plant sterols are the sum of campesterol, stigmasterol, and β-sitosterol. Total sterol concentrations are reported in $\mu g\ g^{-1}$.

ID	Aquatic Sterols	Brassicasterol	Cholesterol	Plant Sterols	Total Sterols ($\mu g\ g^{-1}$)
Soil					
MS1	0.0	9.0	1.8	79.4	1.8
MS2	0.0	8.3	3.0	88.7	2.1
US1	0.0	2.4	5.8	91.8	50.6
US2	0.0	0.0	0.0	0.0	0.0
US3	0.0	0.0	0.0	100.0	1.0
US4	0.0	3.2	2.2	90.6	16.7
US5	0.0	2.6	6.1	91.3	7.8
FS1	0.0	6.8	3.2	90.0	13.1
FS2	0.0	3.3	1.3	94.1	63.4
FS3	0.0	5.5	1.2	91.0	46.2
SS1	0.0	5.8	5.2	89.0	0.4
SS2	0.0	11.7	1.1	87.2	87.2
AS1	0.0	2.1	3.0	94.9	19.0
AS2	0.2	0.1	5.0	69.0	21.1
AS3	0.0	3.9	2.3	93.8	29.5
AS4	0.0	3.6	4.8	91.6	21.2
Charcoal					
CC1	0.0	3.2	0.0	88.1	125.6
CC2	0.0	2.1	1.0	96.9	62.4
Vegetation					

V1	0.0	0.0	0.0	100.0	248.4
V2	0.0	0.0	2.3	97.7	441.8
V3	0.0	0.0	0.0	88.6	370.2
V4	0.0	0.0	0.0	100.0	1171.0
V5	0.0	2.8	0.0	97.2	1413.2
V6	0.0	0.0	0.0	100.0	696.6
V7	0.0	0.0	2.2	97.8	681.8
V8	0.0	0.0	0.0	100.0	5416.4
V9	0.2	2.5	0.3	89.3	496.6
V10	0.0	1.2	0.3	98.5	743.1
V11	0.0	0.0	0.3	99.7	368.1
V12	0.0	0.0	0.8	96.4	704.9
Aquatic					
PL1	2.3	5.7	75.5	16.5	520.3
PL2	4.1	1.3	84.6	9.7	1164.9
PL3	1.5	2.9	32.4	63.2	52.2
POM1	6.6	9.4	18.3	65.7	1.0
POM2	5.8	20.0	16.6	57.6	0.7
POM3	5.9	8.3	19.7	66.1	0.8
ALG	1.4	8.4	25.2	65.1	37.1

Table 3-5. Lignin biomarker values for end member samples.
Lignin data for soil, vegetation and charcoal samples collected from the upper Yuba River watershed. The sum of 8 lignin phenols (Σ8) are reported in mg g^{-1}, and the carbon normalized lignin concentrations (Λ8) are reported in mg g_{OC}^{-1}. Ratios of lignin phenols, including C/V, S/V, (Ad/Al)v, and 3,5-Bd:V are also presented here. Samples for which lignin values are not available are noted as n.a. The mean and standard deviation are reported for soil, char, vegetation, and aquatic sample groups.

ID	Σ8	Λ8	C/V	S/V	(Ad/Al)v	3,5-Bd:V
Soil						
MS1	0.02	0.52	0.70	0.24	0.49	0.20
MS2	0.04	0.95	0.14	0.22	0.51	0.07
US1	1.16	2.51	1.09	1.04	0.37	0.06
US2	0.03	0.26	0.14	0.25	0.81	0.19
US3	0.09	0.79	0.17	0.24	0.43	0.06
US4	0.48	1.35	0.56	0.28	0.31	0.05
US5	0.43	2.34	0.39	0.48	0.44	0.02
FS1	2.22	3.85	0.13	0.14	0.39	0.03
FS2	5.07	3.16	0.26	0.15	0.33	0.06
FS3	2.51	2.70	0.15	0.18	0.32	0.06
SS1	0.01	0.49	1.09	0.43	0.68	0.13
SS2	0.01	0.20	0.73	0.02	1.05	0.10
AS1	0.71	1.65	0.83	0.34	0.41	0.08
AS2	1.06	1.94	0.56	0.18	0.43	0.04
AS3	1.38	2.46	1.05	0.43	0.36	0.07
AS4	0.78	1.57	0.64	0.36	0.45	0.07
Charcoal						
CC1	7.96	2.55	0.11	0.16	0.42	0.06
CC2	2.93	0.99	1.16	0.38	0.69	0.08
Vegetation						

V1	14.90	3.56	1.78	0.19	0.17	0.02
V2	34.13	7.69	0.90	0.08	0.14	0.00
V3	43.95	11.04	1.62	1.43	0.13	0.00
V4	5.90	1.26	0.07	0.56	0.24	0.06
V5	17.29	3.73	0.01	0.18	0.28	0.02
V6	17.78	3.79	0.01	0.31	0.18	0.03
V7	11.82	2.70	0.00	0.73	0.20	0.06
V8	18.04	3.89	1.12	0.31	0.20	0.04
V9	40.36	8.76	4.04	0.10	0.23	0.05
V10	0.76	0.18	0.45	0.74	0.58	0.71
V11	43.31	11.39	5.62	0.58	0.14	0.00
V12	32.93	7.56	1.98	4.78	0.20	0.02
Aquatic						
PL1	n.a.	n.a.	n.a.	n.a.	n.a.	n.a.
PL2	n.a.	n.a.	n.a.	n.a.	n.a.	n.a.
PL3	n.a.	n.a.	n.a.	n.a.	n.a.	n.a.
POM1	n.a.	n.a.	n.a.	n.a.	n.a.	n.a.
POM2	n.a.	n.a.	n.a.	n.a.	n.a.	n.a.
POM3	n.a.	n.a.	n.a.	n.a.	n.a.	n.a.
ALG	n.a.	n.a.	n.a.	n.a.	n.a.	n.a.

CHAPTER 4: ORGANIC MATTER ACCUMULATION IN A GILBERT-TYPE DELTA: ENGLEBRIGHT LAKE, CALIFORNIA, USA

Pondell, C.R.

Canuel, E.A

Abstract

The global proliferation of dams has been one of the most significant anthropogenic impacts on the environment, and as a result, massive loads of sediment and nutrients are trapped in impoundments each year. Few studies, however, have examined the sediments trapped behind dams to understand patterns of organic carbon accumulation and the effects of watershed processes on carbon delivery. This study measured total organic carbon (TOC) and stable isotopes of carbon and nitrogen ($\delta^{13}C$ and $\delta^{15}N$) in Englebright Lake, CA to relate changes of organic carbon (OC) sources and TOC accumulation to natural (i.e., floods) and anthropogenic (i.e., mining and water management) impacts in the watershed and to depositional processes in the lake. Englebright Lake, characterized as a Gilbert-type delta (a wedge shaped delta comprised of topset, foreset and bottomsept deposits), is a representative system for impoundments in small, mountainous rivers, and anthropogenic disturbances (i.e., mining) in the watershed caused high sediment accumulation rates in the lake. $\delta^{13}C$ signatures indicated that more than 50% of OC in Englebright Lake was derived from terrigenous sources, and throughout the 60-year lake history, 0.35 Tg OC was trapped behind Englebright Dam. TOC in topset deposits was less than TOC in foreset and bottomset deposits ($p < 0.001$), and TOC accumulation associated with flood events was higher (up to 231 $kg_{OC}\ m^{-2}\ yr^{-1}$) than TOC accumulation during non-event periods (0.2 to 39 $kg_{OC}\ m^{-2}\ yr^{-1}$). OC burial and TOC accumulation rates in Englebright Lake were up to an order of magnitude higher than previous estimates of OC burial in impoundments, suggesting that as the level of anthropogenic modification (e.g., mining, agriculture, urbanization) intensifies, the potential for impoundments to trap terrestrial OC will continue to increase.

Introduction

Human activities first began to alter sediment delivery to estuaries and coasts approximately 3000 years ago (Ruddiman 2003), but the magnitude of impact from human activities has intensified in the past 100-300 years (Lotze et al. 2006). Changes in land-use, including deforestation (Gomez 2004), agriculture (Restrepo and Syvitski 2006) and mining (Smith and Jol 1997) have increased sediment yields from rivers, while water management projects such as dam and levee construction have decreased riverine sediment yields (Wright and Schoellhamer 2004; McCarney-Castle et al. 2010). On average, human activities have decreased sediment fluxes from rivers to the ocean by more than 2500 Tg yr^{-1} within the past 70 years (Milliman and Farnsworth 2011), with an estimated 100,000 Tg of sediment trapped in man-made impoundments (Syvitski et al. 2005). Since the 1920s, the era of dam building has reduced sediment transport in a majority of the world's rivers by at least 20% and in some extreme cases, including the Colorado, Yellow, Krishna, Indus, Nile, and Rio Grande rivers, dams have reduced the sediment load by 90 to 100% (Walling 2006; Milliman and Farnsworth 2011; Syvitski and Kettner 2011).

The construction of dams has had a major impact not only on sediment loads and fluxes over the last century, but also on the biogeochemical cycling and transfer of nutrients and organic matter between terrestrial and marine systems (Ludwig et al. 2009, Sanchez-Vidal et al. 2013). Reservoirs and lakes are responsible for a majority of the terrestrial carbon sequestration in terrestrial systems (Smith et al. 2001; Stallard 2012), and represent a significant global sedimentary-carbon sink. Annual carbon burial in eutrophic impoundments are estimated at 200 Tg OC yr^{-1} (Mulholland and Elwood 1982; Dean and Gorham 1998), which is similar to the estimated amount of organic carbon buried annually in the world's oceans (Downing et al. 2008). This implies that total carbon burial in impoundments may be twice as high as carbon sequestration in marine sediments (Dean and Gorham 1998), highlighting the impact of man-made reservoirs on the transport of sediment and associated materials to both terrestrial systems and the coastal ocean.

While the socio-economic benefits of dams are numerous, the sediment trapping efficiency of dams is mainly viewed as a negative environmental impact (Kondolf 1997; Bergkamp et al. 2000; Kingsford 2001; Crossland et al. 2005). However, human environmental impacts offer opportunities to explore ecosystem processes using new chemical tracers, such as synthetic compounds or radionuclides, or to use new study systems to examine natural responses to large-scale forcings (Charlesworth and Lees 1999; Wolf et al. 2012). Impoundments, for example, provide high-resolution records of organic matter and sediment accumulation over the past century in relatively well-monitored regions.

Documenting organic carbon accumulation patterns in delta systems also provides an opportunity to better delineate fluvial and biogeochemical systems, and impoundments offer an ideal location for high-resolution investigations of the development of Gilbert-type deltas within a well-constrained basin and time frame. Gilbert-type deltas (Gilbert 1890) are defined according to depositional regimes that are based on sediment accumulation patterns and redistribution processes (Hansen 2004; Rojas and Le Roux 2010). Topset deposition is characterized by gently sloping, coarse-grain sediment horizons, and is typically found in the region of the delta closest to the river influence. Foreset deposits are steeply sloping (~34°) laminations of fine sediments interrupted by layers of coarse material, and are found at the prograding delta front. Bottomset deposits are found in regions with low energy and are identified by horizontal laminations of fine silt and clay. This clinoform depositional pattern has been recognized in modern and ancient lakes (i.e., Smith and Jol 1997; Rojas and Le Roux 2010) and marine deltas worldwide (Kuehl et al. 1997; Falk and Dorsey 1998; Malartre et al. 2004). This study examined organic carbon burial in a representative impoundment in northern California over a 60 year time period to evaluate the amount and sources of organic carbon being trapped, and to investigate the relationship between organic carbon accumulation and the three depositional regimes associated with Gilbert-type deltas.

Study Site

Dam have been built extensively throughout California to prevent flooding, confine mine tailings from the historic Gold Rush, for hydroelectric power and recreation, and to divert water for agricultural needs (Mount 1995). Approximately 1600 dams have been installed along the waterways of Californian rivers (www.damsafety.org), creating a highly managed network of water flow throughout the state. The Sacramento-San Joaquin River Delta drains 67% of California, and over 200 large dams, including three of the largest dams (Shasta, Oroville and Folsom) control the flow to the Sacramento-San Joaquin River Delta.

Englebright Lake, which lies behind the Englebright Dam, is an impoundment on the Yuba River in northern California (Figure 4-1) and its sediments provide a record of changes to its watershed over the past ~60 years (Table 4-1). The Yuba River is a tributary of the Feather River, which flows into the Sacramento River and eventually to northern San Francisco Bay. The Yuba River has three tributaries that drain a 3468 km^2 area of the Sierra Nevada mountain range and that converge just upstream of Englebright Lake (Figure 4-1). Englebright Dam was built in 1940 to trap mine tailings from hydraulic gold mining in the late 19^{th} century (James 2005). Currently, Englebright Dam and its impoundment provide a minor source of hydroelectric power and recreation to the surrounding community.

Previous Work in Englebright Lake. In 2001 the U.S. Geological Survey (USGS) conducted studies in Englebright Lake to determine the feasibility of removing the dam in order to increase spawning areas for anadromous salmon populations. This investigation included a bathymetric survey, which concluded that 21.9 million cubic meters of sediment had accumulated in Englebright Lake during its 60 year history, decreasing the storage capacity of Englebright Lake by 25.5% (Childs et al. 2003). An extensive coring campaign in 2002 obtained cores that were subsequently analyzed for sediment grain size and organic content by loss on ignition (LOI) (Snyder et al. 2004a), trace metal and mercury content (Alpers et al. 2006), and radioisotopic (^{137}Cs and ^{210}Pb) sediment dating (Snyder et al. 2006) to characterize the sediments that accumulated after the construction of the dam. Additionally, conceptual models of sediment accumulation

were constructed using these data and hydrologic records from the system to describe the depositional history (Snyder et al. 2006).

Methods

Sample Collection and Analysis

As a part of the USGS investigation, six sediment cores were collected along the thalweg, or deepest channel, of Englebright Lake in 2002 (Figure 4-1). These cores were subsampled for the present study in 2009 to analyze organic carbon accumulation throughout the lake. Ten-centimeter-thick samples (equivalent to ~40 cm^3 of sediment) were collected at 20-cm intervals from cores 1 and 4 and at 50-cm intervals from cores 6 and 7. Twenty-centimeter samples (~60 cm^3 of sediment) were collected from cores 8 and 9 at 50-cm intervals owing to their coarser texture (Snyder et al. 2004a), thus requiring larger volumes for organic carbon analyses. This sampling strategy provided a 1- to 5-year resolution of sediment accumulation based on sedimentation rates determined by Snyder et al (2006). After sediment cores from Englebright Lake were subsampled from the USGS sediment library in Menlo Park, CA, they were transferred to the Virginia Institute of Marine Science, stored in combusted glass vials at -80 °C and freeze-dried prior to organic carbon analysis.

Total Nitrogen and Organic Carbon Analysis. Freeze-dried sediments were homogenized before analysis for total organic carbon (TOC) and total nitrogen (TN). Aliquots of 18 to 23 mg of sediment (30-100 mg for coarse grain sediments from cores 8 and 9) were weighed into acetone rinsed 5x9 mm tin capsules. The samples were acidified (10% HCl) to remove inorganic carbon prior to analysis (Hedges and Stern 1984) and then dried at 60 °C overnight. They were crimped into small cubes and analyzed with a Carlo Erba Flash EA 1112 series Elemental Analyzer. Standards were run after every ten samples to verify the accuracy of the instrument; replicate analyses showed that variability between samples was generally less than 10%, although the variability was somewhat greater in samples with low organic content (< 0.1 %).

Stable Carbon and Nitrogen Isotope Analyses. Samples for stable isotope analyses were prepared similarly to those analyzed for TOC and TN. Aliquots of sediment were weighed, acidified, and packaged for stable carbon and nitrogen isotope analyses ($\delta^{13}C$ and $\delta^{15}N$) using a Costech ECS 4010 CHNSO Analyzer (Costech Analytical Technologies, Inc.) connected to a Delta V Advantage Isotope Ratio Mass Spectrometer with the Conflo IV interface (Thermo Electron North America, LLC). Carbon and nitrogen stable isotope values are reported using the delta (δ) notation defined relative to isotope ratios in standard reference material (PeeDee belemnite limestone for $\delta^{13}C$ and air for $\delta^{15}N$). Variability between samples was, on average, less than 10%.

Data Analysis

Sediment accumulation rates, determined using plutonium radioisotopic profiles (Pondell et al. in prep.), were used to calculate mass accumulation rates and to identify flood event layers in Englebright Lake sediments. Depth profiles of $^{239+240}Pu$ were used to identify the 1954 and 1963 horizons, and these horizons and their corresponding depths were used to calculate vertical sediment accumulation rates between 1940-1954, 1954-1963 and 1963-2002. A combination of the dating profile provided by plutonium radioisotope concentrations, %TOC profiles for each core, and records of historic events in the watershed (Table 4-1) were used to identify flood layers corresponding to the 1964 and 1997 floods in core 4 and to the 1964 flood in core 7. Additionally, event layers in core 4 were characterized by relatively coarse grain sediments (>150μm), while thick organic deposits dominated the 1964 event horizon in core 7 (Snyder et al. 2004a). Event layers identified in this study agreed well with those identified by the previous USGS study (Snyder et al. 2006).

Rates of mass accumulation of organic carbon in Englebright Lake were calculated using TOC content, dry bulk density data from Snyder et al. (2004), and sediment accumulation

rates determined with $^{239+240}$Pu profiles from Pondell et al. (in prep.). Mass accumulation rates (MAR) were then multiplied by the TOC content to determine mass accumulation rates for TOC (MAR_{OC}). Accumulation was calculated for each of the six regions of the lake by multiplying MAR_{OC} by the area of the lake represented by each core (Table 4-2). Total carbon burial in Englebright Lake since 1940 was then calculated as the sum of carbon buried these six regions. Mass accumulation of TN was calculated similarly using %TN rather than %TOC. MAR_{TN} was not calculated for cores 8 and 9 because only 40% of the samples had reliable measurements of TN (> 15μg).

Stable carbon and nitrogen isotope values from multiple aquatic and terrigenous organic matter sources were used in a 3-end-member mixing model to proportion contributions of these sources to sediments in Englebright Lake. End-member values of soils and C3 plants from terrigenous sources (Source 1) and freshwater plankton, particulate organic matter, and algae from aquatic sources in Englebright Lake (Source 2) had $\delta^{13}C_{TOC}$ values of -28.5 ± 0.9‰ and -31.7 ± 2.4‰, respectively (Pondell and Canuel in prep.). Published $\delta^{13}C_{TOC}$ values for benthic diatoms and freshwater seston were used to represent Source 3 ($\delta^{13}C_{TOC}$ = -21.0 ± 5.3‰ and $\delta^{15}N_{TN}$ = 0.9 ± 2.0‰; Cloern et al. 2002) because the sediment stable isotope values were not captured entirely by a survey of end-members from the watershed (Pondell and Canuel in prep.). The minimum and maximum possible contributions (minmax solutions) from each of these three sources were calculated using the following equations from Fry (2006).

$$f_1 + f_2 + f_3 = 1 \text{ and}$$
$$\delta_1 f_1 + \delta_2 f_2 + \delta_3 f_3 = \delta S * 1$$

f_1, f_2, and f_3 refer to the fraction of organic matter contributed from Source 1, Source 2 and Source 3, respectively, and these fractions are multiplied by the mean $\delta^{13}C$ or $\delta^{15}N$ values from each source to estimate the $\delta^{13}C$ or $\delta^{15}N$ values of the samples (δS). These equations were applied to mean $\delta^{13}C$ and $\delta^{15}N$ values (δS in equation above) for each of the sediment cores. The end-member mixing model was not applied to mean $\delta^{15}N$ for

cores 8 and 9 because the average isotope values for these cores was likely not representative of the total core because less than 40% of these samples had reliable $\delta^{15}N$ values (>15 μg N).

Data were analyzed using R-Studio version 0.97.332, and TOC, MAR_{OC}, and mean grain size data (Snyder et al. 2004) were log-transformed prior to statistical analyses to meet the assumption of normal distribution for the linear regression and t-test analyses.

Results

Sediment characteristics, including grain size and TOC content, varied widely over both spatial and temporal scales in Englebright Lake. Grain size was highest in topset deposits (sand and gravel), lowest in bottomset deposits (silt and clay) and was dominated by sands in the foreset deposits (Table 4-2) (Snyder et al. 2004a). Sediment TOC was inversely related to mean grain size ($R^2 = 0.32$, $p < 0.001$), and this relationship was driven by differences in grain size between depositional regimes (Table 4-2). TOC content ranged from 0.03 to 30.24% of dry weight, and differed across depositional regimes (Figures 4-2 and 4-3). TOC in bottomset (1.15 ± 0.77 %) and foreset deposits (0.89 ± 0.98 %) was higher ($p < 0.001$ for both analyses) than TOC in topset deposits (0.18% ± 0.24%), but there was no statistical difference between TOC in bottomset and foreset deposits (Figure 4-2a). Flood events (Table 4-1) also had a significant impact on TOC in sediments in Englebright Lake, and in all cores, sediments associated with flood events had higher TOC than sediments accumulating during non-flood event periods ($p \leq 0.008$ for all cores). Additionally, there was a trend of increasing %TOC over time in core 4 ($R^2 = 0.66$, $p = 0.04$); however, temporal trends in %TOC content were not detected in the other cores (Figure 4-3).

Across the six cores, $\delta^{13}C$ values ranged between -28‰ and -22‰ and $\delta^{15}N$ values ranged between -4‰ and 4‰. Stable isotope values were relatively constant across depositional regimes, although average $\delta^{13}C$ was significantly higher in foreset deposits

than bottomset deposits ($p = 0.006$; Figure 4-2c and 2d and Figure 4-4a). There was an inverse relationship between depth and $\delta^{13}C$ in cores 4 and 1 ($R^2 = 0.52$ and 0.42, $p = 0.001$ and 0.002, respectively; Figure 4-5). Even though there was a general trend in $\delta^{13}C$ and $\delta^{15}N$ suggesting that TOC and TN sources shift toward more soil and plant inputs during flood events, these trends were not statistically significant (Figure 4-6). As a result, the 3-end-member mixing model was applied to the mean stable isotope values from each core. The isotope mixing model using carbon isotopes indicated a dominance of terrigenous OC sources (> 54%) (Table 4-3), except for core 9 where terrigenous OC contributed as little as 33% of total OC. In contrast, nitrogen isotope data showed that aquatic sources were the dominant (>62%) source of nitrogen in all sediment cores from Englebright Lake, except for core 6 where aquatic inputs were as low as 16% (Table 4-3).

Calculated TOC mass accumulation rates provided estimates for the burial of carbon in Englebright Lake. TOC accumulation rates ranged from 0.66 kg_{OC} m^{-2} yr^{-1} for core 1 during non-event accumulation to 231 kg_{OC} m^{-2} yr^{-1} for event accumulation in core 7 (Table 4-2). On average, accumulation of OC was highest in the foreset region (core 7) and lowest in the topset region (cores 8 and 9) (Figures 4-2b and 4-4). Average TOC accumulation rates in Englebright Lake since 1940 were 4.5 kg_{OC} m^{-2} yr^{-1}, and TOC accumulation was 10- to 20-times greater than TN accumulation rates (Table 4-2). TOC accumulation resulted in the burial of 0.35 Tg of OC in this impoundment since construction of Englebright Dam in 1940. The accumulation of terrestrial OC (OC_T), determined using the terrestrial fraction calculated from the isotope mixing model, was at least 5 Mg OC_T in zone 9 (the area of the lake represented by core 9) and 106 Mg OC_T in zone 4, and between 1940 and 2002 a minimum of 0.23 Tg of OC was sequestered in Englebright Lake.

Discussion

Spatial Trends in Organic Matter Accumulation defined by Depositional Regime

The correlation between organic matter accumulation and grain size in Englebright Lake sediments dictates the connection between sediment depositional patterns and organic mater distribution throughout the lake. The inverse relationship between mean sediment grain size and TOC in Englebright Lake ($R^2 = 0.32, p < 0.001$) is consistent with previous studies showing that a portion of the organic matter associated with sediments is sorbed to mineral grains and fine-grained sediments tend to have higher proportions of organic matter associated with them due to their higher surface area (Keil et al. 1994; Mayer 1994). However, this relationship only applies to Englebright Lake sediments deposited during normal, non-event periods because event horizons, especially in core 7, are characterized by large pieces of organic matter, such as bark and leaves, as well as sediment-associated organic matter.

Organic matter content in the upstream reaches of Englebright Lake, where topset deposits dominate, is lower than in any other depositional setting in the reservoir ($p < 0.01$). Topset deposits usually accumulate where a moving body of water enters a stagnant water body, such as a lake or estuary (Gilbert 1890). At these locations the energy of the system suddenly decreases, and the coarsest particles fall out of suspension or bedload and accumulate. Additionally, these sediments are constantly reworked causing any fine sediment that does accumulate in the topset regions to be winnowed away (Wakeham and Canuel submitted, Rosenbloom et al. 2001) during periods of low river flow or lake surface drawdowns when these deposits are exposed (Snyder et al. 2006). The locations of cores 8 and 9 typify these conditions, which explains the coarse sands and gravels, and subsequently, the low (0.01% to 0.1%) TOC content observed within these deposits.

Bottomset deposition is the most common depositional regime in Englebright Lake, and has been identified in all six cores collected from Englebright Lake. Bottomset deposits characterize sediments of cores 1, 6, and 4, and the bottom approximately seven meters of cores 7, 8 and 9 (Figure 4-4a). Bottomset deposits in cores 1 and 6 show stable accumulation of sediment and OM over time, and reflect a region of low energy due to the presence of the dam, which allows for the settling of fine-grained material from

suspension. Without the presence of Englebright Dam, for instance, the energy from the river's current would be too great to allow the suspended load to settle on the river bed, and this material, with its relatively high organic matter content, would be transported further downstream. Instead, sediments accumulating in cores 1 and 6 likely represent deposition of the suspended load of the Yuba River, and are characterized by fine grain sizes with relatively high OC (mean $TOC_{C1+C6} = 1.0 \pm 0.5$ % during non-event deposition).

Sediments in core 4 are generally defined as bottomset deposits; however, thick layers of coarse silt and sand associated with large events periodically interrupt the accumulation of silt and clay in core 4. These event horizons are characteristic of the highly dynamic nature of distal foreset accumulation typically observed downstream of the delta front (Snyder et al., 2006), and reflect the remobilization of foreset accumulation at the delta front during flood events. As a result, event layers recorded in core 4 have higher TOC due to the accumulation of large pieces of OM (i.e., bark and leaves) during flood events than sediments associated with non-event accumulation ($p < 0.01$), and contribute to the variability in the TOC content of bottomset deposits (Figure 4-2a).

The combination of high variability in both bottomset and foreset deposits associated with the impact of floods influences our ability to resolve differences in the TOC content of these two depositional regimes. In the foreset deposits at the delta front region of Englebright Lake, periods of normal, non-event accumulation are represented as silty deposits, closely resembling characteristics of bottomset deposits in cores 1 and 6 (mean $TOC_{C1+C6} = 1.4\% \pm 0.9\%$ and mean $TOC_{C7} = 0.9\% \pm 0.8\%$). However, sandy deposits interrupt periods of "normal" accumulation during flood events, and high TOC values (15 to 32% TOC) coincide with these event horizons when large amounts of wood and leaf organic matter accumulate. These events result in higher TOC in the foreset deposits relative to bottomset and topset deposits ($p < 0.001$), with 17-fold increases between normal accumulation and event accumulation in core 7.

The greatest response of TOC accumulation to flood events can be seen in the foreset and distal foreset deposits from cores 7 and 4, respectively (Figure 4-3) where TOC ranges from 6 to 10% in the 1964 and 1997 events in core 4, and TOC peaks at 31% in the 1964 event in core 7. However, depth profiles of TOC clearly show the impact of events on TOC accumulation in all cores from Englebright Lake (Figure 4-3) with higher %TOC corresponding to periods of event accumulation ($p < 0.001$ for 1, 4, 7, 8, and 9, and $p = 0.008$ for core 6). The response of TOC to episodic floods is more evident than TOC response to long-term impacts such as mining or agriculture. However, the influence of anthropogenic activities is apparent in the overall high sediment accumulation rates; similar to other study systems, anthropogenic activities in the Englebright watershed have likely increased its vulnerability to erosion during flood events. In the Waipaoa River system in New Zealand, for example, deforestation practices have made the watershed more susceptible to erosion during climate and tectonic events (Goff 1997; Leithold et al. 2013). Similarly, hydraulic mining in California likely altered sediment loads in the tributaries draining into the Sacramento River changing its response to events in the watershed (Schoellhamer et al. 2013). Therefore, the impact of human disturbance (i.e., hydraulic mining) in the Englebright Lake system may have increased the susceptibility of the watershed to high discharge events, resulting in transport of high amounts of organic matter during floods.

Evidence of the impact of hydraulic mining on the Englebright Lake watershed is apparent not only in high sediment accumulation rates and the response of sediment and TOC accumulation to floods, but also in a 10m thick layer of sediment found in the topset deposits that exhibits similar features to mine tailings found throughout the watershed. Coarse (sand and gravel), grey, OC-poor (0.01-0.1%) sediments define this mine tailing deposit between 5 and 15m depth in cores 9 and 8 (Figure 4-3), and are distinct from the finer (silt and sand) tan sediments with higher OC content (mean TOC ~ 1.5%) that characterize the other sediments in Englebright Lake. Additionally, concentrations of trace metals that are naturally found in placer mine tailings, including lead, arsenic, and antimony, are higher in this 10m thick sediment layer, and confirm the placer mine tailing origin of this sediment deposit in cores 8 and 9 (Ashley 2002; Alpers et al. 2006). The

accumulation of this thick layer of mine tailings in Englebright Lake likely results from the mobilization of mine tailings from storage in upstream tributaries during the high discharge events of the early 1960's. Declines in these tailings in more recently deposited sediments may indicate that the impact of hydraulic mining on the Englebright Lake watershed is decreasing as these sediments move out of the tributaries (Schoellhamer et al. 2013).

Sources of Organic Matter to Englebright Lake

Stable isotope values were measured in sediments from Englebright Lake as a proxy for the sources of organic matter delivered to this system, and the values indicate a mixture of freshwater plankton, benthic diatoms and freshwater seston, and terrigenous soil and plant organic matter sources (Figure 4-6). Sources of OM to Englebright Lake, including freshwater plankton, soil, and plants, were characterized by samples of these sources collected throughout the lake and watershed (Pondell et al. in prep.), but these samples only represent a fraction of potential OM sources to Englebright Lake. Based on the distribution of isotopic signatures from Englebright Lake sediments and their relation to freshwater plankton and terrigenous OM sources (Figure 4-6), it appears that stable isotope signatures in the sediments are not completely described by these two end-members. This may be due to an incomplete sampling or potential sources, seasonal changes in OM sources to Englebright Lake, or changing OM sources over the 60-year history of the lake. Diagenesis is another process that alters stable isotope signatures over time and it tends to favor the preservation of lignin and lipids over carbohydrates and proteins, resulting in a 1-2‰ shift toward more negative $\delta^{13}C$ values (Benner et al. 1987). Since all sediment $\delta^{13}C$ signatures in Englebright Lake are more positive than or equal to the OM sources identified from Englebright Lake and its watershed (FW plankton, soils and plants), diagenesis does not explain the $\delta^{13}C$ signatures in the lake sediments and suggests that our sampling of potential sources in Englebright Lake and its watershed did not characterize all possible OM sources. To address the missing OM source to Englebright Lake, a third end-member, benthic diatoms and freshwater seston, was identified as a possible source using results from a more exhaustive study of OM sources

in the San Francisco Bay estuary and delta (Cloern et al. 2002). Benthic diatoms and freshwater seston may be an important OM source to lake sediments, especially in shallow regions where the light availability at the sediment surface is high enough to support benthic communities.

The three end-member model using $\delta^{13}C$ values suggests that terrigenous OM sources (plants and soils) dominate (> 50%) over aquatic sources in Englebright Lake sediments (Table 3). The dominance of terrigenous organic matter in Englebright Lake is similar to previous studies showing the importance of terrestrial sources of carbon in the Sacramento-San Joaquin River Delta, which lies downstream of Englebright Lake (Jassby and Cloern 2000). During event deposits, stable isotope values tend to indicate increased inputs from terrigenous OM sources, but the high variability among sediment isotope signatures prevents us from identifying any significant differences between non-event and event signatures in both the stable isotope values and the relative proportion of OM sources in these samples. Additionally, there are no significant differences in OM sources between depositional regimes, further highlighting the prevalence of the contribution of terrigenous OM to Englebright Lake.

While most $\delta^{13}C$ values from Englebright Lake sediments reflect the dominance of terrigenous OM sources and this source remains relatively constant over time, three cores showed significant changes over time (Figure 4-5). $\delta^{13}C$ values are inversely related to depth in cores 1 and 4 (R^2 = 0.42 and 0.52, p = 0.002 and 0.001 for cores 1 and 4, respectively), and decrease by approximately 2‰ throughout the 60-year accumulation period. Since the freshwater plankton samples have the lowest $\delta^{13}C$ values of the three end-members, these trends might suggest a shift towards greater contributions from aquatic sources over time. This decrease may also reflect increasing diagenetic alteration of the accumulating OM over time associated with changes in delivery (i.e., decreased accumulation rates) or reactivity (i.e., more labile OM from plankton or algae) (Lehmann et al. 2002; Vreča and Muri 2010). These trends are not observed in cores 6, 7 and 8

likely from enhanced preservation due to high sediment accumulation rates or differences in OM inputs.

In core 9, $\delta^{13}C$ shifts from more positive values below 15m to more negative values above 3m. The higher $\delta^{13}C$ values at depth in core 9 are consistent with $\delta^{13}C$ values from benthic diatoms and freshwater seston (Cloern et al. 2002), and may explain why terrigenous inputs at this location are anomalously low relative to inputs to the remaining cores from the lake. $\delta^{13}C$ values in core 9 shift toward more terrigenous inputs after 1970 likely in response to hydrologic changes in the lake. Before 1970, lake levels were drawn down every summer and fall by up to 20m, exposing the shallowest sediments and changing the water depth at core 9 from ~30m to < 10m (Snyder et al. 2006). During these periods of lake drawdowns, the shallower water depths would likely experience increased light availability in some regions of the lake, conditions that promote primary production from benthic autotrophs. Evidence of this is found only in core 9; this may be because core 8 may have been completely exposed during drawdowns while water depths at the location of the remaining cores were likely too deep to support benthic autotrophs. After 1970, the annual lake drawdowns stopped, leaving the whole lake too deep for benthic diatom populations to thrive and resulting in a relative increase in terrigenous inputs to core 9.

Interestingly, while the mixing model using $\delta^{13}C$ values indicates that inputs from aquatic OC sources are lower than inputs from terrigenous OC sources, the model based on $\delta^{15}N$ values suggests that TN in Englebright Lake is dominated by aquatic sources (Table 4-3). This is consistent with the distribution of carbon and nitrogen in aquatic and terrigenous sources. For example, structural components such as cellulose and lignin, which are high in carbon and depleted in nitrogen, are abundant in higher plants, whereas plankton are more nitrogen-rich as evidenced by higher N/C values in plankton than in higher plants (Emerson and Hedges 2008). This suggests that TOC in Englebright Lake sediments derives largely from soil and plant OM sources while TN originates from aquatic plankton.

Temporal trends in OC signatures in Englebright Lake

Profiles of TOC in Englebright respond to periods of increased river discharge, and highlight the impact of flood events on the accumulation of organic carbon in Englebright Lake (Figure 4-3). With the exception of core 4, TOC peaks during flood events, but then returns to a relatively constant baseline during non-event accumulation. There also appears to be a cycle in the TOC content of core 4 over time (Figure 4-3). The periodicity in TOC is approximately 30 years, which is similar to the periodicity of approximately 20-30 years associated with the Pacific Decadal Oscillation (PDO) (Mantua and Hare 2002) and consistent with discharge trends in California. Discharge in California is strongly influenced by climate oscillations, including PDO and the El Niño Southern Oscillation (ENSO). In northern California, discharge from rivers north of ~40°N responds to cold PDO and La Niña events (negative phases of both PDO and ENSO), while river discharge in southern California is controlled by El Niño and warm PDO phases (Milliman and Farnsworth 2011). However, river discharge (from USGS gauging station 11418000 and presented by Snyder et al. 2006) and the corresponding TOC accumulation in Englebright Lake appears to respond similarly to northern California rivers prior to ~1970, and then switches and responds to warm PDO and El Niño during the last 30 years of accumulation (Table 4-1). This shift in the controlling climate patterns on river discharge and sediment and TOC accumulation in Englebright Lake (located at 39°N) may suggest that the latitude at which the influence of PDO and ENSO phases on river discharge in California changes is not fixed, and instead varies by a few degrees north or south over time (personal communication, JD Milliman, March 2014).

On the other hand, this apparent periodicity in TOC from core 4 may simply be the response of organic carbon accumulation to two unusually large floods (i.e., 50- to 100-year flood events) that occurred in the Englebright Lake watershed in 1964 and 1997. Alternatively, it may reflect the changing depositional regimes in the lake over time. The location of the delta front in Englebright Lake, for example, has oscillated between core 8 and core 7 over the 60-year record of sediment accumulation in the lake. The

progradation of the delta front may have caused TOC accumulation in core 4 to increase as the delta front approached its current location during the 1964 and 1997 floods.

TOC Mass Accumulation Rates (MAR_{OC}) in Englebright Lake

In marine systems, the preservation of OC_T depends on energy dynamics and sediment accumulation rates (Blair and Aller 2012). A majority of OC_T preservation takes place on river dominated margins, and Blair and Aller (2012) identify three patterns of OC_T preservation: (1) high energy, mobile muds result in low OC_T preservation (e.g., Amazon Delta), (2) low energy, high accumulation rates lead to high OC_T preservation (e.g., Ganges-Brahmaputra Delta), and (3) high accumulation during episodic events preserves high amounts of OC_T (e.g., small, mountainous rivers). These three OC_T preservation patterns are present in Englebright Lake, and topset deposits preserve OC similar to regions with high energy and mobile muds, bottomset OC accumulation reflects preservation patterns associated with low energy and high sediment accumulation, and OC preservation in foreset deposits imitate OC_T preservation during episodic events in small, mountains river deltas. The conceptual diagram in Figure 4-4 shows that TOC is higher in bottomset deposits (cores 1, 6 and 4) than in topset or foreset deposits, but during events TOC is highest in foreset deposits (core 7). Additionally, MAR_{OC} in foreset deposits (6.7 ± 9.9 kg_{OC} m^{-2} yr^{-1} for non-event accumulation and 256.2 ± 100.3 kg_{OC} m^{-2} yr^{-1} for event accumulation) is strongly influenced by the high vertical accumulation rates associated with episodic events that characterize this depositional region (29 cm yr^{-1} to 161 cm yr^{-1}; Pondell et al. in prep.). However, MAR_{OC} is driven by sediment accumulation rates and TOC content, and while bottomset deposits have higher %TOC than topset deposits (Figure 4-4), the MAR_{OC} is higher in topset deposits than in bottomset deposits (Figure 4-4, Table 4-2) as a result of differences in vertical accumulation rates ($20 - 40$ cm yr^{-1} for topset vs. ~17 cm yr^{-1} for bottomset).

MAR_{OC} were combined with the areas of Englebright Lake represented by the different sediment cores (Childs et al. 2003) to calculate organic carbon burial in these regions (Table 4-2). This approach assumed that sediment accumulation in the core was representative of sediment accumulation over the whole region of the lake, and previous

analyses of longitudinal and transverse variability of sediments in Englebright Lake supports this assumption (Snyder et al. 2004b). The analysis of MAR_{TOC} in Englebright Lake shows that the highest non-event carbon burial is found in cores 4 and 7 at the delta front region, followed by the deep regions closest to the dam (cores 1 and 6), and the region represented by cores 9 and 8 has the lowest non-event carbon burial rates. Figure 4-4 illustrates relationships between TOC, mass accumulation of TOC, depositional regime and sediment supply in Englebright Lake during event and non-event periods of deposition, and highlights the impact of flood events. These events increase organic carbon content and burial by up to an order of magnitude in Englebright Lake. When the TOC content and sediment accumulation rate for each sediment horizon are integrated and then combined with the area of each region for event and non-event periods, carbon burial in Englebright Lake is estimated at 0.35 Tg of carbon since the construction of Englebright Dam in 1940, and of this carbon accumulation more than 0.23 Tg is terrigenous OC and up to 0.16 Tg is aquatic OC.

In Englebright Lake, TOC accumulation ranged from 0.2 to 231 kg OC $m^{-2} yr^{-1}$ and averaged 6.6 kg OC $m^{-2} yr^{-1}$, which is two times greater than TOC accumulation in the Sacramento River prior to 1972 (3.1 kg OC $m^{-2} yr^{-1}$) (Canuel et al. 2009). These data provide evidence to support claims of the impacts of extensive damming on mass accumulation in the Sacramento River and the Sacramento – San Joaquin River Delta (SSJR Delta) (Wright and Schoellhamer 2004). For instance, Englebright Lake only represents about 0.09% of the total 100 km^3 of storage available in all the impoundments in the watershed of the SSJR Delta (California Dept. of Water Resources, Division of Dam Safety), and yet it has trapped about 0.23 Tg of terrigenous OC in 60 years. These data also reveal the potential for organic carbon sequestration in impoundments, and support previous research describing the magnitude of carbon burial and sequestration in other impounded systems (Downing et al. 2008; Tranvik et al. 2009).

Dams are perhaps one of the most significant ways by which humans have altered the environment. They have lasting impacts not only on regional hydrology and sediment transport, but also on nutrient cycling and organic carbon sequestration. In Englebright

Lake 0.23 Tg of terrigenous organic carbon have been buried at an average rate of 3.3 $kg_{OC}\ m^{-2}\ yr^{-1}$ since the construction of the Englebright Dam in 1940. Flood events have a substantial effect on TOC delivery and accumulation in this impoundment, increasing the organic carbon burial rate by an order of magnitude. However, dams also provide more secure water resources and a relatively carbon neutral energy source to a human population whose demand for freshwater and energy is higher than ever. In a time when the proliferation of dams has become a global strategy for controlling freshwater supply, additional studies are needed to investigate the impact of dams on the carbon cycle and provide information to inform decisions regarding dam construction and water resource management.

References

Alpers, C. N., M. P. Hunerlach, M. C. Marvin-DiPasquale, R. C. Antweiler, B. K. Lasorsa, J. F. DeWild, and N. P. Snyder. 2006. Geochemical Data for Mercury, Methylmercury, and Other Constituents in Sediments from Englebright Lake, California, 2002. Page 95. U.S. Geological Survey Data Series 151.

Ashley, R.P. 2002. Geoenvironmental model for low-sulfide gold-quartz vein deposits. Progress on geoenvironmental models for selected mineral deposits types 2:176.

Benner, R., M.L. Fogel, E.K. Sprague, and R.E. Hodson. 1987. Depletion of 13 C in lignin and its implications for stable carbon isotope studies. Nature 329:708–710.

Bergkamp, G., M. McCartney, and P. Dugan. 2000. Dams, ecosystem functions and environmental restoration. Thematic Review Environmental Issuses II.1

Blair, N.E. and R.C. Aller. 2012. The fate of terrestrial organic carbon in the marine environment. Annual Reviews of Marine Science 4:401-423.

Canuel, E., E. Lerberg, R. Dickhut, S. Kuehl, T. Bianchi, and S. Wakeham. 2009. Changes in sediment and organic carbon accumulation in a highly-disturbed ecosystem: The Sacramento-San Joaquin River Delta (California, USA). Marine Pollution Bulletin 59:154–163.

Charlesworth, S.M., and J.A. Lees. 1999. Particulate-associated heavy metals in the urban environment: Their transport from source to deposit, Coventry, UK. Chemosphere 39:833–848. doi: 10.1016/S0045-6535(99)00017-X

Childs J., N. Snyder, and M. Hampton. 2003. Bathymetric and geophysical surveys of Englebright Lake, Yuba-Nevada Counties, California. 20.

Cloern, J.E., E.A. Canuel, and D. Harris. 2002. Stable carbon and nitrogen isotope composition of aquatic and terrestrial plants of the San Francisco Bay estuarine system. Limnology and Oceanography 47:713–729.

Crossland, C.J., H.H. Kremer, and H.J. Lindeboom. 2005. Coastal fluxes in the anthropocene.

Crutzen, P.J. 2002. Geology of mankind. Nature 415:23–23. doi: 10.1038/415023a

Dean, W., and E. Gorham. 1998. Magnitude and significance of carbon burial in lakes, reservoirs, and peatlands. Geology 26:535–538.

Downing, J., J. Cole, J. Middelburg, R. Striegl, C. Duarte, P. Kortelainen, Y. Prairie, and K. Laube. 2008. Sediment organic carbon burial in agriculturally eutrophic impoundments over the last century. Global Biogeochemical Cycles 22:GB1018.

Emerson, S., and J. Hedges. 2008. Chemical Oceanography and the Marine Carbon Cycle. Cambridge University Press, Cambridge

Falk, P.D., and R.J. Dorsey. 1998. Rapid development of gravelly high-density turbidity currents in marine Gilbert-type fan deltas, Loreto Basin, Baja California Sur, Mexico. Sedimentology 45:331–349. doi: 10.1046/j.1365-3091.1998.0153e.x

Fry, B. 2006. Stable Isotope Ecology. Springer, New York

Gilbert, G.K. 1890. Lake Bonneville.

Goff, J.R. 1997. A chronology of natural and anthropogenic influences on coastal sedimentation, New Zealand. Marine Geology 138:105–117. doi: 10.1016/S0025-3227(97)00018-2

Gomez, B. 2004. Organic carbon in floodplain alluvium: Signature of historic variations in erosion processes associated with deforestation, Waipaoa River basin, New Zealand. Journal of Geophysical Research 109:F04011. doi: 10.1029/2004JF000154

Hansen, L. 2004. Deltaic Infill of a Deglaciated Arctic Fjord, East Greenland: Sedimentary Facies and Sequence Stratigraphy. Journal of Sedimentary Research 74:422–437. doi: 10.1306/102703740422

Hedges, J.I., and J.H. Stern. 1984. Carbon and nitrogen determinations of carbonate-containing solids [In sediments, sediment trap materials and plankton]. Limnology and Oceanography

James, L.A. 2005. Sediment from hydraulic mining detained by Englebright and small dams in the Yuba basin. Geomorphology 71:202–226. doi: 10.1016/j.geomorph.2004.02.016

Keil, R.G., E. Tsamakis, C.B Fuh, and J.C. Giddings. 1994. Mineralogical and textural controls on the organic composition of coastal marine sediments: Hydrodynamic separation using SPLITT-fractionation. Geochimica et Cosmochimica Acta 58:879-893.

Kingsford, R.T. 2001. Ecological impacts of dams, water diversions and river management on floodplain wetlands in Australia. Austral Ecology 25:109–127. doi: 10.1046/j.1442-9993.2000.01036.x

Kondolf, G.M. 1997. Hungry Water: Effects of Dams and Gravel Mining on River Channels. Environmental Management 21:533–551. doi: 10.1007/s002679900048

Kuehl, S.A., B.M. Levy, W.S. Moore, and M.A. Allison. 1997. Subaqueous delta of the Ganges-Brahmaputra river system. Marine Geology 144:81–96. doi: 10.1016/S0025-

3227(97)00075-3

Lehmann, M.F., S.M. Bernasconi, A. Barbieri, and J.A. McKenzie. 2002. Preservation of organic matter and alteration of its carbon and nitrogen isotope composition during simulated and in situ early sedimentary diagenesis. Geochimica et Cosmochimica Acta 66:3573–3584. doi: 10.1016/S0016-7037(02)00968-7

Leithold, E.L., N.E. Blair, L.B. Childress, and B.R. Brulet. 2013. Signals of watershed change preserved in organic carbon buried on the continental margin seaward of the Waipaoa River, New Zealand. Marine Geology

Lotze, H.K., H.S. Lenihan, B.J. Bourque, and R.H. Bradbury. 2006. Depletion, degradation, and recovery potential of estuaries and coastal Sseas. Science 312:1806. doi: 10.1126/science.1128035

Malartre, F., M. Ford, and E.A. Williams. 2004. Preliminary biostratigraphy and 3D geometry of the Vouraikos Gilbert-type fan delta, Gulf of Corinth, Greece. Comptes Rendus Geoscience 336:269–280. doi: 10.1016/j.crte.2003.11.016

Mantua, N.J., and S.R. Hare. 2002. The Pacific Decadal Oscillation. Journal of Oceanography 58:35–44. doi: 10.1023/A:1015820616384

Mayer, L.M. 1994. Surface area control of organic carbon accumulation in continental shelf sediments. Geochimica et Cosmochimica Acta 58:1271–1284. doi: 10.1016/0016-7037(94)90381-6

McCarney-Castle, K., G. Voulgaris, and A.J. Kettner. 2010. Analysis of Fluvial Suspended Sediment Load Contribution through Anthropocene History to the South Atlantic Bight Coastal Zone, U.S.A. http://dx.doi.org.proxy.wm.edu/10.1086/652658

Milliman, J.D., and K.L. Farnsworth. 2011. River Discharge to the Coastal Ocean: A Global Synthesis. Cambridge University Press, New York

Mount, J.F. 1995. California Rivers and Streams: The Conflict Between Fluvial Process and Land Use. University of California Press, Berkeley, California

Mulholland, P.J., and J.W. Elwood. 1982. The role of lake and reservoir sediments as sinks in the perturbed global carbon cycle. Tellus 34:490–499. doi: 10.1111/j.2153-3490.1982.tb01837.x

Restrepo, J.D., and J.P.M. Syvitski . 2006. Assessing the Effect of Natural Controls and Land Use Change on Sediment Yield in a Major Andean River: The Magdalena Drainage Basin, Colombia. AMBIO: A Journal of the Human Environment 35:65–74. doi: 10.1579/0044-7447(2006)35[65:ATEONC]2.0.CO;2

Rojas, E., and J.P. Le Roux. 2010. Sedimentary processes on a Gilbert-type delta in Lake Llanquihue, southern Chile. Andean Geology

Ruddiman, W.F. 2003. The Anthropogenic Greenhouse Era Began Thousands of Years Ago. Climatic Change 61:261–293. doi: 10.1023/B:CLIM.0000004577.17928.fa

Schoellhamer, D.H., S.A. Wright, and J.Z. Drexler. 2013. Adjustment of the San Francisco estuary and watershed to decreasing sediment supply in the 20th century. Marine Geology 345:63–71. doi: 10.1016/j.margeo.2013.04.007

Smith, D.G., and H.M. Jol. 1997. Radar structure of a Gilbert-type delta, Peyto Lake, Banff National Park, Canada. Sedimentary Geology 113:195–209. doi: 10.1016/S0037-0738(97)00061-4

Smith, S.V., W.H. Renwick, R.W. Buddemeier, and C.J. Crossland. 2001. Budgets of soil erosion and deposition for sediments and sedimentary organic carbon across the conterminous United States. Global Biogeochemical Cycles 15:697–707. doi: 10.1029/2000GB001341

Snyder, N., J. Allen, C. Dare, M. Hampton, G. Schneider, R. Wooley, C. ALPERS, AND M. MARVIN-DIPASQUALE. 2004a. Sediment grain-size and loss-on-ignition analyses from 2002 Englebright Lake coring and sampling campaigns. Page 46.

Snyder, N. P., D. M. Rubin, C. N. Alpers, J. R. Childs, J. A. Curtis, L. E. Flint, and S. A. Wright. 2004b. Estimating accumulation rates and physical properties of sediment behind a dam: Englebright Lake, Yuba River, northern California. Water Resources Research 40:W11301.

Snyder, N., S. Wright, C. Alpers, L. Flint, C. Holmes, and D. Rubin. 2006. Reconstructing depositional processes and history from reservoir stratigraphy: Englebright Lake, Yuba River, northern California. Journal of Geophysical Research 111:F04003.

Stallard, R.F. 2012. Terrestrial sedimentation and the carbon cycle: Coupling weathering and erosion to carbon burial. Global Biogeochemical Cycles 12:231–257. doi: 10.1029/98GB00741

Syvitski, J., C. Vörösmarty, A. Kettner, and P. Green. 2005. Impact of humans on the flux of terrestrial sediment to the global coastal ocean. Science 308:376–380. doi: 10.1126/science.1109454

Syvitski, J.P.M., and A. Kettner. 2011. Sediment flux and the Anthropocene. Philosophical Transactions of the Royal Society A: Mathematical, Physical and Engineering Sciences 369:957–975. doi: 10.1130/B30125.1

Tranvik, L.J., J.A. Downing, J.B. Cotner, S.A. Loiselle, R.G. Striegl, T.J. Ballatore, P. Dillon, K. Finlay, K. Fortino, and L.B. Knoll. 2009. Lakes and reservoirs as regulators of carbon cycling and climate. Limnology and Oceanography 54:2298–2314.

Vreča, P., and G. Muri. 2010. Sediment organic matter in mountain lakes of north-western Slovenia and its stable isotopic signatures: records of natural and anthropogenic impacts. Hydrobiologia 648:35–49. doi: 10.1007/s10750-010-0148-4

Wakeham SG, Canuel EA. submitted. Density-fractionated sediments in Delta of the Sacramento and San Joaquin Rivers (California). Limnology and Oceanography

Walling, D. 2006. Human impact on land-ocean sediment transfer by the world's rivers. Geomorphology 79:192–216.

Wolf, Ll, C. Zwiener, and M. Zemann. 2012. Tracking artificial sweeteners and pharmaceuticals introduced into urban groundwater by leaking sewer networks. Science of the Total Environment 430:8–19. doi: 10.1016/j.scitotenv.2012.04.059

Wright, S., and D. Schoellhamer. 2004. Trends in the Sediment Yield of the Sacramento River, California, 1957-2001. San Francisco Estuary and Watershed Science 2:Article 2.

Figure 4-1. Map of sediment cores collected from Englebright Lake.
This figure shows the location of Englebright Lake in relation to the Yuba River watershed and the Sacramento-San Joaquin River Delta watershed in CA (see inset). The location of the six cores collected from Englebright Lake for this study are shown on the map, and the lake has been divided into the six regions represented by each core (Childs et al, 2003).

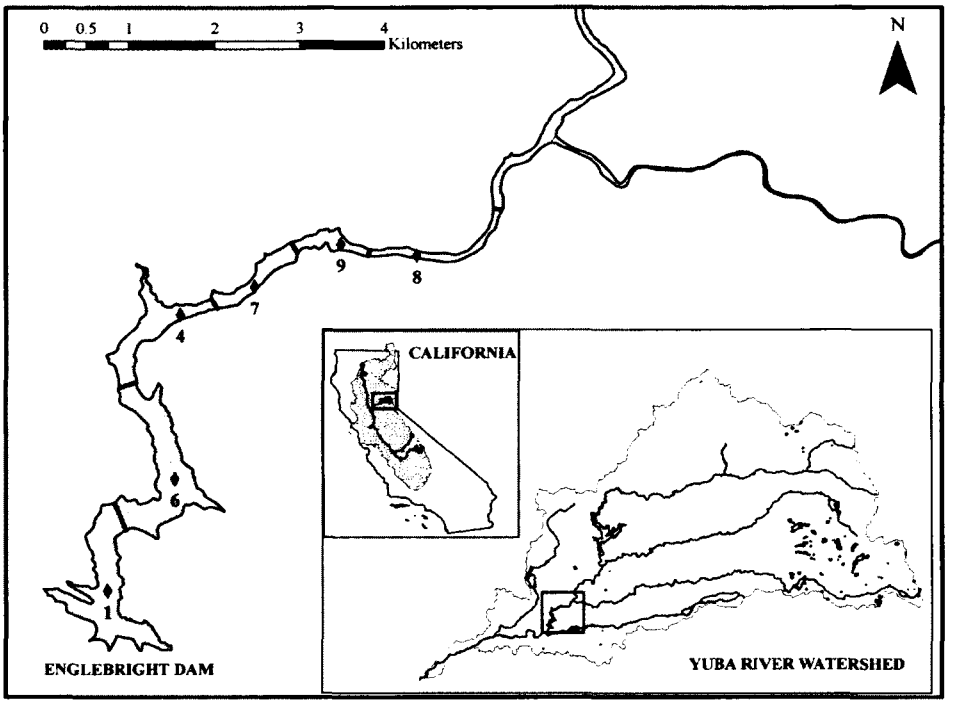

Figure 4-2. Boxplots of TOC, MAR_{OC}, and stable isotopes.
Box plots showing the median (labeled horizontal lines inside boxes), interquartile range (25th to 75th percentiles as boxends), and range from the 5th to 95th percentile as ends of the error bars for TOC content (a), TOC mass accumulation rates (b), and stable carbon (c) and nitrogen (d) isotope values of sediments in Englebright Lake as a function of depositional regime. Outliers, associated with event deposition, were not included to highlight differences in depositional regimes during non-event accumulation.

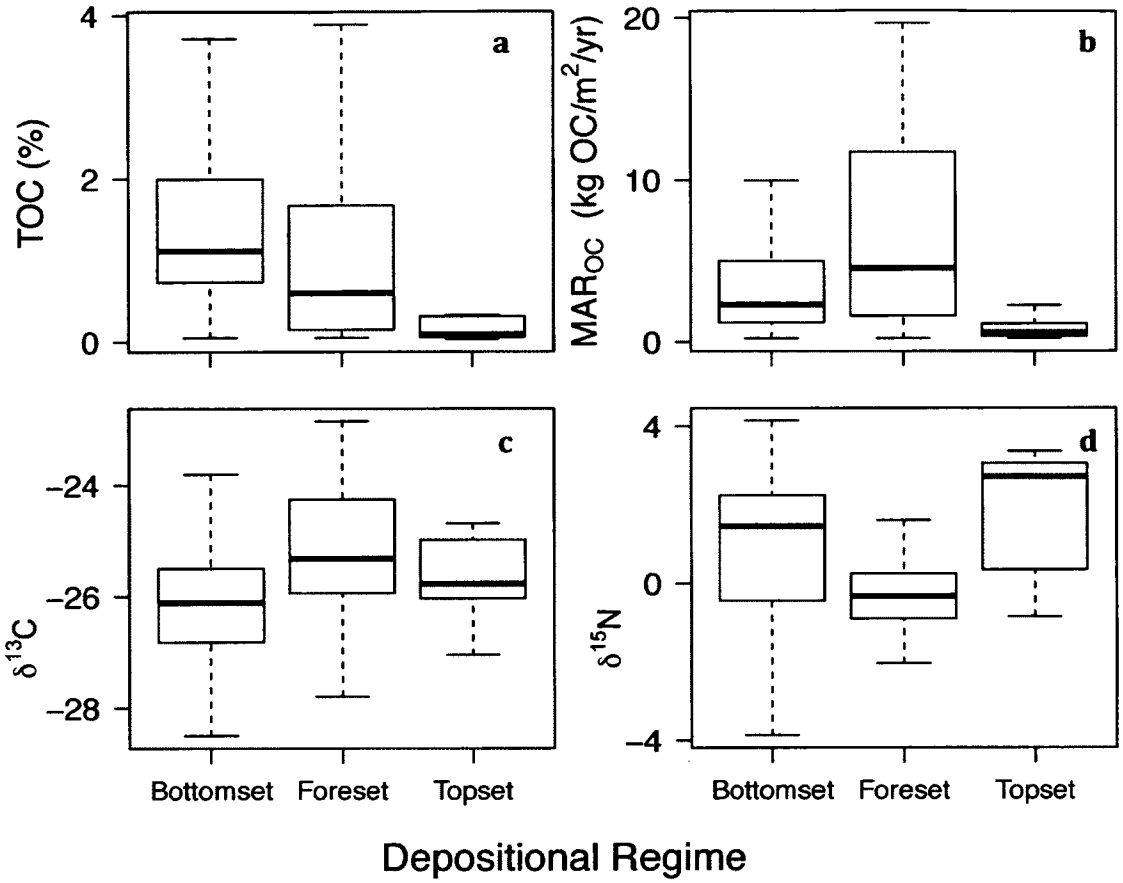

Figure 4-3. Depth profiles of organic carbon content in each core.
Cores are organized with those closest to the dam on the left side of the figure and those closest to the river input are on the right of the figure. Event samples are identified by filled symbols, and error bars represent one standard deviation for all replicate samples. Gray shaded regions represent the 1964 flood horizon identified by Pondell et al. (in prep.). Ticks on the right axis of each plot indicate depths corresponding to the 1997 flood event, the 1970 construction of the New Bullards Bar dam, and the 1950 flood event. Note the different x-axis scale for Cores 4 and 7.

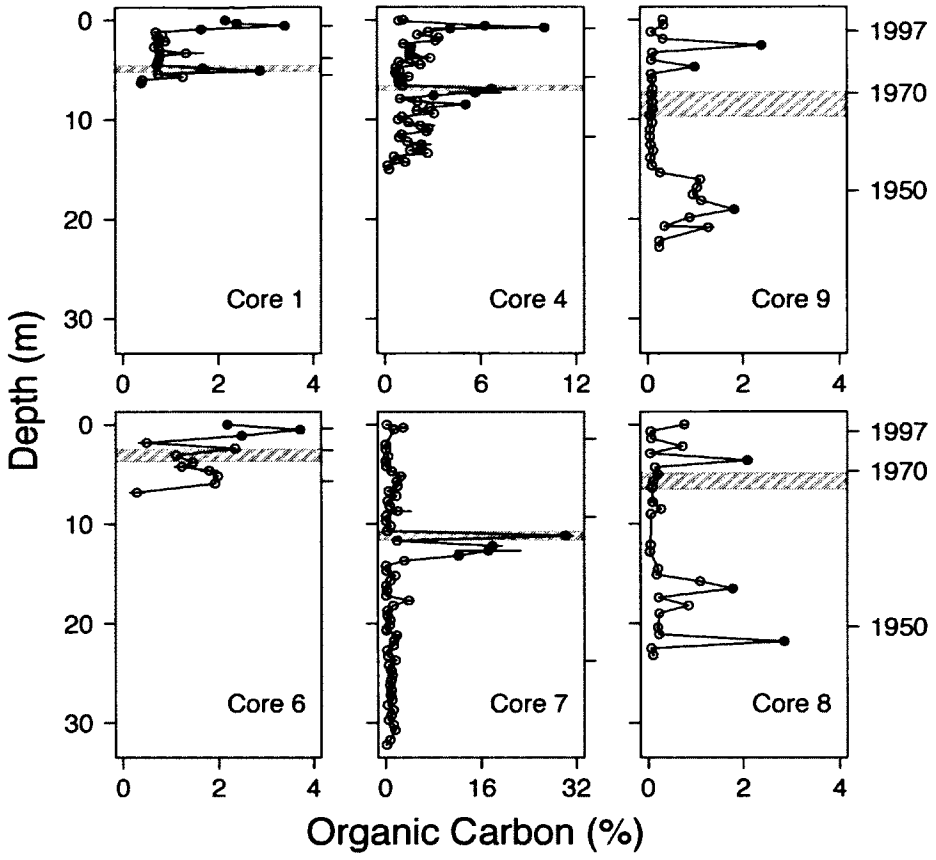

Figure 4-4. Conceptual diagram illustrating event and non-event accumulation of organic carbon in Englebright Lake.
The sediment deposit is shaded in the top panel as the accumulation between the 1939 and 2001 bathymetric profiles (Childs et al, 2003). Sediment load in the Yuba River is high and decreases as it flows downstream (to the left) in the lake, and the dominant depositional regime changes from topset (white) to foreset (grey) to bottomset (black) as the distance from the dam decreases. Average TOC content for each core during non-event (squares) and event (triangles) driven accumulation is shown in the middle two plots, while non-event and event driven mass accumulation rates (MAR) of TOC are shown on the bottom two plots. Note the difference in y-axis scale between event and non-event driven accumulation. Error bars represent the standard deviation of the average core value for non-event and event accumulation rates.

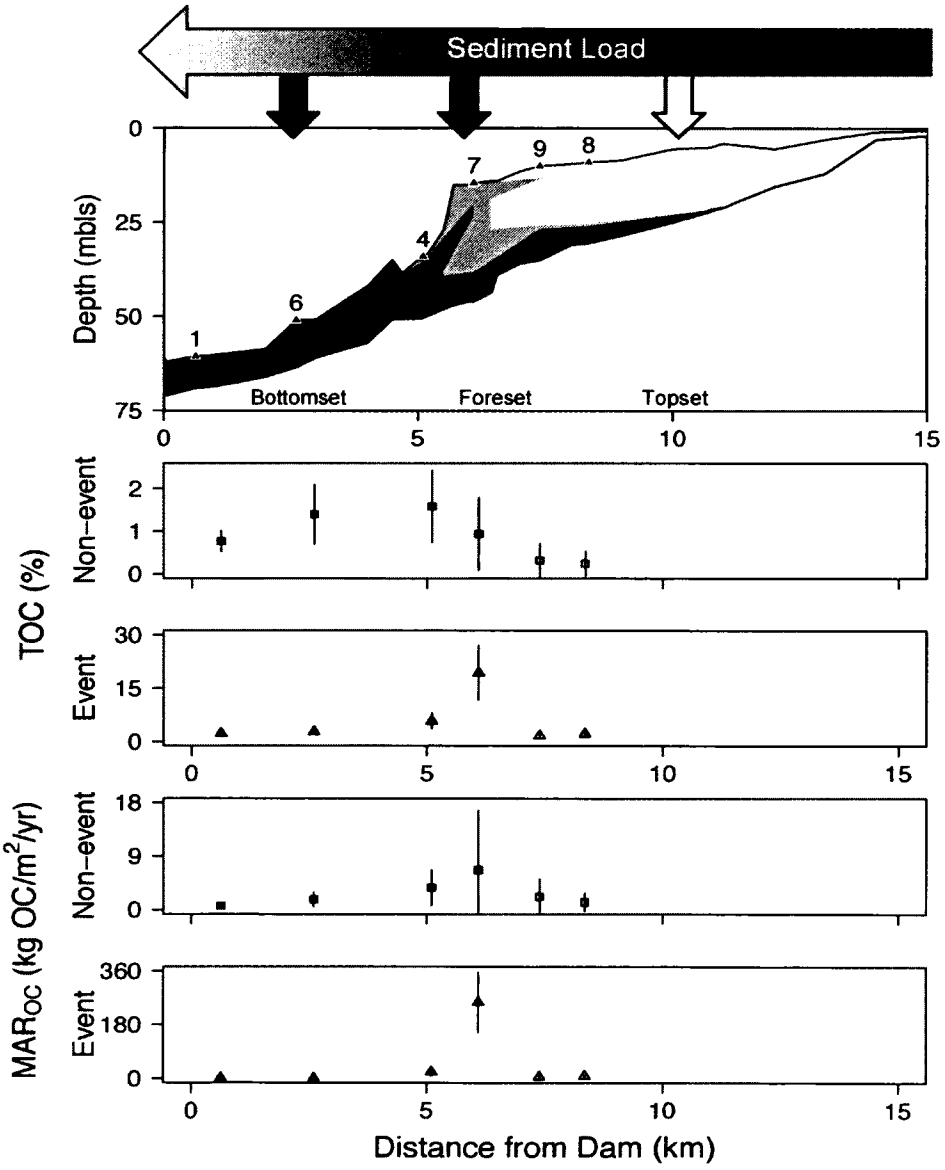

Figure 4-5. Depth profiles of stable carbon isotope values ($\delta^{13}C$) for each core. Cores are organized with those closest to the dam on the left side of the figure and those closest to the river input are on the right of the figure. Event samples are identified by filled symbols, and error bars represent one standard deviation for all replicate samples. Gray shaded regions represent the 1964 flood horizon identified by Pondell et al. (in prep.), and horizons corresponding to the 1997 flood, the construction of New Bullards Bar dam in 1970, and the 1950 flood are indicated with tick marks on the right axis of each profile.

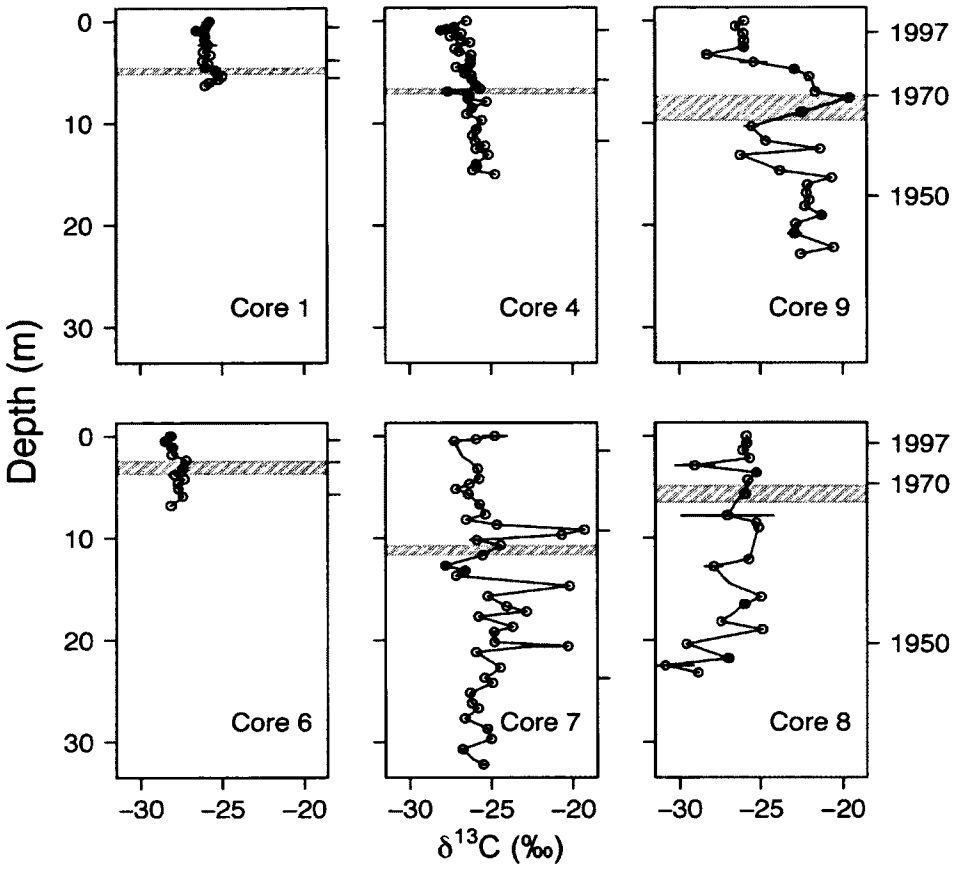

Figure 4-6. Stable isotope bi-plot with mean event and non-event core values. The boxes show the mean ± 1 standard deviation for isotope values of aquatic signatures, including plankton and particulate organic matter (FW Plankton), soils, and plants collected from Englebright Lake and its the watershed (Pondell and Canuel, in prep), and benthic diatoms from Cloern et al (2002). Freshwater algae values are not shown here in order to show variability in sediment stable isotope values. Mean stable isotope values for nonevent (grey) and event (black) accumulation for each core are shown and error bars represent the standard error associated with each mean.

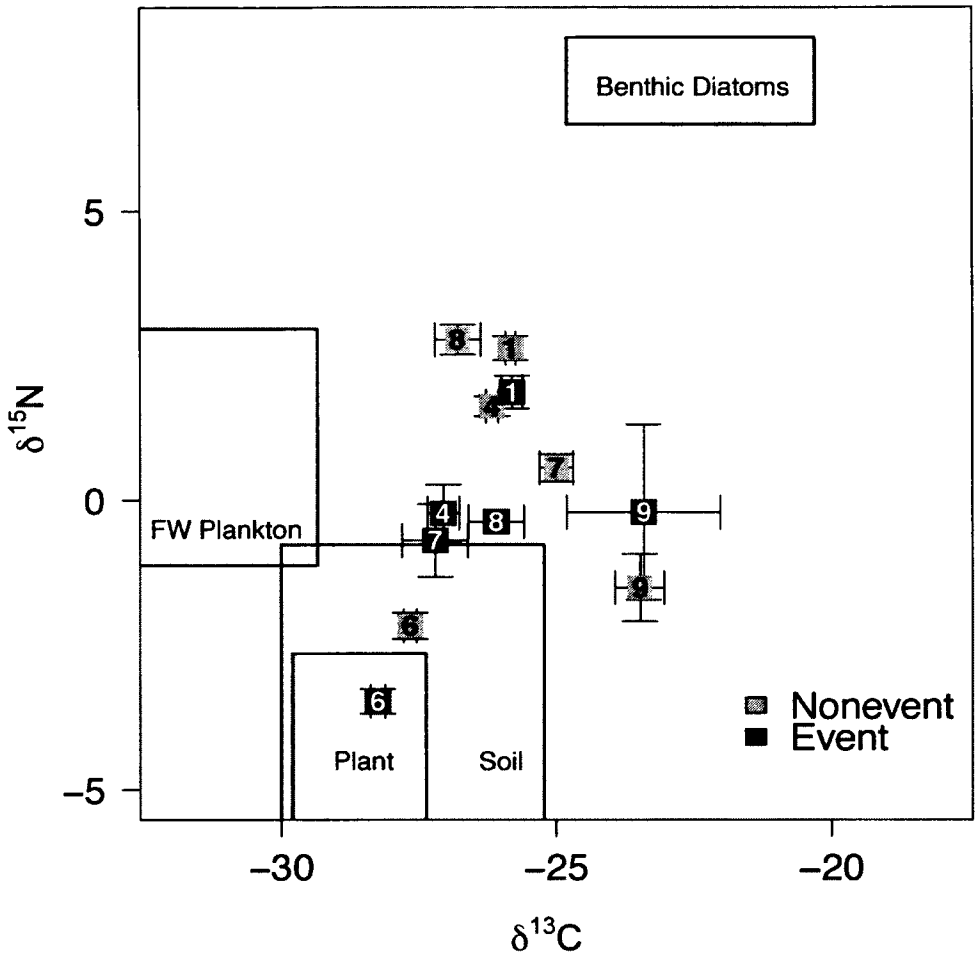

Table 4-1. Events influencing the Yuba River watershed and Englebright Lake. The floods presented include all events where mean daily discharge (Q_d) was greater than 1500 $m^3 s^{-1}$ (US Geological Survey gauging station 11418000). The controlling PDO and ENSO phase are listed for each flood event.

Year	Event	PDO	ENSO
2002	Cores collected from Englebright Lake		
1997	Flood	Warm	El Niño
1986	Flood	Warm	El Niño
1970	Annual lake level draw-downs cease		
1970	Flood	Neutral	La Niña
1964	Flood	Cold	La Niña
1963	Flood	Cold	Neutral
1962	Flood	Cold	La Niña
1960	Flood	Neutral	Neutral
1955	Flood	Cold	La Niña
1950	Flood	Cold	La Niña
1940	Englebright Dam completed		

Table 4-2. Organic carbon accumulation in Englebright Lake cores.
The dominant depositional regime from each core, the area in the lake represented by each core (from Fig. 1), and the mean grain size are listed. The mean and standard deviation of mass accumulation rates for TOC (MAR_{OC}) and for TN (MAR_{TN}), and the estimated terrestrial OC buried in each region are reported.

Core	Area (km^2) [a]	Deposit [b]	Grain Size (μm) [b]	MAR_{OC} Non-event ($kg_{OC}/m^2/yr$)	MAR_{OC} Event ($kg_{OC}/m^2/yr$)	Min OC_T Buried (Mg OC_T)	MAR_{TN} ($kg_{TN}/m^2/yr$)
1	0.739	Bottomset	17.1	0.7 ± 0.2	1.8 ± 0.6	10.2	0.95 ± 0.02
6	0.857	Bottomset	23.0	1.8 ± 1.2	1.5 ± 0.3	15.6	0.83 ± 0.03
4	0.474	Bottomset	35.4	3.7 ± 3.0	22.6 ± 13.0	106.6	6.27 ± 0.12
7	0.232	Foreset	74.8	6.7 ± 9.9	256.2 ± 100.3	85.3	5.68 ± 0.23
9	0.175	Topset	2848.0	2.2 ± 3.0	6.6 ± 5.7	5.0	NA
8	0.187	Topset	2000.0	1.3 ± 1.5	9.1 ± 1.6	8.1	NA

a: Data from Childs et al., 2003.
b: Data from Snyder at al., 2004.

Table 4-3. Aquatic and terrigenous sources in sediment cores.
Ranges of the contributions from terrigenous, freshwater plankton, and benthic diatom and freshwater seston OM sources to Englebright Lake sediments presented as minmax solutions from 3-end-member mixing models using $\delta^{13}C$ and $\delta^{15}N$ for mean core and overall lake values. Mean $\delta^{15}N$ values were not included in the end member analysis because nitrogen values were below detection in more than 60% of these samples, and are indicated here with NA. When a maximum value was greater than 100% or a minimum value was less than 0%, the contribution from that source was identified as either greater or less than the value calculated in the mixing model.

Core	Isotope	Aquatic Source: Benthic Diatoms and Freshwater Seston	Aquatic Source: Freshwater Plankton	Terrigenous Source: Soil and Plant
1	$\delta^{13}C$	36 – 55%	< 45%	> 64%
	$\delta^{15}N$	13 – 35%	> 87%	< 65%
6	$\delta^{13}C$	10 – 37%	< 63%	> 90%
	$\delta^{15}N$	< 0.04%	> 16%	84 – 96%
4	$\delta^{13}C$	29 – 50%	< 48%	> 69%
	$\delta^{15}N$	3 – 28%	> 97%	< 72%
7	$\delta^{13}C$	46 – 62%	< 38%	>54%
	$\delta^{15}N$	< 23%	> 90%	10 – 77%
9	$\delta^{13}C$	66 – 77%	< 23%	> 33%
	$\delta^{15}N$	NA	NA	NA
8	$\delta^{13}C$	25 – 47%	< 53%	> 75%
	$\delta^{15}N$	NA	NA	NA
Lake Average	$\delta^{13}C$	39 – 57%	< 43%	> 61%
	$\delta^{15}N$	> 25%	< 95%	5 – 75%

CHAPTER 5: RESPONSE OF ORGANIC MATTER ACCUMULATION IN ENGLEBRIGHT LAKE, CALIFORNIA (USA) TO CLIMATE AND HUMAN IMPACTS

C.R. Pondell

E.A. Canuel

Abstract

Climate change models predict increasing temperatures and uncertainty surrounding the freshwater supply will lead to greater frequency of drought and intense storms that will threaten systems already vulnerable to climate and anthropogenic change. This study investigates how anthropogenic activities and climate influence organic carbon (OC) delivery using Englebright Lake, a reservoir in California, as an example system. Terrigenous and aquatic OC accumulation in three depositional regimes (bottomset, foreset, topset) were analyzed using fatty acid, sterol and lignin biomarkers and compared to records of watershed changes to determine responses to reservoir management (i.e., lake draw-downs) and flood events. Concentrations of long chain saturated fatty acids (LCFA), plant sterols, and lignin biomarkers increased by an order of magnitude in sediments at the delta front during flood events ($p < 0.007$). A decrease in diacids coincident with an increase in aquatic sterols in bottomset deposits reflect the response of OC accumulation to the discontinuation of ~20m lake level draw-downs in 1970 ($p < 0.007$). OC accumulation in Englebright Lake sediments suggests that multiple processes (e.g., magnitude, duration and depositional regime) govern responses to human- and climate-driven events in lakes, and the potential for the aquatic system to sequester terrigenous and aquatic carbon will increase as the impact of storms and the degree of human modification intensifies in the future.

Introduction

The predicted effects of climate change, including warming, reduced snowpack and altered precipitation patterns are expected to transform river runoff patterns and modify biodiversity and species composition in terrestrial and aquatic habitats (Intergovernmental Panel on Climate Change, 2014). Additionally, the intensity of droughts, fires, and disease outbreaks is expected to effect not only natural systems, but also human modified systems such as agricultural lands (Marshall et al. 2008, Sturrock et al. 2011, Wheeler and Braun 2013). Natural and anthropogenic systems already vulnerable to climate pressures including rising sea level, increasing temperatures, and uncertain freshwater resources (Cloern and Jassby 2012, Moser et al. 2012) will become more threatened under future climate change scenarios (Cloern et al. 2011).

Global climate change is expected to alter carbon cycling between atmospheric, terrestrial, and marine carbon pools, with differing impacts and magnitude of change in arctic, temperate, and tropical systems (Canuel et al. 2012). Temperate systems, for example, are generally predicated to receive more precipitation as temperatures increase, resulting in higher winter-spring stream flow and increased phytoplankton productivity (Paerl et al. 2006, Najjar et al. 2010). In some temperate systems, such as the Mississippi Delta and Mobile Bay, increasing temperatures are expected to lead to extreme salinities and reduced stream flow, resulting in decreased water quality and altered food webs (Twilley et al. 2001). In some estuarine and coastal systems the frequency of intense storm events is expected to rise, increasing inundation and modifying aquatic carbon cycles (Canuel et al. 2012). During extreme events the export of organic carbon may be two to five times greater than the average annual base flow export, and is dominated by particulate, rather than dissolved organic carbon (Dhillon and Inamdar 2013). The burial of particulate carbon in marine sediments is a significant carbon sink, and the potential particulate carbon sink in aquatic systems during flood events may be just as important.

The impact of intense storm events on the transport of carbon through rivers is substantial, and in many small or arid rivers world-wide more than 25% of the annual

carbon flux to the ocean is transported during episodic events over the course of several hours to a few days (Coynel et al. 2005). Predicting when these events will occur in a river is difficult because the response to extreme events depends on several factors, including local climate and geologic and geomorphic controls in the drainage basin (Milliman and Farnsworth 2011). Direct sampling of flood events challenging than due to safety issues and sampling strategies. Sediment records provide an alternate method for analyzing the impact of extreme flood events on organic carbon burial in coastal and lake environments over extended time periods, and offer insights to help increase understanding of responses of sediment and particulate matter to past events (Wheatcroft et al. 2010, Orpin et al. 2010).

The approach employed in this study uses multiple proxies to identify how organic carbon and sediment accumulation respond to anthropogenic- and climate-driven impacts. Multi-proxy studies in terrestrial and aquatic systems prove useful in differentiating between sources of material to depositional environments (Muri et al. 2004, Pierce et al. 2012, Routh et al. 2014), and offer powerful tools to trace changes to organic matter (OM) over time (Zimmerman and Canuel 2001, Houel et al. 2006). Human activities, such as urbanization and agriculture, and climate are both significant drivers that may translate to simultaneous responses in environmental records, such as sediments. It is often difficult to distinguish between these response signals (Parmesan and Yohe 2003), especially if the magnitude of the events or responses is not equal. This study measured the effects of different impacts, including the modification of the hydrological regime and major flood events on the transport and accumulation of carbon in aquatic systems by analyzing multiple organic biomarkers from an impoundment in a small, mountainous watershed in northern California.

Study System

Englebright Lake on the Yuba River is a reservoir in the foothills of the Sierra Nevada Mountains in northern California (Figure 5-1a) created by construction of Englebright Dam in 1940. The impoundment is a 14km long lake with depths ranging from 70m near the dam to less than 3 meters at the river confluence (Figure 5-1b). Three tributaries, the

North, Middle, and South Yuba Rivers, converge just upstream of the Englebright Lake and drain 3468 km^2 of conifer and hardwood forest dominated area in the Sacramento River watershed. Hydraulic mining impacts from gold mining in the 19th century mobilized an estimated 344 million cubic meters of sediments in Sacramento River watershed, and Englebright Dam is one of the many dams built in this system to trap this mining debris. Several flood events impacted the Englebright Lake watershed since the construction of Englebright Dam in 1940, leading to extended periods of high discharge (Table 5-1) that have influenced sediment and organic carbon (OC) transport to the Englebright Lake.

Depositional patterns in Englebright Lake are an example of a Gilbert-type delta (Snyder et al. 2006) with three distinct depositional regimes (Figure 5-1b). Topset deposits in the shallow, upstream region of the lake designate the accumulation of bedload material. Foreset deposits at the top of the delta front are influenced by the changing slope of the river bottom, and bottomset deposits in the deep-water region of the lake closest to the dam represent the accumulation of the suspended sediment load (Pondell et al. in prep.).

Methods

Sediment Sample Collection

Sediment cores were collected from Englebright Lake in 2002 by the U.S. Geological Survey (Snyder et al. 2004) to characterize the sediment deposit. Parameters, including grain size, organic matter content (from loss-on-ignition analysis), sediment density, trace metals, and radioactive cesium isotope profiles for geochronological dating were measured from sediment samples collected from these cores. In 2009, six of these sediment cores were resampled for organic carbon and biomarker analyses. Samples (~40g of sediment) were collected at depth intervals that provided a temporal resolution of one to five years in each core. Sampling size and intervals increased for cores 8 and 9, where larger samples (~60g of sediment) were needed to ensure enough organic material was available for biomarker analysis from the coarse (1-3mm) sediments. Sediment samples for organic carbon analyses were transported to the Virginia Institute of Marine

Science and stored at -80°C until they could be freeze-dried and homogenized for biomarker analysis.

Lipid Biomarker Analysis

Total lipids were extracted from 167 sediment samples (~10-50g) with CH_2Cl_2: CH_3OH (2:1 v/v) at 80°C and 1800 psi using a Dionex ASE 200 accelerated solvent extractor (Waterson and Canuel 2008). Samples were partitioned with a 1:1:0.9 solution of CH_2Cl_2: CH_3OH:NaCl (20% aqueous solution) to separate the extracts into organic and aqueous phases. The organic phase was isolated, dried, and saponified using 1N KOH in aqueous methanol (10% H_2O) (Canuel and Martens 1993). Neutral lipids (SAP-N) were isolated from the saponified residue using hexane. The pH of the residue was reduced to 2 and the acidic lipids (SAP-A) were isolated by hexane extraction. The SAP-A fraction was methylated with 3% BF_3 in methanol and the methyl esters were extracted into hexane. Sterols (from SAP-N fraction) and fatty acid methyl esters (FAME) and were isolated from other lipid classes using silica gel chromatography. Prior to analysis by gas chromatography (GC), sterol fractions were derivatized with N,O-Bis(trimethylsilyl)trifluoroacetamide (BSTFA). Sterols were analyzed with an Agilent 7890A GC (DB-5MS 30m x 0.32mm column with 0.25μm film) connected to an Agilent 5975C mass spectrometer, and FAMEs were analyzed with an HP5890 series II GC (DB-23 60m x 0.32mm, 0.25μm film). FAMEs and sterols were quantified relative to C_{21} FAME and 5α-cholestane internal standards, respectively. Methodological blanks were run in parallel and samples were blank corrected prior to data analysis. Average recovery of nonadecanol and 5α-androstanol (surrogate compounds added at the beginning of the analysis) was greater than 55%, and variation between blank corrected replicate samples was less than 20%.

Lignin Biomarker Analysis

Lignin phenols were extracted from 146 sediment samples following the CuO method described by Hedges and Ertel (1982) and modified by Louchouarn et al. (2000). Briefly, sediments (enough for the extraction of ~4mg OC), 330mg CuO, 150mg $Fe(NH_4)Mg$, and

2-3mL 2N NaOH were added to stainless steel reaction vessels and heated at 154°C for 3 hours. For sediments where the organic carbon content was low (i.e., less than 4mg OC per 1g sediment), ~5mg of glucose was added to prevent the super oxidation of lignin oxidation products (Louchouarn et al. 2010). Prior to closing the vessels, samples were purged with nitrogen to ensure the reaction occurred without oxygen. After samples cooled, surrogate standards *trans*-cinnamic acid and ethyl-vanillin were mixed into samples, which were then decanted with 2 successive rinses of 1N NaOH. Samples were acidified with HCl and extracted three times with ethyl acetate. Water was removed from samples using Na_2SO_4, and samples were dried, re-dissolved in pyridine, and derivatized with BSTFA prior to analysis by GC-mass spectrometry. Lignin oxidation products were analyzed with an Agilent 7890A GC (DB-5MS 30m x 0.32mm column with 0.25μm film) connected to an Agilent 5975C mass spectrometer using 1,3,5-triisopropylbenzene as an internal standard to quantify 13 lignin compounds. Quantification peaks were blank corrected, and variation between replicate samples was ~20%.

Data Analysis

Statistical analysis of sediment biomarker data was performed using R-Studio software (version 0.98.507). All biomarker data were log transformed to meet the assumption of normal distribution prior to statistical analysis. Analysis of variance (ANOVA) was used to identify differences between biomarker concentrations in depositional regimes, during events, and interactions between these variables. Tukey HSD (highly significant difference) post hoc test compared differences between variables to determine which differences were significant. In order to reduce the dimensionality of the data set, fatty acid, sterol, and lignin biomarkers for all samples were analyzed together using principal components analysis (PCA) (Table 5-2). Prior to PCA, data were transformed to remove negative bias. This transformation included normalizing all biomarker values to the total biomarker class concentration (i.e., total fatty acids or total sterol concentration), and then values that were below detection (BD) were replaced with one half the minimum biomarker concentration. Biomarker values were divided by their geometric mean and log normalized. Then, the mean was subtracted from each biomarker value and divided by the standard deviation of that mean to transform the biomarker mean and standard

deviation to 1 and 0, respectively (Yunker et al. 2005). Based on results from the initial PCA, biomarker compounds were grouped when appropriate (i.e., when they reflected common biological sources and grouped similarly in the PCA) to reduce the number of variables. A final PCA was run using these grouped biomarkers, and factor loadings were used to determine which biomarker compounds explained the dominant principal components (PC).

Terrestrial to aquatic ratios of fatty acids (TAR_{FA}) were calculated to provide an estimate of contributions from terrigenous and aquatic sources using the equation presented in Meyers (1997).

$$TAR_{FA} = \frac{C_{24} + C_{26} + C_{28}}{C_{12} + C_{14} + C_{16}}$$

C_X indicates a saturated fatty acid of carbon length X. TAR_{FA} less than one suggest an aquatic source, while TAR_{FA} greater than one imply a terrigenous OM source.

Results

Factor Analysis

Despite considerable variation in biomarkers signatures across Englebright Lake sediment samples, results from the PCA identified three distinct core groupings. Cores 1, 8 and 9 grouped together, cores 4 and 7 were similar, and core 6 was different from all other cores (Figure 5-2a). PCA loadings suggested differences in organic matter sources reflected by the terrigenous and aquatic biomarkers (Figure 5-2b). Biomarkers with the highest positive loadings on Principal Component 1 (PC-1) were aquatic sterols (0.431), cholesterol (0.329), polyunsaturated fatty acids (PUFA; 0.284), and ratios of vanillic acid to vanillin ((Ad/Al)v; 0.298). In contrast, long chain fatty acids (LCFA) (-0.339), total lignin phenols (Σ8) (-0.407) and plant sterols (-0.263) had the most negative loadings on PC-1. Short chain fatty acids (SCFA) and diacids had the most positive loadings on PC2 (0.318 and 0.368, respectively) and branched fatty acids (BrFA), C_{18}PUFA, and odd-numbered monounsaturated fatty acids (Odd MUFA) had the most negative loadings on PC2 (-0.417, -0.475 and -0.347, respectively). Together PC-1 and PC-2 explained ~35%

of the variability in the data set and this paper will discuss trends in the biomarkers most strongly correlated to these PC.

Lipid Biomarkers

Total FA and total sterol concentrations tracked total organic carbon (TOC) content in sediment samples ($R^2 = 0.81$ and $p < 0.001$ for total FA vs. TOC; $R^2 = 0.72$ and $p < 0.001$ for total sterol vs. TOC). Overall, total FA concentrations ranged from 0.6 to 832.6 μg g^{-1} and total sterols ranged from below detection (BD) to 280.6 μg g^{-1} in sediments from Englebright Lake. Concentrations of lipid biomarkers representing aquatic sources, including SCFA (total range = BD – 128.5 μg g^{-1}), PUFA (total range = BD – 74.4 μg g^{-1}), aquatic sterols (total range = BD – 0.3 μg g^{-1}), and cholesterol (total range = BD – 2.1 μg g^{-1}), for each sediment core are presented in Table 5-3. (See Appendices for concentrations of biomarkers for each sediment sample). Overall, aquatic biomarkers did not differ significantly during flood events, but in bottomset deposits aquatic sterol concentrations were higher in sediments accumulating after 1970 (0.03 ± 0.05 μg g^{-1}) than they were in sediments deposited before1970 (0.008 ± 0.006 μg g^{-1}; $p < 0.001$)(Table 5-3). Additionally, bacterial biomarkers, including BrFA and Odd MUFA, were higher in recent deposits (after 1970) (BrFA = 1.13 ± 1.15 μg g^{-1}, Odd MUFA = 0.19 ± 0.37 μg g^{-1}) than in sediments accumulating before 1970 (BrFA = 0.65 ± 0.85 μg g^{-1}, Odd MUFA = 0.37 ± 0.49 μg g^{-1}; $p < 0.001$ for all biomarkers).

LCFA (total range = BD – 303.1 μg g^{-1}), diacids (total range = BD – 57.1 μg g^{-1}), C_{18}PUFA (total range = BD – 21.2 μg g^{-1}), and plant sterols (total range = BD – 247.0 μg g^{-1}) characterized terrigenous organic matter sources, including plants and soils (Table 5-3). Concentrations of diacids in cores 1 and 6 were higher in sediments deposited before 1970 than in the more recently deposited sediments ($p < 0.007$) (Table 5-3; Figure 5-3). Diacid concentrations decreased from 0.83 ± 0.85 μg g^{-1} and 1.09 ± 0.60 μg g^{-1} in sediments deposited before 1970 to 0.04 ± 0.12 μg g^{-1} and BD in sediments deposited post-1970 from cores 1 and 6, respectively (Table 5-3 Figure 5-3). LCFA and plant sterol concentrations differed between flood event and non-event deposits in core 7 (Table 5-3,

Figure 5-4). Concentrations of these biomarkers were significantly higher in the 1964 flood deposit than in the rest of the sediments that accumulated in core 7 ($p < 0.001$ for both biomarkers) (Table 5-2). Concentrations of plant sterols (24-methylcholesta-5-en-3B-ol [campesterol], 24-ethylcholesta-5,22-dien-3B-ol [stigmasterol], and 24-ethylcholest-5-en-3B-ol [sitosterol]) 35 times higher in this event deposit than the average concentrations measured during normal, non-event accumulation, and LCFA concentrations were over 50 times greater in event deposits (Table 5-2). TAR_{FA} were generally greater than 1, except in cores 8 and 9 where the average TAR_{FA} was 0.9 and 0.99, respectively (Table 5-4).

Lignin Biomarkers

Lignin phenol concentrations (Σ8), or the sum of the concentration of the vanillyl, syringyl and cinnamyl phenols, ranged from BD to 54.2 mg g^{-1} in Englebright Lake, and responded to the 1964 and 1997 flood events in the watershed (Figure 5-5). In cores 4 and 7, Σ8 increased by an order of magnitude during the 1964 and 1997 flood events ($p < 0.001$) from 0.62 ± 0.94 mg g^{-1} during non-event accumulation to 7.14 ± 5.88 mg g^{-1} in flood event deposits in core 4 and from 0.75 ± 1.26 mg g^{-1} to 31.70 ± 16.89 mg g^{-1} in core 7 (Table 5-3).

Additional lignin proxies showed few significant differences over time or between cores in Englebright Lake, but provide information about terrestrial sources of OM to the lake. Syringyl to vanillyl phenol ratios (S/V), used to distinguish between angiosperm and gymnosperm plant tissues (Hedges and Mann, 1979), ranged from 0.04 to 1.26 in Englebright Lake sediments, but average values for each core ranged between 0.27 and 0.49. Ratios of cinnamyl to vanillyl phenols (C/V) ranged from 0.003 to 0.40, and all mean core C/V values were less than 0.13. C/V ratios differentiate between hard and soft plant tissue, such as bark and leaves or needles. Acid to aldehyde ratios of vanillyl phenols [(Ad/Al)v] provide information about the degree of degradation of lignin (Goni et al. 1993). (Ad/Al)v values in Englebright Lake ranged from 0.22 to 3.29, and were higher in topset deposits (0.78 ± 0.65) than in bottomset (0.57 ± 0.33) or foreset deposits (0.48 ± 0.23, $p < 0.04$). Finally, ratios of 3,5-benzoic acid to vanillin (3,5-Bd:V), an

indicator of degradation of soil organic matter inputs, ranged from 0.005 to 0.62, with an overall mean of 0.07 ± 0.09. Ratios of 3,5-Bd:V were correlated with (Ad/Al)v ratios ($r = 0.49$, $p < 0.001$) and had similar PCA scores for the initial PCA run, so these two biomarkers were combined for the final PCA (Figure 5-2).

Discussion

Sources of organic matter to Englebright Lake

Biomarker results are consistent with a complementary study using stable carbon and nitrogen isotopes, showing that more than ~60% of OM delivered to Englebright Lake is terrigenous in origin (Pondell and Canuel in prep.). Concentrations of terrigenous lipid biomarkers are greater than aquatic biomarkers (e.g., plant sterol > aquatic sterol [$p < 0.001$] and cholesterol [$p < 0.001$]), and lignin concentrations are two to three orders of magnitude greater than lipid biomarker concentrations, indicating the importance of terrigenous OM inputs to Englebright Lake. However, the amount of terrigenous OM differs by location in the lake, and in some cores the aquatic sources contribute more to the sediment OM pool than terrigneous sources (i.e., aquatic OM is at least 66% of OM in core 9, Pondell and Canuel in prep.). Cores 1, 9 and 8, with positive PC-1 scores, are more strongly influenced by aquatic sources, whereas terrigenous OM biomarkers (negative PC-1 loadings) characterize cores 6, 4 and 7 (Figure 5-3).

Cores 4 and 7 group together based on PCA loadings of LCFA, Σ8, plant sterols, and diacids (Figure 5-2), and these biomarkers, as well as the high TAR_{FA} (Table 5-4), are indicative of terrigneous OM sources. LCFA, Σ8, plant sterols are well-known biomarkers for terrigenous plant sources (e.g., Volkman 1986, Houel et al. 2006, Waterson and Canuel 2008), C_{18} PUFA derive from higher plants and fungi (Ruess and Chamberlain 2010), and diacid biomarkers indicate contributions from plant leaf waxes (Volkman et al. 1980). Additionally, concentrations of theses biomarkers were greatest in higher plant OM sources from the Englebright Lake watershed (Pondell and Canuel in prep.), confirming that their origins in Englebright Lake are from terrigenous plants.

While contributions of LCFA, plant sterols, diacids, and Σ8 imply that OM inputs to cores 4 and 7 are dominated by terrigenous sources, ratios of other lignin phenols identify specific vascular plant sources. The biplot of C/V and S/V (Figure 5-6) indicates that the OM in cores 4 and 7 is a mixture of hard and soft tissues from gymnosperm and angiosperm plants (Goni and Hedges 1992), reflecting conifer and hardwood forests , the two dominant land covers in the Englebright Lake watershed (Figure 5-1a) (Federal 2000). Biomarkers from both of these OM sources accumulate are common throughout Englebright Lake, and are not specific only to cores 4 and 7 (Figure 5-6). (Ad/Al)v ratios provide a measure of the oxidative state of lignin (Hedges & Mann, Goñi et al. 1993) and values of this ratio range from fresh plant tissues ([Ad/Al]v ~ 0.3) to highly degraded ([Ad/Al]v ~ 1) in cores 4 and 7. Mean (Ad/Al)v values of ~0.48 in cores 4 and 7 suggest that, in general, vascular plant sources at these locations are fresh relative to the other core locations in Englebright Lake (Table 5-4).

Biomarkers suggest that cores 1, 9 and 8 are influenced by aquatic OM sources to a greater extent than cores 4 and 7 (Figure 5-2), although differences in concentrations of aquatic biomarkers implies that the aquatic source is not consistent across these three cores. Freshwater plankton collected in Englebright Lake were dominated by 27-nor-24-cholesta-5,22-dien-3β-ol and cholesta-5,22-dien-3β-ol (Pondell and Canuel in prep.) but only 27-nor-24-cholesta-5,22-dien-3β-ol was detected in sediments from Englebright Lake, and mainly in core 1. 27-nor-24-cholesta-5,22-dien-3β-ol has been identified as a product of the bacterial degradation of diatoms (Holba et al. 1998), and suggests that diatoms are important components of the freshwater community contributing to OM signatures in core 1 (Pondell and Canuel in prep.).

High contributions from SCFA (> 25% for cores 8 and 9 as compared to < 23% for all other cores) and low contributions from LCFA (<17% for cores 8 and 9, and >25% for all other cores) are consistent with aquatic sources in these two cores. Stable carbon isotope values suggest that the aquatic community, especially for core 9, may be influenced by benthic diatoms (Pondell and Canuel in prep.). Similarities between SCFA, LCFA, and

(Ad/Al)v in cores 8 and 9 indicate similar OM sources, and an examination of the hydrologic history of Englebright Lake may explain organic matter proxies in these two cores. Prior to 1970, annual lake level draw-downs exposed the shallowest sediments in Englebright Lake during summer and autumn (Snyder et al. 2006). Biomarker signatures in cores 8 and 9 suggest that changing lake levels may cause winnowing of sediments and OM (Wakeham and Canuel submitted), leaving behind the OM most closely bound to sediment particles. High (Ad/Al)v, and correspondingly high 3,5-Bd:V, in cores 8 and 9 (> 0.69) suggests that terrigenous OM accumulating in these cores is likely soil organic matter that has undergone more degradation than the bark, leave and needles that accumulated in cores 4 and 7, providing evidence to support the winnowing of loosely associated coarse OM during lake level draw-downs at these core locations. TAR_{FA} (core 9 = 0.9 and core 8 =0.99) indicates that OM in these cores was derived from approximately equal proportions of aquatic and terrigenous sources. During Englebright Lake's early history, lake level draw-downs may have increased benthic primary production in the shallowest region of the lake. The decreased water levels at core 9 (from ~30 m in winter and spring to < 10 m in summer and autumn) may have stimulated benthic diatom productivity. Benthic diatom communities may have also influenced sediments accumulating in core 8, but in this location lake-levels draw-downs likely exposed these sediments, leading to more scouring and less aquatic influence when water levels were extremely low.

Biomarkers in core 6 are unique relative to all other cores in Englebright Lake. While PCA results indicate a dominance of terrigenous sources in this core (PC-1 < 0), the terrigenous source for core 6 (PC-2 < 0) differs from the higher plant source dominating biomarker signatures in cores 4 and 7 (PC-2 ≥ 0). PCA loadings indicate that higher contributions from BrFA, C_{18} PUFA and Odd MUFA, biomarkers for bacterial and fungal/higher plant OM sources (Volkman et al. 1980, Canuel and Martens 1993, Zelles 1999), distinguish core 6 from cores 4 and 7. One interpretation of these microbial biomarkers is that soils are the dominant source of OM to core 6, which is supported by sediment stable isotope values from core 6 (Pondell and Canuel in prep.) that are consistent with stable isotope values of soils collected from the Englebright Lake

watershed (Pondell and Canuel in prep.). The unique stable isotope and biomarker signatures associated with core 6 suggest a local source and may reflect OM inputs from the nearby Keystone Ravine. Keystone Ravine drains a small area (< ~100^2m) and core 6 was collected at the mouth of this ravine. Overall, differences in the biomarkers found in core 6 relative to the other cores from Englebright Lake suggest a localized OM source, and implies that runoff from this small creek controls OC accumulation at this location.

In summary, the organic biomarkers, PCA and stable isotope mixing models (Pondell and Canuel in prep.) indicate that sediments in Englebright Lake are influenced by a mixture of sources but that that proportion of these sources varies by location.

Response of biomarker signatures to anthropogenic and climate influences

Flood events. In Englebright Lake, the response to climate, specifically floods, is evident in profiles of terrigenous biomarkers, but records of flood layers vary across events and depositional regime. The strongest signal from flood events was observed at the delta front in cores 4 and 7 (Figure 5-5). Overall, lignin concentrations during flood events are an order of magnitude higher in cores 4 and 7 than during non-event deposition. However, only two flood events are recorded in these cores, and the response of OC accumulation during these two events differs between cores 4 and 7. While both the 1964 and 1997 flood events are recorded in core 4, $\Sigma 8$ is higher for the 1997 flood than for the 1964 flood. In contrast, only the 1964 flood is recorded in core 7. In addition to higher $\Sigma 8$ concentrations in core 7, the 1964 flood is also characterized by elevated concentrations of other terrigenous biomarkers in flood deposits relative to non-flood deposition (e.g., plant sterols [$p = 0.02$], and LCFA [$p = 0.003$]; Figure 5-4). Interestingly, the relative contribution of LCFA and plant sterols did not change during flood and non-event accumulation ($p > 0.9$), indicating that even though more terrigenous material from the watershed is delivered to the lake during flood events, the sources of this OM remain constant.

While flood events from 1964 and 1997 seem to have the greatest impact on allochthonous OM accumulation in Englebright Lake, other flood events impacting the

watershed are also recorded in the sediments. For example, the maximum peak in $\sum 8$ and other terrigenous biomarkers in core 7 corresponds to the 1964 event, but there is also a peak just below this one that shows a response to the 1960, 1962 and/or 1963 floods (Figure 5-4, Table 5-2). Profiles of $\sum 8$ concentration from Englebright Lake (Figure 5-5) suggest that not all of the nine large floods, as defined by a mean daily discharge >1500 $m^3 s^{-1}$ (Snyder et al. 2006), are recorded in the lake sediments, and that those flood events that are preserved differ in timing and magnitude across the cores (Figure 5-5).

The 1997 and 1964 floods had the most significant impact on OM accumulation in Englebright Lake. (i.e., largest increase in biomarker concentrations). The 1964 and 1997 floods were not only two of the largest floods in terms of peak discharge, but they were also the two longest lasting floods in the Englebright Lake watershed with 5 or 6 consecutive days of discharge greater than 1500 $m^3 s^{-1}$ (Table 5-2) (Snyder et al, 2006). The combination of high discharge and extended duration of flood events (i.e., > 4 days) may contribute to increased terrigenous OM accumulation, similar to other riverine and lacustrine systems (Enzel and Wells 1997, Orpin et al. 2010). This suggests that extended periods of high discharge may be needed to mobilize large enough loads of sediment and organic matter to accumulate as event layers in Englebright Lake. In the case of the 1964 flood, approximately 1.5 m of sediment were preserved in the foreset deposits in core 7 (based on accumulation rates from Pondell et al., in prep), and some of that event, sediments were remobilized as turbidity currents or hyperpycnal flows and deposited in core 4 at the bottom of the delta front. In contrast, flood events of shorter duration (<four days) are not recorded consistently in the sediments of Englebright Lake.

The record of flood events may also reflect differences in physical processes by location in Englebright Lake. Sediments accumulating in shallow regions of the lake (i.e., cores 7, 8, and 9), for example, are likely influenced by physical re-working (i.e., winnowing) to a greater degree than sediments in deep waters due to lake surface drawdowns that are part of the management of Englebright Lake (Snyder et al. 2006). As a result, sediments accumulating in the deeper regions of Englebright Lake are more protected from physical

mixing processes, which may explain why the magnitude and number of event signatures recorded in the bottomset deposits (cores 1 and 6) is greater than in the topset deposits (cores 8 and 9) (Figure 5-5).

Overall, the deposition patterns reveal that a host of factors influence delivery and accumulation of OM associated with flood events in Englebright Lake including the magnitude and duration of storm events, depositional regime and post depositional processes.

Lake level draw-downs. Englebright Dam was the first large dam (height > 15m) constructed on the Yuba River, and it was built to trap debris from upstream hydraulic mining sites. Between 1940 and 1970 Englebright Dam and its reservoir also supplied hydroelectric power and water for irrigation to the surrounding communities (Snyder et al. 2006). In order to provide these services, the lake surface level was drawn down from an average of 157m to ~137m between summer and autumn every year, and was recharged during the winter storm season (Snyder et al. 2006). In 1970, these annual draw-downs ceased with the construction of the New Bullards Bar (NBB) dam upstream of Englebright Lake. The NBB was constructed to provide hydroelectric power, and became the source of water for irrigation as well; the need to draw water from Englebright was reserved only for periods when maintenance on Englebright Dam was required. The construction of the NBB across the North Yuba River changed the hydrograph of the river, and discharge to Englebright Lake was controlled by discharge from the hydroelectric plant associated with the NBB (Snyder et al. 2006). The NBB is the second tallest dam in California (194 m high, reservoir volume = 1.196 km^3) with a residence time of approximately 4 years and a trapping efficiency over 95% (calculated from equations described in Vörösmarty et al. (2003). However, the impact of the NBB on the delivery of OM to Englebright Lake was diminished because it inundated a dam constructed before the construction of Englebright Dame. Therefore, the analysis of biomarker signatures before and after 1970 will focus on hydrologic changes in the lake rather than changes in the delivery of sediments and organic matter due to the upstream dam.

Biomarkers from select sediment cores show a response to the hydrologic changes in 1970. Fatty acid biomarkers, specifically diacids, decrease significantly from an average of 5 to 20% before 1970 to values below detection in cores 1 and 6 ($p = 0.006$ for core 1 and $p < 0.001$ for core 6) (Figure 5-3). The absence of diacids in the more recent (post-1970) sediment samples suggests a shift from terrigenous to aquatic OM sources in cores 1 and 6. In the bottomset deposits, where most of the accumulation of suspended sediment load occurs, decreases in the concentration of diacids correspond to increases in aquatic sterol concentrations. Aquatic sterols were significantly higher in bottomset sediments deposited after 1970 than in sediments from before 1970 ($p < 0.001$). The combination of decreasing diacid concentrations and increasing concentrations of aquatic sterols after 1970 suggests that autochthonous OM sources increased after the annual lake level draw-downs stopped.

Changes to the hydrologic regime likely influence the suspended sediment load in Englebright Lake, and after 1970 remobilized sediments from topset deposits in the lake would no longer be incorporated into the suspended load. This should decrease the overall suspended sediment load and decrease terrigenous OM inputs from the winnowed shallow water sediments. Increases in aquatic OM in response to the changing hydrologic regime may reflect increasing production due to increased light availability as the suspended sediment load decreases (Friedl and Wuest 2002) or a relative increase due to decreasing transport of terrigenous OM from shallow sediments in the lake.

The role of depositional regime in the identification of specific responses to watershed events

Organic biomarkers document responses to climate and human impacts in the Englebright Lake watershed but these responses are not recorded uniformly within the lake sediment record. Bottomset deposits (cores 1 and 6) contain biomarker evidence documenting the impact of changing hydrologic regime on the accumulation of OC throughout the lake. When the lake level draw-downs stopped, the transport of remobilized materials from upstream areas to downstream regions of the lake decreased.

This could result in a few different circumstances that would increase the proportion of aquatic OC in bottomset deposits. First, a decrease in suspended sediments resulting from decreased upstream material loads could increase the light availability in the deep-water region of Englebright Lake, stimulating primary production from freshwater plankton communities. Conversely, a decrease in the delivery of terrigenous OM from remobilized sediments from upstream regions of Englebright Lake would result in a relative increase in aquatic OM sources in bottomset deposits of the lake.

Foreset accumulation records OC accumulation related to the two largest floods at the delta front in Englebright Lake. High concentrations of terrestrial biomarkers reflect the accumulation of large pieces of organic matter, such as leaves and branches (based on visual observations), and the records of events in core 4 and at the bottom of the delta front likely result from sediment remobilization during turbidity currents (Gilbert et al. 2006) or subsequent lake level drawdowns (Snyder et al. 2006).

Conversely, sediments in the topset deposits (5 to 15 m in cores 8 and 9) have the lowest concentrations of terrigenous biomarkers (~5$\mu g\ g^{-1}$) and are likely associated with the accumulation of coarse bedload sediments. These coarse sediments are arguably the most impacted by the changing lake hydrography. Before 1970, these sediments were exposed every year, and fine sediment and organic matter was winnowed away. Biomarkers from core 9 in the topset deposits indicate a dominance of aquatic biomarkers during the first 30 years of accumulation that is not observed in any other core, and there is a trend toward increasing contributions from terrigneous OM sources after 1970 as hydrologic conditions in the topset region of the lake become more similar to conditions seen throughout the rest of Englebright Lake.

This study shows that responses to anthropogenic and climate events can be differentiated in this system, and suggests that a multi-proxy study of organic carbon is needed in systems like Englebright Lake where multiple drivers of events influence OC accumulation over time. The spatial separation of event records in Englebright Lake by depositional regime demonstrates how the energy associated with an event controls the

transport and accumulation of OC. This separation of event signals is obvious from the data measured for this small system, but may also be applied to large riverine systems. For instance, in large river systems (i.e., the Mississippi River) records of high energy, episodic events like storms may be retained in upstream tributaries where the localized event impact is strongest (e.g. paleo-event records in Lake Tutira; Orpin et al. 2010) while long term records of land-use change (i.e., agriculture or dams) may accumulate estuarine or coastal sediment deposits as evidence of the watershed response to a more large-scale event (i.e., decreased organic carbon accumulation in the Sacramento-San Joaquin River Delta coincident with dam proliferation; Canuel et al. 2009).

Conclusions

Sediment and organic carbon accumulation in Englebright Lake provide evidence showing that terrestrial OC accumulation responds to anthropogenic and climate stressors in the watershed. Based on the biomarker results, organic matter in Englebright Lake has the following general characteristics: (1) the dominant source of material is allochthonous and derived primarily from higher plants and soils in the watershed based on the high relative contribution of terrestrial biomarkers, (2) organic matter sources to the lake do not change during floods, but a greater volume of this terrigenous material accumulates during these events. Additionally, inputs from aquatic OM sources increased significantly in bottomset deposits after 1970, coincident with the construction of a mega-dam upstream causing changes to the hydrology of Englebright Lake. The response of sediment and organic carbon accumulation is contingent on several factors that are unique to individual environmental systems, including the history of land-use in the watershed, the magnitude and duration of disturbance events, and the connectivity between terrestrial and aquatic systems. This study provides a framework for evaluating influences of specific events based on unique watershed characteristics, and offers insights into the importance of reservoirs as recorders of watershed responses to local and regional events and as potential terrestrial carbon sinks.

References

Canuel, E. A. 2001. Relations between river flow, primary production and fatty acid composition of particulate organic matter in San Francisco and Chesapeake Bays: a multivariate approach. Organic Geochemistry 32:563–583.

Canuel, E. A., S. S. Cammer, H. A. McIntosh, and C. R. Pondell. 2012. Climate Change Impacts on the Organic Carbon Cycle at the Land-Ocean Interface. Annual Review of Earth and Planetary Sciences 40:685–711.

Canuel, E., and C. Martens. 1993. Seasonal variations in the sources and alteration of organic matter associated with recently-deposited sediments. Organic Geochemistry 20:563–577.

Canuel, E., E. Lerberg, R. Dickhut, S. Kuehl, T. Bianchi, and S. Wakeham. 2009. Changes in sediment and organic carbon accumulation in a highly-disturbed ecosystem: The Sacramento-San Joaquin River Delta (California, USA). Mar Pollut Bull 59:154–163.

Cloern, J. E., and A. D. Jassby. 2012. Drivers of change in estuarine-coastal ecosystems: Discoveries from four decades of study in San Francisco Bay. Reviews of Geophysics 50:RG4001.

Cloern, J. E., N. Knowles, L. R. Brown, D. Cayan, M. D. Dettinger, T. L. Morgan, D. H. Schoellhamer, M. T. Stacey, M. van der Wegen, R. W. Wagner, and A. D. Jassby. 2011. Projected evolution of California's San Francisco Bay-Delta-River system in a century of climate change. PLoS ONE 6:e24465.

Coynel, A., H. Etcheber, G. Abril, E. Maneux, J. Dumas, and J.-E. Hurtrez. 2005. Contribution of small mountainous rivers to particulate organic carbon input in the Bay of Biscay. Biogeochemistry 74:151–171.

Dhillon, G. S., and S. Inamdar. 2013. Extreme storms and changes in particulate and dissolved organic carbon in runoff: Entering uncharted waters? Geophysical Research Letters 40:1322–1327.

Enzel, Y., and S. G. Wells. 1997. Extracting Holocene paleohydrology and paleoclimatology information from modern extreme flood events: An example from southern California. Geomorphology 19:203–226.

Federal, M. (Ed.). 2000. Landsat GeoCover EMT+2000 Edition Mosaics, 1st edition. USGS. http://www.landcover.org.

Friedl, G., and A. Wuest. 2002. Disrupting biogeochemical cycles - Consequences of

damming. Aquatic Sciences 64:55–65.

Gilbert, R., S. Crookshanks, K. R. Hodder, J. Spagnol, and R. B. Stull. 2006. The Record of an Extreme Flood in the Sediments of Montane Lillooet Lake, British Columbia: Implications for Paleoenvironmental Assessment. Journal of Paleolimnology 35:737–745.

Goad, L. J., and N. Withers. 1982. Identification of 27-nor-(24R)-24-methylcholesta-5,22-dien-3β-ol and brassicasterol as the major sterols of the marine dinoflagellateGymnodinium simplex. Lipids 17:853–858.

Goni, M. 1997. Record of terrestrial organic matter composition in Amazon Fan sediments. Proceedings of the Ocean Drilling Program; scientific results, Amazon Fan; covering Leg 155 of the cruises of the drilling vessel JOIDES Resolution, Bridgetown, Barbados, to Bridgetown, Barbados, sites 930-946, 25 March-24 May 1994 155:519–530.

Goni, M., and J. Hedges. 1992. Lignin dimers: Structures, distribution and geochemical applications. Geochimica et Cosmochimica Acta 56:4025–4043.

Goni, M., K. Ruttenberg, and T. Eglinton. 1998. A reassessment of the sources and importance of land-derived organic matter in surface sediments from the Gulf of Mexico. Geochimica et Cosmochimica Acta 62:3055–3075.

Goñi, M. A., B. Nelson, and R. A. Blanchette. 1993. Fungal degradation of wood lignins: Geochemical perspectives from CuO-derived phenolic dimers and monomers. Geochimica et Cosmochimica Acta 57:3985–4002.

Hedges, J., and D. Mann. 1979. The characterization of plant tissues by their lignin oxidation products. Geochimica et Cosmochimica Acta 43:1803–1807.

Hedges, J., and J. Ertel. 1982. Characterization of lignin by gas capillary chromatography of cupric oxide oxidation products. Anal. Chem. 54:174–178.

Holba, A. G., L. I. P. Dzou, W. D. Masterson, W. B. Hughes, B. J. Huizinga, M. S. Singletary, J. M. Moldowan, M. R. Mello, and E. Tegelaar. 1998. Application of 24-norcholestanes for constraining source age of petroleum. Organic Geochemistry 29:1269–1283.

Houel, S., P. Louchouarn, M. Lucotte, R. Canuel, and B. Ghaleb. 2006. Translocation of soil organic matter following reservoir impoundment in boreal systems: Implications for in situ productivity. Limnology and Oceanography 51:1497–1513.

Huang, W.-Y., and W. G. Meinschein. 1979. Sterols as ecological indicators. Geochimica et Cosmochimica Acta 43:739–745.

Louchouarn, P., R. M. W. Amon, S. Duan, C. Pondell, S. M. Seward, and N. White.

2010. Analysis of lignin-derived phenols in standard reference materials and ocean dissolved organic matter by gas chromatography/tandem mass spectrometry. Marine Chemistry 118:85–97.

Louchouarn, P., S. Opsahl, and R. Benner. 2000. Isolation and quantification of dissolved lignin from natural waters using solid-phase extraction and GC/MS. Analytical Chemistry 72:2780–2787.

Marshall, J. D., J. M. Blair, D. P. Peters, G. Okin, A. Rango, and M. Williams. 2008. Predicting and understanding ecosystem responses to climate change at continental scales. Frontiers in Ecology and the Environment 6:273–280.

Meyers, P. A. 1997. Organic geochemical proxies of paleoceanographic, paleolimnologic, and paleoclimatic processes. Organic Geochemistry.

Milliman, J. D., and K. L. Farnsworth. 2011. River Discharge to the Coastal Ocean: A Global Synthesis. Cambridge University Press, New York.

Moser, S. C., S. Jeffress Williams, and D. F. Boesch. 2012. Wicked Challenges at Land's End: Managing Coastal Vulnerability Under Climate Change. Annual Review of Environment and Resources 37:51–78.

Mount, J. F. 1995. California Rivers and Streams: The Conflict Between Fluvial Process and Land Use. University of California Press, Berkeley, California.

Muri, G., S. G. Wakeham, T. K. Pease, and J. Faganeli. 2004. Evaluation of lipid biomarkers as indicators of changes in organic matter delivery to sediments from Lake Planina, a remote mountain lake in NW Slovenia. Organic Geochemistry 35:1083–1093.

Najjar, R. G., C. R. Pyke, M. B. Adams, and D. Breitburg. 2010. Potential climate-change impacts on the Chesapeake Bay. Estuarine, Coastal and Shelf Science 86:1–20.

Opsahl, S., and R. Benner. 1995. Early diagenesis of vascular plant tissues: Lignin and cutin decomposition and biogeochemical implications. Geochimica et Cosmochimica Acta 59:4889–4904.

Orpin, A. R., L. Carter, M. J. Page, U. A. Cochran, N. A. Trustrum, B. Gomez, A. S. Palmer, D. C. Mildenhall, K. M. Rogers, H. L. Brackley, and L. Northcote. 2010. Holocene sedimentary record from Lake Tutira: A template for upland watershed erosion proximal to the Waipaoa Sedimentary System, northeastern New Zealand. Marine Geology 270:11–29.

Paerl, H. W., L. M. Valdes, M. F. Piehler, and C. A. Stow. 2006. Assessing the Effects of Nutrient Management in an Estuary Experiencing Climatic Change: The Neuse River

Estuary, North Carolina - Springer. Environmental Management.

Parmesan, C., and G. Yohe. 2003. A globally coherent fingerprint of climate change impacts across natural systems. Nature 421:37–42.

Pierce, D. W., T. Das, D. R. Cayan, E. P. Maurer, N. L. Miller, Y. Bao, M. Kanamitsu, K. Yoshimura, M. A. Snyder, L. C. Sloan, G. Franco, and M. Tyree. 2012. Probabilistic estimates of future changes in California temperature and precipitation using statistical and dynamical downscaling. Climate Dynamics 40:839–856.

Rojas, E., and J. P. Le Roux. 2010. Sedimentary processes on a Gilbert-type delta in Lake Llanquihue, southern Chile. Revista Geológica de Chile 32:19–31.

Routh, J., G. Hugelius, P. Kuhry, T. Filley, P. K. Tillman, M. Becher, and P. Crill. 2014. Multi-proxy study of soil organic matter dynamics in permafrost peat deposits reveal vulnerability to climate change in the European Russian Arctic. Chemical Geology 368:104–117.

Ruess, L., and P. M. Chamberlain. 2010. The fat that matters: Soil food web analysis using fatty acids and their carbon stable isotope signature. Soil Biology and Biochemistry 42:1898–1910.

Snyder, N., C. Alpers, L. Flint, J. Curtis, M. Hampton, B. Haskell, and D. Nielson. 2004. Report on the May-June 2002 Englebright Lake deep coring campaign. Page 32.

Snyder, N., S. Wright, C. Alpers, L. Flint, C. Holmes, and D. Rubin. 2006. Reconstructing depositional processes and history from reservoir stratigraphy: Englebright Lake, Yuba River, northern California. Journal of Geophysical Research 111:F04003.

Sturrock, R. N., S. J. Frankel, A. V. Brown, P. E. Hennon, J. T. Kliejunas, K. J. Lewis, J. J. Worrall, and A. J. Woods. 2011. Climate change and forest diseases. Plant Pathology 60:133–149.

Twilley, R. R., E. J. Barron, H. L. Gholz, M. A. Harwell, R. L. Miller, D. J. Redd, J. B. Rose, E. H. Siemann, R. G. Wetzel, and R. J. Zimmerman. 2001. Confronting climate change in the Gulf Coast region: Prospects for sustaining our ecological heritage. Union of Concerned Scientistis, Cambridge, Massachusetts and Ecological Society of America.

Volkman, J. 2003. Sterols in microorganisms. Applied microbiology and Biotechnology 60:495–506.

Volkman, J. K. 1986. A review of sterol markers for marine and terrigenous organic matter. Organic Geochemistry 9:83–99.

Volkman, J. K., J. W. Farrington, and R. B. Gagosian. 1987. Marine and terrigenous lipids in coastal sediments from the Peru upwelling region at 15°S: Sterols and triterpene alcohols. Organic Geochemistry 11:463–477.

Volkman, J. K., R. B. Johns, F. T. Gillan, G. J. Perry, and H. J. Bavor Jr. 1980. Microbial lipids of an intertidal sediment—I. Fatty acids and hydrocarbons. Geochimica et Cosmochimica Acta 44:1133–1143.

Volkman, J. K., S. W. Jeffrey, P. D. Nichols, G. I. Rogers, and C. D. Garland. 1989. Fatty acid and lipid composition of 10 species of microalgae used in mariculture. Journal of Experimental Marine Biology and Ecology 128:219–240.

Volkman, J., A. Revill, D. Holdsworth, and D. Fredericks. 2008. Organic matter sources in an enclosed coastal inlet assessed using lipid biomarkers and stable isotopes. Organic Geochemistry 39:689–710.

Vörösmarty, C., M. Meybeck, B. Fekete, K. Sharma, P. Green, and J. Syvitski. 2003. Anthropogenic sediment retention: major global impact from registered river impoundments. Global and Planetary Change 39:169–190.

Wakeham, S. G., and E. A. Canuel. submitted. Density-fractionated sediments in Delta of the Sacramento and San Joaquin Rivers (California).

Waterson, E., and E. Canuel. 2008. Sources of sedimentary organic matter in the Mississippi River and adjacent Gulf of Mexico as revealed by lipid biomarker and [delta] 13CTOC analyses. Organic Geochemistry 39:422–439.

Wheatcroft, R. A., M. A. Goni, J. A. Hatten, G. B. Pasternack, and J. A. Warrick. 2010. The role of effective discharge in the ocean delivery of particulate organic carbon by small, mountainous river systems. Limnology and Oceanography 55:161.

Wheeler, T., and J. von Braun. 2013. Climate Change Impacts on Global Food Security. Science 341:508–513.

Yunker, M. B., L. L. Belicka, H. R. Harvey, and R. W. Macdonald. 2005. Tracing the inputs and fate of marine and terrigenous organic matter in Arctic Ocean sediments: A multivariate analysis of lipid biomarkers. Deep Sea Research Part II: Topical Studies in Oceanography 52:3478–3508.

Zelles, L. 1999. Fatty acid patterns of phospholipids and lipopolysaccharides in the characterisation of microbial communities in soil: a review. Biology and Fertility of Soils 29:111–129.

Zimmerman, A. R., and E. A. Canuel. 2001. Bulk Organic Matter and Lipid Biomarker Composition of Chesapeake Bay Surficial Sediments as Indicators of Environmental Processes. Estuarine, Coastal and Shelf Science 53:319–341.

Figure 5-1. Map of the Yuba River and Englebright Lake sediments.
The land cover and dams are shown for the Yuba River and Englebright lake watersheds (a). The bottom panel shows a transect of Englebright Lake with the location of the six cores and their depth in meters below the lake surface (mbls). Sediment deposited in the lake between the construction of Englebright Dam and when the cores were collected (1939-2001) based on bathymetric survey data (Childs et al. 2003) is shaded and is separated into bottomset (black), foreset (grey), and topset (white) deposits.

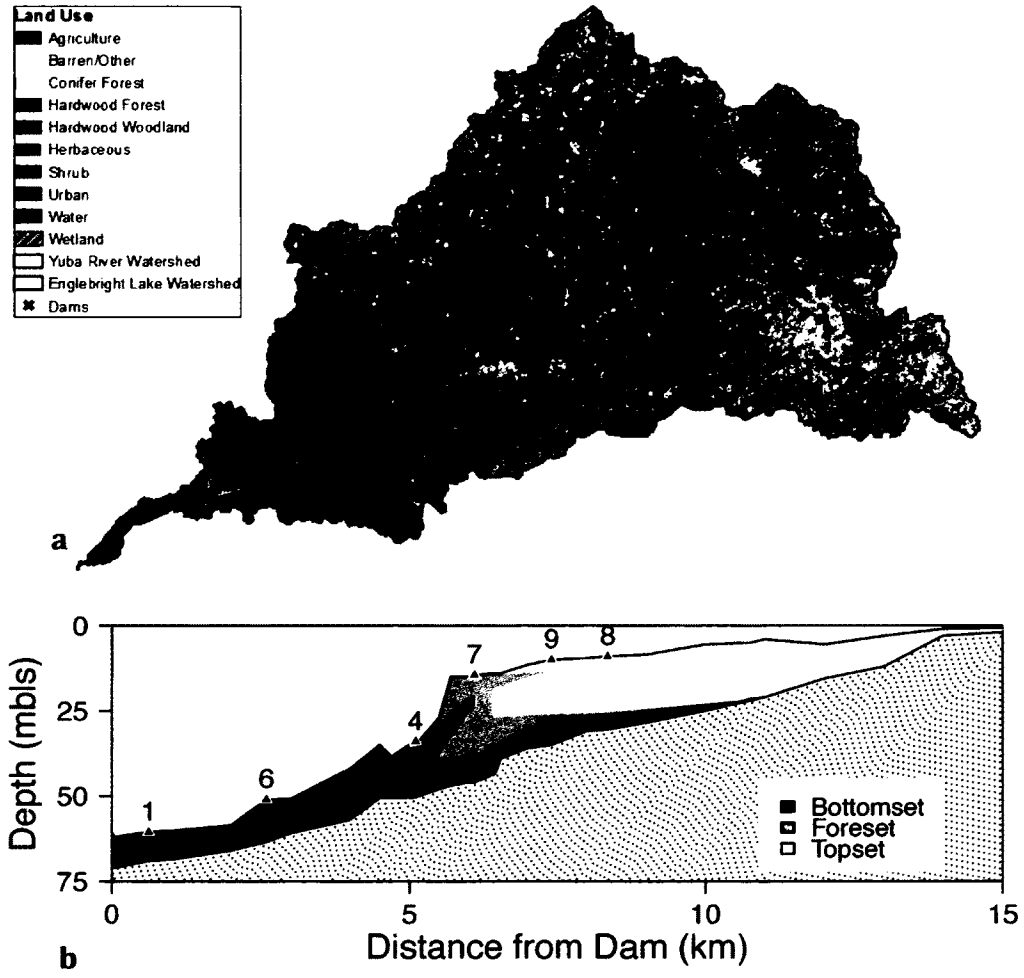

Figure 5-2. Mean core results from Principal Component Analysis (PCA). PCA scores for principal components 1 and 2 (PC-1 and PC-2) are shown for the mean and standard error of each core (a). Boxes highlight groups of cores with similar PCA scores. PCA loadings (b) show that PC-1 separated samples by source with positive loadings for aquatic sources (e.g., aquatic sterols, cholesterol [$C_{27}\Delta^5$], etc.) and negative loadings for terrigenous sources (lignin (Σ8), plant sterols, LCFA, etc.). Diacids had the most positive loadings on PC-2 and Odd MUFA, BrFA, SCFA and C18 PUFA had negative loadings on PC-2.

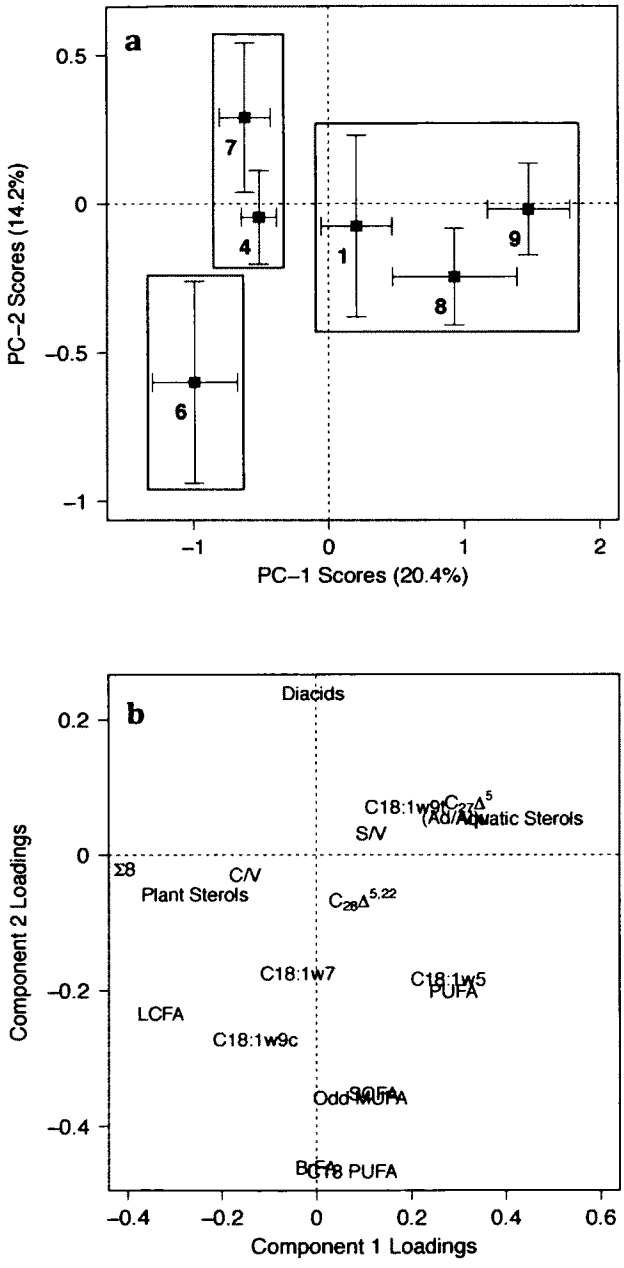

Figure 5-3. Diacid concentrations before and after 1970 for all sediment cores. Cores are plotted with respect to their distance form the dam, with cores 1 and 6 closest to the dam, and cores 8 and 9 furthest from the dam. Error bars represent 1 standard error of the mean. The 1970 horizon coincides with the construction of the New Bullards Bar dam and the discontinuation of the annual lake level drawdowns in Englebright Lake. Shifts in diacid concentrations before vs after 1970 are significant in core 1 ($p = 0.002$), core 6 ($p < 0.001$).

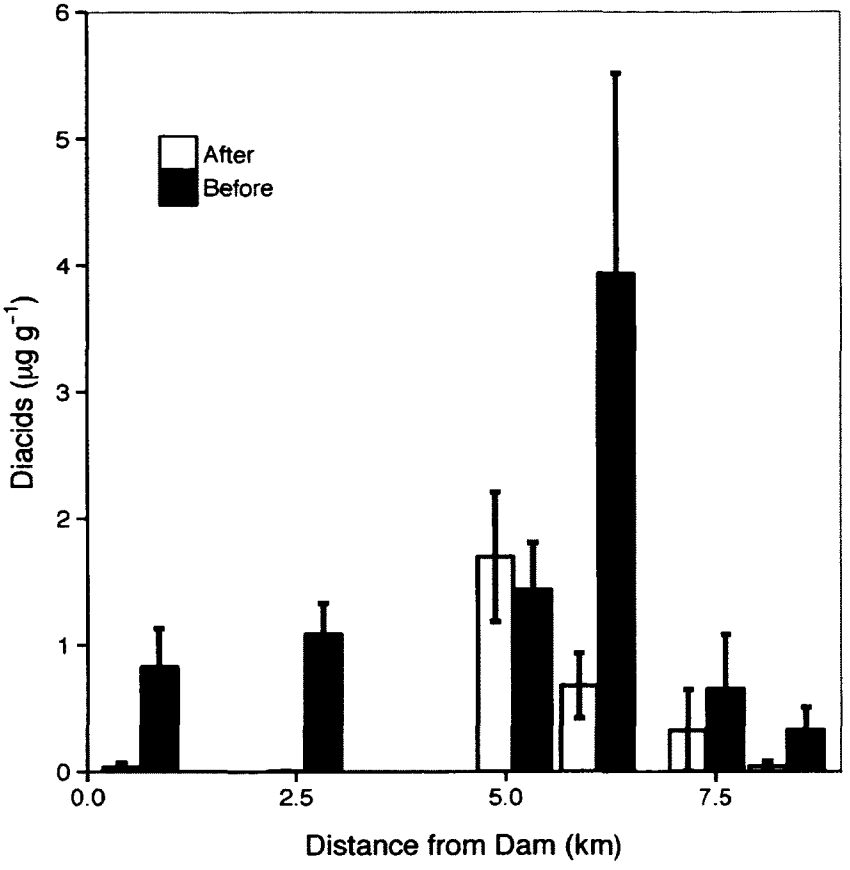

Figure 5-4. Profiles of select terrigenous biomarkers in core 7.
Concentrations of biomarkers are significantly greater in core 7 only. The grey shaded bar highlights the 1962-1964 flood events in the watershed. Concentrations of lignin phenols (Σ8), LCFA, and plant sterols show significant increases during this event ($p < 0.001$). Note the concentration of lignin biomarkers is two orders of magnitude higher than concentrations of lipid biomarkers.

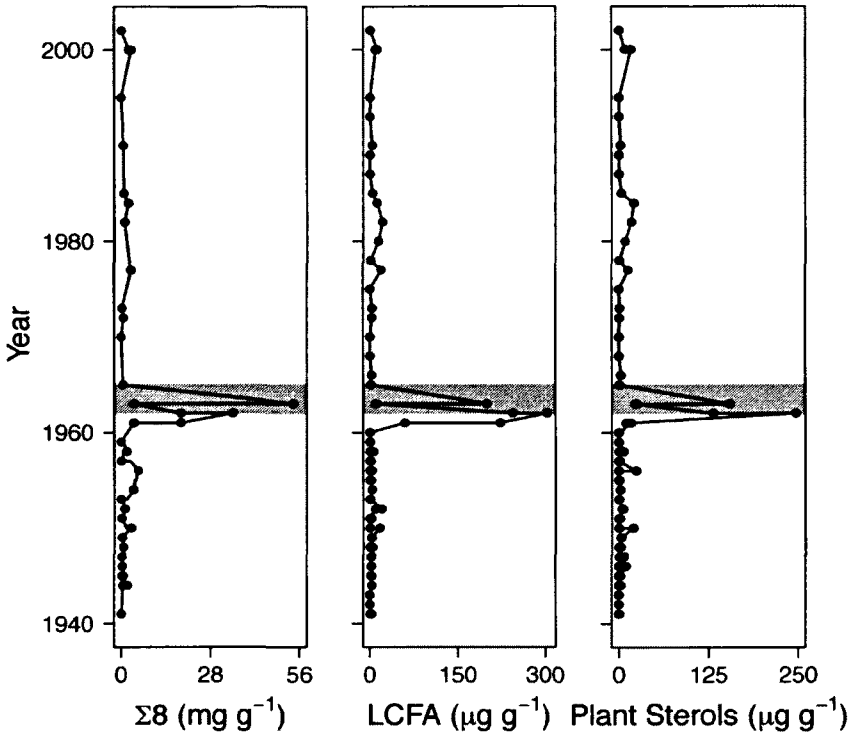

Figure 5-5. Profiles of lignin phenols for Englebright Lake cores.
The mean (solid vertical line) and standard error (dotted vertical lines) of Σ8 values for non-event layers are shown for all cores. Grey shaded bars identify the layers where statistical increases in Σ8 concentrations are coincident with flood events in the watershed, highlighting the magnitude and differential preservation of flood events throughout Englebright Lake.

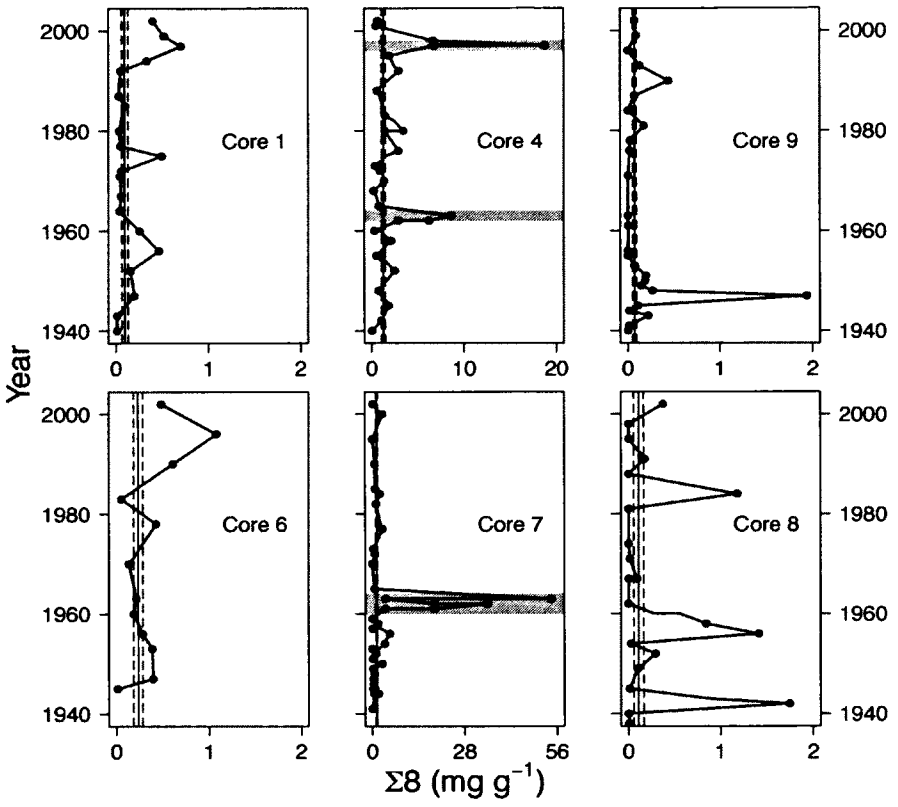

Figure 5-6. Biplot of ratios of C/V and S/V lignin phenols.
Mean values of C/V and S/V are shown for each core, and error bars represent one standard error of the mean. Boxes indicate compositional ranges of gymnosperm woods (G), angiosperm woods (A), gymnosperm needles (g), and angiosperm leaves (a) (Goni 1997, Goni et al. 1998). The biplot shows that signatures from Englebright Lake sediments represent a mixture of vascular plant sources.

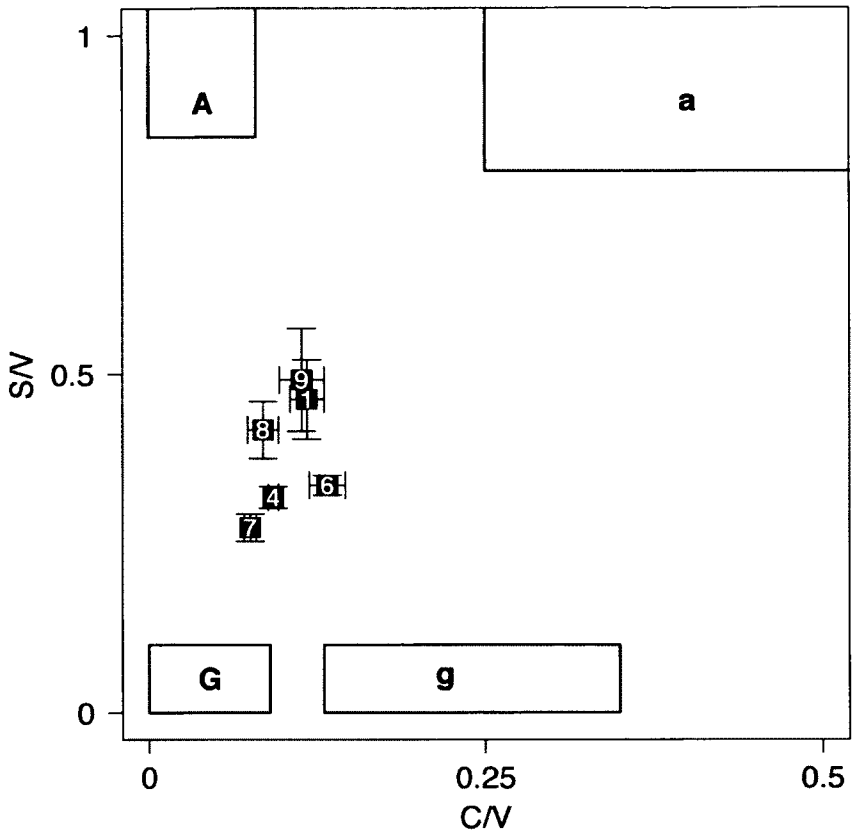

Figure 5-7. Climate and discharge records for Englebright Lake (1940-2010). Annual index Pacific Decadal Oscillation (PDO) (a), multivariate ENSO index (MEI) (b), and mean daily discharge (c) from Englebright Lake (USGS gauging station 11418000) throughout the history of Englebright Lake. Positive PDO values indicate warm PDO phase and negative values show cold PDO phase. La Niña events have low (< -0.5) MEI values and El Niño have high (> 0.5) MEI values. Horizontal lines reference 0 (PDO and ENSO) and -0.5 and 0.5 (ENSO). Discharge from Englebright Lake responds similarly to the natural river discharge, and shown by the comparison the discharge from Englebright Lake and from the South Yuba River (shown in blue). Flood events in Englebright Lake are identified as periods when mean daily discharge exceeds 1500 m^3s^{-1} (dashed line), and includes 9 events between 1940 and 2002.

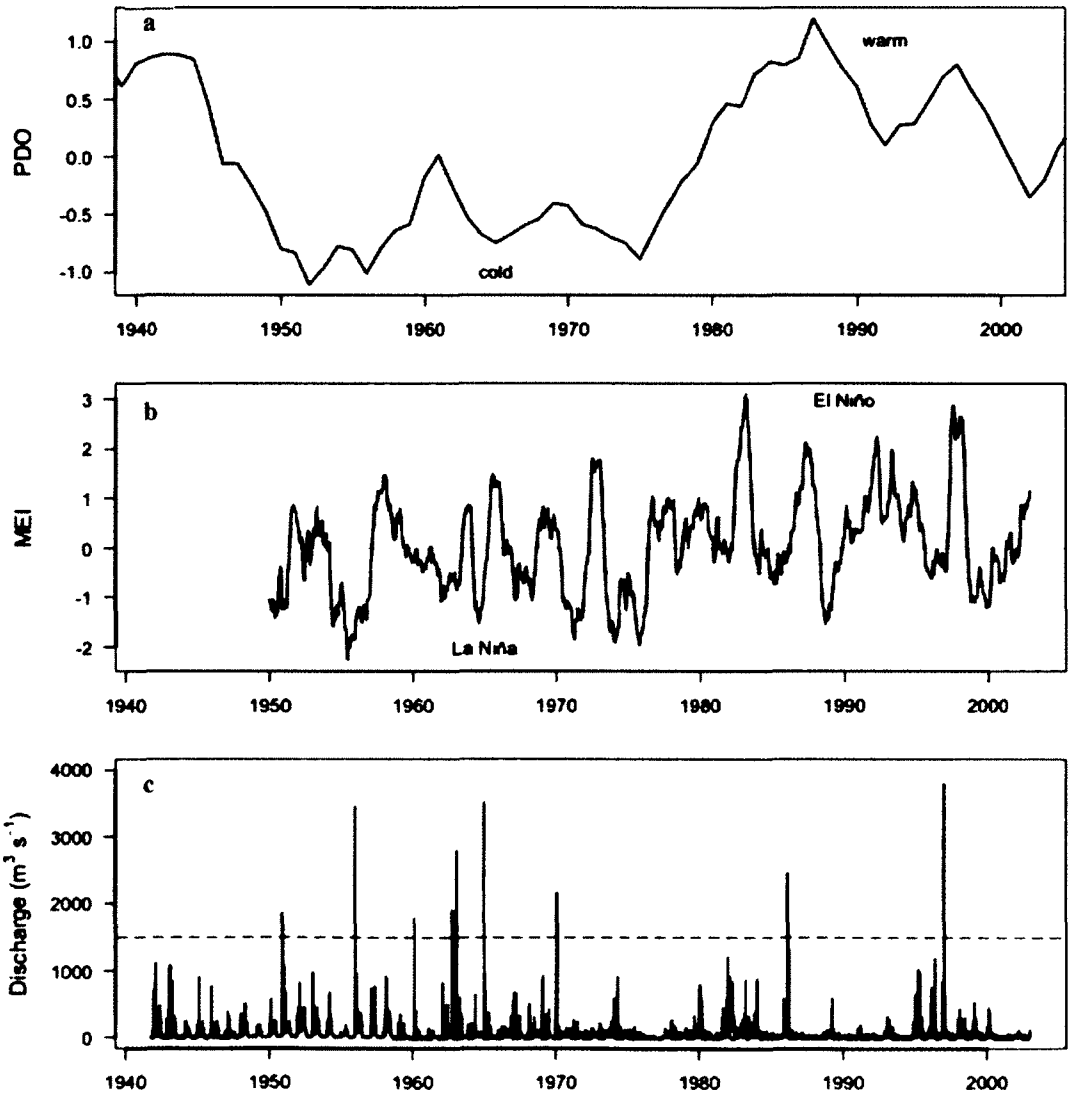

Table 5-1. Description of events impacting Englebright Lake.
For each large flood event (defined as mean daily discharge > 1500 $m^3 s^{-1}$), the mean daily discharge (Q_d), peak discharge (Q_p), and duration is listed. PDO and ENSO phases the each event year are also provided.

Year	Event	Q_d ($m^3 s^{-1}$)	Q_P ($m^3 s^{-1}$)	Duration (days)	PDO Phase	ENSO
2002	USGS Coring Campaign					
1997	Flood	3794	3821	5	warm	El Nino
1986	Flood	2469	2030	4	warm	El Nino
1970	Annual lake level drawdowns cease					
1970	Flood	2163	2663	4	neutral	La Nina
1964	Flood	3511	4839	6	cold	La Nina
1963	Flood	2801	4245	2	cold	neutral
1962	Flood	1903	na	2	cold	La Nina
1960	Flood	1770	2434	1	neutral	neutral
1955	Flood	3455	4188	3	cold	La Nina
1950	Flood	1853	3085	3	cold	La Nina
1940	Englebright Dam Completed					
1848	Start of Gold Mining					

Table 5-2. List of biomarker variables used in Principal Components Analysis.

Variable	Biomarker	Source	Reference
PUFA	16:2+16:3+16:4+20:2+ 20:3ω(6,3)+20:4ω(6,3)+20:5ω3+22 :2+22:5ω3+22:6ω3	Labile Phytoplankton	(Volkman et al. 1989, Canuel 2001)
SCFA	12:0+14:0+16:0+18:0	Algal	(Canuel and Martens 1993)
Aquatic Sterols	Cholesta-5,22-dien-3β-ol+ 27-nor-24-cholesta-5,22-dien-3β-ol	Diatoms, dinoflagellates	(Goad and Withers 1982, Volkman 1986)
$C_{28}\Delta^{5,22}$	Brassicasterol	Diatoms	(Volkman 1986)
$C_{27}\Delta^{5}$	Cholesterol	Zooplankton, algae (trace)	(Volkman et al. 1987, Volkman 2003)
C16:1	16:1ω9+16:1ω7+16:1ω5	Phytoplankton and bacteria	(Volkman et al. 1980)
C18:1w9t	18:1ω9t	Green algae, higher plants	(Volkman et al. 2008)
C18:1w9c	18:1ω9c	Green algae, higher plants	(Volkman et al. 2008)
C18:1w7	18:1ω7	Fungi and bacteria	(Zelles 1999, Ruess and Chamberlain 2010)
C18:1w5	18:1ω5	Fungi and bacteria	(Zelles 1999, Ruess and Chamberlain 2010)
Odd MUFA	15:1+17:1+19:1	Bacteria	(Volkman et al. 1980)
BrFA	i15+a15+i17+a17+i19+a19	Bacteria	(Volkman et al. 1980, Canuel and Martens 1993)
C_{18} PUFA	18:2ω6+18:3ω6+18:3ω3+18:4	Higher plants, fungi	(Zelles 1999)
Diacids	14α,ω+16α,ω+18α,ω+ 20α,ω+22α,ω+24α,ω	Higher plants	(Volkman et al. 1980, Zelles 1999)
LCFA	22:0+24:0+25:0+26:0+27:0 +28:0+29:0+30:0	Higher plants	(Zimmerman and Canuel 2001, Waterson and Canuel 2008)
Plant Sterols	Stigmasterol+Campesterol+ Sitosterol	Higher plants	(Huang and Meinschein 1979, Volkman et al. 1987)
Σ8	Cinnamyl+Vanillyl+Syringyl phenols	Vascular plants	(Hedges and Mann 1979)
S/V	Syringyl/ Vanillyl phenols	Angiosperm vs. gymnosperm	(Hedges and Mann 1979)
C/V	Cinnamyl/Vanillyl phenols	Hard vs. soft plant tissue	(Hedges and Mann 1979)
(Ad/Al)v	Acid to aldehyde ratios of vanillyl phenols	Degradation of plant tissue	(Goñi et al. 1993, Opsahl and Benner 1995)

Table 5-3. List of significant biomarker responses to lake and watershed events. Mean values for biomarkers in cores and depositional regimes where significant differences were measured in response to hydrologic history (i.e., lake level draw-downs) or flood events). The table is divided by event type to highlight the biomarkers and cores (or bottomset depositional regime [B]) that are responding to each event. Standard deviations are reported for every mean, and p-values from one-way Student's t-test are reported for every significant difference. The "normal" classification refers to non-event accumulation. BD indicates values that are below detection.

		Σ8 (mg g^{-1})	LCFA (μg g^{-1})	Diacids (μg g^{-1})	Plant Sterols (μg g^{-1})	Aquatic Sterols (ng g^{-1})
Draw-downs						
C1	After	-	-	0.04± 0.12	-	-
	Before	-	-	0.83 ± 0.85	-	-
	p-value	-	-	0.002	-	-
C6	After	-	-	BD	-	-
	Before	-	-	1.09 ± 0.60	-	-
	p-value	-	-	<0.001	-	-
B	After	-	-	-	-	29.61 ± 49.91
	Before	-	-	-	-	8.37 ± 5.95
	p-value	-	-	-	-	<0.001
Flood Event						
C4	Normal	0.62 ± 0.94	-	-	-	-
	Event	7.14 ± 5.88	-	-	-	-
	p-value	0.008	-	-	-	-
C7	Normal	0.75 ± 1.26	4.64 ± 8.98	-	3.87 ± 6.49	-
	Event	31.70 ± 16.89	242.50 ± 44.10	-	135.71 ± 97.7	-
	p-value	<0.001	<0.001	-	<0.001	-

Table 5-4. Average biomarker concentrations in each core.
The minimum, maximum, and mean values of select aquatic, bacterial, and terrigenous biomarkers are presented for each core. TAR_{FA} and (Ad/Al)v are also shown. Concentrations that were below detection are indicated with BD.

		Aquatic				Bacterial		Terrigenous						
		SCFA	PUFA	Aquatic Sterols	$C_{27}\Delta^5$	BrFA	Odd MUFA	LCFA	C_{18}PUFA	Diacids	Plant Sterols	Σ8[a]	TAR_{FA}	(Ad/Al)v
1	min	0.53	0.21	0.01	0.02	0.11	0.09	1.01	0.41	0.29	0.39	0.01	0.09	0.33
	max	25.2	0.66	0.27	0.72	5.52	1.46	50.21	28.87	2.37	15.74	0.7	8.15	1.08
	mean	4.9	0.43	0.05	0.25	0.92	0.32	7.87	5.97	1.01	3.55	0.2	2.46	0.67
6	min	0.95	BD	0.02	0.00	0.31	0.11	1.58	1.24	0.69	1.71	0.01	0.12	0.42
	max	50.87	BD	0.13	0.97	3.91	0.88	24.94	21.34	2.19	20.40	1.08	2.94	0.93
	mean	11.12	BD	0.07	0.34	1.4	0.38	12.43	6.41	1.09	8.56	0.36	1.75	0.55
4	min	1.02	0.24	0.02	0.04	0.16	0.07	1.53	0.94	0.32	0.73	0.02	0.32	0.31
	max	51.53	74.41	0.13	2.17	5.44	2.26	107.41	51.82	11.43	40.08	18.76	5.03	0.69
	mean	12.38	13.2	0.07	0.4	1.08	0.39	18.93	9.33	2.22	11.8	2.8	2.02	0.44
7	min	0.15	0.03	0.14	0.01	0.03	0.04	0.07	0.38	0.04	0.06	0.01	0.04	0.23
	max	128.45	0.95	0.14	0.91	5.46	13.54	303.05	211.54	57.06	247.04	54.22	8.34	1.25
	mean	13.11	0.23	0.14	0.17	0.69	0.97	26.56	15.56	5.51	17.23	4.41	1.77	0.47
9	min	0.06	3.68	0.06	0.00	0.00	0.02	0.01	0.22	0.01	0.00	0.00	0.02	0.29
	max	13.84	3.68	0.06	0.19	2.38	0.63	19.51	10.84	9.55	4.6	1.94	2.65	2.28
	mean	2.85	3.68	0.06	0.03	0.31	0.12	2.46	2.32	1.49	0.92	0.16	0.9	0.69
8	min	0.04	BD	0.03	0.00	0.01	0.00	0.03	0.04	0.12	0.01	0.00	0.06	0.23
	max	29.03	BD	0.03	0.19	1.92	0.5	56.51	27.83	2.87	31.56	1.74	3.59	3.3
	mean	5.28	BD	0.03	0.04	0.4	0.14	5.97	3.97	0.74	4.22	0.3	0.99	0.85

a: All concentrations are in $\mu g\ g^{-1}$, except for Σ8, which is presented in $mg\ g^{-1}$

CHAPTER 6: SUMMARY & CONCLUSIONS

The impacts of dams on the transport of sediments and nutrients through rivers have been well documented (Friedl and Wuest 2002, Wright and Schoellhamer 2004, Walling 2006), and within the last 20 years, research has shown that dams and their impoundments can be significant global sinks for terrestrial organic carbon (Downing et al. 2008, Stallard 2012). These impoundments have profound effects on the global carbon cycle, increasing the evasion of CO_2 and CH_4 greenhouse gases from reservoir surfaces in aquatic systems (St Louis et al. 2000, Friedl and Wuest 2002), while simultaneously decreasing carbon export to the coastal ocean (Stallard 2012). Investigations of the downstream impact of dams are numerous (e.g., Kondolf 1997, Wright and Schoellhamer 2004, Walling 2006, Singer 2007, Canuel et al. 2009), but few studies have focused on the organic carbon (OC) accumulation behind dams (Houel et al. 2006, Downing et al. 2008), and few have used multi-proxy approaches to study organic matter sources. This study explored trends in the signatures of OC trapped in Englebright Lake, an impoundment in northern California, to: (1) determine organic matter sources to the impoundment, (2) examine OC accumulation over spatial and temporal scales, and (3) relate OC signatures in the impounded sediments to events in the watershed. This chapter will discuss some of the implications of the data presented in this dissertation, limitations associated with the data analysis and interpretation, and potential avenues for future research.

A comparison of stable carbon and nitrogen isotopes and biomarker signatures between end-member samples collected from the Yuba River watershed and sediments collected from Englebright Lake indicated that terrigenous OC sources (i.e., higher plants and soils) dominated (>55%) OC signatures in Englebright Lake, while the aquatic signatures were consistent with diatoms and zooplankton. Flood events significantly impacted OC accumulation in Englebright Lake, and during periods of high discharge, large amounts of coarse, terrigenous organic matter (i.e., leaves and twigs) accumulated in foreset deposits near the delta front. Bottomset and topset deposits, while less influenced by flood events, recorded the impacts of changing hydrologic regime in the lake. Biomarkers in bottomset sediments shifted toward more aquatic signatures, whereas in the topset

deposits biomarkers became increasingly terrigenous in response to the construction of an upstream dam and the resulting discontinuation of annual lake level draw-downs. Patterns in OC accumulation showed that the depositional regimes associated with Gilbert-type deltas strongly influenced the distribution of OC, which was higher in bottomset and foreset deposits than in topset deposits. However, due to the magnitude of impact from flood events, the highest rates of OC accumulation in Englebright Lake were measured in foreset deposits.

This dissertation offers the first detailed analysis of organic carbon accumulation in a lake in relation to depositional regimes associated with Gilbert-type deltas. OC mass accumulation in Englebright Lake is comparable or greater than estimates of OC accumulation in other reservoirs (Downing et al. 2008, Tranvik et al. 2009), but the source of this OC (i.e., soils and vegetation) suggests more allochthonous inputs in Englebright Lake than measured in other reservoirs (Downing et al. 2008). This is likely due to low levels of agriculture in the watershed and lower nutrient inputs to Englebright Lake compared with the more eutrophic systems that have been studied previously, in addition to lower light attenuation resulting from high sediment loads due to hydraulic mining activity.

Comparisons to other reservoir systems highlight the massive amount of OC buried in Englebright Lake, but the total OC buried in Englebright Lake between 1940 and 2002. However, despite these high rates of OC burial, this only represents two-fold more carbon than phytoplankton primary productivity in San Francisco Bay during 1980, a year of especially low productivity (Jassby et al. 1993). However, data from this study provide information that can be extrapolated to reservoirs throughout California to compare total reservoir OC accumulation to total primary production derived OC burial in the San Francisco Bay. Using modeled estimates of sediment accumulation for 69 reservoirs in California (Minear and Kondolf 2009), the average dry bulk density reported for California sediments (960 kg m^{-3}; Dendy and Champion 1978), and average total organic carbon content from Englebright Lake sediments, the total mass of OC

buried in reservoirs across California between 1880 and 2008 is 30.85 Tg OC. Based on data from the 3-end-member mixing model in Englebright Lake, at least 18.85 Tg of this OC is derived from terrigenous sources.

The amount of OC buried in California reservoirs (~30Tg OC) is similar to estimated OC buried in the San Francisco Bay (~22 Tg OC) during the same time period (1880-2008) based on the OC mass accumulation rates presented in Jassby et al. (1993). This measurement is a conservative estimate since it does not reflect the increasing rates of primary production over the last decade in response to climate shifts observed in 1998 (Cloern and Jassby 2012). However, this comparison shows that the amount of OC produced by phytoplankton in the San Francisco Bay is similar to the amount of OC that has accumulated behind dams in California. Data from this dissertation suggest that the proliferation of dams has had, and will continue to have, significant impacts on global carbon cycling. As a result, OC cycling in reservoirs requires more study to predict how climate and anthropogenic change will influence the impact of dams on downstream environments.

Limitations of this study and directions for further research

This study offered insights into the impact of dams on the transport and sequestration of terrestrial organic carbon, and biomarkers describe the responses to anthropogenic and climate driven events in the watershed. A few limitations associated with the methodology of this dissertation should be considered when interpreting results of this analysis. First, the sampling resolution between cores is not equal. Therefore, discussions about the impact of events being restricted only to a few cores, for example, may be due to higher resolution in one core that captured the event, while low resolution in another core missed the event signature. Second, analysis of OC sources depends on literature values as well as biomarker signatures from end-member sources analyzed from the watershed. The limited literature on many of the potential sources that characterize the study system, and evidence that the end-member sampling strategy did not capture all OC sources, restricted interpretation of the sediment cores. A more thorough investigation of

local OC sources is needed to more accurately determine how changing biomarker signatures reflect the response of OC to events in the watershed. Finally, uncertainty associated with plutonium dating profiles may result in misinterpretations of the responses of accumulation in sediments to events in the watershed. In order to improve the age model, additional chronometers (e.g., organic contaminants such as the pesticide dichlorodiphenyltrichloroethane (DDT) with well-established use records) could be measured to support accumulation rates calculated from plutonium isotopes (Canuel et al., 2009).

Results presented in this dissertation add to the current knowledge of biogeochemical cycling of organic carbon in reservoirs by examining sources of aquatic and terrigenous OC using biomarkers and relating changes in biomarkers to events in the watershed. With growing concerns about mitigating impacts from anticipated climate change scenarios, there is a need to understand how environmental systems have responded to past and current events. Therefore, future research may explore the following topics in order to meet this need:

- Investigate the response of terrestrial systems to additional anthropogenic impacts (road construction, fire/drought, increasing population density, etc.) using different biomarkers (i.e., PAH, carbohydrates, contaminants)
- Develop more robust biomarker signature of aquatic and terrigenous end-members that can be applied to lake and freshwater systems
- Determine the role of watershed priming in the response of terrestrial systems to large events in order to predict when an event will have a significant impact on the transport of water, sediment, and/or nutrient in watersheds
- Quantify carbon accumulation, burial, transformation, and evasion in reservoirs to establish the role of dams (i.e., source or sink) in the global carbon cycle

Accumulation in Englebright Lake demonstrates the response of substantial amounts of terrestrial organic carbon to multiple events in the watershed, and the sequestration of this

organic carbon load emphasizes the role of impoundments as terrestrial carbon sinks. While the impact of impoundments on the global carbon cycle is just beginning to be understood, the demonstrated storage capacity of these systems suggests that they could have significant implications for climate mitigation strategies in the future.

Literature Cited

Canuel, E., E. Lerberg, R. Dickhut, S. Kuehl, T. Bianchi, and S. Wakeham. 2009. Changes in sediment and organic carbon accumulation in a highly-disturbed ecosystem: The Sacramento-San Joaquin River Delta (California, USA). Marine Pollution Bulletin 59:154–163.

Cloern, J. E., and A. D. Jassby. 2012. Drivers of change in estuarine-coastal ecosystems: Discoveries from four decades of study in San Francisco Bay. Reviews of Geophysics 50:RG4001.

Dendy, F. E., and W. A. Champion. 1978. Sediment deposition in U.S. reservoirs: summary of data reported through 1975. Page 68. Miscellaneous Publication 1362, U.S. Dept. of Agric, Washington, D.C.

Downing, J., J. Cole, J. Middelburg, R. Striegl, C. Duarte, P. Kortelainen, Y. Prairie, and K. Laube. 2008. Sediment organic carbon burial in agriculturally eutrophic impoundments over the last century. Global Biogeochemical Cycles 22:GB1018.

Friedl, G., and A. Wuest. 2002. Disrupting biogeochemical cycles - Consequences of damming. Aquatic Sciences 64:55–65.

Houel, S., P. Louchouarn, M. Lucotte, R. Canuel, and B. Ghaleb. 2006. Translocation of soil organic matter following reservoir impoundment in boreal systems: Implications for in situ productivity. Limnology and Oceanography 51:1497–1513.

Jassby, A., J. Cloern, and T. Powell. 1993. Organic carbon sources and sinks in San Francisco Bay: variability induced by river flow. Marine Ecology Progress Series 95:39–54.

Kondolf, G. M. 1997. Hungry Water: Effects of Dams and Gravel Mining on River Channels. Environmental Management 21:533–551.

Minear, J. T., and G. M. Kondolf. 2009. Estimating reservoir sedimentation rates at large spatial and temporal scales: A case study of California. Water Resources Research 45:W12502.

Singer, M. B. 2007. The influence of major dams on hydrology through the drainage network of the Sacramento River basin, California. River Research and Applications 23:55–72.

St Louis, V., C. Kelly, E. Duchemin, J. Rudd, and D. Rosenberg. 2000. Reservoir surfaces as sources of greenhouse gases to the atmosphere: A global estimate. BioScience 50:766–775.

Stallard, R. F. 2012. Terrestrial sedimentation and the carbon cycle: Coupling weathering and erosion to carbon burial. Global Biogeochemical Cycles 12:231–257.

Tranvik, L. J., J. A. Downing, J. B. Cotner, S. A. Loiselle, R. G. Striegl, T. J. Ballatore, P. Dillon, K. Finlay, K. Fortino, and L. B. Knoll. 2009. Lakes and reservoirs as regulators of carbon cycling and climate. Limnology and Oceanography 54:2298–2314.

Walling, D. 2006. Human impact on land-ocean sediment transfer by the world's rivers. Geomorphology 79:192–216.

Wright, S., and D. Schoellhamer. 2004. Trends in the Sediment Yield of the Sacramento River, California, 1957-2001. San Francisco Estuary and Watershed Science 2:Article 2.

APPENDIX 1: ORGANIC CARBON PROXIES FOR CORE SAMPLES

Values of TOC, TN, C:N_a, $\delta^{13}C$, and $\delta^{15}N$ are presented for each sample analyze from the six sediment cores collected from Englebright Lake. Each core is presented in a separate table, and the depth of each sample is included in these tables. Values below detection are indicated with b.d., and samples that were not analyzed for these are indicated with n.a.

Table A1-1. Organic carbon proxies for Core 1.

Sample ID	Depth (m)	TOC (%)	TN (%)	$C:N_a$	$\delta^{13}C_{TOC}$	$\delta^{15}N_{TN}$
1A-1H-1 5-15	0.00	2.15	0.11	20.05	-25.74	2.27
1A-1H-1 35-45	0.30	2.39	0.12	19.42	-25.89	1.89
1A-1H-1 65-75	0.60	3.40	0.17	20.23	-25.98	1.20
1D-1H-1 71-81	0.90	1.64	0.10	16.12	-26.56	0.92
1D-1H-1 101-111	1.20	0.69	0.05	13.38	-26.06	1.32
1D-1H-1 130-137	1.50	0.82	0.06	14.41	-26.01	2.74
1D-1H-2 21-31	1.80	0.73	0.05	15.43	-26.03	2.13
1D-1H-2 51-61	2.10	0.88	0.06	15.76	-25.97	2.67
1D-1H-2 71-81	2.30	0.74	0.04	17.12	-25.84	0.81
1B-2E-2 24-34	2.70	0.66	0.05	13.05	n.a.	n.a.
1B-2E-2 54-64	3.00	0.76	0.06	13.25	-26.11	3.32
1B-2E-2 84-94	3.30	1.32	0.06	21.23	-25.69	3.27
1B-2E-2 114-124	3.60	0.77	0.06	13.36	n.a.	n.a.
1B-2E-3 9-19	3.90	0.76	0.05	14.02	-26.17	2.91
1B-2E-3 39-49	4.20	0.74	0.05	13.43	-25.80	2.76
1B-2E-3 69-79	4.50	0.71	0.05	13.36	-25.97	3.37
1B-2E-3 99-109	4.80	1.68	0.09	18.62	-25.38	2.19
1B-2E-3 129-139	5.10	2.88	0.14	20.56	-25.26	2.76
1B-3E-1 9-19	5.40	0.74	0.05	15.97	-24.98	2.20
1B-3E-1 39-49	5.70	1.26	0.07	18.49	-25.20	2.83
1B-3E-1 69-79	6.00	0.41	0.04	9.83	-25.74	3.25
1B-3E-1 99-109	6.30	0.39	0.03	11.24	-26.01	3.32

Table A1-2. Organic carbon proxies for Core 6.

Sample ID	Depth (m)	TOC (%)	TN (%)	$C:N_a$	$\delta^{13}C_{TOC}$	$\delta^{15}N_{TN}$
6F-1H-1 77-97	0.00	2.18	0.10	22.69	-28.15	-3.04
6F-1H-2 19-39	0.52	3.72	0.17	21.50	-28.50	-3.68
6E-1H-2 49-69	1.12	2.48	0.10	23.86	-28.06	-3.70
6E-1H-2 119-139	1.82	0.49	0.03	15.27	-28.06	-2.48
6F-2H-1 50-70	2.39	2.34	0.09	26.02	-27.20	-2.56
6E-2H-2 43-63	3.12	1.11	0.06	19.93	-27.40	-1.63
6F-2H-2 80-100	3.81	1.46	0.07	20.05	-27.92	-1.72
6F-2H-2 123-143	4.23	1.23	0.06	19.64	-27.31	-1.21
6B-2H-2 35-55	4.62	1.80	0.09	19.85	-27.72	-2.06
6F-3E-1 41-61	5.19	1.98	0.08	24.19	-27.70	-3.44
6E-3E-1 71-91	5.93	1.92	0.09	22.40	-27.42	-1.73
6E-3E-2 38-58	6.82	0.28	0.03	8.25	-28.14	-2.66

Table A1-3. Organic carbon proxies for Core 4.

Sample ID	Depth (m)	TOC (%)	TN (%)	$C:N_a$	$\delta^{13}C_{TOC}$	$\delta^{15}N_{TN}$
4B-1H-1 7-17	0.00	1.14	0.07	15.66	-26.47	1.49
4B-1H-1 17-27	0.10	0.85	0.06	15.12	n.a.	n.a.
4A-1H-1 33-43	0.60	6.26	0.20	31.96	-27.21	-1.23
4A-1H-1 53-63	0.80	10.00	0.34	29.60	-27.68	-2.01
4A-1H-1 63-73	0.90	4.12	0.16	25.92	-28.04	0.94
4A-1H-1 93-103	1.20	2.72	0.15	18.11	-26.78	-0.44
4A-1H-2 13-23	1.50	2.02	0.09	21.43	-27.46	1.36
4A-1H-2 43-53	1.80	3.37	0.14	24.17	-26.81	-0.31
4A-1H-2 73-83	2.10	3.18	0.16	20.48	-26.25	0.86
4A-1H-2 103-113	2.40	1.15	0.06	17.94	n.a.	n.a.
4A-1H-2 133-143	2.70	1.63	0.10	17.08	-27.17	1.59
4B-2H-1 26-36	3.00	1.59	0.09	16.96	-26.91	1.52
4B-2H-1 56-64	3.30	1.57	0.09	18.24	-26.20	1.09
4B-2H-1 86-95	3.60	1.56	0.08	20.50	n.a.	n.a.
4A-2H-2 61-71	3.82	2.85	0.12	24.01	n.a.	n.a.
4B-2H-1 110-118	3.84	1.92	0.11	17.62	-26.24	0.97
4B-2H-2 18-28	4.20	0.87	0.06	14.32	-26.24	1.57
4B-2H-2 48-58	4.50	2.23	0.08	29.43	-27.09	0.33
4A-2H-3 17-27	4.80	0.67	0.04	16.21	-26.46	1.87
4A-2H-3 47-57	5.10	0.91	0.05	18.13	-26.58	2.04
4A-2H-3 67-77	5.30	0.66	0.05	14.47	-26.18	1.45
4A-2H-3 77-87	5.40	0.69	0.04	16.80	n.a.	n.a.
4A-2H-3 107-117	5.70	1.48	0.08	18.29	-26.15	1.18
4B-3H-1 17-27	6.00	0.86	0.07	12.48	n.a.	n.a.
4B-3H-1 47-57	6.30	0.88	0.04	20.55	-25.91	1.67

4B-3H-1 74-85	6.60	1.11	0.05	23.22	-25.66	3.76
4B-3H-1 107-117	6.90	6.69	0.22	29.78	-27.59	1.86
4A-4H-1 59-69	7.30	5.66	0.17	33.22	-26.31	-0.31
4A-4H-1 89-99	7.60	3.06	0.10	32.09	-26.38	-0.76
4A-4H-2 1-11	7.90	0.94	0.05	17.50	-25.26	2.58
4A-4H-2 31-41	8.20	2.05	0.08	25.51	n.a.	n.a.
4A-4H-2 61-71	8.50	5.07	0.17	29.34	-26.13	-0.03
4A-4H-2 91-101	8.80	2.82	0.12	23.74	n.a.	n.a.
4A-4H-2 121-131	9.10	1.99	0.10	19.98	-26.46	1.75
4B-4H-1 61-71	9.40	3.08	0.16	19.00	n.a.	n.a.
4B-4H-1 91-101	9.70	1.06	0.07	15.27	-25.55	1.90
4B-4H-1 121-131	10.00	0.81	0.06	14.11	n.a.	n.a.
4B-4H-2 31-41	10.30	1.47	0.08	19.57	n.a.	n.a.
4B-4H-2 61-71	10.60	2.21	0.10	22.00	-25.88	1.65
4A-5H-2 42-52	10.90	2.74	0.12	22.34	n.a.	n.a.
4A-5H-2 72-82	11.20	2.61	0.12	21.51	-26.11	1.03
4A-5H-2 102-112	11.50	1.05	0.07	14.30	n.a.	n.a.
4A-5H-2 132-142	11.80	0.88	0.06	14.75	-25.94	2.24
4B-5H-1 75-85	12.20	1.40	0.07	19.06	-25.35	1.83
4B-5H-1 105-115	12.50	2.29	0.08	27.41	-25.91	1.29
4B-5H-1 137-147	12.81	2.29	0.09	26.32	n.a.	n.a.
4B-5H-2 24-34	13.10	1.58	0.08	18.65	-25.15	3.01
4B-5H-2 54-64	13.40	2.68	0.11	23.69	n.a.	n.a.
4B-5H-2 84-94	13.70	0.56	0.04	14.45	n.a.	n.a.
4B-5H-2 114-124	14.00	0.76	0.05	15.31	-25.90	2.22
4B-5H-2 140-150	14.26	1.27	0.07	17.67	-25.87	1.83
4B-6H-1 23-33	14.60	0.17	0.02	7.90	-26.10	4.15
4B-6H-1 53-63	15.00	0.25	0.02	12.15	-24.74	1.32

Table A1-4. Organic carbon proxies for Core 7.

Sample ID	Depth (m)	TOC (%)	TN (%)	$C:N_a$	$\delta^{13}C_{TOC}$	$\delta^{15}N_{TN}$
7C-1H-1 27-37	0.00	0.25	0.01	17.31	-24.79	0.88
7C-1H-2 60-70	0.33	2.99	0.09	31.87	-25.93	-0.78
7C-1H-1 77-87	0.50	1.46	0.04	33.12	-27.24	-0.86
7C-1H-2 110-120	2.00	0.05	0.01	8.49	n.a.	n.a.
7C-2H-1 39-49	2.50	0.05	0.00	22.17	n.a.	n.a.
7C-2H-1 109-119	3.20	0.45	0.02	29.54	-25.83	-0.57
7C-2H-2 9-19	3.70	0.07	0.01	6.63	n.a.	n.a.
7C-2H-2 59-69	4.20	0.15	0.01	13.87	-25.74	-0.94
7A-2H-2 32-42	4.70	1.04	0.03	32.68	-26.34	1.61
7A-2H-2 82-92	5.20	2.59	0.11	24.03	-27.16	1.39
7C-3H-1 66-76	5.70	1.87	0.10	19.49	-26.41	1.14
7C-3H-1 124-134	6.20	2.01	0.10	20.35	n.a.	n.a.
7C-3H-2 25-35	6.70	0.52	0.02	23.40	-25.72	3.53
7C-3H-2 95-105	7.20	1.83	0.05	35.58	n.a.	n.a.
7C-3H-2 125-135	7.70	0.34	0.02	14.17	-25.37	0.06
7C-4H-1 14-24	8.20	0.68	0.04	16.17	-26.54	3.08
7C-4H-2 20-30	8.70	2.05	0.03	62.00	-24.66	1.49
7C-4H-2 66-76	9.20	0.08	0.01	7.62	-19.29	-1.01
7C-4H-3 37-47	9.70	0.10	0.01	6.59	-20.68	-1.57
7C-4H-3 87-97	10.20	0.86	0.05	17.12	-25.90	2.77
7A-4H-2 44-54	10.70	0.26	0.01	18.36	-24.44	-0.02
7A-4H-2 94-104	11.20	30.24	0.57	53.47	n.a.	n.a.
7C-5H-1 78-88	11.70	1.92	0.06	32.51	-25.55	-0.57
7C-5H-1 128-138	12.20	17.86	0.41	44.08	n.a.	n.a.
7C-6H-1 20-30	12.70	17.15	0.59	29.02	-27.79	-0.06

7C-6H-1 70-80	13.20	12.26	0.50	24.49	-26.59	-1.32
7C-6H-1 120-137	13.70	3.13	0.12	26.04	-27.13	2.09
7C-6H-2 19-29	14.20	0.07	0.02	3.30	n.a.	n.a.
7C-6H-2 69-79	14.70	0.14	0.02	8.26	-20.21	-0.46
7C-6H-2 119-129	15.20	1.61	0.06	25.50	n.a.	n.a.
7C-7H-1 20-30	15.70	0.82	0.03	25.38	-25.23	0.32
7C-7H-1 60-70	16.20	0.12	0.02	6.37	n.a.	n.a.
7C-7H-1 110-120	16.70	0.28	0.02	12.32	-24.07	-2.03
7C-7H-2 25-35	17.20	0.11	0.02	6.30	-22.85	-0.98
7C-7H-2 75-85	17.70	3.89	0.12	33.82	-25.79	-0.57
7C-7H-2 110-120	18.20	1.27	0.06	21.08	n.a.	n.a.
7C-8H-1 20-30	18.70	0.30	0.02	12.75	-23.69	-0.20
7C-8H-1 70-80	19.20	0.31	0.02	17.82	-24.83	-0.73
7C-8H-1 116-126	19.66	0.78	0.05	16.41	n.a.	n.a.
7C-9H-2 33-43	20.20	0.64	0.03	22.62	-24.81	0.19
7C-9H-2 73-83	20.60	0.15	0.02	8.50	-20.30	-1.86
7C-9H-2 83-93	20.70	0.17	0.03	5.65	n.a.	n.a.
7C-9H-2 132-142	21.19	1.89	0.09	20.50	-25.94	0.85
7C-9H-3 38-48	21.70	1.43	0.10	14.96	n.a.	n.a.
7C-9H-3 88-98	22.20	1.34	0.09	15.35	n.a.	n.a.
7C-10H-1 25-35	22.70	0.27	0.02	10.91	-24.45	-0.11
7C-10H-1 75-85	23.30	0.41	0.04	9.63	n.a.	n.a.
7C-10H-1 125-135	23.70	1.67	0.04	38.76	-25.42	-0.08
7C-10H-2 30-40	24.20	0.57	0.04	15.64	-24.92	0.06
7C-10H-2 70-80	24.70	0.91	0.07	13.20	n.a.	n.a.
7C-10H-2 120-130	25.17	1.13	0.07	15.58	-26.29	2.13
7C-11H-1 10-20	25.70	0.92	0.06	15.28	n.a.	n.a.
7C-11H-1 60-70	26.20	0.75	0.05	14.71	-26.19	2.49

7C-11H-2 22-32	26.70	0.94	0.07	14.24	-25.81	1.84
7C-11H-2 72-82	27.20	0.87	0.07	12.71	n.a.	n.a.
7C-11H-2 120-130	27.68	1.11	0.06	17.58	-26.61	1.91
7C-12H-1 6-16	28.20	0.35	0.04	9.37	n.a.	n.a.
7C-12H-1 56-66	28.70	1.29	0.05	26.62	-25.25	1.25
7C-12H-1 116-126	29.20	0.95	0.08	11.63	n.a.	n.a.
7C-12H-2 24-34	29.70	0.52	0.05	11.27	-25.01	3.32
7C-12H-2 74-84	30.20	1.35	0.09	14.81	n.a.	n.a.
7C-12H-2 124-134	30.70	1.60	0.10	16.59	-26.74	2.64
7C-13H-3 23-33	31.70	0.78	0.08	9.40	n.a.	n.a.
7C-13H-3 73-83	32.20	0.19	0.03	5.42	-25.50	0.24

Table A1-5. Organic carbon proxies for Core 9.

Sample ID	Depth (m)	TOC (%)	TN (%)	C:N_a	$\delta^{13}C_{TOC}$	$\delta^{15}N_{TN}$
9A-1H-1 12-32	0.00	0.32	0.01	30.20	-26.01	b.d.
9A-1H-1 82-102	0.53	0.33	0.01	23.85	-26.56	b.d.
9C-1H-2 65-85	1.23	0.06	b.d.	b.d.	-26.06	b.d.
9C-1H-2 115-135	1.93	0.32	0.02	18.69	-26.02	b.d.
9C-2H-1 15-35	2.57	2.38	0.15	16.02	-26.03	2.68
9C-2H-1 85-105	3.30	0.10	b.d.	b.d.	-28.27	b.d.
9C-2H-2 47-67	4.05	0.07	b.d.	b.d.	-25.41	b.d.
9C-2H-2 117-137	4.73	0.99	0.05	19.46	-22.92	-0.85
9C-3H-1 27-47	5.46	0.07	0.01	8.27	-22.03	b.d.
9A-3H-1 98-118	5.93	0.08	0.01	12.51	n.a.	n.a.
9A-3H-2 57-77	6.93	0.10	0.01	15.22	-21.67	b.d.
9A-3H-2 111-131	7.53	0.08	0.01	10.78	-19.59	b.d.
9C-4H-1 33-53	8.25	0.09	b.d.	b.d.	n.a.	n.a.
9C-4H-2 16-36	8.94	0.09	b.d.	b.d.	-22.47	b.d.
9C-4H-2 86-106	9.64	0.05	b.d.	b.d.	n.a.	n.a.
9A-5H-1 61-81	10.33	0.09	b.d.	b.d.	-25.55	6.78
9A-5H-2 16-36	11.03	0.04	b.d.	b.d.	n.a.	n.a.
9A-5H-2 86-106	11.73	0.04	b.d.	b.d.	-24.69	-0.51
9C-6H-1 52-72	12.53	0.06	b.d.	b.d.	-21.37	-3.87
9C-6H-2 24-44	13.13	0.11	b.d.	b.d.	-26.24	b.d.
9C-6H-2 94-114	13.85	0.05	b.d.	b.d.	n.a.	n.a.
9A-8H-2 70-90	14.63	0.09	b.d.	b.d.	-23.80	-3.87
9C-7H-1 33-53	15.34	0.25	0.01	19.30	-20.67	b.d.
9C-7H-1 103-123	16.03	1.10	0.05	20.80	-22.15	-1.61
9A-9H-2 40-60	16.83	1.04	0.05	20.14	-22.22	-1.35

9A-9H-2 80-100	17.53	0.95	0.05	18.73	-22.03	-1.24
9C-8H-1 16-36	18.13	1.12	0.05	22.54	-22.31	-1.73
9C-8H-1 106-136	19.03	1.82	0.07	25.72	-21.27	-2.45
9C-8H-4 46-66	19.84	0.88	0.05	17.02	-22.84	-1.58
9A-10H-3 13-33	20.72	0.35	0.03	10.54	-22.92	2.73
9A-10H-3 83-103	20.83	1.27	0.08	16.96	-22.91	-2.05
9C-9H-3 41-61	22.18	0.24	0.02	12.65	-20.55	b.d.
9C-9H-3 110-130	22.82	0.23	0.02	11.36	-22.56	b.d.

Table A1-6. Organic carbon proxies for Core 8.

Sample ID	Depth (m)	TOC (%)	TN (%)	$C:N_a$	$\delta^{13}C_{TOC}$	$\delta^{15}N_{TN}$
8A-1H-2 0-20	0.00	0.76	0.04	17.49	-25.89	1.89
8A-1H-2 79-90	0.69	0.05	b.d.	b.d.	-25.86	1.20
8A-1H-3 51-71	1.40	0.06	b.d.	b.d.	-26.11	3.32
8A-1H-3 140-155	2.19	0.73	0.04	18.43	-25.69	b.d.
8A-2H-1 8-28	2.90	0.04	0.00	29.67	-29.07	b.d.
8A-2H-2 40-55	3.60	2.09	0.06	36.58	-25.26	b.d.
8A-2H-2 110-130	4.30	0.14	b.d.	b.d.	-25.80	2.76
8B-2H-1 100-120	5.00	0.21	0.02	12.28	n.a.	n.a.
8B-2H-2 48-68	5.70	0.10	b.d.	b.d.	-25.97	3.37
8B-2H-2 118-133	6.38	0.08	b.d.	b.d.	n.a.	n.a.
8B-3H-1 56-76	7.80	0.09	0.00	52.88	-27.05	b.d.
8B-3H-2 43-63	8.50	0.27	b.d.	b.d.	-25.28	2.86
8B-3H-2 93-113	9.00	0.05	b.d.	b.d.	-25.13	2.80
8C-3H-1 15-35	12.10	0.04	b.d.	b.d.	-25.74	3.25
8C-3H-2 78-98	12.80	0.03	b.d.	b.d.	-27.88	b.d.
8C-4H-1 54-74	14.50	0.20	b.d.	b.d.	n.a.	n.a.
8C-4H-1 114-134	15.10	0.17	b.d.	b.d.	n.a.	n.a.
8C-4H-2 43-58	15.78	1.09	0.05	23.48	-24.98	b.d.
8C-4H-2 113-133	16.50	1.78	0.05	34.26	-26.01	b.d.
8C-5H-1 52-72	17.40	0.21	b.d.	b.d.	n.a.	n.a.
8C-5H-2 22-42	18.20	0.85	0.03	30.85	-27.44	b.d.
8C-5H-2 102-118	18.98	0.23	b.d.	b.d.	-24.91	b.d.
8C-6H-1 27-47	20.40	0.20	0.01	25.61	-29.56	3.59
8C-6H-1 97-117	21.10	0.22	b.d.	b.d.	n.a.	n.a.
8C-6H-3 20-40	21.80	2.84	0.11	26.97	-26.99	-0.37
8A-14H-2 3-23	22.50	0.06	b.d.	b.d.	-30.88	b.d.
8A-14H-2 73-93	23.20	0.10	0.01	8.97	-28.86	b.d.

APPENDIX 2: FATTY ACID BIOMARKERS FOR CORE SAMPLES

Values of long chain fatty acids (LCFA), short chain fatty acids (SCFA), C_{18} and C_{20+22} polyunsaturated fatty acids (PUFAs), branched fatty acids (BrFA), and diacids are presented as a percent of the total fatty acid (FA) content for each sample analyze from the six sediment cores collected from Englebright Lake. The total FA is reported in mg g^{-1} and the TAR_{FA} is shown for each sample as well. Each core is presented in a separate table. Values that are below detection are indicated with b.d., and samples that were not analyzed for these are indicated with n.a.

Table A2-1. Fatty acid biomarkers for Core 1.

Sample ID	LCFA	SCFA	C_{18} PUFA	PUFA	BrFA	Diacids	Total FA	TAR_{FA}
1A-1H-1 5-15	36.68	18.24	3.82	b.d.	4.68	b.d.	31.21	1.95
1A-1H-1 35-45	36.81	23.46	3.10	b.d.	4.64	b.d.	35.70	1.60
1A-1H-1 65-75	42.01	17.41	2.42	b.d.	4.62	b.d.	119.53	2.22
1D-1H-1 71-81	37.21	19.13	3.79	b.d.	4.77	b.d.	26.74	1.80
1D-1H-1 101-111	34.92	19.01	2.31	b.d.	3.93	b.d.	7.58	1.84
1D-1H-1 130-137	n.a.	n.a.	n.a.	n.a.	n.a.	n.a.	n.a.	n.a.
1D-1H-2 21-31	28.45	11.70	1.71	b.d.	3.81	b.d.	5.32	2.43
1D-1H-2 51-61	35.53	10.88	1.56	b.d.	4.10	b.d.	7.38	2.59
1D-1H-2 71-81	n.a.	n.a.	n.a.	n.a.	n.a.	n.a.	n.a.	n.a.
1B-2E-2 24-34	37.82	14.09	3.91	b.d.	3.48	b.d.	10.83	2.23
1B-2E-2 54-64	33.95	17.74	3.03	b.d.	2.19	b.d.	15.18	1.73
1B-2E-2 84-94	32.09	21.79	3.80	b.d.	4.44	b.d.	20.89	1.55
1B-2E-2 114-124	20.84	33.45	3.15	b.d.	2.76	b.d.	16.47	0.86
1B-2E-3 9-19	31.88	4.01	2.52	b.d.	3.00	3.16	14.09	5.44
1B-2E-3 39-49	32.46	3.98	2.16	b.d.	2.60	4.10	14.98	5.56
1B-2E-3 69-79	7.29	3.57	0.58	0.45	0.23	0.63	46.57	1.76
1B-2E-3 99-109	10.85	6.76	0.98	0.70	1.66	1.80	93.98	1.59
1B-2E-3 129-139	13.52	6.26	0.69	b.d.	1.46	3.58	66.32	1.83
1B-3E-1 9-19	10.94	3.53	0.64	b.d.	1.59	1.57	27.87	2.49
1B-3E-1 39-49	39.57	3.26	2.14	b.d.	2.31	5.05	23.57	8.15
1B-3E-1 69-79	3.47	72.62	0.32	b.d.	2.27	b.d.	34.70	0.09
1B-3E-1 99-109	24.09	12.70	0.99	b.d.	6.97	b.d.	4.18	1.44

Table A2-2. Fatty acid biomarkers for Core 6.

Sample ID	LCFA	SCFA	C_{18} PUFA	PUFA	BrFA	Diacids	Total FA	TAR_{FA}
6F-1H-1 77-97	17.74	b.d.	2.03	b.d.	3.71	b.d.	105.33	0.56
6F-1H-2 19-39	38.14	b.d.	2.58	b.d.	4.71	b.d.	65.40	1.95
6E-1H-2 49-69	41.14	b.d.	3.39	b.d.	4.56	b.d.	42.05	2.30
6E-1H-2 119-139	23.59	b.d.	1.96	b.d.	4.14	b.d.	7.52	1.32
6F-2H-1 50-70	49.04	b.d.	1.36	b.d.	3.08	b.d.	35.70	2.92
6E-2H-2 43-63	34.78	b.d.	1.60	b.d.	4.64	b.d.	11.02	1.99
6F-2H-2 80-100	25.62	3.48	1.05	b.d.	2.16	3.48	19.61	0.94
6F-2H-2 123-143	21.31	1.35	0.30	b.d.	1.18	1.35	101.20	2.79
6B-2H-2 35-55	24.14	1.53	0.28	b.d.	1.30	1.53	44.26	2.94
6F-3E-1 41-61	41.15	2.27	0.67	b.d.	3.28	2.27	32.82	1.77
6E-3E-1 71-91	35.87	2.44	1.63	b.d.	3.60	2.44	35.39	1.38
6E-3E-2 38-58	3.77	5.20	0.48	b.d.	3.34	5.20	42.01	0.12

Table A2-3. Fatty acid biomarkers for Core 4.

Sample ID	LCFA	SCFA	C_{18} PUFA	PUFA	BrFA	Diacids	Total FA	TAR_{FA}
4B-1H-1 7-17	34.47	2.44	2.08	21.97	2.91	5.83	17.64	1.73
4B-1H-1 17-27	10.69	2.49	1.48	b.d.	1.38	2.49	39.48	0.98
4A-1H-1 33-43	31.94	7.69	2.18	21.87	1.56	5.61	203.87	1.76
4A-1H-1 53-63	21.50	2.67	1.86	b.d.	2.17	2.67	90.20	0.91
4A-1H-1 63-73	18.80	2.86	2.73	b.d.	1.60	2.86	142.13	1.24
4A-1H-1 93-103	45.23	5.72	1.49	26.32	1.84	5.60	66.32	3.09
4A-1H-2 13-23	n.a.	n.a.	n.a.	n.a.	n.a.	n.a.	n.a.	n.a.
4A-1H-2 43-53	16.02	1.18	2.02	b.d.	1.51	1.18	141.96	0.77
4A-1H-2 73-83	41.46	6.66	1.83	30.03	2.89	5.91	55.58	2.92
4A-1H-2 103-113	10.58	1.97	0.76	b.d.	1.21	1.97	55.58	0.81
4A-1H-2 133-143	n.a.	n.a.	n.a.	n.a.	n.a.	n.a.	0.00	n.a.
4B-2H-1 26-36	n.a.	n.a.	n.a.	n.a.	n.a.	n.a.	0.00	n.a.
4B-2H-1 56-64	11.26	1.91	b.d.	b.d.	1.89	1.91	63.76	0.86
4B-2H-1 86-95	n.a.	n.a.	n.a.	n.a.	n.a.	n.a.	n.a.	n.a.
4A-2H-2 61-71	18.48	1.59	0.84	b.d.	1.31	1.59	112.09	1.40
4B-2H-1 110-118	42.85	5.77	1.96	29.70	2.50	7.64	30.38	2.79
4B-2H-2 18-28	49.65	3.34	1.26	35.66	1.86	9.75	14.24	3.46
4B-2H-2 48-58	n.a.	n.a.	n.a.	n.a.	n.a.	n.a.	n.a.	n.a.
4A-2H-3 17-27	n.a.	n.a.	n.a.	n.a.	n.a.	n.a.	n.a.	n.a.
4A-2H-3 47-57	8.09	1.25	0.29	b.d.	0.68	1.25	39.15	0.80
4A-2H-3 67-77	3.79	0.92	0.50	b.d.	0.84	0.92	57.41	0.32
4A-2H-3 77-87	n.a.	n.a.	n.a.	n.a.	n.a.	n.a.	n.a.	n.a.
4A-2H-3 107-117	43.65	3.76	1.87	46.44	3.10	10.58	14.80	1.89
4B-3H-1 17-27	6.51	0.80	b.d.	b.d.	0.77	0.80	39.86	0.66
4B-3H-1 47-57	n.a.	n.a.	n.a.	n.a.	n.a.	n.a.	n.a.	n.a.
4B-3H-1 74-85	37.48	3.46	2.90	b.d.	2.64	3.46	25.28	2.56

4B-3H-1 107-117	42.08	2.19	2.03	b.d.	2.13	2.19	255.22	2.60
4A-4H-1 59-69	40.49	8.78	1.13	16.93	1.32	5.17	192.10	3.49
4A-4H-1 89-99	47.52	9.13	0.95	33.21	1.44	5.16	68.69	3.80
4A-4H-2 1-11	44.84	3.81	2.46	65.70	2.49	15.77	7.30	3.03
4A-4H-2 31-41	n.a.	n.a.	n.a.	n.a.	n.a.	n.a.	n.a.	n.a.
4A-4H-2 61-71	n.a.	n.a.	n.a.	n.a.	n.a.	n.a.	n.a.	n.a.
4A-4H-2 91-101	26.58	2.30	0.55	b.d.	1.85	2.30	49.54	1.27
4A-4H-2 121-131	46.97	5.38	1.36	23.37	2.95	7.67	25.48	2.33
4B-4H-1 61-71	43.29	6.60	1.33	28.85	2.67	7.40	27.88	2.44
4B-4H-1 91-101	58.95	2.31	0.65	b.d.	1.88	2.31	18.84	5.03
4B-4H-1 121-131	n.a.	n.a.	n.a.	n.a.	n.a.	n.a.	n.a.	n.a.
4B-4H-2 31-41	46.96	2.84	0.60	b.d.	2.39	2.84	53.49	2.81
4B-4H-2 61-71	n.a.	n.a.	n.a.	n.a.	n.a.	n.a.	n.a.	n.a.
4A-5H-2 42-52	37.95	3.54	1.32	b.d.	2.42	3.54	75.82	1.65
4A-5H-2 72-82	50.21	4.02	0.70	0.59	1.77	4.02	68.02	3.11
4A-5H-2 102-112	19.63	2.65	1.08	0.30	1.71	2.65	45.32	0.58
4A-5H-2 132-142	35.48	4.88	2.42	b.d.	1.91	4.88	21.63	1.72
4B-5H-1 75-85	34.66	4.34	0.69	b.d.	2.70	4.34	13.68	1.55
4B-5H-1 105-115	49.37	6.80	1.00	27.44	1.97	7.66	29.55	3.01
4B-5H-1 137-147	n.a.	n.a.	n.a.	n.a.	n.a.	n.a.	n.a.	n.a.
4B-5H-2 24-34	n.a.	n.a.	n.a.	n.a.	n.a.	n.a.	n.a.	n.a.
4B-5H-2 54-64	38.80	3.11	0.48	b.d.	1.67	3.11	48.20	1.62
4B-5H-2 84-94	n.a.	n.a.	n.a.	n.a.	n.a.	n.a.	n.a.	n.a.
4B-5H-2 114-124	52.56	3.98	1.82	23.03	1.54	7.97	13.58	3.06
4B-5H-2 140-150	27.75	4.75	1.28	b.d.	2.48	4.75	16.55	0.99
4B-6H-1 23-33	n.a.	n.a.	n.a.	n.a.	n.a.	n.a.	n.a.	n.a.
4B-6H-1 53-63	20.72	3.30	1.37	22.36	2.22	7.96	7.41	1.97

Table A2-4. Fatty acid biomarkers for Core 7.

Sample ID	LCFA	SCFA	C_{18} PUFA	PUFA	BrFA	Diacids	Total F	TAR_{FA}
7C-1H-1 27-37	13.43	3.59	2.16	0.60	0.63	3.59	4.98	0.69
7C-1H-2 60-70	29.52	4.21	3.92	0.47	0.81	4.21	41.87	1.45
7C-1H-1 77-87	18.42	3.05	8.85	0.26	0.81	3.05	50.82	1.29
7C-1H-2 110-120	3.49	2.73	1.26	b.d.	0.53	2.73	5.53	0.12
7C-2H-1 39-49	n.a.	n.a.	n.a.	n.a.	n.a.	n.a.	n.a.	n.a.
7C-2H-1 109-119	23.33	5.59	3.17	b.d.	b.d.	5.59	16.19	1.59
7C-2H-2 9-19	n.a.	n.a.	n.a.	n.a.	n.a.	n.a.	n.a.	n.a.
7C-2H-2 59-69	n.a.	n.a.	n.a.	n.a.	n.a.	n.a.	n.a.	n.a.
7A-2H-2 32-42	20.27	2.89	4.06	0.93	1.43	2.89	20.03	1.12
7A-2H-2 82-92	10.99	1.19	1.48	0.26	1.42	1.19	107.09	0.32
7C-3H-1 66-76	44.84	1.29	2.56	b.d.	1.46	1.29	47.46	2.66
7C-3H-1 124-134	29.01	0.30	3.51	b.d.	1.71	0.30	48.06	1.24
7C-3H-2 25-35	23.23	b.d.	1.92	b.d.	1.91	b.d.	3.87	1.22
7C-3H-2 95-105	16.87	3.84	3.44	0.41	1.11	3.84	114.40	0.68
7C-3H-2 125-135	n.a.	n.a.	n.a.	n.a.	n.a.	n.a.	n.a.	n.a.
7C-4H-1 14-24	36.69	b.d.	1.86	b.d.	1.87	b.d.	10.03	1.79
7C-4H-2 20-30	21.54	4.35	6.14	0.35	1.90	4.35	14.41	1.27
7C-4H-2 66-76	1.07	b.d.	8.67	b.d.	1.31	b.d.	6.88	0.04
7C-4H-3 37-47	n.a.	n.a.	n.a.	n.a.	n.a.	n.a.	n.a.	n.a.
7C-4H-3 87-97	33.97	6.55	b.d.	b.d.	2.41	6.55	7.74	2.18
7A-4H-2 44-54	20.09	0.55	1.57	b.d.	1.06	0.55	7.68	1.02
7A-4H-2 94-104	34.16	4.57	1.44	b.d.	0.75	4.57	586.06	1.68
7C-5H-1 78-88	12.55	6.21	2.45	0.29	0.68	6.21	82.63	1.42
7C-5H-1 128-138	43.44	5.14	1.45	0.17	0.97	5.14	561.80	3.82
7C-6H-1 20-30	42.45	3.99	2.96	b.d.	0.73	3.99	713.83	2.43

7C-6H-1 70-80	26.74	6.85	b.d.	b.d.	b.d.	6.85	832.64	4.25
7C-6H-1 120-137	51.23	1.28	1.26	b.d.	0.96	1.28	116.06	3.11
7C-6H-2 19-29	n.a.	n.a.	n.a.	n.a.	n.a.	n.a.	n.a.	n.a.
7C-6H-2 69-79	6.26	7.51	1.08	b.d.	1.41	7.51	5.62	0.29
7C-6H-2 119-129	n.a.	n.a.	n.a.	n.a.	n.a.	n.a.	n.a.	n.a.
7C-7H-1 20-30	36.56	2.05	2.93	b.d.	1.82	2.05	16.49	1.93
7C-7H-1 60-70	6.75	8.29	5.50	b.d.	b.d.	8.29	2.89	0.28
7C-7H-1 110-120	17.72	1.35	2.62	b.d.	1.36	1.35	10.61	1.08
7C-7H-2 25-35	n.a.	n.a.	n.a.	n.a.	n.a.	n.a.	n.a.	n.a.
7C-7H-2 75-85	3.76	10.08	0.48	0.29	0.67	10.08	91.92	0.32
7C-7H-2 110-120	n.a.	n.a.	n.a.	n.a.	n.a.	n.a.	n.a.	n.a.
7C-8H-1 20-30	n.a.	n.a.	n.a.	n.a.	n.a.	n.a.	n.a.	n.a.
7C-8H-1 70-80	5.80	32.98	b.d.	b.d.	b.d.	32.98	33.17	8.34
7C-8H-1 116-126	23.27	3.97	3.48	0.76	1.61	3.97	15.57	1.37
7C-9H-2 33-43	n.a.	n.a.	n.a.	n.a.	n.a.	n.a.	n.a.	n.a.
7C-9H-2 73-83	3.37	b.d.	0.91	b.d.	1.50	b.d.	4.16	0.17
7C-9H-2 83-93	2.30	21.01	b.d.	b.d.	b.d.	21.01	24.13	2.29
7C-9H-2 132-142	53.89	b.d.	1.26	b.d.	1.80	b.d.	37.16	3.19
7C-9H-3 38-48	46.24	b.d.	0.91	b.d.	1.15	b.d.	20.07	2.61
7C-9H-3 88-98	n.a.	n.a.	n.a.	n.a.	n.a.	n.a.	n.a.	n.a.
7C-10H-1 25-35	28.78	b.d.	2.05	b.d.	1.32	b.d.	8.26	1.24
7C-10H-1 75-85	n.a.	n.a.	n.a.	n.a.	n.a.	n.a.	n.a.	n.a.
7C-10H-1 125-135	38.74	2.77	3.76	0.23	0.92	2.77	43.43	3.67
7C-10H-2 30-40	35.16	b.d.	1.55	b.d.	1.08	b.d.	7.91	1.81
7C-10H-2 70-80	n.a.	n.a.	n.a.	n.a.	n.a.	n.a.	n.a.	n.a.
7C-10H-2 120-130	44.51	b.d.	1.05	b.d.	1.41	b.d.	9.62	2.87
7C-11H-1 10-20	8.83	3.55	b.d.	b.d.	b.d.	3.55	34.15	1.88
7C-11H-1 60-70	23.20	7.20	1.91	b.d.	b.d.	7.20	9.03	0.93

7C-11H-2 22-32	18.76	6.62	2.90	1.01	1.31	6.62	12.20	0.64
7C-11H-2 72-82	30.56	4.92	1.18	b.d.	2.34	4.92	8.82	1.18
7C-11H-2 120-130	28.17	2.71	0.75	b.d.	2.37	2.71	12.04	1.04
7C-12H-1 6-16	40.10	b.d.	2.00	b.d.	1.64	b.d.	4.47	2.99
7C-12H-1 56-66	22.08	2.37	2.04	b.d.	2.01	2.37	16.72	0.96
7C-12H-1 116-126	42.40	b.d.	0.56	b.d.	1.23	b.d.	8.79	2.54
7C-12H-2 24-34	n.a.	n.a.	n.a.	n.a.	n.a.	n.a.	n.a.	n.a.
7C-12H-2 74-84	n.a.	n.a.	n.a.	n.a.	n.a.	n.a.	n.a.	n.a.
7C-12H-2 124-134	n.a.	n.a.	n.a.	n.a.	n.a.	n.a.	n.a.	n.a.
7C-13H-3 23-33	47.31	b.d.	1.72	b.d.	1.40	b.d.	5.98	3.66
7C-13H-3 73-83	7.15	3.56	2.09	0.87	1.73	3.56	8.49	0.28

Table A2-5. Fatty acid biomarkers for Core 9.

Sample ID	LCFA	SCFA	C_{18} PUFA	PUFA	BrFA	Diacids	Total FA	TAR_{FA}
9A-1H-1 12-32	28.58	0.19	8.54	b.d.	2.32	0.19	4.07	2.06
9A-1H-1 82-102	27.23	b.d.	5.90	b.d.	1.85	b.d.	6.43	1.56
9C-1H-2 65-85	14.04	b.d.	4.78	b.d.	0.45	b.d.	0.59	1.41
9C-1H-2 115-135	34.43	b.d.	5.47	b.d.	1.72	b.d.	3.59	2.65
9C-2H-1 15-35	40.75	b.d.	1.55	b.d.	3.00	b.d.	47.88	1.85
9C-2H-1 85-105	13.20	b.d.	22.46	b.d.	2.04	b.d.	1.47	0.76
9C-2H-2 47-67	0.70	b.d.	18.61	b.d.	0.39	b.d.	1.25	0.05
9C-2H-2 117-137	39.05	b.d.	2.34	b.d.	2.89	b.d.	46.30	2.10
9C-3H-1 27-47	3.84	b.d.	12.24	b.d.	1.58	b.d.	1.64	0.28
9A-3H-1 98-118	12.19	b.d.	9.39	b.d.	1.04	b.d.	4.29	0.35
9A-3H-2 57-77	1.12	19.65	b.d.	b.d.	3.74	19.65	18.04	0.06
9A-3H-2 111-131	5.80	b.d.	6.06	b.d.	1.94	b.d.	0.85	0.46
9C-4H-1 33-53	n.a.	n.a.	n.a.	n.a.	n.a.	n.a.	n.a.	n.a.
9C-4H-2 16-36	0.83	5.34	1.95	b.d.	0.76	5.34	3.71	0.03
9C-4H-2 86-106	2.37	2.41	5.01	b.d.	1.70	2.41	1.06	0.10
9A-5H-1 61-81	20.62	b.d.	15.44	b.d.	0.32	b.d.	1.49	1.40
9A-5H-2 16-36	n.a.	n.a.	n.a.	n.a.	n.a.	n.a.	n.a.	n.a.
9A-5H-2 86-106	n.a.	n.a.	n.a.	n.a.	n.a.	n.a.	n.a.	n.a.
9C-6H-1 52-72	b.d.	7.75	0.70	b.d.	1.46	7.75	20.39	b.d.
9C-6H-2 24-44	2.26	11.51	b.d.	b.d.	1.74	11.51	5.80	0.12
9C-6H-2 94-114	4.94	8.91	b.d.	b.d.	1.06	8.91	5.57	0.25
9A-8H-2 70-90	12.38	b.d.	1.62	b.d.	1.42	b.d.	1.65	0.64
9C-7H-1 33-53	29.49	b.d.	2.41	b.d.	2.56	b.d.	1.94	1.42
9C-7H-1 103-123	45.42	b.d.	1.57	b.d.	2.60	b.d.	13.02	2.62
9A-9H-2 40-60	31.89	3.98	0.76	b.d.	2.34	3.98	13.17	1.12

9A-9H-2 80-100	16.71	2.20	0.45	b.d.	1.87	2.20	25.63	0.44
9C-8H-1 16-36	35.75	2.25	0.91	b.d.	3.15	2.25	15.32	1.46
9C-8H-1 106-136	3.93	8.29	2.04	b.d.	1.78	8.29	4.32	0.07
9C-8H-4 46-66	n.a.	n.a.	n.a.	n.a.	n.a.	n.a.	n.a.	n.a.
9A-10H-3 13-33	n.a.	n.a.	n.a.	n.a.	n.a.	n.a.	n.a.	n.a.
9A-10H-3 83-103	7.84	b.d.	3.80	27.92	18.75	75.02	12.73	0.02
9C-9H-3 41-61	3.64	b.d.	0.64	b.d.	0.29	b.d.	3.46	0.30
9C-9H-3 110-130	11.78	b.d.	1.34	b.d.	1.48	b.d.	6.65	0.68

Table A2-6. Fatty acid biomarkers for Core 8.

Sample ID	LCFA	SCFA	C_{18} PUFA	PUFA	BrFA	Diacids	Total FA	TAR_{FA}
8A-1H-2 0-20	34.74	b.d.	4.64	b.d.	2.35	b.d.	23.88	1.72
8A-1H-2 79-90	3.93	b.d.	10.06	b.d.	b.d.	b.d.	0.72	0.70
8A-1H-3 51-71	15.01	b.d.	13.53	b.d.	0.99	b.d.	1.43	1.11
8A-1H-3 140-155	37.39	b.d.	1.64	b.d.	2.16	b.d.	11.69	2.13
8A-2H-1 8-28	3.37	b.d.	4.97	b.d.	1.64	b.d.	0.98	0.20
8A-2H-2 40-55	36.11	b.d.	4.79	b.d.	1.41	b.d.	58.12	3.37
8A-2H-2 110-130	1.93	b.d.	11.23	b.d.	1.34	b.d.	1.76	0.09
8B-2H-1 100-120	n.a.	n.a.	n.a.	n.a.	n.a.	n.a.	n.a.	n.a.
8B-2H-2 48-68	3.13	b.d.	7.93	b.d.	b.d.	b.d.	1.21	0.19
8B-2H-2 118-133	2.81	1.76	1.74	b.d.	1.32	1.76	22.22	0.08
8B-3H-1 56-76	8.09	b.d.	3.77	b.d.	1.87	b.d.	0.65	0.86
8B-3H-2 43-63	36.28	b.d.	3.85	b.d.	1.47	b.d.	7.47	3.59
8B-3H-2 93-113	3.48	7.28	1.80	b.d.	1.03	7.28	3.18	0.09
8C-3H-1 15-35	4.07	4.21	0.85	b.d.	0.52	4.21	2.77	0.09
8C-3H-2 78-98	5.30	10.43	0.65	b.d.	2.47	10.43	1.61	0.11
8C-4H-1 54-74	n.a.	n.a.	n.a.	n.a.	n.a.	n.a.	n.a.	n.a.
8C-4H-1 114-134	n.a.	n.a.	n.a.	n.a.	n.a.	n.a.	n.a.	n.a.
8C-4H-2 43-58	40.03	b.d.	3.36	b.d.	1.71	b.d.	43.35	1.58
8C-4H-2 113-133	31.88	4.70	1.07	b.d.	2.31	4.70	61.10	1.15
8C-5H-1 52-72	17.43	2.94	1.21	b.d.	1.63	2.94	9.75	0.69
8C-5H-2 22-42	25.31	4.81	1.03	b.d.	2.57	4.81	10.85	0.93
8C-5H-2 102-118	1.75	2.98	0.69	b.d.	3.76	2.98	44.89	0.06
8C-6H-1 27-47	19.54	b.d.	1.73	b.d.	1.08	b.d.	4.25	0.88
8C-6H-1 97-117	n.a.	n.a.	n.a.	n.a.	n.a.	n.a.	n.a.	n.a.
8C-6H-3 20-40	47.26	b.d.	0.74	b.d.	1.60	b.d.	119.58	2.31
8A-14H-2 3-23	14.15	b.d.	0.51	b.d.	0.76	b.d.	0.83	0.80
8A-14H-2 73-93	2.33	b.d.	0.56	b.d.	0.73	b.d.	7.20	0.08

APPENDIX 3: STEROL BIOMARKERS FOR CORE SAMPLES

Values of aquatic sterols (27-nor-24-cholesta-5,22-dien-3β-ol and cholesta-5,22-dien-3β-ol), brassicasterol, cholesterol, and plant sterols (campesterol, stigmasterol, and sitosterol) are presented as a percent of the total sterol content for each sample analyze from the six sediment cores collected from Englebright Lake. Total sterol concnetration is reported in mg g^{-1}. Each core is presented in a separate table. Values that are below detection are indicated with b.d., and samples that were not analyzed for these are indicated with n.a.

Table A3-1. Sterol biomarkers for Core 1.

Sample ID	Aquatic Sterols	Brassicasterol	Cholesterol	Plant Sterols	Total Sterols
1A-1H-1 5-15	0.67	3.47	3.34	73.82	11.90
1A-1H-1 35-45	0.33	3.22	2.58	75.39	11.79
1A-1H-1 65-75	0.14	2.15	2.15	79.01	19.93
1D-1H-1 71-81	0.58	3.79	6.97	59.87	10.31
1D-1H-1 101-111	0.52	2.72	5.91	47.81	4.50
1D-1H-1 130-137	n.a.	n.a.	n.a.	n.a.	n.a.
1D-1H-2 21-31	0.66	1.65	5.33	52.05	2.08
1D-1H-2 51-61	1.01	2.29	6.91	15.31	2.58
1D-1H-2 71-81	n.a.	n.a.	n.a.	n.a.	n.a.
1B-2E-2 24-34	1.41	3.22	8.16	43.92	3.29
1B-2E-2 54-64	1.18	3.18	9.38	44.12	3.38
1B-2E-2 84-94	5.59	1.63	4.29	22.70	4.89
1B-2E-2 114-124	0.86	2.71	6.62	55.35	4.28
1B-2E-3 9-19	3.04	3.62	9.15	43.89	2.12
1B-2E-3 39-49	0.92	3.93	6.07	46.53	1.96
1B-2E-3 69-79	1.02	3.13	5.63	49.73	2.91
1B-2E-3 99-109	b.d.	2.29	2.30	67.28	12.33
1B-2E-3 129-139	b.d.	2.24	1.44	71.31	8.05
1B-3E-1 9-19	1.15	2.87	3.06	52.74	3.71
1B-3E-1 39-49	b.d.	2.03	2.01	62.24	1.10
1B-3E-1 69-79	2.25	6.93	14.64	50.03	1.10
1B-3E-1 99-109	1.10	4.01	20.88	49.45	1.80

Table A3-2. Sterol biomarkers for Core 6.

Sample ID	Aquatic Sterols	Brassicasterol	Cholesterol	Plant Sterols	Total Sterols
6F-1H-1 77-97	b.d.	4.54	4.39	91.07	11.05
6F-1H-2 19-39	b.d.	4.61	4.33	91.06	22.41
6E-1H-2 49-69	0.87	4.89	4.35	89.89	14.63
6E-1H-2 119-139	b.d.	5.73	9.15	85.12	2.07
6F-2H-1 50-70	b.d.	2.09	1.06	96.84	14.92
6E-2H-2 43-63	0.43	4.44	0.07	94.78	3.96
6F-2H-2 80-100	b.d.	2.04	2.85	67.52	9.96
6F-2H-2 123-143	b.d.	1.87	2.30	67.50	12.27
6B-2H-2 35-55	b.d.	2.09	2.22	65.53	7.81
6F-3E-1 41-61	b.d.	2.32	2.05	63.49	11.52
6E-3E-1 71-91	b.d.	1.75	1.71	74.35	13.49
6E-3E-2 38-58	b.d.	b.d.	13.76	63.12	2.70

Table A3-3. Sterol biomarkers for Core 4.

Sample ID	Aquatic Sterols	Brassicasterol	Cholesterol	Plant Sterols	Total Sterols
4B-1H-1 7-17	0.33	3.66	5.57	66.79	5.06
4B-1H-1 17-27	b.d.	2.84	6.36	74.26	3.81
4A-1H-1 33-43	b.d.	2.04	0.92	86.57	46.30
4A-1H-1 53-63	b.d.	1.24	1.92	86.43	45.84
4A-1H-1 63-73	b.d.	1.44	3.10	85.49	23.60
4A-1H-1 93-103	b.d.	2.89	3.97	74.81	16.99
4A-1H-2 13-23	n.a.	n.a.	n.a.	n.a.	n.a.
4A-1H-2 43-53	0.47	1.88	3.08	82.30	27.56
4A-1H-2 73-83	b.d.	2.11	1.83	73.70	15.46
4A-1H-2 103-113	b.d.	2.60	7.21	62.51	4.53
4A-1H-2 133-143	n.a.	n.a.	n.a.	n.a.	n.a.
4B-2H-1 26-36	n.a.	n.a.	n.a.	n.a.	n.a.
4B-2H-1 56-64	b.d.	2.66	6.11	63.30	5.91
4B-2H-1 86-95	n.a.	n.a.	n.a.	n.a.	n.a.
4A-2H-2 61-71	b.d.	2.58	2.92	79.71	25.55
4B-2H-1 110-118	b.d.	2.14	1.93	70.46	10.37
4B-2H-2 18-28	b.d.	1.92	4.78	58.15	3.05
4B-2H-2 48-58	n.a.	n.a.	n.a.	n.a.	n.a.
4A-2H-3 17-27	n.a.	n.a.	n.a.	n.a.	n.a.
4A-2H-3 47-57	n.a.	n.a.	n.a.	n.a.	n.a.
4A-2H-3 67-77	b.d.	2.90	10.77	51.85	2.71
4A-2H-3 77-87	n.a.	n.a.	n.a.	n.a.	n.a.
4A-2H-3 107-117	b.d.	1.62	2.63	66.93	6.19
4B-3H-1 17-27	b.d.	2.57	7.51	54.34	3.09
4B-3H-1 47-57	n.a.	n.a.	n.a.	n.a.	n.a.

4B-3H-1 74-85	n.a.	n.a.	n.a.	n.a.	n.a.
4B-3H-1 107-117	b.d.	1.21	4.35	78.01	49.96
4A-4H-1 59-69	b.d.	2.47	1.37	82.57	39.15
4A-4H-1 89-99	b.d.	1.49	0.66	82.59	26.03
4A-4H-2 1-11	b.d.	2.11	1.83	57.19	2.38
4A-4H-2 31-41	n.a.	n.a.	n.a.	n.a.	n.a.
4A-4H-2 61-71	n.a.	n.a.	n.a.	n.a.	n.a.
4A-4H-2 91-101	b.d.	1.66	1.64	78.71	27.12
4A-4H-2 121-131	b.d.	1.99	1.70	76.22	16.03
4B-4H-1 61-71	b.d.	1.94	1.53	80.15	11.88
4B-4H-1 91-101	b.d.	1.85	3.56	59.42	4.05
4B-4H-1 121-131	n.a.	n.a.	n.a.	n.a.	n.a.
4B-4H-2 31-41	b.d.	1.67	2.41	78.36	15.78
4B-4H-2 61-71	n.a.	n.a.	n.a.	n.a.	n.a.
4A-5H-2 42-52	b.d.	1.65	3.97	84.18	16.54
4A-5H-2 72-82	b.d.	1.45	3.20	76.24	15.98
4A-5H-2 102-112	b.d.	2.38	6.61	56.42	4.25
4A-5H-2 132-142	b.d.	1.92	8.42	57.83	3.40
4B-5H-1 75-85	b.d.	1.45	2.18	70.74	4.71
4B-5H-1 105-115	b.d.	2.00	1.37	77.32	22.22
4B-5H-1 137-147	n.a.	n.a.	n.a.	n.a.	n.a.
4B-5H-2 24-34	n.a.	n.a.	n.a.	n.a.	n.a.
4B-5H-2 54-64	b.d.	1.74	2.08	68.18	12.23
4B-5H-2 84-94	n.a.	n.a.	n.a.	n.a.	n.a.
4B-5H-2 114-124	b.d.	1.44	3.76	61.46	3.85
4B-5H-2 140-150	b.d.	1.64	3.62	64.64	3.62
4B-6H-1 23-33	n.a.	n.a.	n.a.	n.a.	n.a.
4B-6H-1 53-63	b.d.	0.53	4.13	52.28	1.40

Table A3-4. Sterol biomarkers for Core 7.

Sample ID	Aquatic Sterols	Brassicasterol	Cholesterol	Plant Sterols	Total Sterols
7C-1H-1 27-37	b.d.	b.d.	b.d.	100.00	0.30
7C-1H-2 60-70	b.d.	4.52	2.53	92.95	8.56
7C-1H-1 77-87	b.d.	3.11	1.77	95.12	17.48
7C-1H-2 110-120	b.d.	b.d.	100.00	b.d.	0.02
7C-2H-1 39-49	n.a.	n.a.	n.a.	n.a.	n.a.
7C-2H-1 109-119	b.d.	3.56	2.66	93.78	2.23
7C-2H-2 9-19	n.a.	n.a.	n.a.	n.a.	n.a.
7C-2H-2 59-69	n.a.	n.a.	n.a.	n.a.	n.a.
7A-2H-2 32-42	b.d.	3.12	3.19	93.69	3.50
7A-2H-2 82-92	b.d.	1.17	1.17	97.66	20.83
7C-3H-1 66-76	b.d.	b.d.	b.d.	71.57	23.60
7C-3H-1 124-134	b.d.	2.20	1.62	71.42	11.53
7C-3H-2 25-35	b.d.	b.d.	b.d.	69.73	0.33
7C-3H-2 95-105	b.d.	2.61	3.39	94.00	13.64
7C-3H-2 125-135	n.a.	n.a.	n.a.	n.a.	n.a.
7C-4H-1 14-24	b.d.	1.43	0.66	77.14	1.48
7C-4H-2 20-30	b.d.	5.64	17.80	76.57	0.79
7C-4H-2 66-76	b.d.	5.22	5.13	89.65	0.16
7C-4H-3 37-47	n.a.	n.a.	n.a.	n.a.	n.a.
7C-4H-3 87-97	b.d.	2.97	3.05	65.91	4.08
7A-4H-2 44-54	b.d.	1.71	0.98	82.18	1.07
7A-4H-2 94-104	b.d.	2.05	0.55	97.40	158.96
7C-5H-1 78-88	b.d.	1.51	0.53	91.28	25.64
7C-5H-1 128-138	b.d.	0.86	0.56	98.58	133.10
7C-6H-1 20-30	b.d.	1.79	0.32	88.05	280.57

7C-6H-1 70-80	b.d.	2.28	1.54	89.26	10.95
7C-6H-1 120-137	b.d.	0.79	0.22	87.90	19.43
7C-6H-2 19-29	n.a.	n.a.	n.a.	n.a.	n.a.
7C-6H-2 69-79	b.d.	b.d.	13.71	56.46	0.16
7C-6H-2 119-129	n.a.	n.a.	n.a.	n.a.	n.a.
7C-7H-1 20-30	b.d.	0.76	0.58	82.48	8.40
7C-7H-1 60-70	b.d.	b.d.	7.06	36.75	1.29
7C-7H-1 110-120	b.d.	2.80	1.87	95.33	1.43
7C-7H-2 25-35	n.a.	n.a.	n.a.	n.a.	n.a.
7C-7H-2 75-85	b.d.	0.62	0.81	85.66	27.52
7C-7H-2 110-120	n.a.	n.a.	n.a.	n.a.	n.a.
7C-8H-1 20-30	n.a.	n.a.	n.a.	n.a.	n.a.
7C-8H-1 70-80	b.d.	0.93	0.96	71.55	1.02
7C-8H-1 116-126	b.d.	1.77	1.43	84.30	2.48
7C-9H-2 33-43	n.a.	n.a.	n.a.	n.a.	n.a.
7C-9H-2 73-83	b.d.	b.d.	5.96	53.57	0.36
7C-9H-2 83-93	b.d.	b.d.	9.63	39.87	0.15
7C-9H-2 132-142	b.d.	1.04	1.49	74.35	7.80
7C-9H-3 38-48	b.d.	0.95	1.29	79.48	5.94
7C-9H-3 88-98	n.a.	n.a.	n.a.	n.a.	n.a.
7C-10H-1 25-35	b.d.	0.84	0.80	75.42	1.97
7C-10H-1 75-85	n.a.	n.a.	n.a.	n.a.	n.a.
7C-10H-1 125-135	0.67	1.43	1.09	96.80	20.56
7C-10H-2 30-40	b.d.	0.97	1.40	80.97	3.46
7C-10H-2 70-80	n.a.	n.a.	n.a.	n.a.	n.a.
7C-10H-2 120-130	b.d.	1.39	2.60	64.07	3.54
7C-11H-1 10-20	b.d.	1.83	2.51	52.70	2.49
7C-11H-1 60-70	b.d.	0.57	0.93	79.84	9.40

7C-11H-2 22-32	b.d.	b.d.	b.d.	41.74	0.96
7C-11H-2 72-82	b.d.	2.08	3.54	49.32	20.89
7C-11H-2 120-130	b.d.	1.64	2.08	59.68	3.61
7C-12H-1 6-16	b.d.	2.50	4.66	12.95	1.40
7C-12H-1 56-66	b.d.	3.71	3.80	92.48	2.85
7C-12H-1 116-126	b.d.	2.28	3.25	77.38	0.37
7C-12H-2 24-34	n.a.	n.a.	n.a.	n.a.	n.a.
7C-12H-2 74-84	n.a.	n.a.	n.a.	n.a.	n.a.
7C-12H-2 124-134	n.a.	n.a.	n.a.	n.a.	n.a.
7C-13H-3 23-33	b.d.	4.08	2.23	49.10	1.18
7C-13H-3 73-83	b.d.	b.d.	b.d.	b.d.	0.40

Table A3-5. Sterol biomarkers for Core 9.

Sample ID	Aquatic Sterols	Brassicasterol	Cholesterol	Plant Sterols	Total Sterols
9A-1H-1 12-32	b.d.	1.06	0.75	90.64	1.15
9A-1H-1 82-102	b.d.	0.66	0.92	91.82	2.49
9C-1H-2 65-85	b.d.	9.76	5.37	23.40	0.02
9C-1H-2 115-135	b.d.	0.56	0.38	88.60	0.90
9C-2H-1 15-35	1.01	2.35	3.12	77.62	5.93
9C-2H-1 85-105	b.d.	10.65	10.87	78.48	0.17
9C-2H-2 47-67	b.d.	29.32	13.16	42.18	0.03
9C-2H-2 117-137	b.d.	0.98	0.85	78.61	4.98
9C-3H-1 27-47	b.d.	2.16	5.63	52.94	0.04
9A-3H-1 98-118	b.d.	4.64	6.93	61.29	0.11
9A-3H-2 57-77	n.a.	n.a.	n.a.	n.a.	n.a.
9A-3H-2 111-131	b.d.	b.d.	13.19	76.64	0.05
9C-4H-1 33-53	n.a.	n.a.	n.a.	n.a.	n.a.
9C-4H-2 16-36	b.d.	b.d.	18.59	81.41	0.05
9C-4H-2 86-106	n.a.	n.a.	n.a.	n.a.	n.a.
9A-5H-1 61-81	b.d.	2.42	1.55	76.01	0.20
9A-5H-2 16-36	n.a.	n.a.	n.a.	n.a.	n.a.
9A-5H-2 86-106	n.a.	n.a.	n.a.	n.a.	n.a.
9C-6H-1 52-72	b.d.	b.d.	1.72	80.60	1.43
9C-6H-2 24-44	b.d.	b.d.	7.52	58.85	0.07
9C-6H-2 94-114	b.d.	b.d.	25.13	37.10	0.09
9A-8H-2 70-90	b.d.	1.19	4.41	94.40	0.18
9C-7H-1 33-53	b.d.	1.79	1.14	78.06	0.51
9C-7H-1 103-123	b.d.	1.71	1.21	59.49	1.98
9A-9H-2 40-60	b.d.	1.16	2.62	57.40	2.40

9A-9H-2 80-100	b.d.	1.25	2.23	72.74	2.09
9C-8H-1 16-36	b.d.	0.63	1.20	77.05	5.27
9C-8H-1 106-136	b.d.	b.d.	41.25	40.10	0.03
9C-8H-4 46-66	n.a.	n.a.	n.a.	n.a.	n.a.
9A-10H-3 13-33	n.a.	n.a.	n.a.	n.a.	n.a.
9A-10H-3 83-103	b.d.	0.69	1.16	11.12	4.35
9C-9H-3 41-61	b.d.	1.84	2.41	41.19	0.34
9C-9H-3 110-130	b.d.	12.96	16.01	44.57	0.28

Table A3-6. Sterol biomarkers for Core 8.

Sample ID	Aquatic Sterols	Brassicasterol	Cholesterol	Plant Sterols	Total Sterols
8A-1H-2 0-20	0.43	2.52	3.20	76.53	5.81
8A-1H-2 79-90	b.d.	4.92	2.44	39.51	0.05
8A-1H-3 51-71	b.d.	11.08	6.30	39.54	0.08
8A-1H-3 140-155	b.d.	1.61	2.29	61.36	5.21
8A-2H-1 8-28	b.d.	6.31	8.64	51.23	0.06
8A-2H-2 40-55	b.d.	1.22	0.59	84.89	10.33
8A-2H-2 110-130	b.d.	9.11	11.68	48.10	0.07
8B-2H-1 100-120	n.a.	n.a.	n.a.	n.a.	n.a.
8B-2H-2 48-68	b.d.	13.78	4.99	41.03	0.05
8B-2H-2 118-133	b.d.	b.d.	2.02	97.98	0.99
8B-3H-1 56-76	b.d.	1.09	9.30	55.40	0.06
8B-3H-2 43-63	b.d.	0.72	0.43	83.01	3.97
8B-3H-2 93-113	b.d.	2.68	7.73	89.59	0.10
8C-3H-1 15-35	b.d.	b.d.	22.38	77.62	0.02
8C-3H-2 78-98	b.d.	b.d.	24.08	b.d.	0.01
8C-4H-1 54-74	n.a.	n.a.	n.a.	n.a.	n.a.
8C-4H-1 114-134	n.a.	n.a.	n.a.	n.a.	n.a.
8C-4H-2 43-58	b.d.	0.82	0.28	83.65	15.85
8C-4H-2 113-133	b.d.	1.43	0.88	97.68	21.96
8C-5H-1 52-72	b.d.	b.d.	2.69	97.31	1.30
8C-5H-2 22-42	b.d.	1.16	1.61	95.69	3.15
8C-5H-2 102-118	b.d.	b.d.	2.07	97.93	0.99
8C-6H-1 27-47	b.d.	1.36	2.85	52.63	0.53
8C-6H-1 97-117	n.a.	n.a.	n.a.	n.a.	n.a.
8C-6H-3 20-40	b.d.	1.41	0.36	80.79	39.08
8A-14H-2 3-23	b.d.	1.90	11.39	31.44	0.04
8A-14H-2 73-93	b.d.	b.d.	15.71	22.61	0.09

APPENDIX 4: LIGNIN BIOMARKERS FOR CORE SAMPLES

Values of total lignin phenol concentrations ($\Sigma 8$ in mg g^{-1}), carbon normalized lignin yields ($\Lambda 8$ in mg / 100 mg_{OC}), and ratios of syringyl to vanillyl (S/V) and cinnamyl to vanillyl (C/V) phenols, vanillic acid to vanillyln [(Ad/Al)v], and benzoinc acid to vanillyln (3,5-Bd:V) are presented for all sediment samples collected from the Englerbight lake cores. Each core is presented in a separate table. Values that are below detection are indicated with b.d., and samples that were not analyzed for these are indicated with n.a.

Table A4-1. Lignin biomarkers for Core 1.

Sample ID	Σ8	Λ8	S/V	C/V	(Ad/Al)v	3,5-Bd:V
1A-1H-1 5-15	0.40	1.87	0.30	0.13	0.53	0.06
1A-1H-1 35-45	0.52	2.18	0.31	0.12	0.45	0.05
1A-1H-1 65-75	0.70	2.07	0.29	0.12	0.45	0.05
1D-1H-1 71-81	0.33	2.03	0.85	0.16	0.59	0.07
1D-1H-1 101-111	0.05	0.75	0.41	0.16	0.87	0.13
1D-1H-1 130-137	n.a.	n.a.	n.a.	n.a.	n.a.	n.a.
1D-1H-2 21-31	0.03	0.44	0.37	0.08	0.78	0.07
1D-1H-2 51-61	0.10	1.14	0.82	0.17	0.50	0.06
1D-1H-2 71-81	n.a.	n.a.	n.a.	n.a.	n.a.	n.a.
1B-2E-2 24-34	0.04	0.56	0.48	0.06	1.08	0.09
1B-2E-2 54-64	0.05	0.67	0.47	0.11	0.99	0.12
1B-2E-2 84-94	0.50	3.76	0.05	0.03	0.33	0.02
1B-2E-2 114-124	0.06	0.81	0.40	0.13	0.86	0.12
1B-2E-3 9-19	0.05	0.60	0.44	0.13	0.91	0.12
1B-2E-3 39-49	0.06	0.78	0.48	0.10	0.96	0.09
1B-2E-3 69-79	0.04	0.55	0.46	0.15	0.34	0.14
1B-2E-3 99-109	0.26	1.52	0.33	0.17	0.45	0.07
1B-2E-3 129-139	0.47	1.63	0.21	0.18	0.44	0.07
1B-3E-1 9-19	0.16	2.09	1.29	0.15	0.50	0.07
1B-3E-1 39-49	0.20	1.57	0.36	0.19	0.49	0.08
1B-3E-1 69-79	0.01	0.29	0.50	0.01	1.08	0.07
1B-3E-1 99-109	0.01	0.30	0.46	0.00	0.87	0.04

Table A4-2. Lignin biomarkers for Core 6.

Sample ID	Σ8	Λ8	S/V	C/V	(Ad/Al)v	3,5-Bd:V
6F-1H-1 77-97	0.49	2.23	0.30	0.14	0.49	0.06
6F-1H-2 19-39	1.08	2.91	0.33	0.14	0.42	0.05
6E-1H-2 49-69	0.61	2.45	0.31	0.13	0.47	0.05
6E-1H-2 119-139	0.05	1.05	0.38	0.06	0.93	0.06
6F-2H-1 50-70	0.43	1.83	0.27	0.17	0.51	0.06
6E-2H-2 43-63	0.13	1.20	0.33	0.20	0.59	0.09
6F-2H-2 80-100	0.21	1.45	0.38	0.15	0.48	0.04
6F-2H-2 123-143	0.19	1.51	0.30	0.13	0.48	0.06
6B-2H-2 35-55	0.28	1.57	0.31	0.15	0.48	0.07
6F-3E-1 41-61	0.39	1.95	0.30	0.12	0.46	0.05
6E-3E-1 71-91	0.40	2.06	0.36	0.18	0.48	0.07
6E-3E-2 38-58	0.01	0.41	0.45	0.03	0.79	0.07

Table A4-3. Lignin biomarkers for Core 4.

Sample ID	Σ8	Λ8	S/V	C/V	(Ad/Al)v	3,5-Bd:V
4B-1H-1 7-17	0.63	5.14	0.36	0.11	0.48	0.06
4B-1H-1 17-27	0.46	5.43	0.39	0.08	0.36	0.03
4A-1H-1 33-43	6.68	12.25	0.31	0.10	0.58	0.03
4A-1H-1 53-63	18.77	18.56	0.39	0.08	0.60	0.03
4A-1H-1 63-73	6.77	15.08	0.38	0.09	0.69	0.02
4A-1H-1 93-103	1.94	7.61	0.37	0.11	0.42	0.03
4A-1H-2 13-23	n.a.	n.a.	n.a.	n.a.	n.a.	n.a.
4A-1H-2 43-53	2.95	8.36	0.29	0.11	0.52	0.02
4A-1H-2 73-83	n.a.	n.a.	n.a.	n.a.	n.a.	n.a.
4A-1H-2 103-113	0.57	4.91	0.31	0.09	0.33	0.03
4A-1H-2 133-143	n.a.	n.a.	n.a.	n.a.	n.a.	n.a.
4B-2H-1 26-36	n.a.	n.a.	n.a.	n.a.	n.a.	n.a.
4B-2H-1 56-64	1.48	8.87	0.35	0.09	0.46	0.05
4B-2H-1 86-95	n.a.	n.a.	n.a.	n.a.	n.a.	n.a.
4A-2H-2 61-71	3.43	12.06	0.21	0.08	0.49	0.03
4B-2H-1 110-118	1.45	7.65	0.34	0.09	0.46	0.04
4B-2H-2 18-28	n.a.	n.a.	n.a.	n.a.	n.a.	n.a.
4B-2H-2 48-58	2.91	12.65	0.51	0.06	0.40	0.02
4A-2H-3 17-27	n.a.	n.a.	n.a.	n.a.	n.a.	n.a.
4A-2H-3 47-57	0.38	3.95	0.38	0.09	0.38	0.06
4A-2H-3 67-77	0.89	13.42	0.28	0.10	0.46	0.04
4A-2H-3 77-87	n.a.	n.a.	n.a.	n.a.	n.a.	n.a.
4A-2H-3 107-117	1.36	8.91	0.52	0.15	0.35	0.05
4B-3H-1 17-27	0.22	2.55	0.35	0.14	0.40	0.07
4B-3H-1 47-57	n.a.	n.a.	n.a.	n.a.	n.a.	n.a.

4B-3H-1 74-85	0.76	6.61	0.18	0.08	0.37	0.04
4B-3H-1 107-117	8.62	10.26	0.24	0.09	0.54	0.03
4A-4H-1 59-69	6.20	9.13	0.17	0.11	0.55	0.03
4A-4H-1 89-99	2.91	9.53	0.26	0.07	0.43	0.03
4A-4H-2 1-11	0.31	3.50	0.29	0.12	0.42	0.07
4A-4H-2 31-41	n.a.	n.a.	n.a.	n.a.	n.a.	n.a.
4A-4H-2 61-71	n.a.	n.a.	n.a.	n.a.	n.a.	n.a.
4A-4H-2 91-101	2.11	7.49	0.24	0.07	0.33	0.03
4A-4H-2 121-131	n.a.	n.a.	n.a.	n.a.	n.a.	n.a.
4B-4H-1 61-71	n.a.	n.a.	n.a.	n.a.	n.a.	n.a.
4B-4H-1 91-101	0.50	4.71	0.32	0.11	0.41	0.06
4B-4H-1 121-131	n.a.	n.a.	n.a.	n.a.	n.a.	n.a.
4B-4H-2 31-41	n.a.	n.a.	n.a.	n.a.	n.a.	n.a.
4B-4H-2 61-71	n.a.	n.a.	n.a.	n.a.	n.a.	n.a.
4A-5H-2 42-52	2.49	9.11	0.23	0.08	0.41	0.03
4A-5H-2 72-82	n.a.	n.a.	n.a.	n.a.	n.a.	n.a.
4A-5H-2 102-112	n.a.	n.a.	n.a.	n.a.	n.a.	n.a.
4A-5H-2 132-142	n.a.	n.a.	n.a.	n.a.	n.a.	n.a.
4B-5H-1 75-85	0.75	5.29	0.34	0.08	0.31	0.04
4B-5H-1 105-115	n.a.	n.a.	n.a.	n.a.	n.a.	n.a.
4B-5H-1 137-147	n.a.	n.a.	n.a.	n.a.	n.a.	n.a.
4B-5H-2 24-34	n.a.	n.a.	n.a.	n.a.	n.a.	n.a.
4B-5H-2 54-64	1.84	6.87	0.28	0.06	0.40	0.03
4B-5H-2 84-94	n.a.	n.a.	n.a.	n.a.	n.a.	n.a.
4B-5H-2 114-124	n.a.	n.a.	n.a.	n.a.	n.a.	n.a.
4B-5H-2 140-150	1.03	7.94	0.37	0.09	0.41	0.04
4B-6H-1 23-33	n.a.	n.a.	n.a.	n.a.	n.a.	n.a.
4B-6H-1 53-63	0.02	0.90	0.23	0.07	0.43	0.06

Table A4-4. Lignin biomarkers for Core 7.

Sample ID	Σ8	Λ8	S/V	C/V	(Ad/Al)v	3,5-Bd:V
7C-1H-1 27-37	0.15	6.94	0.32	0.08	0.39	0.04
7C-1H-2 60-70	2.41	7.36	0.13	0.04	0.34	0.02
7C-1H-1 77-87	3.07	20.80	0.58	0.08	0.46	0.02
7C-1H-2 110-120	0.01	1.78	0.19	0.05	0.79	0.12
7C-2H-1 39-49	n.a.	n.a.	n.a.	n.a.	n.a.	n.a.
7C-2H-1 109-119	0.65	14.34	0.09	0.03	0.28	0.01
7C-2H-2 9-19	n.a.	n.a.	n.a.	n.a.	n.a.	n.a.
7C-2H-2 59-69	n.a.	n.a.	n.a.	n.a.	n.a.	n.a.
7A-2H-2 32-42	0.82	12.16	0.18	0.06	0.30	0.02
7A-2H-2 82-92	2.23	7.94	0.24	0.06	0.38	0.03
7C-3H-1 66-76	1.09	6.67	0.36	0.09	0.41	0.04
7C-3H-1 124-134	n.a.	n.a.	n.a.	n.a.	n.a.	n.a.
7C-3H-2 25-35	n.a.	n.a.	n.a.	n.a.	n.a.	n.a.
7C-3H-2 95-105	3.12	17.02	0.42	0.04	0.41	0.02
7C-3H-2 125-135	n.a.	n.a.	n.a.	n.a.	n.a.	n.a.
7C-4H-1 14-24	0.30	4.35	0.36	0.10	0.39	0.06
7C-4H-2 20-30	0.77	15.89	0.44	0.06	0.24	0.01
7C-4H-2 66-76	0.02	3.11	0.11	0.09	0.83	0.29
7C-4H-3 37-47	n.a.	n.a.	n.a.	n.a.	n.a.	n.a.
7C-4H-3 87-97	n.a.	n.a.	n.a.	n.a.	n.a.	n.a.
7A-4H-2 44-54	0.64	17.89	0.05	0.03	0.36	0.02
7A-4H-2 94-104	54.22	17.45	0.27	0.07	1.25	0.02
7C-5H-1 78-88	4.03	18.06	0.10	0.07	0.36	0.02
7C-5H-1 128-138	18.79	9.79	0.36	0.06	0.54	0.02
7C-6H-1 20-30	35.02	17.59	0.22	0.13	0.47	0.03

7C-6H-1 70-80	18.75	14.80	0.42	0.12	0.49	0.03
7C-6H-1 120-137	3.92	11.94	0.26	0.08	0.46	0.03
7C-6H-2 19-29	n.a.	n.a.	n.a.	n.a.	n.a.	n.a.
7C-6H-2 69-79	0.01	0.40	0.33	0.11	0.61	0.18
7C-6H-2 119-129	n.a.	n.a.	n.a.	n.a.	n.a.	n.a.
7C-7H-1 20-30	1.76	20.76	0.17	0.07	0.46	0.03
7C-7H-1 60-70	n.a.	n.a.	n.a.	n.a.	n.a.	n.a.
7C-7H-1 110-120	0.08	2.88	0.14	0.05	0.38	0.05
7C-7H-2 25-35	n.a.	n.a.	n.a.	n.a.	n.a.	n.a.
7C-7H-2 75-85	5.34	16.15	0.31	0.08	0.86	0.03
7C-7H-2 110-120	n.a.	n.a.	n.a.	n.a.	n.a.	n.a.
7C-8H-1 20-30	n.a.	n.a.	n.a.	n.a.	n.a.	n.a.
7C-8H-1 70-80	n.a.	n.a.	n.a.	n.a.	n.a.	n.a.
7C-8H-1 116-126	3.81	48.86	0.04	0.03	0.23	0.01
7C-9H-2 33-43	n.a.	n.a.	n.a.	n.a.	n.a.	n.a.
7C-9H-2 73-83	0.01	0.78	0.33	0.05	0.42	0.03
7C-9H-2 83-93	n.a.	n.a.	n.a.	n.a.	n.a.	n.a.
7C-9H-2 132-142	1.08	6.68	0.27	0.08	0.40	0.03
7C-9H-3 38-48	1.14	8.01	0.32	0.08	0.34	0.03
7C-9H-3 88-98	n.a.	n.a.	n.a.	n.a.	n.a.	n.a.
7C-10H-1 25-35	0.20	7.61	0.39	0.05	0.29	0.02
7C-10H-1 75-85	n.a.	n.a.	n.a.	n.a.	n.a.	n.a.
7C-10H-1 125-135	3.03	19.42	0.08	0.12	0.87	0.04
7C-10H-2 30-40	0.30	5.20	0.32	0.06	0.34	0.03
7C-10H-2 70-80	n.a.	n.a.	n.a.	n.a.	n.a.	n.a.
7C-10H-2 120-130	0.66	5.59	0.38	0.09	0.41	0.04
7C-11H-1 10-20	n.a.	n.a.	n.a.	n.a.	n.a.	n.a.
7C-11H-1 60-70	0.37	5.11	0.34	0.08	0.38	0.05

7C-11H-2 22-32	0.43	4.72	0.33	0.11	0.42	0.05
7C-11H-2 72-82	n.a.	n.a.	n.a.	n.a.	n.a.	n.a.
7C-11H-2 120-130	0.73	6.75	0.34	0.07	0.39	0.04
7C-12H-1 6-16	0.31	8.80	0.31	0.07	0.36	0.04
7C-12H-1 56-66	1.92	15.04	0.24	0.08	0.44	0.03
7C-12H-1 116-126	0.52	5.48	0.46	0.10	0.37	0.05
7C-12H-2 24-34	n.a.	n.a.	n.a.	n.a.	n.a.	n.a.
7C-12H-2 74-84	n.a.	n.a.	n.a.	n.a.	n.a.	n.a.
7C-12H-2 124-134	n.a.	n.a.	n.a.	n.a.	n.a.	n.a.
7C-13H-3 23-33	0.08	1.01	0.36	0.12	0.52	0.03
7C-13H-3 73-83	0.05	2.92	0.11	b.d.	0.82	0.03

Table A4-5. Lignin biomarkers for Core 9.

Sample ID	Σ8	Λ8	S/V	C/V	(Ad/Al)v	3,5-Bd:V
9A-1H-1 12-32	0.07	2.28	0.36	0.40	0.36	0.06
9A-1H-1 82-102	0.09	2.64	0.21	0.07	0.46	0.05
9C-1H-2 65-85	0.00	0.13	0.49	0.07	1.41	0.47
9C-1H-2 115-135	0.13	4.06	0.53	0.15	0.40	0.04
9C-2H-1 15-35	0.45	1.87	0.45	0.16	0.51	0.06
9C-2H-1 85-105	0.07	7.42	2.16	0.10	0.36	0.04
9C-2H-2 47-67	0.00	0.14	0.60	0.10	1.11	0.45
9C-2H-2 117-137	0.17	1.76	0.41	0.12	0.44	0.06
9C-3H-1 27-47	0.02	3.43	0.13	0.16	0.50	0.06
9A-3H-1 98-118	0.02	2.23	1.09	0.30	0.57	0.06
9A-3H-2 57-77	0.00	0.35	0.38	0.07	0.73	0.09
9A-3H-2 111-131	n.a.	n.a.	n.a.	n.a.	n.a.	n.a.
9C-4H-1 33-53	n.a.	n.a.	n.a.	n.a.	n.a.	n.a.
9C-4H-2 16-36	0.00	0.04	0.64	0.11	1.75	0.62
9C-4H-2 86-106	n.a.	n.a.	n.a.	n.a.	n.a.	n.a.
9A-5H-1 61-81	0.00	0.55	0.16	0.06	0.53	0.05
9A-5H-2 16-36	n.a.	n.a.	n.a.	n.a.	n.a.	n.a.
9A-5H-2 86-106	n.a.	n.a.	n.a.	n.a.	n.a.	n.a.
9C-6H-1 52-72	n.a.	n.a.	n.a.	n.a.	n.a.	n.a.
9C-6H-2 24-44	0.00	0.23	0.19	0.07	0.37	0.11
9C-6H-2 94-114	0.00	0.18	0.42	0.04	0.70	0.15
9A-8H-2 70-90	n.a.	n.a.	n.a.	n.a.	n.a.	n.a.
9C-7H-1 33-53	0.07	2.87	0.32	0.13	0.37	0.04
9C-7H-1 103-123	0.20	1.77	0.46	0.15	0.38	0.06
9A-9H-2 40-60	0.18	1.78	0.46	0.12	0.38	0.05

9A-9H-2 80-100	0.14	1.52	0.42	0.12	0.40	0.07
9C-8H-1 16-36	0.27	2.37	0.42	0.11	0.36	0.05
9C-8H-1 106-136	1.94	10.65	0.30	0.09	0.29	0.03
9C-8H-4 46-66	0.11	1.21	0.47	0.12	0.46	0.06
9A-10H-3 13-33	0.02	0.44	0.47	0.01	1.09	0.05
9A-10H-3 83-103	0.22	1.74	0.43	0.12	0.38	0.05
9C-9H-3 41-61	0.01	0.52	0.52	0.01	1.31	0.03
9C-9H-3 110-130	0.00	0.11	0.28	0.00	2.28	0.00

Table A4-6. Lignin biomarkers for Core 8.

Sample ID	Σ8	Λ8	S/V	C/V	(Ad/Al)v	3,5-Bd:V
8A-1H-2 0-20	0.38	4.98	0.67	0.16	0.58	0.05
8A-1H-2 79-90	0.00	0.24	0.55	0.07	1.16	0.29
8A-1H-3 51-71	0.00	0.58	0.12	0.02	3.30	0.08
8A-1H-3 140-155	0.17	2.40	0.35	0.19	0.52	0.06
8A-2H-1 8-28	0.00	0.53	0.64	0.12	0.52	0.10
8A-2H-2 40-55	1.18	5.66	0.34	0.10	0.32	0.03
8A-2H-2 110-130	0.00	0.12	0.53	0.09	1.27	0.40
8B-2H-1 100-120	n.a.	n.a.	n.a.	n.a.	n.a.	n.a.
8B-2H-2 48-68	0.00	0.18	0.62	0.08	1.08	0.27
8B-2H-2 118-133	0.01	1.87	0.09	0.13	0.23	0.04
8B-3H-1 56-76	n.a.	n.a.	n.a.	n.a.	n.a.	n.a.
8B-3H-2 43-63	0.09	3.36	0.79	0.08	0.27	0.02
8B-3H-2 93-113	0.00	0.80	0.32	0.04	0.52	0.05
8C-3H-1 15-35	n.a.	n.a.	n.a.	n.a.	n.a.	n.a.
8C-3H-2 78-98	0.00	0.12	0.52	0.11	1.46	0.54
8C-4H-1 54-74	n.a.	n.a.	n.a.	n.a.	n.a.	n.a.
8C-4H-1 114-134	n.a.	n.a.	n.a.	n.a.	n.a.	n.a.
8C-4H-2 43-58	0.85	7.74	0.56	0.18	0.34	0.04
8C-4H-2 113-133	1.41	7.92	0.27	0.08	0.34	0.02
8C-5H-1 52-72	0.03	1.21	0.49	0.03	0.47	0.02
8C-5H-2 22-42	0.29	3.47	0.14	0.07	0.30	0.02
8C-5H-2 102-118	0.10	4.43	0.16	0.03	0.35	0.01
8C-6H-1 27-47	0.01	0.65	0.43	0.02	0.96	0.03
8C-6H-1 97-117	n.a.	n.a.	n.a.	n.a.	n.a.	n.a.
8C-6H-3 20-40	1.75	6.15	0.32	0.11	0.28	0.03
8A-14H-2 3-23	0.00	0.27	0.43	0.06	1.54	0.27
8A-14H-2 73-93	0.01	0.74	0.45	0.01	1.92	0.09

VITA

CHRISTINA ROSE PONDELL

Born on June 29, 1986 in Libertyville, Illinois. Graduated from Antioch Community High School in 2004. Earned a bachelor's degree from Texas A&M University at Galveston in marine science in 2007. Worked as a geotechnical laboratory technician at C&C Technologies, Inc. before entering the master's program at the Virginia Institute of Marine Science. Bypassed into the Ph.D. program in 2010 studying organic geochemistry under Dr. Elizabeth Canuel. Defended dissertation in July 2014.